Etude expérimentale des dynamiques temporelles du comportement normal et pathologique chez le rat et la souris

Maria Isabel Carreno-Muñoz

THÈSE EN COTUTELLE PRÉSENTÉE POUR OBTENIR LE GRADE DE

DOCTEUR DE

L'UNIVERSITÉ DE BORDEAUX

ET DE L'UNIVERSITÉ DU PAYS BASQUE

ÉCOLE DOCTORALE SCIENCES DE LA VIE ET DE LA SANTE

ÉCOLE DOCTORALE DE l'UPV

Par Maria Isabel CARRENO-MUÑOZ

Etude expérimentale des dynamiques temporelles du comportement normal et pathologique chez le rat et la souris

Sous la direction de Xavier LEINEKUGEL
et de Abdelmalik MOUJAHID

Soutenue le 22 Septembre 2017

Membres du jury :

M. HERAULT, Yann	Université de Strasbourg	Rapporteur (Président)
M. SANCHEZ-SANTED, Luis Fernando	Université d'Almeria	Rapporteur
Mme DESMEDT, Aline	Université de Bordeaux	Examinateur
Mme LOPEZ DE IPIÑA, Karmele	Université du Pays Basque	Examinateur
Mme PIETROPAOLO, Susana	Université de Bordeaux	Examinateur

Titre : Etude expérimentale des dynamiques temporelles du comportement normal et pathologique chez le rat et la souris

Résumé : Le développement d'outils de phénotypage comportemental sophistiqués est indispensable pour comprendre le fonctionnement cognitif. A partir d'une analyse élaborée de tests comportementaux classiques, mes résultats suggèrent que l'hypersensibilité sensorielle associée à un canal potassique spécifique (BkCa) participe aux divers troubles comportementaux du syndrome de l'X-Fragile et du spectre autistique. Grâce à un dispositif expérimental nouveau et original, comprenant des capteurs de pression hyper-sensibles à même de détecter les moindres mouvement d'un rat ou d'une souris avec une sensibilité et une précision temporelle exceptionnelles, j'ai pu identifier des composantes comportementales normales et pathologiques inédites, telles que des tremblements ou la dynamique des forces mises en jeu dans divers mouvements, qui modifieront certainement nos capacités d'investigation des mécanismes impliqués dans la douleur, la peur ou la locomotion, dans les conditions normales et pathologiques.

Mots clés : comportement, computation, éthologie, Syndrome de l'X fragile, autisme, Alzheimer, Parkinson

---

Title : Supervised and unsupervised investigation of the temporal dynamics of normal and pathological behaviour in the mouse and rat

Abstract : Modern neuroscience highlights the need for designing sophisticated behavioral readout of internal cognitive states. From a thorough analysis of classical behavioural tests, my results support the hypothesis that sensory hypersensitivity might be the cause of other behavioural deficits, and confirm the potassium channel BKCa as a potentially relevant molecular target for the development of drug medication against Fragile X Syndrome / Autism Spectrum Disorders. I have also used an innovative device, based on pressure sensors that can non-invasively detect the slightest animal movement with unprecedented sensitivity and time resolution, during spontaneous behaviour. Analysing this signal with sophisticated computational tools, I could demonstrate the outstanding potential of this methodology for behavioural phenotyping in general, and more specifically for the investigation of pain, fear or locomotion in normal mice and models of neurodevelopmental and neurodegenerative disorders.

Keywords : behaviour, computation, ethology, Fragile X Syndrome, autism, Alzheimer, Parkinson

Unité de recherche I
Neurocentre Magendie, INSERM U1215
A. Frick Lab, "Cortical plasticity"
146 Rue Léo-Saignat
33000 Bordeaux
France

Unité de recherche II
Basque University (UPV/EHU), Facultad de Informática, M. Graña's Lab "Computational Intelligence Group".
Pº Manuel Lardizabal 1
20018 Donostia
(Gipuzkoa - Spain)

Comprendre les mécanismes sous-jacents aux comportements complexes et aux anomalies comportementales produites par des maladies neuropsychiatriques représente un défi critique dans la recherche biomédicale. En particulier, l'étude du comportement spontané des animaux non apprivoisés peut révéler des informations très importantes sur toute une variété de composants psychologiques, moteurs et cognitifs de manière non invasive. Récemment, certains outils computationnels ont été développés pour étudier le comportement spontané chez les rongeurs. Cependant, l'évolution des besoins des utilisateurs (c'est-à-dire des scénarios plus complexes et une plus grande résolution spatio-temporelle) ainsi que l'apparition de nouveaux capteurs (capteurs de pression) et la possibilité de synchroniser avec les lectures de l'activité neuronale, donne de nouvelles perspectives à la recherche actuelle. Le principal objectif de cette thèse est d'étudier le comportement spontané chez les rongeurs de points de vue différents mais complémentaires.

Afin d'obtenir une description la plus précise du comportement et d'extraire des résultats descriptifs de la corrélation et causalité du comportement, dans la première partie de ma thèse, j'ai exploré l'intérêt pour le phénotypage comportemental d'un nouveau dispositif expérimental, basé sur des capteurs de mouvement (en utilisant la technologie piézoélectrique). Il s'agit d'une plate-forme ouverte « open field » reposant sur plusieurs capteurs de pression, qui sont capables de détecter le moindre mouvement de l'animal placé sur elle, comme la respiration et le rythme cardiaque. Des mouvements individuels (comme chaque pas) peuvent être détectés pour être après plus précisément caractérisés. Le profil du signal est spécifique à chaque comportement et il apporte des précieuses informations quantitatives et qualitatives. Cet outil non invasif nous a permis également de décrire des comportements très subtiles, impossibles à distinguer par d'autres systèmes, tels que des tremblements (lies à la douleur, à la peur, à la maladie de Parkinson (MP)), des changements de rythmes respiratoire et cardiaque et des anomalies dans la marche (comment le décours temporel de la force et de la coordination des mouvements au sein de chaque pas lors de la locomotion). Mes analyses basées sur la décomposition temps-fréquence et le recours à des algorithmes de machine learning

démontrent le potentiel exceptionnel de cette approche pour le phénotypage comportemental.

Un avantage très important de ce système de phénotypage comportemental est la possibilité d'effectuer l'acquisition des enregistrements électrophysiologiques (EEG) simultanément au signal mécanique et au signal vidéo, ce qui permet de caractériser l'activité cérébrale sous-jacent aux comportements. Par exemple, pendant cette thèse on a pu étudier comment la force appliqué à chaque pas pendant la locomotion de l'animal fluctue d'une façon corrélationnelle a l'amplitude des ondes thêta hippocampiques (5-12 Hz).

En utilisant cet appareil, nous avons identifié également des symptômes moteurs chez des souris 3xTg-AD (un modèle transgénique de la Maladie d'Alzheimer) et souris 6-OHDA (modèle de souris de la Maladie de Parkinson), comme des épisodes éphémères de tremblement de haute fréquence, et des altérations de la démarche locomotrice par rapport aux animaux control du même âge. Les théories classiques assument que la Maladie d'Alzheimer est principalement liée d'un déficit cognitif en raison de déficits dans les systèmes cholinergiques et la Maladie de Parkinson est lie des altérations motrices en raison de déficits dans les systèmes dopaminergiques. Toutefois, des études cliniques prospectives ont montré que les symptômes moteurs précèdent souvent les symptômes cognitifs dans la Maladie d'Alzheimer. Ici, nous montrons comment ces symptômes moteur communes chez les souris 3xTg-AD et souris 6-OHDA ont été soulagés par la L-dopa (précurseur dopaminergique et médicaments de référence pour Maladie de Parkinson), ce qui suggère l'implication potentielle de déficit dopaminergique dans la Maladie d'Alzheimer. Des enregistrements de l'EEG ont également révélé l'expression de l'activité hippocampique altérée pendant la locomotion où la modulation de l'amplitude de thêta est altérée. Nos résultats préliminaires chez la souris 3xTg-AD, démontrent l'expression inattendue d'une bande bêta (caractéristique du Maladie de Parkinson) qui est sensible à la L-DOPA. Ces observations renforcent l'idée d'une potentielle affectation du système dopaminergique dans la Maladie d' Alzheimer.

Dans la deuxième partie de ma thèse, j'ai aussi étudié l'effet du changement d'environnement sur un modèle murin de Syndrome de Fragile X (SFX), une pathologie neurodéveloppementale fréquemment associée à des troubles autistiques. Il a été proposé, mais jamais démontré, que l'intolérance au changement qui caractérise les patients SFX serait due à leur hypersensibilité sensorielle (dérivée d'une hyperexcitabilité neuronale) et à un déficit du mécanisme neuronal d'habituation. Ces défauts de connectivité neuronale (hypo ou hyper connectivité en fonction du contexte et de la nature des stimuli présentés) sont présumé d'etre la cause physiologique des déficits d'attention et diverses anomalies comportementales déclenchés en réaction à une charge excessive d'information environnementale qui serait normalement ignorée. Ce phénomène, appelé « défensive sensorielle », a été proposé comme la cause potentielle de l'hyperactivité, hyperexcitation et des réactions comportementales négatives aux changements de routine qui sont souvent néfastes pour les patients SFX. Pour tester cette hypothèse, dite de l'hyper-réactivité ou "défensive sensorielle", j'ai utilisé le BMS-204352, une drogue agoniste des canaux potassiques de type gKCa, qui restaure une sensibilité sensorielle normale chez les souris Fmr1-KO, un modèle de SFX. Au moyen des tests comportementaux classiques, j'ai observé que comme les patients SFX, les souris Fmr1-KO étaient fortement perturbées par l'exposition à un environnement nouveau ou inhabituel, une situation se traduisant par des anomalies comportementales telles que l'hyperactivité, l'incapacité à construire leur nid ou le toilettage du dos excessif. Mais ces anomalies ont disparu après traitement par le BMS-204352, ce qui constitue un argument en faveur de l'hypothèse de l'hyper-réactivité et confirme l'intérêt thérapeutique potentiel de la voie potassique gkCa dans les pathologies de l'X Fragile et de l'autisme.

Finalement, afin de pouvoir étudier la complexité du comportent globale des animaux Fmr1-KO j'ai appliqué au signal issu des capteurs de pression des approches computationnelles dérivées de la physique (entropie et des analyses fractals). Il a été déjà observé que le signal electrophysiologique cortical et la motricité des patients Alzheimer révèlent une diminution de la complexité en comparaison aux sujets control. D'ailleurs, d'après un grand nombre d'observations qu'on peut trouver dans la littérature, la complexité des systèmes naturels a été lie à la richesse comportementale, à

l'imprédictibilité, au chaos…, et donc la perte de cette complexité est lié la prédictibilité, aux maladies et au vieillissement. L'apparition des comportements répétitifs et des stéréotypies sont unes de caractéristiques plus limitantes chez les patients de syndrome de troubles autistes et de l'X Fragile. Pendant ma thèse on a aussi analysé la complexité du comportement globale comment indicateur de pathologie et stéréotypies comportementaux. Nous avons développé des algorithmes qui nous ont permis de quantifier l'entropie et des coefficients de la dimension fractale (coefficient de dimension et exposant de Lyapunov) du signal mécanique (décrite avant) et les coordonnées XY (comportement exploratoire de l'animal) pendant une heure d'enregistrement dans un environnement nouveau. En effet, on a pu observer que le comportement global des souris Fmr1-KO montre une complexité significativement plus basse que chez les souris control. Cependant, des études complémentaires sont requises pour identifier les composantes comportementales sous-jacentes à cette baisse de complexité globale.

ACKNOWLEDGMENTS

I am very grateful to my supervisor Xavier Leinekugel (Neurocentre Maendie, Inserm, France) for giving me the opportunity to work in his lab, for helping, guiding and supporting me throughout my PhD and Master studies. His mentorship has been a keystone in my research career. I will always be grateful to him for believing in my capacities, encouraging me to never give up and showing me that we can always do better. I specially want to thank him for introducing me to this wonderful field which is neuroscience and teaching me everything I know, always with a good sense of humour.

I would like to thank all the team members of the Cortical Plasticity team: Andreas Frick, Melanie Ginger, Isabel del Pino, Maria del Carmen Medrano, Olivier Dubanet, Maelys Bompart, Fabienne Martins, Senka Hadzibegovic, Guillaume Bony, Katy LeCorf, Arjun Bhaskaran, Rafael De Sa and Vladimir Kouskoff, for being always happy to help me and teach me new things, for their cooperation and altruism, but specially for providing a stimulating and fun environment every day at the lab. It has been a great pleasure to work with all of you. In particular I am very grateful to Maria del Carmen Medrano who has supported me inside and outside the lab, being not only a great college, but also a great friend. A real friend who every single day has shared with me her motivation, knowledge, skills and smile to make me move forward.

I want to thank my co-supervisor Abdelmalik Moujahid for teaching me computational and physical concepts that I would have never understood better. I would also like to thank Manuel Graña and all his lab members, in particular Oier and Leire who were always so welcoming to me and shared with me their passion for computational sciences and many good moments in the beautiful city of San Sebastian.

I wish to thank also Karmele Lopez de Ipiña for her work on alternative analysis of the piezo-electricic signals and XY coordinates. I really appreciate the time she spent teaching and explaining me how to make “churreras”.

I am grateful to all my friends in- and outside the lab for their every-day support and encouragement, Giovanna, Maria, Melody, Mari, Giulia, Nuria and many others, thank you for your moral support. To all my friends who, despite being far away from me during this

wonderful experience, have always supported and sent me their best every day. Eri, Cuchi, Maki and Caro, thank you for being always there for me.

Above all, I would like to thank my parents for the constant support they gave me all my life, for their unconditional love, for being able to cross seas and mountains in a second just to push me up, for their patience and encouragement, for everything they did for me, thank you. I'll be always grateful to my sister for her unconditional support, for teaching me how to appreciate the important things of life and for being always close to me. Laura, thank you for being always you and for pushing me to be more "me". I would also like to thank my entire family for being there for me anytime.

For your love, for your dedication, for making me smile every day, for your constant support, for turning our lives into pure joy even in the hard times, for your energy, for being who you are, everyday, I thank you, Manu!

This project has benefited from state funding, managed by the National Research Agency (France). The funding is allocated to the project "IdEx Bordeaux" within the framework of the programme "Investments for the Future", reference number ANR - n ° ANR-10-IDEX-03 -02".

SUMMARY

The presumably limited introspection and language capabilities of laboratory animals promote the need for designing sophisticated behavioral readout of internal cognitive states. During the first part of my PhD, I have investigated the behavioural phenotype of *Fmr1*-KO mice, a model of Fragile-X Syndrome (FXS), which is a neurodevelopmental disorder very frequently associated with Autism Spectrum Disorders (ASD). In FXS, sensory-hypersensitivity and impaired habituation has been proposed as the potential cause of hyperactivity, hyperarousal, and negative reactions to changes in routine that are often deleterious for FXS patients. However, the lack of tools for manipulating sensory-hypersensitivity has not allowed the experimental testing required to evaluate the relevance of this hypothesis. Here, I have used BMS-204352, a BK_{Ca} channel agonist recently shown to reverse the cortical hyper-excitability and related sensory hypersensitivity in the *Fmr1*-KO mouse model of FXS. With classical behavioural tests, I have found that exposing *Fmr1*-KO mice to novel or unfamiliar environments resulted in multiple behavioural perturbations, ranging from hyperactivity to impaired nest building and excessive grooming of the back. Reversing sensory hypersensitivity with BMS-204352 prevented these behavioral abnormalities in *Fmr1*-KO mice. These results are in support of the sensory defensiveness hypothesis, and confirm BK_{Ca} as a potentially relevant molecular target for the development of drug medication against FXS / ASD.

In the second part of my PhD, I have explored the potential of an innovative device offering new opportunities for behavioural phenotyping. It consists of an open-field platform resting on very sensitive pressure-sensors, so that the slightest animal movement can be detected with unprecedented sensitivity and time resolution, in a totally non-invasive manner and during spontaneous behaviour. For example, we can resolve up to individual heart beats and breathing cycles during rest, the time course of strength and muscle/limb coordination over individual footsteps during locomotion, or internal shaking events expressed during pain or fear. Analyses based on time-frequency decomposition and machine learning algorithms demonstrate the outstanding potential of this methodology for behavioural phenotyping in general. More specifically, I have observed differential expression of fear (freezing immobility vs internal body shaking) in different behavioural conditions such as fear conditioning, exploration of a novel environment, or the presence of a predator. This suggests that we may identify different levels or even possibly different types of fear. Investigating the behavioural phenotype of 3xTg-AD and APP-PS1 mice, two transgenic models of Alzheimer's disease, I

have also identified motor symptoms expressed as altered gait and intermittent high-frequency (80-100Hz) shaking events. These are rescued by the dopaminergic agonist L-DOPA, induced in WT mice by 6-OHDA lesions of the dopaminergic system, and expressed already at the age of 3 weeks. These results echo the clinical observation that motor symptoms can be found several years prior to cognitive deficits in Alzheimer patients, and the pre-clinical data indicating a significant rescue of cognitive performance with L-DOPA in Alzheimer mice. Altogether, these results point to very early deficits in the DA system in Alzheimer's disease, a perspective yet poorly explored in clinical studies.

Interestingly, computational approaches derived from physics have identified specific properties of motor behaviour in Alzheimer patients. Applying these to my data, I have found that the signal obtained from the pressure sensors during spontaneous open-field behaviour differed in complexity (entropy and Lyapunov exponents) between WT and *Fmr1*-KO mice. Further investigation is required to identify the specific aspects of behaviour underlying these differences in signal complexity.

RESUME

Le développement d'outils de phénotypage comportemental sophistiqués est indispensable pour mieux comprendre le fonctionnement cognitif. Dans la première partie de ma thèse, j'ai étudié le comportement des souris *Fmr1*-KO, un modèle du syndrome de l'X Fragile (SXF) qui est une pathologie neurodéveloppementale fréquemment associée à des troubles autistiques. Il a été proposé, mais jamais démontré, que l'intolérance au changement qui caractérise les patients SXF serait due à leur hypersensibilité sensorielle et un déficit du mécanisme neuronal d'habituation. Pour tester cette hypothèse, dite de l'hyper-réactivité ou "défensive sensorielle", j'ai utilisé le BMS-204352, une drogue agoniste des canaux potassiques de type gKCa, qui restaure une sensibilité sensorielle normale chez les souris *Fmr1*-KO, un modèle de SXF. Au moyen de tests comportementaux classiques, j'ai observé que comme les patients SXF, les souris *Fmr1*-KO étaient fortement perturbées par l'exposition à un environnement nouveau ou inhabituel, une situation se traduisant par des anomalies comportementales telles qu'hyperactivité, incapacité à construire leur nid ou toilettage du dos excessif. Mais ces anomalies ont disparu après traitement par le BMS-204352, ce qui constitue un argument en faveur de l'hypothèse de l'hyper-réactivité et confirme l'intérêt thérapeutique potentiel de la voie potassique BkCa dans les pathologies de l'X Fragile et de l'autisme.

Dans la deuxième partie de ma thèse, j'ai exploré l'intérêt pour le phénotypage comportemental d'un dispositif expérimental nouveau, constitué d'une plateforme (open-field) reposant sur des capteurs de pression extrêmement sensibles et permettant de détecter de façon totalement non invasive les moindres mouvements de l'animal, au cours du comportement spontané, avec une sensibilité et une précision temporelle sans équivalent dans les systèmes existants. On peut ainsi résoudre chaque battement de coeur ou chaque cycle de respiration pendant l'immobilité, le décours temporel de la force et de la coordination des mouvements au sein de chaque pas lors de la locomotion, ou des tremblements/frissons exprimés en réponse à la douleur ou à la peur. Mes analyses basées sur la décomposition temps-fréquence et le recours à des algorithmes de machine learning démontrent le potentiel exceptionnel de cette approche pour le phénotypage comportemental. Plus spécifiquement, j'ai observé l'expression distincte d'immobilité totale ou de frissons en réponse à différentes situations stressantes telles qu'un conditionnement aversif, l'exploration d'un nouvel environnement ou la présence d'un prédateur, ce qui suggère la possibilité de différencier plusieurs niveaux, voire différents types de peur. Sur des souris 3xTg-AD et APP-PS1, deux modèles transgéniques de la maladie d'Alzheimer (MA), j'ai également identifé une altération de la marche et l'expression de tremblements intermittents à haute fréquence (80-100Hz), déjà exprimées à l'âge de 3

semaines, corrigées par l'administration de l'agoniste dopaminergique L-DOPA, et reproduits chez des souris sauvages par des lésions dopaminergiques (6-OHDA). Ces résultats suggèrent l'expression de déficits très précoces des systèmes dopaminergiques dans la maladie d'Alzheimer, une voie peu explorée en clinique malgré la description de symptômes moteurs précédant de plusieurs années l'expression des symptômes cognitifs chez les patients et l'amélioration cognitive apportée par la L-DOPA sur des souris modèles de MA.

Finalement, j'ai appliqué au signal issu des capteurs de pression des approches computationnelles dérivées de la physique, et observé comme ça l'avait été pour la motricité de patients Alzheimer, une diminution de la complexité du signal (entropie et fonction de Lyapunov) chez les souris MA par rapport à des souris sauvages. Des études complémentaires sont requises pour identifier les composantes comportementales sous-jacentes à cette baisse de complexité globale.

RESUMEN

Para una mejor comprensión del funcionamiento cognitivo, resulta indispensable el desarrollo de herramientas de caracterización comportamental sofisticadas. La primera parte de mi tesis estudia el comportamiento de ratones FMR1-KO, un modelo animal de síndrome del X frágil (SFX), una neuropatología del desarrollo frecuentemente asociada con el autismo. Aunque aún no se ha demostrado científicamente, se ha propuesto en trabajos anteriores que la aversión al cambio que caracteriza a los pacientes de SFX podría ser debida a una hipersensibilidad neuronal y a un déficit del mecanismo neuronal de habituación. Este trabajo pone a prueba esta teoría de hiperreactividad, también llamada "defensa sensorial". Utilizando BMS-204352, una sustancia agonista de los canales de potasio del grupo gKCa, hemos conseguido restablecer la sensibilidad sensorial de los ratones FMR1-KO a niveles normales. Mediante la aplicación de test comportamentales clásicos, hemos observado que al igual que los pacientes SFX, los ratones FMR1-KO son fuertemente perturbados ante la exposición a un ambiente nuevo o inhabitual, situaciones que se traducen en anomalías comportamentales, como la hiperactividad, la incapacidad de construir su nido, o el lavado excesivo del lomo. Una única dosis de BMS-204352 fue suficiente para recuperar todas estas anomalías, resultado que apoya la teoría de la hiperreactividad, y confirma el interés terapéutico de la vía potásica gkCa, en patologías como el X frágil y el autismo.

La segunda parte de esta tesis, explora el potencial de un dispositivo experimental diseñado para la caracterización comportamental. Se trata de una plataforma que descansa sobre sensores de presión extremadamente sensibles, y que permiten detectar de forma nada invasiva los más sutiles movimientos del animal. Esta herramienta ofrece la posibilidad de explorar el comportamiento espontaneo del animal con una gran sensibilidad y precisión temporal previamente inexistente. Con ella podemos, por ejemplo, observar cada latido cardiaco, o ciclo respiratorio durante periodos de inmovilidad, la evolución temporal de la fuerza y la coordinación de los movimientos que se acontecen en cada paso durante la locomoción, así como los temblores producidos por dolor, o miedo. Nuestros análisis basados en la descomposición espectral y machine learning, demuestran el potencial excepcional de esta herramienta de fenotipaje comportamental. En concreto, hemos podido observar la distinta expresión entre inmovilidad absoluta y temblores en respuesta a diferentes situaciones estresantes, como son, un condicionamiento aversivo a un contexto y sonido, la exploración de un ambiente desconocido, o la presencia de un depredador, lo que sugiere la posibilidad de diferenciar distintos niveles o tipos de miedo. Por otro lado, hemos podido identificar una

alteración en la locomoción y la aparición de temblores de alta frecuencia (80-10 Hz) en ratones 3xTg-AD y APP-PS1, dos modelos transgénicos de la patología de Alzheimer (PA). Estas, expresiones comportamentales, que observamos también en juveniles de 3 semanas y en animales con lesiones en nucleos dopaminergicos (modelo animal de Parkinson, 6OHDA), han podido ser corregidas tras una única dosis de L-dopa. Estos resultados sugieren la expresión de déficits precoces de sistemas dopaminergicos, en el caso de la PA, una vía poco explorada en clínica pese a la descripción de síntomas motores precedentes a la expresión de síntomas cognitivos en los pacientes, y a la mejora cognitiva observada tras tratamientos de L-Dopa en varios modelos de PA.

Por último, la realización de análisis computacionales derivados de la física, han evaluado la complejidad (entropía y exponente de Lyapunov) de la señal derivada de los captores de presión, revelando una disminución de la complejidad de la señal en ratones FMR1-KO. Estudios complementarios son necesarios para la identificación de componentes comportamentales subyacentes a esta base de complejidad global.

LIST OF ABBREVIATIONS

6-OHDA	6-Hydroxidopamine
AP	Action Potentials
AD	Alzheimer's Disease
APP	β-amyloid precursor protein
ASD	Autism Spectrum Disorder
BK	Big conductance K+ channels
BKCa	Ca2+-activated K+ Channels
CFA	Complete Freund's Adjuvant
CS	Conditioned Stimulus
CPP	Conditioned Place Preference
D2	Correlation Dimension
DA	Dopamine
DAT	Dopamine transporter
DG	Dentate gyrus
DSM-IV	Diagnostic and Statistical Manual of Mental Disorders, 5th Edition
EC	Entorhinal Cortex
EEG	Electrophysiological
EMG	Electromyogram
FFT	Fast Fourier Transform
FMRP	Fragile X Mental Retardation Protein
FXS	Fragile X Syndrome
GP	Globus Pallidus
KO	Knockout
LE	Lyapunov exponents
MFB	Median Forebrain Bundle
MGS	Mouse Grimace Scale
MS	Medial Septum
mPFC	Medial Prefrontal Cortex
MPTP	1-methyl 4-phenyl 1,2,3,6-tetrahydropyridine
NET	Noradrenaline Transporter
NREM	Non– Rapid Eye Movement
PD	Parkinson's Disease
PE	Permutation Entropy

PSD	Power Spectrum Density
REM	Rapid Eye Movement
SEM	Standard Error of Means
SN	Substantia Nigra
STN	Subthalamic Nucleus
TJM	Tremulous Jaw Movement
US	Unconditioned Stimulus
VGKCs	Voltage-Gated K+ Channels
WBP	Whole Body Plethysmography
WT	Wild Type

GENERAL INTRODUCTION

Understanding the underlying mechanisms of complex behavior and the behavioral abnormalities that result from neuropsychiatric disorders represent a critical issue in biomedical research. With the advent of molecular genetics and techniques allowing to manipulate neuronal physiology with unprecedented versatility and precision, the number of animal models is growing considerably, supporting a renewed interest for integrative physiology and behavioral phenotyping. The possibility to generate animal models in which psychological, cognitive and physiological functions can be manipulated experimentally is a considerable source of progress in neuroscience and medical research, allowing to establish causal relationships between brain structure and function, as well as to reproduce and rescue the pathological changes responsible for pathologies that are a major societal concern. However, the presumably limited introspection and language capabilities of laboratory animals promote the need for designing sophisticated behavioral readout of internal cognitive states. Behavioral phenotyping is therefore a fundamental requirement for the exploitation of a growing number of available animal models and potentially useful pharmacological agents made available by academic and industrial medical research.

Comparative psychology and ethology are two main but very different ways to approach the question of how to study animal behavior. Comparative psychologists argue that the design of a laboratory experiment must implement precise procedural control, so that all possible experimental factors will be considered at the time of interpretation. This approach emphasizes cross-species similarities and focusses on common features that may represent the fundamental core of behavioral mechanisms and/or brain functions. Ethologists on the other hand argue that instead of forcing the animal to conform the rigid boundaries set by the test design, allowing the animal to exhibit its natural spontaneous behavior provides a better ground for the study of behavioral mechanisms and functional aspects of the brain. Given that each species possesses a broad and complex behavioral repertoire that may manifest in a species-specific and test-situation-dependent manner not easily quantifiable using restricted behavioral techniques, ethologists often prefer observation-based quantification of behavior (Crusio et al., 2013). A fundamental difference in these approaches also lies in the interpretation of the data. Behavioural tests are designed with the idea to test a specific aspect of cognition, largely based on anthropomorphism that is the extrapolation to animals of human concepts. Anthropomorphism can also be used for the interpretation of spontaneous behaviour, but in that case it comes a posteriori, in a more optional manner than in a test designed to evaluate a specific cognitive function such as memory, anxiety... Because we find that the problem of

interpreting animal behaviour with human and scientific standards is not trivial, we deliberately chose to develop this PhD work from an ethologic perspective and to investigate the expression of spontaneous behavior. In this respect, we sympathize very much with the development of techniques allowing to identify and quantify all sorts of aspects of spontaneous behaviour, with the idea to explore with increasing resolution and detail the full range of behaviours that constitutes the ethogram of laboratory animals.

We therefore believe that there is a real and timely need for developing ways of quantitatively and accurately measuring behavior, in all its richness and complexity. This refers to data acquisition, with the development of new sensors and recording techniques, as well as data analysis using sophisticated algorithms, all served by an ever-increasing digital storage and computing power. In this context, the emergence of a new field called "Computational Ethology" has made possible the development of tools to automate the measurement and the analysis of animal behavior(Gomez-Marin et al., 2012). For example, pixel by pixel analysis and sophisticated computational procedures such as pattern recognition or template matching, are now available and allow not only sophisticated position tracking but also to automatically identify and score a number of behaviors such as rest, locomotion, grooming, social interactions, etc... Technological and computational advances in the automatic detection of individual actions with a fine resolution provide a new avenue to better understand the diversity, functional structure and temporal organization of behavior (Anderson & Perona, 2014)(Gomez-Marin et al., 2012). This a major opportunity for neuroscience, because refining our understanding of the behavioural repertoire will undoubtedly refine our understanding of brain function as well.

My PhD has been performed in co-tutelle between two supervisors and research laboratories with very different background: Xavier Leinekugel from Neurocentre Magendie (INSERM U1215, Bordeaux, France), and Abdelmalik Moujahid from the Computational Intelligence Group (University of the Basque Country (UPV/EHU), Donostia, Spain). X. Leinekugel is a specialist of brain rhythms, neuronal circuits and behaviour, who has recently developped a novel device for behavioural phenotyping. It consists of an open-field platform resting on very sensitive pressure-sensors, so that the slightest animal movement can be detected with unprecedented sensitivity and time resolution, in a totally non-invasive manner and during spontaneous behaviour. In addition to classical behavioural approaches such as video tracking and quantified analysis of open-field exploration, self grooming or nest building, I have explored the potential of this innovative device for behavioural phenotyping, in normal

animals as well as in several mouse models of neurodevelopmental (Fragile-X Syndrome) and neurodegenerative (Alzheimer's and Parkinson's) diseases.

With my Spanish supervisors, A. Moujahid and M. Grana, both specialists in computational sciences, I have learned matlab programming, and we have applied computational approaches to analyse the experimental data collected in Bordeaux. Exploring the relevance of computational approaches derived from physics, and already successfully applied for the study of motor function in Alzheimer patients, we have found that the signal obtained from the pressure sensors during spontaneous open-field behaviour differed in complexity (entropy and Lyapunov exponents) between wild type (WT) and *Fmr1*-KO mice. Further investigation is required to identify the specific aspects of behaviour underlying these differences in signal complexity.

Implementing analyses based on time-frequency decomposition and machine learning algorithms on my data, we also demonstrate the outstanding potential of this methodology for behavioural phenotyping in general. For example, we can resolve up to individual heart beats and breathing cycles during rest, the time course of strength and muscle/limb coordination over individual footsteps during locomotion, or internal shaking events expressed during pain or fear. Using this approach, I have observed differential expression of fear (freezing immobility vs internal body shaking) in different behavioural conditions such as fear conditioning, exploration of a novel environment, or the presence of a predator, suggesting that we may in fact be able to identify different levels or even possibly different types of fear. Moreover, investigating the behavioural phenotype of 3xTg-AD and APP-PS1 mice, two transgenic models of Alzheimer's disease, I have identified motor symptoms expressed as altered gait and intermittent high-frequency (80-100Hz) shaking events. These are rescued by the dopaminergic agonist L-DOPA, induced in WT mice by 6-OHDA lesions of the dopaminergic system, and expressed already at the age of 3 weeks. These results echo the clinical observation that motor symptoms can be found several years prior to cognitive deficits in Alzheimer patients, and the pre-clinical data indicating a significant rescue of cognitive performance with L-DOPA in Alzheimer mice. Altogether, these results point to very early deficits in the DA system in Alzheimer's disease, a perspective yet poorly explored in clinical studies.

In the coming chapters, I will introduce the background of my work with an overview of existing behavioural phenotyping methods, both in terms of acquisition systems (sensors) and analysis methods. I will provide details about how the specific evaluation of fear, pain, tremor, sleep, self grooming and locomotion is classically performed, in order to highlight my

contribution to new approaches in the evaluation of these behaviours. I will also present in detail the different mouse models of pathologies I have used in my work, emphasizing its potential relevance to (pre-)clinical research, a major societal consideration. Overall, I believe this work may contribute to further progress in computational ethology, a recent but most promising and rapidly developing field of neuroscience. At the interface between multiple disciplines such as neurobiology, ethology, physics, mathematics and computational sciences, this approach should help us better understand the behavioural readout of brain functioning, both in health and disease.

Chapter 1: BEHAVIOURAL CHARACTERIZATION

Traditional behavioural tests

Locomotion and balance

During my PhD, I have investigated several aspects of locomotion, from basic and classical measures such as total running time and distance run as index of global activity, to more original and complex parameters such as balance and strength involved in individual footstep or the dynamics of successive footsteps during locomotion.

Basic locomotor function can be assessed during spontaneous activity in an open field. Nowadays, most **open field** devices are equipped with videotracking systems, more rarely with photocell beams. The photocell beams technology employs an array of light emitter and light detection (each in opposite side of the arena). When the animal moves through a beam, the beam path is broken so the photocell analyzer records the beam break and computes the distance travelled by the animal (Crawley, 2007b). The main advantage of the photocells technology over the video tracking is that it when using several layers of photocells at different heigths, it brings information about the vertical movements of the animal (rearing). Nevertheless, the spatio-temporal resolution of photocells technology is poor compared to video tracking (Kafkafi et al., 2003), and they are not adapted to the monitoring of large arenas. Softwares available for video tracking are usually based on pixel-by-pixel analysis if successive images, and completed by more sophisticated algorithms to identify the position and orientation of the animal, recognising the head, body and tail. The level of details captured by video systems depends on the quality of the camera in terms of spatial and temporal resolution, most often around 1200x800 pixels at 30 frames/s.

The principal methods currently used for evaluating motor coordination and balance in rodents are the rotarod, the grid test, the balance beam, the Catwalk (foot-print analysis), the vertical grid and the suspended wire test (Lalone and Strazielle, 2013).

The **rotarod** is one of the most commonly used tests of motor function in mice. It consist in a rotating cylinder of approximately 3 cm in diameter where the mouse must maintain its balance and continuously walk forward to keep from falling off the rotating cylinder (Crawley, 2007b). Motor performance is measured as the amount of time before falling from the turning rod. In the **grid test**, the mouse is placed in an enclosed box with a wire mesh floor, 1 cm above a metal floorplate. When the mouse slips on the wire mesh floor and touches the metal plate below, an error is automatically counted. Thus impaired motor coordination is proportional to the number of times the mouse slips through the grid. The grid test requires concurrent assessment of locomotor activity, which is a potential confounding variable when measuring motor incoordination. Because more active mice will have a higher probability of making foot-slips independently of their coordination skills, ataxia in the grid test is taken as a ratio of foot slips over the distance traveled in the apparatus (Crabbe et al., 2003). A variant of this test is the **parallel rod floor apparatus**, in which the floor is composed of parallel steel rods (Kamens et al., 2005). Motor coordination and balance is also evaluated by the ability of rodents to traverse a graded series of **narrow beams** to reach an enclosed safety platform (Carter et al., 1999). The beams are long strips of wood horizontally placed at 50 cm high above the table (figure 1). The latency to traverse and the number of times the hind feet slip off a beam are indexes of fine motor coordination and balance. However, this test is so stressful that it has also been used to evaluate the level of anxiety in rodents by measuring the amount of exploration along the alley (Kalueff et al., 2008).

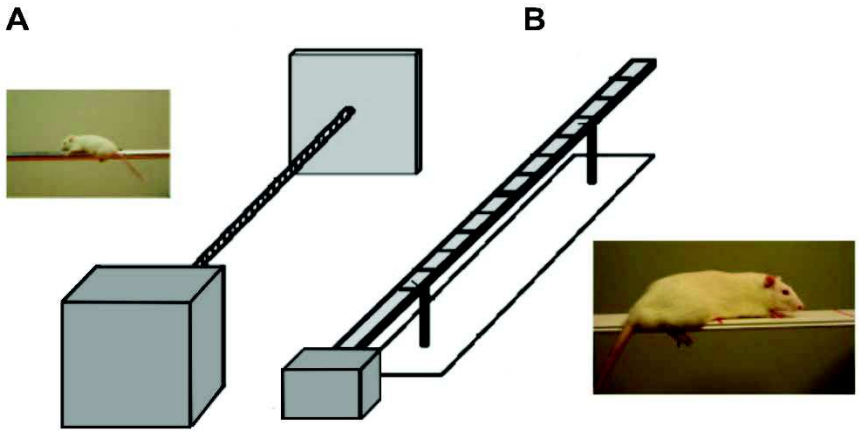

Figure1: Regular balance beams. A, shows a scheme of the mouse version and B, the rat version

A more detailed analysis of motor coordination is provided by examining gait during normal walking. The most commonly used method for assessing gait is the **'footprint' test** (figure 2). The fore and hind paws are painted with dyes of different colours and the mouse is encouraged to walk in a straight line over absorbent paper (Clarke and Still, 2001). This method provide measures of the ability of the mouse to walk in a straight line, with regular, even steps (Crawley, 2007b). The footprint patterns are then analysed for a range of measurements, such as the distance between each stride and the variability in stride length. For example ataxic mice show a gait pattern characterized by highly variable stride length and path (Barlow et al., 1996). A fully automated version of this method is the **CatWalk** System (CatWalk XT, Noldus Information Technology, Netherlands), which consists in an enclosed walkway (glass plate) illuminated by fluorescent light. The animal's gait is recorded with a high speed camera placed above the plate.

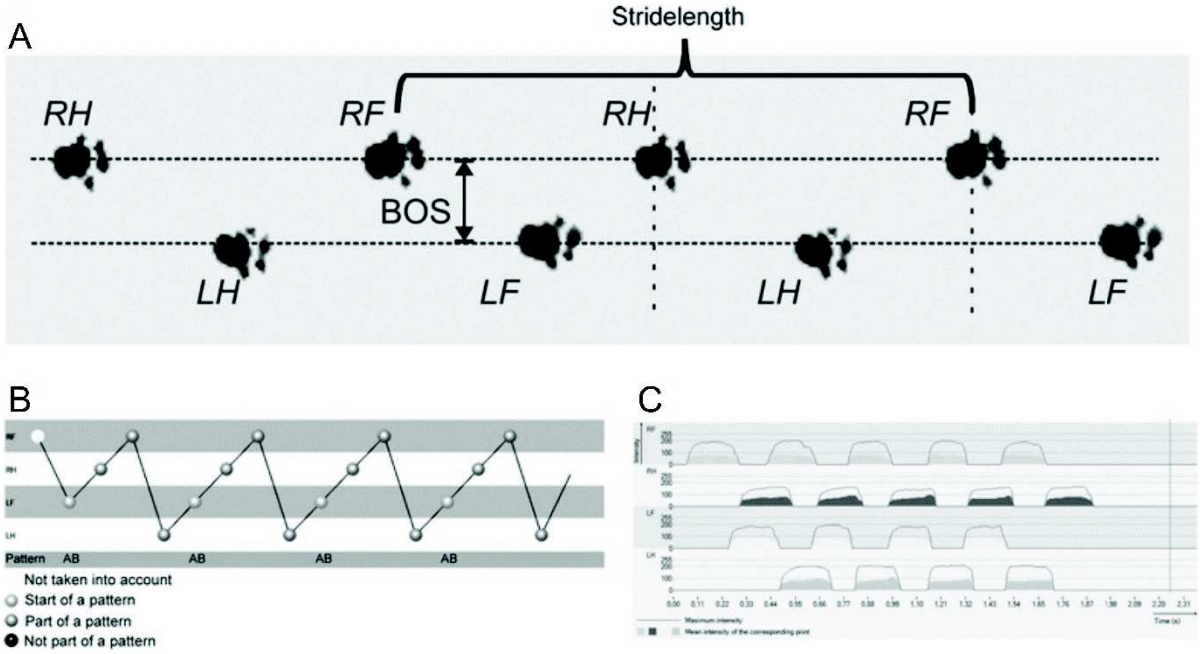

Figure 2: From Herold et al, 2016 (Herold et al., 2016). Dynamic parameters for gait analysis in BN-rats. A Section from original footprints recorded from a healthy BN-rat. The animal is running to the right. B Normal step-pattern in healthy BN-rats is quite constant and usually gives a regularity index of almost 100%. C Mean footprint intensity from all four limbs is comparable under healthy conditions. RF right forelimb, RH right hindlimb, LF left forelimb, LH left hindlimb, BOS base of support.

Motor coordination may also be assessed by **swimming and climbing tests**. In the swimming test a mouse must swim from one end of a water tank to a visible escape platform

at the other. In the **suspended wire test** the mouse is simply placed at the bottom of a suspended piece of rope with regularly placed knots, and the time to reach the end is measured (Thifault et al., 1996).

Another climbing test is the **vertical grid**, where the latency to fall from the grid or to reach the top brings information about mice motor abilities (Lalone and Strazielle, 2013). These tests of motor dysfunction are relatively simple and fast. However, since climbing and swimming involves several aspects of motor function, these tasks are very unspecific. Thus their quantification is relatively coarse, they provide little information about the nature of the underlying disorder and they are difficult to standardize.

Among these tests, the open field test is the only one relevant to study spontaneous locomotor activity without adding stressful conditions (Svensson et al., 2016) that could affect the behavioural outcome and its interpretation. The open field has however other limitations as the impossibility to precisely detect each individual movement of the animal, making impossible to study the animal gait, balance or muscles coordination. This highlights the necessity to develop new observational and non-invasive techniques to evaluate spontaneous locomotion, gait and balance in a precise manner.

Emotional behaviour: dyscomfort, anxiety, distress

Anxiety and fear are psychological, and behavioural states induced in all animals by a threat to well-being or survival. It is characterized by increased arousal, expectancy, autonomic and neuroendocrine activation, and specific defensive behavioural patterns. This is actually an adaptive response to confront an adverse or unexpected situation. Animals may learn from previous fear situations in which they have been exposed to pain or stress, and subsequently show avoidance behaviour when they reencounter that situation. However, if the adaptive function of anxiety and fear is generalized, these emotions can become a pathological state, which may later on interfere with the ability to face other challenges or stressful events in daily life. Pathological anxiety can also be a consequence of predisposing factors (or traits), which result from numerous gene-environment interactions during development (particularly during the perinatal period), and experience (life events). Conceptually, for some authors, fear and anxiety are undistinguishable, whereas others believe that they are distinct phenomena, with fear being a response to an immediate, real danger and anxiety a response to threat, i.e., a potential danger (Steimer, 2002b). However, the fact that anxiety and fear are probably distinct emotional states does not exclude some overlap in underlying brain and behavioural

mechanisms. In fact, anxiety may just be a more elaborate form of fear, which provides the individual with an increased capacity to adapt and plan for the future (Steimer, 2002b).

Behavioural responses associated with fear or anxiety have been observed in many animal species, from insect to mammals, suggesting that the neuronal structures related to fear processing are conserved across species. One challenging question in modern behavioural neuroscience is to understand how modifications of neuronal activity in determined neuronal circuits give rise to appropriate behaviour associated with simple experiences. In this thesis we have investigated different forms of anxiety and fear responses. In particular, we describe in the results section that animals shake as a contextual fear-related response. We explore here the evolution in time of this behaviour and its relationship with other well-known fear-related responses such as thigmotaxis and freezing behaviour, in different threatning contexts. We got also interested in the nest building and grooming behaviour and how its evaluation could bring information about the emotional state of *Fmr1*-KO mice (mouse models of Fragile X syndrome).

Evaluation of anxiety

The **Geller-Seifter conflict test** was the first pharmacologically validated measure of anxiety-related behaviour in rodents (Crawley, 2007a). Here, rats learn to press a lever for a food reinforcement while a mild shock is delivered on every tenth or twentieth lever press. Anxiolytic drugs increase the number of shocks accepted to obtain the food rewards. Subsequently, many classes of potential anxiolytic agent have been characterized employing this procedure. However, the major disadvantages are the necessity for long-term (months) and daily training of subjects and their repeated utilization. An analogous to the Geller-Seifter test but using water reinforcement, instead of food, is the **Vogel conflict test** (Vogel et al., 1971). This task has also been well validated for specificity to anxiolytic drugs and has been used extensively by the pharmaceutical industry to discover new anxiolytics (Millan and Brocco, 2003).

The **Open Field test** is one of the most commonly used platforms to measure anxiety-like behaviour in different animal models (Seibenhener and Wooten, 2015) and to investigate the anxiolytic effect of pharmacological compounds (Choleris et al., 2001). When placed in the centre of an unfamiliar open field, a mouse will typically run to the walled edge and then explore its way around the whole arena while remaining close to the wall (thigmotaxis). Over time, as the animal habituates to the new environment and its anxiety reduces, the mouse will

increasingly venture out towards central parts of the arena before returning to the edges. Based on this behavioural profile we can get a preliminary indication of fear-related behaviour: more time spent in the center of an open field indicates a possible anxiolytic-like (anti-anxiety) effect of a mutation or drug treatment, and less time in the center may reflect fear-related traits. However, the time spent in center may be affected by many other factors, such as altered locomotion or sensory perception (Crawley, 2007a).

The **light/dark box** was first developed by Crawley and coworkers as a simple, automated test for the anxiolytic properties of drugs in mice (Crawley and Goodwin, 1980). The test is based on the innate aversion of rodents for brightly illuminated and open areas, and on the spontaneous novelty-induced exploratory behavior. It is actually a modification of the Open Field test where the arena is divided into two unequally sized compartments by a partition with an opening that allows transitions, where one-third of the area is darkened and two-thirds are illuminated. The mice are allowed to freely explore the space, and the ratio of the time spent in the lit vs dark compartments is taken as a measure of anxiety (Kulesskaya and Voikar, 2014).

The **Elevated Plus-Maze** test uses the same conflict between the tendency of mice to explore a novel environment and the aversive properties of bright light, height, and openness. It consists of a maze in the form of a plus sign which is elevated to about 1 meter above the ground by a pole situated under its center. Two opposing arms are enclosed by walls, whereas the other two opposing arms are open, such that the mouse can see the cliff. The mouse is placed in the central intersection, from which it can walk down any of the four narrow runways. Naturally, mice prefer the closed arms but will venture out into the open arms driven by curiosity. The number of entries into each arm and the time spent in each arm is taken as an indicator of anxiety (Crawley, 2007a, Holter et al., 2015). Anxiolytic drugs specifically increase the number of entries and the time spent in the open arms (Pellow et al., 1985). Anxiogenic effects are also detectable (Mechiel Korte and De Boer, 2003).

Evaluation of fear

Fear results in the expression of a range of adaptive or defensive behaviours, which are aimed at escaping from the source of danger or motivational conflict. These behaviours depend on the context and the repertoire of each species. Active coping strategies are used when escape from threat is possible, and the autonomic changes associated with these active strategies are mediated predominantly by sympathetic activation (hypertension, tachycardia). Alternative strategies, such as immobilization or freezing, are usually elicited when threat is inescapable,

and are usually characterized by autonomic inhibition (hypotension, bradycardia), and a more pronounced increase in the neuroendocrine response (Steimer, 2002a).

Because fear is a robust behavior and can be learned, very popular laboratory tests evaluate fear-learning dependent plasticity mechanisms using **contextual and cued fear conditioning** paradigms. In these rapid and robust emotional learning paradigms, an animal learns to associate a previously neutral stimulus (the conditioned stimulus, or CS, such as a sound or a specific context) with a coincident aversive stimulus (the unconditioned stimulus, or US), such as a mild footstock. Twenty-four and/or forty-eight hours following the training session, the presentation of the CS alone elicits a broad range of conditioned behavioural responses including freezing immobility, the most widely used behavioural variable to quantify fear memory (figure 3). Freezing is measured as complete immobility, beside respiration. This measure is highly sensitive to parametric manipulations that are expected to affect the level of learning and the level of fear. For instance, freezing increases with both the number of trials and with the intensity of the shocks (Blanchard, 2008).

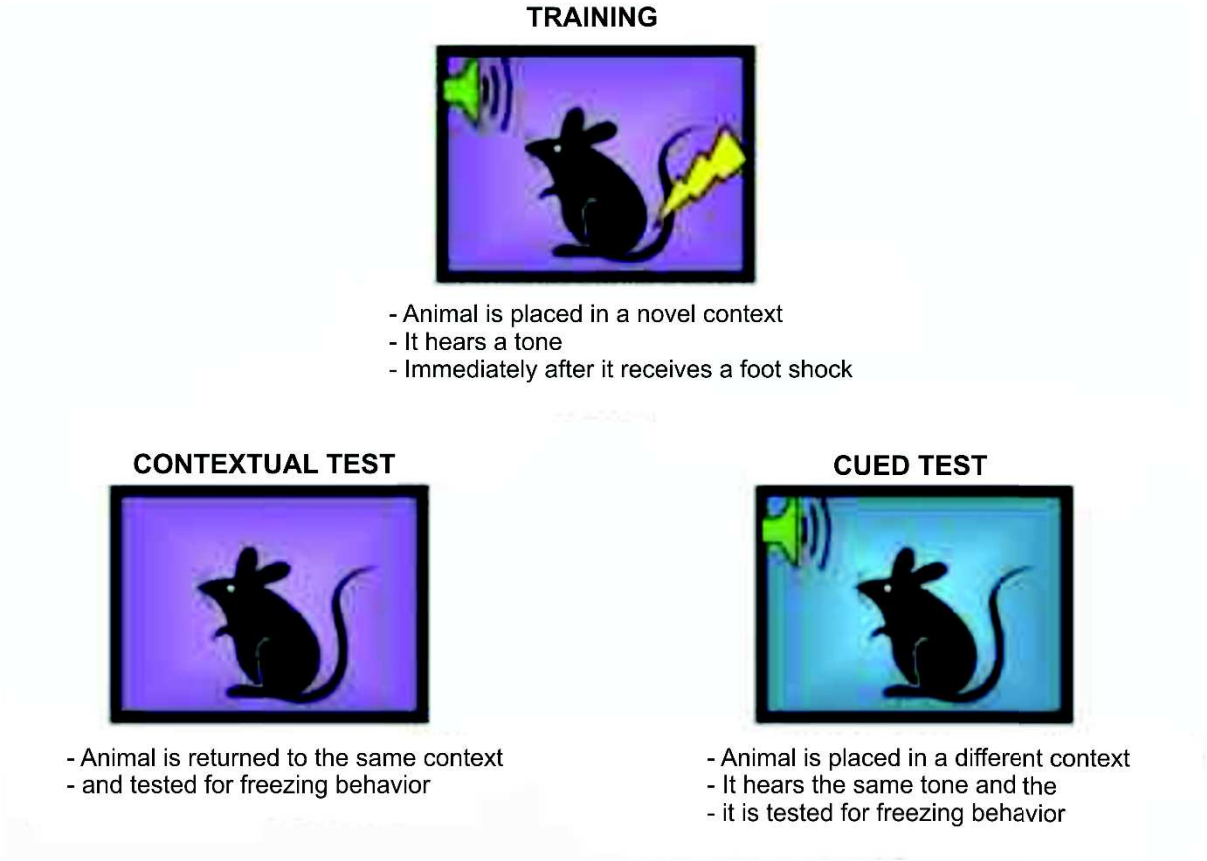

Figure 3: Fear condition paradigm where the animal learn to associate a conditioned stimulus (context, on the right or sound on the left) to an unconditioned stimulus (foot shock).

Another behavioural response that can be measured in fear conditioned animals is the startle reflex. Above a certain intensity, sensory stimulations such as sounds induce a startle reflex. **Fear-potentiated startle** refers to the increase or potentiation of the acoustic startle reflex during fear states elicited by the anticipation of an aversive stimulus (as a footshock). In a typical fear-potentiated startle experiment, the amplitude of the startle reflex elicited by a loud noise is measured either in the presence or in the absence of a CS previously paired with an aversive US (Daldrup et al., 2015). Under these conditions, the amplitude of the startle reflex is greater in the presence than in the absence of the CS. One significant advantage of potentiated startle as a measure of fear is that it can assess the level of fear at a precise moment in time. This is not possible for diffuse responses such as freezing. However, to be reliable fear-potentiated startle test requires more training than the typical context or cue fear-conditioning techniques using freezing as a measure (Blanchard et al., 2011).

Fear of a predator is an innate fear response directly related with the presence of the predator per se or predator cues (odors, sounds, and ambiguous visual stimuli). When confronted to a rat, its natural predator, both wild and laboratory mice show clear innate defensive behaviours (Blanchard, 2008). The rat exposure test is therefore taken as an animal model of anxiety and fear (Yang et al., 2004). This test is conducted in a chamber with three compartment: a safe zone (home chamber), an approaching zone (neutral compartment) and an aversive zone (exposure cage). When the confrontation is with the actual predator, the exposure cage is divided in two compartments, separated by a wire mesh screen. If the exposure is to predator odors then the exposure cage is a single compartment impregnated by the predator odors. The home chamber is connected to the exposure cage by a clear Plexiglas tunnel. The behavioural parameters analysed usually comprise spatiotemporal and ethological measures. The spatiotemporal measures are time spent in the home chamber, tunnel, and on the surface. The ethological measures are frequency and duration of stretch attend posture (SAP, a posture in which the body is stretched forward and the animal is motionless), stretch approach (a movement toward the stimulus with the animal's body in a stretched position), and freezing (complete cessation of movement except breathing) (Yang et al., 2004, de Oliveira Crisanto et al., 2015).

Both the foot-shock and predator exposure are contextual fear conditioning models that involve an acclimation period, followed by delivery of the US, and subsequent testing for contextual fear behaviour. However, important procedural differences are apparent in these two models that extend beyond obvious differences in US modality. First, the traditional foot-shock conditioning model using rodents generally involves delivery of brief foot-shocks, e.g.,

1 s duration, and freezing is measured after each post-shock interval. Here, the time spent freezing is measured as a conditioned response and the unconditioned responses to shock (such as jumping, vocalization, or flinching) are often not measured. In the typical predator odor conditioning model, the US delivered over a period of minutes also generates robust unconditioned responses, such as freezing and avoidance, which are the primary fear conditioning measures. Second, training or repeated foot-shocks delivered at spaced intervals provide an acquisition index of contextual fear learning, i.e., contextual freezing, whereas the current predator odor conditioning model, which provides an assessment of unconditioned fear, does not provide a critical evaluation of the animal's magnitude of learning to associate the context with the US due to the absence of measuring a conditioned response. Thus, when an animal exhibits unconditioned fear to predator odor, but subsequently exhibits deficits in contextual fear, the impairment in contextual fear behaviour may result from incomplete learning at the time of training (Takahashi et al., 2008). Then, although the predator exposure test does not represent the best option to evaluate learning and memory in rodents, this test allows to measure innate fear response. On the other hand, fear conditioning paradigm is mostly used as a memory test and not necessary to study the state of fear or anxiety.

Well-being

Factors that determine well-being in rodents remain poorly understood. Nest building and burrowing are complex and spontaneous goal-directed behaviours that have been proposed as an index of well-being in rodents (Jirkof, 2014). Wild mice nests are an essential thermoregulatory adaptation that provides shelter from elements, predators, and competitors and allows successful survival of offspring (Deacon, 2006, Jirkof, 2014). Nest shape, density and composition may vary depending on the environmental condition. Thus, wild mice are expert and flexible nest builders, and this behavior is central to their survival, particularly in terms of dealing with environmental challenges (Hess et al., 2008). In laboratory animals, a good performance in nest building is considered a reliable index of well-being. High anxiety levels have been also related with impaired nest building and burrowing behavior (Keisala et al., 2007, Line et al., 2011). The nest material provided to the laboratory animal is usually about 3 g, 2.5 cm/side, and 5 mm thick compressed cotton. After a short exploratory delay, normal mice show interest in the Nestlet and start crafting it into a functional nest, a process that can take several hours (goal-directed behavior). The resulting nest quality is usually scored according to the following standard criteria stablish by Deacon in 2006: 1 – Nestlet not

noticeably shredded. 2 – Nestlet 50% shredded, not used as a nest. 3 – Nestlet shredded up to 90%, but the shredded material remains scattered in the cage and is not where nest quality is often quantified with complexity scores used as nest. 4 – Nestlet shredded >90%, and shredded material used as a flat nest. 5 – 100% Nestlet shredded and used as a rounded nest with sides covering the mouse. Of note, with this discrete scale, the 3-level represents an important qualitative break point between the stages of shredding and actual nest building. Both, scores of 4 and 5 represent functional nests (Heller et al., 2014, Pedersen et al., 2014). Other authors choose to weight the amount of used vs unused nest material after the testing periods (Angoa-Perez et al., 2013). Parameters such as latency to use the nest material, time to build a "proper nest" and duration of the nest building have been also used to quantify nest building behaviour (Jirkof, 2014).

The **burrowing test** was first described by Deacon and collabrators (Deacon et al., 2001). This simple test is based on the species-typical behavior of mice to spontaneously displace items (normally with a type of push digging) from tubes within their home cage. The tube probably represents semi-natural circumstances imitating the natural environment of burrow digging animals. Burrowing very likely represents tunnel construction and maintenance, like burrow cleaning behaviour (Jirkof, 2014).

During my PhD, I have used nest building as an evaluation of well-being in *Fmr1* KO mice, model of the Fragile X syndrome.

Stereotypic behaviour

In children, rituals, repetitive, and compulsive-like activity is part of the normal behavioural repertoire, thought to ward off anxiety (Evans et al., 1997) and to represent a mechanism for organizing, accommodating to and eventually mastering the environment (Langen et al., 2011a), or in a way to calibrate the system (Boyer and Lienard, 2006). However repetitive behaviour can become excessive, injurious and time persistent. Thus aberrant repetitive behaviours are common signs in many neurodevelopmental disorders (Wolff et al., 2013). In particular, they are core symptoms of autism spectrum disorders (ASD) and form an essential part of the classification criteria for ASD as described in the DSM-IV. Repetitive movements in ASD patients include body rocking, finger tapping or even sometimes self-injurious stereotypies such as biting of the hands (Staal, 2015). Abnormal repetitive behaviour also occurs in animals and can take numerous forms, from jumping and somersaulting to crib- and bar-biting, rocking and self-injurious behaviour (Langen et al.,

2011b). Adverse environmental circumstances can cause an animal to develop abnormal repetitive behaviour. Confinement and environmental restriction are well-established risk factors; indeed, repetitive behaviour is the most common category of abnormal behaviour observed in confined animals (Lewis et al., 2007). In this terms stereotypies in animals are also hypothesized to function as a coping mechanism to reduce the arousal level of the animal when it is exposed to stressful events or environments.

Initially, repetitive behaviour research was directed by fundamental animal studies and was mostly limited to **motor stereotypies**. Later, research advanced to developing translational animal models for human disorders, extending its scope to cognitive and emotional domains. In particular, excessive **self-grooming** behaviour is widely assumed to be a good indicator of stereotypic and compulsive behaviour. In rodent , self-grooming is observed in stressful situations such as novelty-based anxiety tests (e.g. elevated plus-maze, open field, and hole-board tests)(Canavello et al., 2013). Self-grooming is a complex, ethologically-rich ritual which normally proceeds in a cephalocaudal direction and consists in several stages: licking the paws, washing movements over the head, body fur licking (progressively shifting to a more posterior body focus), and tail /genital cleaning). Dissectible at a number of levels, ranging from individual organ kinematics to sequencing and habituation in grooming patterns and their association with non-grooming behaviours, such complex patterned structure is particularly attractive for behavioural phenotyping (Canavello et al., 2013). This behaviour may be assessed in different environmental conditions, such as home cage, open field or in a social test (Sun et al., 2010, Walsh et al., 2012, Arentsen et al., 2015).

Another test commonly used to investigate stereotypies is **marble burying**, which consists in a repetitive digging behaviour. In this case, stereotypy is scored by counting the remaining unburied marbles (Silverman et al., 2010, Angoa-Perez et al., 2013). **Nestlet shredding** has also been suggested to be sensitive to the expression of compulsive-like behaviours (Angoa-Perez et al., 2013). Although it is controversial (Crawley, 2007b), repetitive patterns in locomotion such as circling (Kovalenko, 2015) or rearing (Moy et al., 2014) have been also suggested to be an expression of stereotypy in mice. In all these cases, behavioural evaluation has several limitations. First, the manual detection is a very time demanding task and a subjective measure. Depending on the quality and the position of the camera, static behaviours such as grooming, sniffing, eating or chewing are sometimes very difficult to discriminate. Although with less performance than trained human operators, some behaviours like grooming can be automatically identified by commercially available algorithms, reducing the time cost of the behavioural evaluation, although ignoring the specific body part involved

at each time. Second, the temporal resolution is typically low, allowing only the counting of events and the total time spent grooming, but making impossible to quantify the strength of the movements and to examine the quality of each body-part grooming.

Pain

The capacity to experience pain has a protective role: it warns us of imminent or actual tissue damage and elicits coordinated reflex and behavioural responses to keep such damage to a minimum. Depending on the pain experience, humans and animals gain knowledge about potential dangerous stimuli in the environment, and pain-related unpleasantness help to form long-term avoidance memory in order to protect themselves (Zhuo, 2007). By contrast, persistent pain syndromes offer no biological advantage and cause suffering and distress, turning into a maladaptive process (Woolf and Mannion, 1999). Pathological pain is not protective but maladaptive, resulting from abnormal functioning of the nervous system. It may occur after a damage of the nervous system (neuropathic pain) but also in conditions in which there is no such damage or inflammation (dysfunctional pain). Conditions that evoke dysfunctional pain include fibromyalgia and tension-type headache.

Pain is known to be a complex perceptual experience that is in addition to conveying sensory information such as location, type, and intensity stimulus, also has profound affective (emotional) and cognitive features. Whether or not a particular stimulus will be perceived as painful depends not only on the nature of the stimulus, but also on the context within which it is experienced, memories, emotions, etc. It can be modulated by the environment, in the broadest meaning of the term (affective, sociocultural, geographic, and other factors), and by the individual's psychological status (Calvino and Grilo, 2006). In this work we were interested in measuring spontaneous pain in rodent in a non-invasive way. Before discussing animal models and test currently used to measure spontaneous pain, I would like to briefly introduce the categories of pain that have been classified.

Nociceptive pain is an early warning physiological protective system, essential to detect and minimize contact with damaging or noxious stimuli. Because this pain is concerned with the sensing of noxious stimuli, a high-threshold pain is only activated in the presence of intense stimuli (Basbaum et al., 2009). This everyday acute pain occurs when a strong, noxious stimulus impact the skin or deep tissue. Noxious stimuli are either natural events, such as mechanical (pinch), thermal (hot or cold), and chemical (bee sting) or artificial ones (electric

shock). Acute pain results from the activation of nociceptors which fire impulses in response to these stimuli. The impulses travel along the peripheral nerve, past the sensory cell bodies in the dorsal root ganglion, along the dorsal roots and into the spinal cord or the brain stem. There they activate populations of second and third-order neurons in the central nervous system, this activity is interpreted as pain by a conscious brain.

Inflammatory pain is a spontaneous pain felt when the skin or other tissue is inflamated, hot red, and swollen. This kind of pain is also adaptative and protective. By heightening sensory sensitivity after unavoidable tissue damage, this pain assist in the healing of the injured body art by creating a situation that discourages physical contact and movement.

Neuropathic pain is defined as "pain arising as a direct consequence of a lesion or disease affecting the somatosensory system" (Finnerup et al., 2016). Neuropathic pain conditions express themselves with spontaneous and /or abnormal stimulus-evoked pain. People with chronic pain suffer from spontaneous, ongoing pain. Besides, often in this pathological state stimuli that normally are innocuous, become painful. This phenomenon is called allodynia. Hyperalgesia is a term used to define an increase in pain sensitivity evoked by a normally painful stimulus. It is an exacerbated response to a stimulus that is expected to be only mildly painful.

Most commonly used tests to study pain in laboratory animal measure states of hyperalgesia, an exaggerated response to a noxious stimulus, and/or allodynia, a nocifensive response to a normally innocuous stimulus. Many nociceptive assays are described in the literature, in which states of pain are induced by applying a painful stimulus and the behavioural outcome is scored. Regarding the intensity of these stimuli is important to have in mind that some assays (e.g., **hot-plate**, **paw-withdrawal**, **tail-flick**, **von Frey filaments**, **paw-pressure**, and **flinch/jump** tests) involve the determination of nociceptive thresholds; in these, altering the stimulus intensity will alter the latency to reach that threshold. By contrast, other assays (e.g. abdominal constriction test, formalin test) are suprathreshold; in these, altering the stimulus intensity will alter the frequency/duration or intensity of the response (Wilson and Mogil, 2001). However, pain is not a unitary phenomenon, and thus a wide variety of assays have been developed to model different types of pain. Although acute thermal and mechanical assays exhibit more than adequate empirical validity (i.e. predictive power) for many analgesics, acute pain is virtually non-existent as a clinical entity. Thus, a number of animal models of "chronic" pain have been developed, generally involving an injury of inflammatory or neuropathic (i.e. secondary to nerve damage) nature. Therefore, in most of the chronic pain

models, the dependent measure is a hypersensitivity state, generally overlooking spontaneous pain. There are at least two limitations to this approach. First, although assays of pain-stimulated behaviour are thought to be predictive of many acute pain states, they may not be adequate models of clinical chronic pain (e.g., sustained inflammatory and/or neuropathic pain states). In support of this, assessment of chronic pain in clinical medicine (both human and veterinary) relies heavily on measurement of pain-depressed behaviour (Martin et al., 2004). Another limitation of using pain-stimulated behaviour is that candidate analgesic drugs may decrease pain-stimulated behaviour by producing motor effects that impair the subject's ability to respond, thus producing a false positive analgesic result (Stevenson et al., 2006). Thus, although very few, some tests have been developed in order to test spontaneous pain. For instance, after inflammatory injections with complete Freund's adjuvant (CFA) or arthritic lesions in the hind paw, **hind limb weight bearing** is a behaviour often interpreted as spontaneous pain (Tappe-Theodor and Kuner, 2014). The evaluation of this behaviour relies on an incapacitance tester that determine hind paw weight distribution. The incapacitance system basically consist in an angled Plexiglas chamber so that each hind paw rests on a separate force plate. The change in hind paw weight distribution (the difference in the amount of weight (g) between the left and right limbs) is automatically calculated by the Incapacitance tester placed below (figure 4). Essentially, the apparatus calculates an average weight distribution over the span of 5 sec. The primary dependent measure is % weight on ipsilateral hind paw. This technique has been proven to be good assay to evaluate spontaneous pain (Stevenson et al., 2011). However it requires the animal to be restrained by the tail to assure the proper location of animal pads during the test, which could affect other parameters (such as stress or anxiety) leading so to either stress-induced analgesia (Terman et al., 1984) or stress-induced hyperalgesia (Imbe et al., 2006).

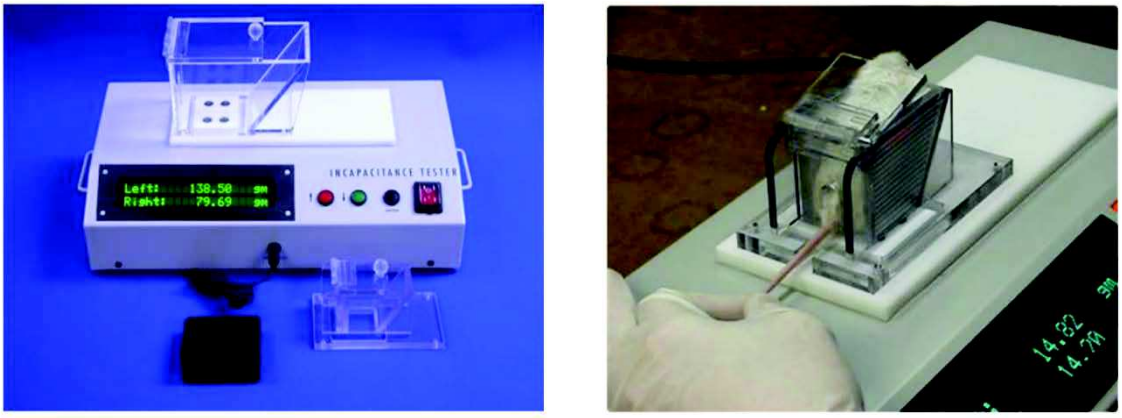

Figure 4: Incapacitance tester from Columbus Instruments.

Gait analysis imaging systems have been used to analyse significant gait changes in pain due to arthritis in rats (Masocha and Pavarthy, 2009, Ängeby Möller et al., 2012). By measuring the paw print area and interlimb coordination over a catwalk instrument, these studies can evaluate the weight bearing on each paw during locomotion. Mogil and collaborators showed significant gait changes in the spared nerve injury model of neuropathic pain using the 'CatWalk' system (Mogil et al., 2010). These changes were detected and peaked just 1 day post-surgery and lasted less than the observed mechanical allodynia, leading to the interpretation that the mechanisms of spontaneous and evoked pain are distinct.

Another test commonly used to evaluate spontaneous pain is the **conditioned place preference** (CPP) test. This test combines pain evaluation with the reward system as a measure of ongoing pain. It utilizes a three-chamber system with a small middle neutral chamber and two outer chambers that are distinguishable by different visual, floor and odor cues. After preconditioning of the animals with free access to all chambers, spinal administration of an analgesic is paired with a chamber. When animals are permitted free access to all chambers post-conditioning, a preference for the analgesic drug-paired chamber is observed, which is indicative of the animal having ongoing pain. This test has been shown to be applicable to several models of chronic pain (Tappe-Theodor and Kuner, 2014).

Recent studies have also demonstrated the potential and promising use of complex behavioural indicators, such as **voluntary wheel running**, **ultrasound vocalization**, **nest building** or **burrowing** in the assessment of spontaneous pain, distress and suffering in the laboratory mouse in veterinary research (Jirkof et al., 2010, Gaskill et al., 2013). However these methods do not offer the temporal precision that the acute induced pain test does. Also, the complexity of this type of behaviours, makes very difficult a specific etiological description.

Evaluation of **facial expression** has been recently demonstrated to be a useful method to assess pain in rodents. The coding system designed by (Langford et al., 2010) show high accuracy and reliability. This is actually a mouse grimace scale (MGS) based on the description of five facial features in rodent in analogy with the human facial pain expressions (figure 5). These facial features in rodent are:

- orbital tightening: is narrowing of the orbital area, with a tightly closed eyelid or an eye squeeze (denoted by wrinkle around eye);
- nose bulge: is a rounded extension of skin visible on the bridge of the nose;
- cheek bulge refers to convex appearance of the cheek muscle (between eye and whiskers) from its baseline position.

- ear position: refers to ears pulled apart and back from their baseline position or featuring vertical ridges that form owing to tips of ears being drawn back

-whisker change: is movement of whiskers from their baseline position either backward, against the face or forward, as if standing on end; whiskers may also clump together.

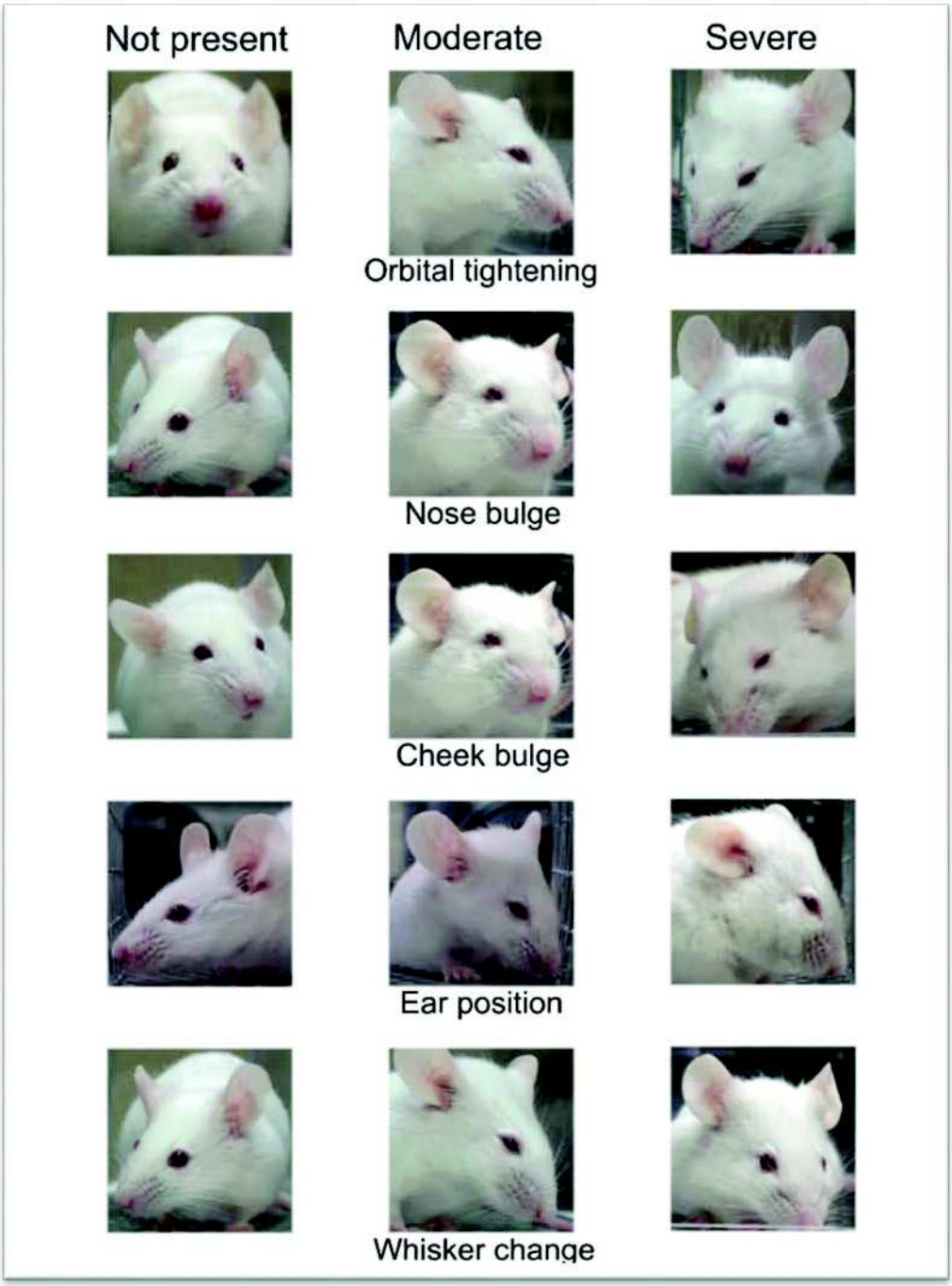

Figure 5: Images of the three values (not present, moderate and severe) of mice exhibiting behavior corresponding to each one of the five facial features characterized in this scale. Figure modified form (Langford et al., 2010).

As it can be notice, three of these features are identical to those observed in humans: orbital tightening, nose bulge and cheek bulge. This is in accordance with Darwin conviction that facial expressions are evolutionarily conserved (Langford et al., 2010).

Although in recent years there has been an important development of spontaneous pain research, there is still an important lack of tools to evaluate this behaviour. Indeed, there is increasing evidence about the necessity to better-characterized behavioural tests in unrestrained animals to be able to fully analyse diverse components of pain, wellbeing and pain-related disorders, such as fear, depression and negativity. While most studies continue to measure stimulus-evoked pain-related behaviours, there is an urgent need to develop and optimize free-choice and operant-based behavioural readouts.

Sleep and Breathing

Sleep is an important behavioural and physiological adaptation very well conserved over vertebrates. In mammals Sleep is composed of periods of rapid eye movement (REM) sleep defined by the presence of fast activity in the brain (8 Hz, theta waves) and periods of non–rapid eye movement (NREM) sleep characterized by the abundance of slow waves accompanied by the apparition of fast ripples in the hippocampus, (150-200Hz) (Buzsaki et al., 1983). A major focus of current research in mice is to elucidate gene products that (1) regulate sleep and wake, (2) are regulated by sleep and wake, or (3) are affected by sleep deprivation. This evaluation is mostly performed by assessing changes in the electroencephalogram (**EEG**) and electromyogram (**EMG**) (Tagaito et al., 2001). These are invasive techniques that requires the chronic implantation of electrodes and a recovery time from the surgery. Because of the obvious technical and behavioural limitations, EEG experiments cannot be successfully developed in new-born freely moving animals. EMG instrumentation in neonates also requires some restraint during measurement, which has been proven to induce stress and behavioural changes including ventilation (Balbir et al., 2008). Other studies (Pack et al., 2007, McShane et al., 2012) have investigated non-invasive alternatives for sleep-wake characterization from digital video analysis. Relying on simultaneous EEG recording and based on the mouse movements and measuring pixel-by-pixel changes in the area and shape of the body, these studies claimed to be able to distinguish REM from non-rapid eye movement NREM sleep in mice. However the performance is so poor that finally this approach could up to now only discriminate sleep from wakefulness but not REM from NREM.

Primary sleep-disordered breathing include apneas and hypopneas, that are reductions in overall ventilation during sleep (hypoventilation) resulting in arousals, arrhythmia, hypercapnia, acidosis, and/or hypoxic stress responses such as pulmonary hypertension or polycythemia. The availability of genetically-modified mouse models has the potential to accelerate our understanding of the underlying pathophysiology of such disorders. Mice which lack leptin (Yao et al., 2016), orexin (Nakamura et al., 2007) or the endocannabinoid receptor-1 (Silvani et al., 2014), are particularly susceptible to subtle disturbances in the regulation of breathing during sleep. But beside breathing pathologies, it is interesting to note that brain states during sleep are associated with distinct breathing patterns, so that a non invasive characterisation of breathing during sleep may allow to infer the perids af REM vs NREM sleep. As illustrated in figure 6, while awake and NREM sleep states show a regular respiratory pattern, REM sleep is characterized by an irregular breathing pattern (Hernandez et al., 2012, Bastianini et al., 2017). Although it has been also shown that genetic background affects features of ventilatory behaviour during NREM and REM sleep (Friedman et al., 2004), ventilatory systems have been developed in order to identify those different brain states and other respiratory anomalies during sleep. The whole body plethysmography (WBP) chamber is the most common non-invasive method for assessing ventilation as it enables monitoring of the magnitude, frequency, and patterns of breathing concurrent with observations of the animal's behaviour, as well as analysis of changes during exposure to varying gas concentrations and other stimuli. This approach provides an indirect measure of tidal volume, which is directly proportional to the cyclic chamber pressure signal produced during respiration in a sealed chamber (closed systems) or open chamber (open systems). Although closed systems provide an accurate monitoring of the ventilatory changes and they have been successfully used to assess rodent respiration during sleep and wake in unrestrained mice, they present several key limitations regarding the continuous monitoring of breathing during sleep and wakefulness. First, closed chambers can not be used to record long periods, since the lack of airflow makes rise the CO2 concentrations. To prevent CO2 from accumulating in a sealed chamber, airflow (bias flow) must be periodically applied to the chamber via inlet and outlet ports (traditional open system). Thus in traditional open-flow systems errors can arise due to inappropriate flow rates and inaccurate measurement of flow. Besides, the detection of the small pressure deflections caused by animals breathing are easily corrupted. This fact implies the necessity to reduce the air volume and so, the chamber area, making this and inappropriate approach for long lasting recording (Stephenson and Gucciardi, 2002) since it can induce stress. Thus traditional WBP methods (close an open chamber) provide intermittent high-fidelity tidal

volume measurement, but techniques for recording a continuous and accurate tidal volume signal have not been validated yet (Hernandez et al., 2012). Some improvement has been developed by Hernandez and collaborators.

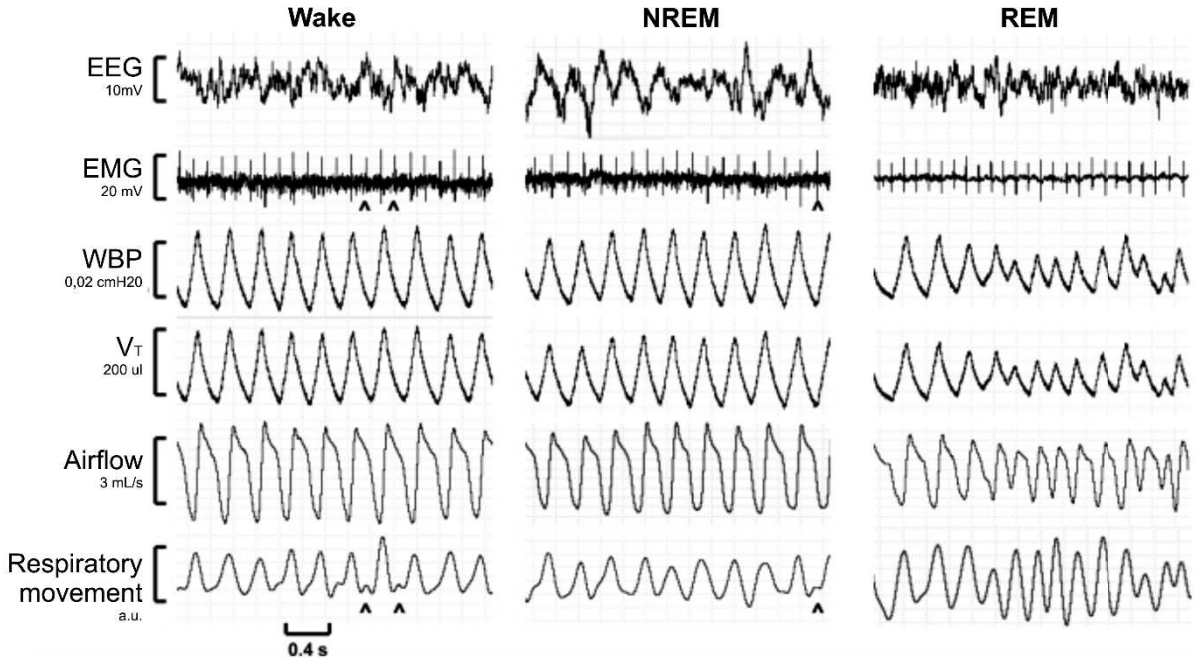

Figure 6: Recording sections of a WBP full polysomnographic study demonstrating respiratory waveforms during quiet wakefulness (left), non-rapid eye movement (NREM) sleep (middle), and rapid eye movement (REM) sleep (right) in one mouse. Signals (from top to bottom) include electroencephalographic (EEG) signal, nuchal electromyographic (EMG) signal, WBP chamber pressure, WBP Vt (tidal volume), WBP airflow, and respiratory movement (surrogate for respiratory effort). Intermittent cardiac artefact (carets) can be seen in the EMG and respiratory movement channels. Figure from (Hernandez et al., 2012)

By placing high-resistance elements and mass flow controller interposed at the chamber's inflow and outflow ports, this adapted open system achieve continuous and unattenuated signal recordings in an open system. Minor pressure fluctuations are also minimized by a slow leak to allow the chamber pressure to equilibrate with atmospheric pressure avoiding the need for implementing a separate computer-feedback system to control chamber pressure. Air bladders are placed above (sensor bladder) and below (reference bladder) the WBP platform (figure 7), so that they were completely isolated from each other. When the mouse lay on the platform, the mechanical displacement of its torso during breathing is transduced by the upper sensor bladder. To cancel out ambient barometric pressure changes

and noise, the WBP animal chamber was referenced to a reference chamber with a similar time constant using a differential pressure transducer.

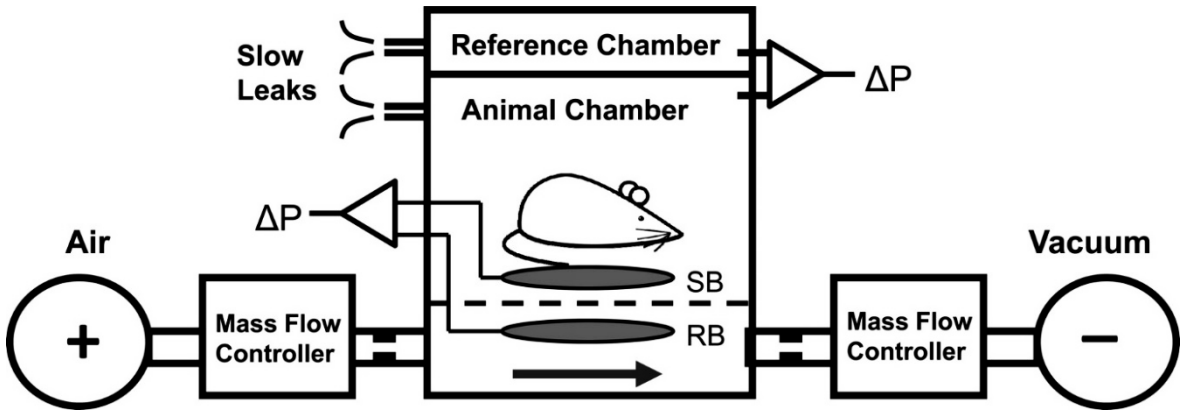

Figure 7: Whole body plethysmography (WBP) open-system schematic. Positive and negative pressure sources are introduced in series by mass flow controllers to generate a continuous bias flow through the animal chamber. The reference chamber served to filter ambient noise from the pressure signal. Slow leaks present on both chambers allowed for equilibration with atmospheric pressure. The sensor bladder (SB) transduced the mechanical pressure changes associated with mouse breathing, while the reference bladder (RB) signal allowed for cancellation of the contaminating chamber pressure signal via the differential pressure transducer. +, Pressurized air source; −, vacuum source; arrow, bias flow; dashed line, platform; ΔP, differential pressure transducer. Figure form (Hernandez et al., 2012)

Therefore, although this technique allows to measure breathing rhythms in mice and rats, it still requires the animal to be restrained in a small chamber, being a source of stress. During my PhD, I have used a device allowing to monitor basic parameters of the breathing pattern that allow to discriminate REM from NREM sleep in an open field in a totally non-invasive manner.

Tremor

Tremor, defined as a rhythmic and unvoluntary movement of any body part, is a highly prevalent movement disorder (Elias and Shah, 2014). This is a prominent behavioral outcome of central nervous system dysfunction caused by disease (e.g. Parkinson's disease) or by toxins (e.g. heavy metal intoxication). Different types of tremor can be distinguished. In human, essential tremor is in a range of 7-12 Hz and Parkinson tremor is at 4-6 Hz. The relative lack

of published reports on parkinsonian tremor in rats may reflect merely the absence of an obvious whole-body tremor (Salamone et al., 1998). However mandibular tremor or tremulous jaw movement (TJM) described as “mouth movements” or “spontaneous chewing” have been described as a resembling Parkinsonism behaviour. TJMs are generated when the ventrolateral region of the striatum suffers an electrolytic lesion. These movements are generated after a dopamine depletion, when the ventrolateral region of the striatum suffers an electrolytic lesion (animal model of Parkinson). In rats, this tremor presents a frequency range of 3 to 9Hz (Herrera-Meza et al., 2014). Harmaline-induced tremor is a well-known model of essential tremor Harmaline (7-methoxy-3.4-dihydro-β-carboline) is a compound especially rich in the seeds of Peganum harmala (Syrian Rue) and in the Banisteriopsis caapi vine(Handforth, 2012). In rats, harmaline-induced tremor is present a frequency range of 9–15 Hz band (Ossowska et al., 2015), while in mice it this tremor tends to be a slightly faster (12–18 Hz).

Despite its importance in neuroscience research, tremor measurement in rodents has often rested on the use of **rating scales by human observers** (Dickinson et al., 1983). Disadvantages of such observation methods include: (I) the insensitivity to relatively small changes in tremor activity, (2) the possible bias of the observer, and (3) the sometimes relatively large group of animals that is needed to obtain reproducible results (Meert et al., 1997). Other studies have investigated rodent induced tremor by EMG implantation (Herrera-Meza et al., 2014), which has the main drawback to be invasive and potentialy affect behaviour (Anagnostaras et al., 2010).

Nevertheless, sophisticated direct-measurement, instrumental methods have been developed for the specific purpose of quantifying whole-body tremor. One example of this is Young and collaborators, who developed a combined system for measuring animal motion activities, able to detect from locomotion to tremor. Inspired by the photocell method (described above) Young and colleagues designed a modularized **infra-red (IR) light matrix system** (Young et al., 1993) combined with an **ultrasonic subsystem**. The IR light matrix subsystem could record the sequences of an animal’s motion activities with a resolution of 0.2 s in time and 1.6 cm in space. Ultrasonic phase shift subsystem adapted to the IR light matrix is used to transmit ultrasound toward the animal in the cage, while an ultrasonic receiver is used to receive the ultrasound reflected from it. This system can simultaneously acquire both gross and minute animal motion data from the IR light matrix and ultrasonic phase shift subsystems. Given the high temporal and spatial resolution, this system is able to measure the presence of induced tremor in a non-invasive manner.

Another instrument extensively used to assess tremor in rodents is the **force-plate actometer**. This system can quantify whole-body tremor, rotational behaviour and locomotor activity from a single session of data recorded from either rats or mice. The term "force-plate" is used for measurement systems that employ three or more transducers to define a plane in which displacement of the centre of force or centre of pressure can be recorded. The force-plate actometer is an ensemble of mechanical, electronic, and computing elements that embody mathematical and physical principles so as to produce measurement of whole-organism behavioural attributes. This system is able to track the animals' movements across a plate. Four force transducers below the corners of the plate record the animal's position on a Cartesian plane and measure the force exerted on the plate at each time point (Fowler et al., 2001). The force-plate actometer, can be used to quantitate whole-body tremor, such as harmaline-induced tremor (Ossowska et al., 2015), where tremor is usually analysed by using Fast Fourier Transform (FFT) on each frame of the experiment.

Computational ethology

Introduction to computational ethology

While the examination of behaving animals under controlled conditions can be used to evaluate specific aspects of mood or cognition such as anxiety or memory, analysing spontaneous behaviour in unsupervised conditions can also be very informative about a whole variety of psychological, motor and cognitive components. Nevertheless, behavioural characterization is a very complex matter and the more precise and sensitive the tool, the more potential categories to classify behaviour, so that it may finally become a very tedious and difficult task. Accordingly, it has been reported recently that trained human operators requested to classify each second of a recording session had major problems attributing up to 44% of individual seconds to any specific behaviour (Brodkin et al., 2014). This fact highlights the necessity to develop sensitive tools able to accurately identify animal behaviour with a fine temporal precision.

Innate behaviours are sculpted by evolution into stereotyped forms that enable animals to accomplish particular goals (such as exploring or avoiding a predator). Ultimately understanding how neural circuits create these patterned behaviours requires a clear framework for characterizing how behaviour is organized and evolves over time. One conceptual approach

to addressing this challenge arises from ethology, which proposes that the brain builds coherent behaviours by expressing stereotyped modules of simpler action in specific sequences. The possibility to correlate neuronal activity with quantitative analysis of behaviour has been essential for the development of neuroethology. Neuroscience is in the midst of a revolution fueled by spectacular new technologies for mapping, monitoring, and manipulating neural activity based on genetic targeting of specific neuron subtypes. These methods offer the ability to move beyond correlation to establishing causal relationships between neural circuit activity and behaviour. New tools, such as optogenetics and pharmacogenetics, connectomics and optical imaging of neuronal activity are transforming our ability to understand how neural circuits control sensory perception, cognitive processes, internal brain states, and behaviour. Exploiting this transformative technology is, however, critically dependent on the ability to assess quantitatively, and with a high degree of spatiotemporal precision, the behavioural consequences of neural circuit manipulations. However, the technology for measuring behaviour has not kept pace with the rapid development of these new methods; manual scoring of behaviour is (with notable exceptions described below) still the dominant approach in the field. This has hampered progress in both understanding the neural circuit control of ethologically relevant behaviours and in using behaviour as a readout for manipulations aimed at uncovering fundamental principles of neural circuit function. Reliance on human observation to score behaviour imposes a number of limitations on data acquisition and analysis. These limitations has raised an emerging field called “computational ethology”, which involves collaborations between physics and biology. This term emphasizes both its roots in the study of natural behaviour in freely moving animals and the application of modern quantitative tools for measuring, describing, and analysing behaviour. This emerging field exploits recent advances in machine learning to automatically identify and quantify instances of known, observer-defined behaviours, as well as to discover potentially new behaviours. With the new technology available for neural circuit analysis, this field should improve the ability to move beyond correlations to establish causal relationships between molecular and cellular mechanisms, circuit-level computations, and behaviour.

Sensors to measure behaviour

Today, **video cameras** offer high spatial and temporal resolution and can, in principle, access many aspects of behaviour without constraining the animal’s movements. The recent advances in machine vision make the video camera the sensor most commonly used for behavioural characterization (Schwarting et al., 1993, Drai and Golani, 2001, Spink et al., 2001,

Jhuang et al., 2010). Machine vision is the discipline concerned with enabling machines to "see," similarly to biological organisms that use their eyes to measure properties of their environment. Images collected by the camera(s) are transferred to the computer, where appropriate calculations are performed to extract the relevant information, e.g., the position, shape, and identity of objects in the scene. Based on pixel by pixel analysis and sophisticated computational procedures such as pattern recognition or template matching, a number of behaviours such as rest, locomotion or grooming can be automatically identified by commercially available algorithms, although with less performance than trained human operators (Brodkin et al., 2014). A challenge in machine vision is computing invariant descriptors from images, i.e., descriptors of image content (e.g., the colour of a surface, the shape of an object's boundary) that are invariant with respect to irrelevant variations in the environment, such as the distribution and intensity of light (Anderson & Perona, 2014). Indeed, many limitations of machine learning and machine vision are the sensitivity of the sensors providing the signal to analyse. In particular, a limitation of video signal is that sometimes it is difficult to discriminate between behaviors involving "stationary" movement such as grooming, sniffing, eating or drinking, making impossible a fine temporal characterization of animal behaviour. Arrangements including multiple cameras and depth sensors may facilitate the measurement of position and motion in 3D. For example, Ou-Yang and collaborators developed a system based on IR range camera depth images for locomotion analysis of rodents, providing superior robustness, rapidity, and reliability, and high temporal and spatial resolution (Ou-Yang et al., 2011). By combining 3D imaging and machine learning methods Wiltschko and collaborators also developed a system and identified basic behavioral modules underlying the thogram at the subsecond timescale (Wiltschko et al., 2015a).

Some other non-invasive tools have been developed taking advantage of different **pressure and acceleration sensors** technology. These tools, allows a quite complete and precise evaluation of spontaneous behaviour in rat and mice. The **LABORAS** (Laboratory Animal Behaviour Observation, Registration, and Analysis System) homecage observation (Metris b.v., Hoofddorp, the Netherlands) is a system that uses a carbon fibre platform lying on sensors to detect behaviour-specific vibration patterns produced by the animal. This apparatus allow to place cages of different sizes on top of the carbon fibber platform, removing like this any stress induced by a novel environment. The vibrations evoked by the movements of the animal are picked up by the force transducers below the platform. The specific LABORAS software processes the produced vibrations into various behavioural parameters. Thus, this system can continuously detect a wide range of behaviours such as climbing,

grooming, rearing, locomotion, immobility, eating, drinking and resting. Figure 2 shows some examples of those behaviours' vibrational patterns. This system is also able to identify stereotyped behaviours such as wet dog shakes, tremors, skin twitches, convulsions or scratching. The LABORAS software uses a range of pattern recognition and signal analysis techniques to reliably recognize the physical properties of the signal generated by those behaviours. The gain and offset of the pre-amplifier are adjusted based on the weight of the laboratory animal that is entered by the experimenter. Therefore this system is able to automatically perform a precise and complete ethogram over time (Pitzer et al., 2016).

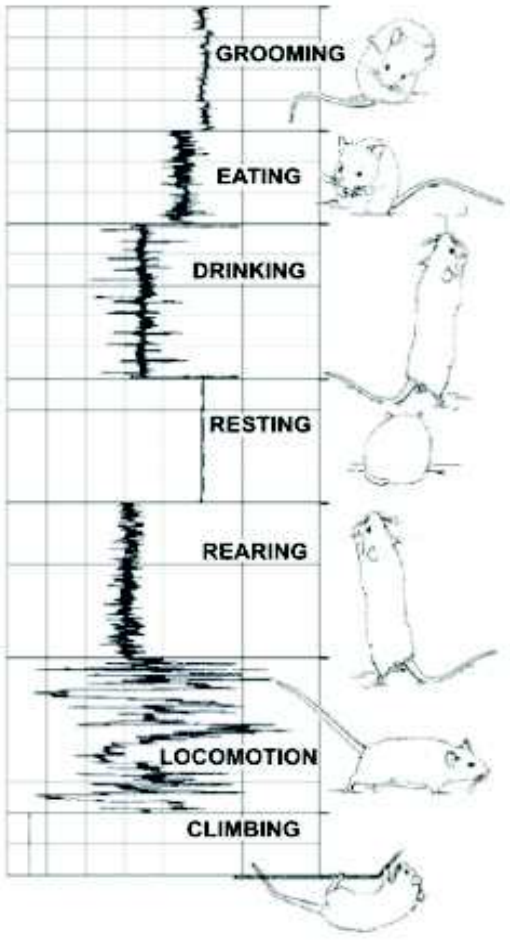

Figure 8: sample of behaviours' vibrational patterns. From LABORAS

Another non-invasive system to evaluate animal behaviour is the **Behavioural Spectrometer** (Behavioural Instruments, NJ and BiObserve, DE who market it under the name Behaviour Sequencer). It consists of a 40 cm by 40 cm square arena enclosed at a height of 45 cm. The removable floor is made of aluminium honeycomb sheet that rests on three accelerometers embedded in the floor support, which capture the platform vibrations generated

by the animal movements. A miniature colour CCD camera is mounted in the ceiling above the centre of the arena. A row of 32 infrared transmitter and receiver pairs is embedded in the walls at a height of 6.5 cm. The Spectrometer is equipped with 4 dimmable 10-W halogen lights placed on the ceiling of the enclosure. One side of the enclosure is a door allowing access to the arena. This apparatus integrates three types of signals to capture animal behaviour: a camera captures video, from which position and posture are extracted (Viewer3, BiObserve); accelerometers embedded in the platform capture the mouse's vibrations; and the infrared beams detect when the animal rears. The software contains 23 different patterns of sensor readings against which to compare any current readings. Through use of a proprietary algorithm utilizing multidimensional clustering to the nearest neighbour in the sensor data space the computer determines the most likely behaviour being emitted by the mouse at every second. This "forced fit" method ensures that all behavioural abnormalities show up in the data (Brodkin et al., 2014). A video record synchronized with the computer scored behaviour is available for post-session inspection. One drawback of this system is that the fine calibration does not allow the insertion of a tether for combined electrophysiological recordings. Wireless systems may nevertheless allow to do so.

In my PhD, I have used a similar based on similar principles, made of an open field plateform relying on piezoelectric pressure sensors. The word piezo comes from the Greek word piezein, meaning to press or squeeze. Piezoelectricity refers to the generation of electricity or of electric polarity in dielectric crystals when subjected to mechanical stress and conversely, the generation of stress in such crystals in response to an applied voltage. The basic theory behind piezoelectricity is based on the electrical dipole. At the molecular level, the structure of a piezoelectric material is typically an ionic bonded crystal. At rest, the dipoles formed by the positive and negative ions cancel each other due to the symmetry of the crystal structure, and an electric field is not observed. When stressed, the crystal deforms, symmetry is lost, and a net dipole moment is created. This dipole moment forms an electric field across the crystal. The electrical charge produced decays with time due to the internal impedance of the sensor and the input impedance of the signal conditioning circuits. Thus piezoelectric sensors are not suited for static applications but they are well suited for dynamic applications, as it is animal behaviour (Karki, 2000). Although piezoelectric technology is commonly used in nanomotion studies regarding engineering applications, some advances have been done regarding biomedical studies. For example, piezoelectric technology has been used to monitor patients' respiration (Rymut et al., 2003, Kim et al., 2009), fetal movements (Sadovsky et al., 1977), and even to classify human leg motion (Tuncel et al., 2009). Because piezo electric

sensors are able to detect fine pressure changes elicited by animal movements, they have a great potential as a non-invasive tool for behavioural monitoring. Taking advantage of this innovative instrument, some studies have been able to identify subtle movements with a fine temporal precision. One application of this technology is the measurement the whisking behaviour (Sachdev, 2001). Piezoelectric technology has also been used for the non-invasive study of animal behaviour, for example placing a piezo-film underneath the floor of a test cage (Meert et al., 1997, Flores et al., 2007). Animal movement then generates a strength over the piezo sensors which is transduced into an electrical signal. For instance, characterization of sleep has been achieved by using these piezoelectric platforms (Flores et al., 2007, Fisher et al., 2012). In these works sleep states were classified using a novel pattern recognition algorithm to identify regular motions associated with respiration when the animal assumed a specific sleep posture. This made possible to specifically distinguish between sleep and awake periods, where the amplitude spikes in the piezoelectric signal is much larger. Depending on the precision of the sensors, the composition of the platform, and the animal position, during sleep, breathing movements might be detected by these sensors through the contact between the chest and the platform. However, the developed algorithm did not have sufficient predictive power to automatically distinguish REM from NREM sleep (Mang et al., 2014, Yaghouby et al., 2016)

Induced-tremor behaviour has been also characterized by using piezo electric film. In their work, Meert evaluated the tremor-induced behaviour in rats by a quantitative analysis of the voltage outputs derived from deformations of two pieces of piezo-film (Meert et al., 1997). Another behaviour successfully evaluated with this technology is fear-potentiated startle. Fear-potentiated startle, as previously described is a reflex response during fear states elicited by the anticipation of an aversive stimulus (e.g. footshock). This response has been largely studied in rats where the amplitude of the acoustic startle reflex is large enough to be used as a measure of fear. However, when it comes to mice, startle responses and fear-potentiated alterations of startle reflexes are notoriously difficult to study. Regarding this issue, piezoelectric sensors has been shown to be sensitive enough to accurately detect these movements in mice (Daldrup et al., 2015). Although the principle is the same, individual piezo pressure sensors appear to have much higher resolution than piezo-films.

In my PhD, I have used a novel device made of an open field plateform relying on piezoelectric pressure sensors with exquisite sensitivity, allowing to access extremely fine components of movement with the resolution of individual moves such as heart beat or individual footsteps. One interesting property of this approach is that it reflects the summed

activity of all the muscles of the animal. Depending on the coordination of these myriads of muscles, their mechanical signature can sum up or cancel each other. This is therefore a very rich but also very complex signal to be characterized. To better understand the complexity of this signal we also explored different computational techniques (such as Machine learning and complexity measures) that could describe its dynamic properties.

Data analysis: classifiers and signal complexity

Computational ethology relies on sophisticated analysis methods. During my PhD, we have used classifiers and machine learning algorithm to discriminate locomotor patterns in different animal models. We have also used concepts originating from physics such as permutation entropy and Lyapunov exponent, to investigate the global properties of behavioral signals.

Classifiers

Classifiers are algorithms used to classify data, that is to use or define criteria to sort items into categories. The sophisticated version of classifiers is machine learning, a type of algorithms which performance increases with experience. A dataset is provided for training, and then validated on a distinct testing set of data. In the supervised approach (figure 9-A), the categories to discriminate are pre-defined, the training data set already classified accordingly, and the objective of the algorithm is to find rules that will allow to make similar classification of any data set automatically in the future. This procedure may allow the characterization of complex actions (e.g., grooming), even though a human programmer would not be able to define explicitly the rules necessary to detect this specific behaviour in an automated manner. The classifier is iteratively trained and tested, and more training examples may be added, until it achieves satisfactory performance, minimising false positives (ie samples detected as the targetted behaviour although they are not) and false negatives (samples of targetted behaviour not recognised as such). In the unsupervised approach, the data set is not annotated or classified a priori. The algorithm is then designed to produce classifications by finding dimensions that separate the data into distinct subsets. Applied to behavioural analysis, supervised machine learning would ideally lead to automatic detection of a predefined set of behaviours, and unsupervised machine learning to automatic identification of various types of behaviour, the relevance of which can be defined a posteriori by the experimenter.

Depending on the properties of the data samples, classification can be performed by linear or nonlinear methods. In the case of linearly separable training data, an infinite number of hyperplanes exists that correctly classify the data. Support vector machines (SVMs) are supervised machine learning algorithms that construct the best fit separation line, classifying the different data sets as well as possible. Given a two class classification problem, specified by a sample$(\overrightarrow{x_1}, y_1)$, …, $(\overrightarrow{x_n}, y_n)$ where x_i are the feature vectors, and y_i are the class labels, the hyperplane chosen by the SVM is the hyperplane that maximizes the distance from the closest training data to the hyperplane (called margin). This so-called maximum margin hyperplane minimizes the 'structural risk' of overfitting and optimizes the generalization of the classifier (figure 9-B)(Heikamp and Bajorath, 2014). Non-linear class separability can be also achieved by application of kernel classifiers, but linear classification such as SVM might show that the features found are robust enough to allow linear separation. Thus when data sets can be linearly separated, the use of linear classifiers is strongly recommended (Huang and Lin). Besides, the application of non-linear classifiers needs a careful, unstable and costly parameter fitting process, often carried out by brute force grid search. Therefore the main inconvenience of non-linear SVM is its instability: often the parameter settings optimal for a sample are not good for the subsequent samples of the same population.

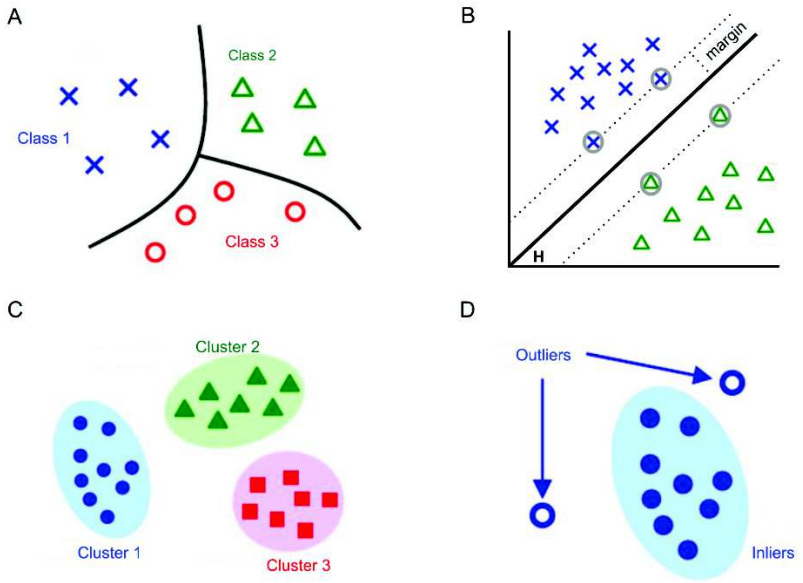

Figure 9. A, Classification process. B. SVM classification. The maximum margin hyperplane H (solid line) separates two classes (blue crosses and green triangles, respectively). Support vectors are encircled in grey. These support vectors either lie on the edge of the margin (parallel to H) or within the margin. Data points that are incorrectly classified are illustrated by dotted lines. C, unsupervised classification by clustering. D, example of outlier detection.

An unsupervised method for classification is clustering (figure 9-C), which objective is to categorize input samples into different clusters (1,2,. . . , c) without any supervision. Usually, similar samples are supposed to belong to the same cluster, and dissimilar samples are supposed to belong to different clusters. Thus, how to measure the similarity between samples is the key issue in clustering. One of the most fundamental algorithms for clustering is the method of k-means clustering, which aims at finding cluster labels based on the mean of the data set (Sugiyama, 2016). Outlier detection (figure 9-D), which is also referred to as anomaly detection, is aimed at finding irregular samples in a given data set. In the same way as clustering, the definition of similarity between samples plays a central role in outlier detection, because samples that are dissimilar from others are usually regarded as outliers.

Classifier algorithms have been successfully used to quantify components of innate exploratory, grooming, approach, aggressive and reproductive behaviours, replacing the tedious and unreliable step of human scoring. These novel approaches open a new horizon to further ethological investigation, which enable more comprehensive characterization of the behavioural components. In their work, Jhuang and colleagues used SVM to accurately identify 8 home cage behaviours (reaching an accuracy of the 90%), allowing a complete characterization of the behavioural organization (ethogram) over the recorded session (Jhuang et al., 2010). Interesting works has also been done regarding the organization of behaviours in time. For example, recent studies has investigated the presence of ultradian cycles regulating locomotor activity and eating in rats (Ootsuka et al., 2009, Blessing et al., 2012) and mice (Miyata et al., 2016). In invertebrates, behavioural modules and their associated transition probabilities can now be discovered systematically through automated machine vision, clustering and classification algorithms (Anderson and Perona, 2014). Identifying behavioural modules and transition probabilities has uncovered context-specific strategies used by invertebrate brains to adapt behaviour to changes in the environment. For instance, sophisticated analysis have developed models of how animals make decisions and control their actions based on their internal state and on external stimuli (Karbowski et al., 2008, Garrity et al., 2010, Luo et al., 2010). A recent study has been able to identify the behavioural organization of the mouse at a sub-second spatiotemporal scale without human supervision (Wiltschko et al., 2015b). In this work, Wiltschko and collaborators uses 3D imaging to capture the animals' pose dynamics and by applying an autoregressive model were able to automatically identify each behavioural pattern of the animal at a fine time scale. They also

implemented a hidden Markov model, to study the switching dynamics between different behavioural modules and extract their associated transition probabilities. Although with some limitations, their model provide automatic identification of specific behavioural pattern and information about adaptive changes in the architecture of behaviour. During my PhD, we have used support vector machines to classify different autoregressive features of foot step patterns from different animal groups. These algorithms made possible to characterize altered locomotion in CFA mice as well in mouse models of Alzheimer's and Parkinson's diseases.

Signal temporal dynamics and complexity

Biological systems are typically characterized by complex dynamics (Goldberger et al., 2002). Many physiological systems are indeed highly complex networks (Varela et al., 2010), with many recursive feed-back and feed-forward circuits, and thus they may be especially prone to develop chaotic behaviours and display fractal structures. Therefore, nonlinear measures such as permutation entropy (PE), autoregression and fractal models have been increasingly applied in physiology and medicine, where they can bring important information about physical properties of the signal, such as periodicity, productivity, complexity, and so reveal its temporal dynamics. Thus temporal dynamic characteristic of a given time series can be quantified, and the resulting parameters may be used to perform the machine learning classification (Wiltschko et al., 2015b, Xi and Zhu, 2015).

Permutation Entropy (PE) and fractal analysis are measures commonly used to characterize the non-linear dynamics of biosignals, an approach well suited to studying biological system's complexity and periodicity. A defining feature of healthy function is adaptability, the capacity to respond to often unpredictable stimuli. Physiologic plasticity requires a broad range of integrated multiscale outputs. Complexity in physiological systems, such as heartbeat and breathing dynamics, may be adaptive for at least two reasons: (1) long-range correlations serve as an organizing mechanism for highly complex processes that generate fluctuations across a wide range of time scales and (2) the absence of a characteristic scale may inhibit the emergence of very periodic behaviours that greatly narrow system responsiveness.

Thus, the theory of complexity loss in aging and disease, as currently formulated, has two central postulates:

1. The output of healthy systems, under certain parameter conditions, reveals a type of complex variability associated with long-range (fractal) correlations, along with distinct classes of nonlinear interactions;
2. This type of multi-scale, nonlinear complexity breaks down with aging and disease, reducing the adaptive capabilities of the individual (Goldberger et al., 2002).

The paradoxical resemblance of highly ordered dynamics with pathological states exemplifies the concept of complexity loss (decomplexification) in aging and disease, where nonlinear analysis have proven lower complexity index in pathological signal (Inouye and Shinosaki, 1991, Goldberger, 1996, Ivanov et al., 1999, Goldberger et al., 2002). Physiological stability appears to relate in part to complex patterns of variability that incorporate long-range correlations, together with distinct classes of nonlinear interactions (Goldberger et al., 2002). Furthermore, physiological systems having only one (or a few) dominant scale(s) become especially easy to recognize clinically because they stereotypically repeat their behaviour in a highly predictable fashion (Goldberger, 1997). This fact make nonlinear analysis especially attractive regarding early diagnostic.

The characterization of brain electrical activities in terms of complexity of the EEG has been demonstrated to be a useful tool in different contexts. For example, the time evolution of PE shows evident changing complexity in the transition between inter-ictal and ictal states in the epileptic brain As it is the case for Lyapuvnov exponents and Correlation dimension of attractors, PE has been used to detect seizure onset and also to predict upcoming seizures before they actually occur (Bruzzo et al., 2008, Nicolaou and Georgiou, 2012). These studies show that EEG during epileptic seizures is characterized by lower PE than normal EEG, lower complexity. Other studies have also shown lower PE in the EEG activity of Alzheimer's disease patients in comparison to control (Abasolo et al., 2006, Morabito et al., 2012, Cao et al., 2015). In this work we have used fractal analysis (including correlation dimension and Lyapunov exponent) and permutation entropy to investigate mice spontaneous behaviour.

Chapter 2: MOUSE MODELS OF PATHOLOGIES

Fragile X Syndrome

Fragile X Syndrome is a neurodevelopmental disorder, the most common inherited form of mental retardation, and a leading known cause of Autism Spectrum Disorder (ASD). Both males and females can be affected, however the degree of cognitive disability is typically more severe in males. Fragile X Syndrome has an estimated frequency of 1/4000 males and 1/7000 females worldwide. The gene involved in FXS was discovered in 1991 and it was called fragile X mental retardation 1 (*Fmr1*) gene (Willemsen et al., 2011).

A CGG trinucleotide repeat expansion in the promoter region of the *Fmr1* gene, located in the X chromosome, is responsible for its transcriptional silencing (Bassell and Warren, 2008). Expansion in this triplet sequence gives rise to FXS, which is the prototype of unstable triplet expansion disorders. The number of CGG repeats is normally ~6-54, 55-200 in permutation carriers and >200 in FXS patients (Willemsen et al., 2011). When more than 200 CGG repeats are accumulated, the CpG island in the 5'-untranslated region (UTR) becomes hypermethylated, which causes a suppressed transcription and therefore a lack of FMRP, an mRNA-binding protein. FMRP is implicated in the regulation of neuronal development and plasticity, in both the central and peripheral nervous system. FMRP targets a large variety of mRNA molecules, with up to as many as 800 mRNAs as binding partners (Brown et al., 2001). This equals ~ 4% percent of all mRNA transcripts that occur in the mammalian brain (Bassell and Warren, 2008). A recent study identified that hundreds of targets of FMRP are mRNAs encoding part of the pre- and postsynaptic proteome (Darnell et al., 2011). In addition to its strong effects on the translational level, FMRP is also thought to have a role in the dendritic mRNAs transport (Dictenberg et al., 2008). Recent studies using mosaic Fmr1 KO mice (FXS mouse model lacking FMRP) revealed extensive connectivity defects in the hippocampal circuit that have a cell-autonomous presynaptic origin (Hanson and Madison, 2007). Together, these findings suggest that several major neuronal and circuit abnormalities attributed to loss of FMRP arise from the requirement for FMRP in presynaptic functions. This large number of interactions explains why a single-gene deficit leads to such a complex sequence of events and makes it difficult to assess the full extent of the consequences of this cognitive disorder. It could further explain why FXS is one of the few single gene mental retardation disorders, since the loss FMRP might affect so many other genes that compensatory mechanisms are insufficient to avoid strong cognitive defects.

Dendritic spines, small protrusions along neuronal dendrites, are sites of excitatory synaptic input, which contain receptors and signaling molecules that are essential for synaptic neurotransmission (Nimchinsky et al., 2002). Postmortem analysis of human cortical tissue revealed that individuals with FXS have an increased density of dendritic spines relative to controls. Moreover, a majority of spines appear elongated and immature (Rudelli et al., 1985), suggesting that FMRP expression is necessary for the development of normal dendritic spine morphology. Classic physical features often seen in adults with FXS include an elongated face with a prominent forehead and macroorchidism, 2 or 3 times the normal size by mid-adolescence. Structural longitudinal magnetic resonance imaging (MRI) study of preschoolers with FXS observed generalized brain overgrowth compared to controls, evident at age two and maintained across ages 4–5 (Hazlett et al., 2012). In this regard, preclinical studies have demonstrated that FMRP inhibits the generation of progenitor neurons from glia cells but enhances the glial cell number in mouse cerebral cortex, suggesting that the lack of FMRP, as seen in FXS might result in an increased proliferation of progenitor glial cells and subsequent cerebral cortical overgrowth (Harlow et al., 2010). In addition, FMRP also regulates the phosphatase and tensin homolog gene translation that in turn regulates growth (Lozano et al., 2016). Other physical features characteristic of FXS patients include abnormalities of elastin fibers in connective tissue, such as prominent ears, soft skin, flat feet, and hyper-extensible finger joints. Medical problems often seen in males with FXS include strabismus (8 to 36%), seizures (20%), sleep problems (26–47%), mitral valve prolapse (50%) and otitis media (85%) (McLennan et al., 2011, Lozano et al., 2016). Fragile X syndrome patients show a complex behavioral phenotype that often includes intellectual disability, social and communication impairment, stereotypic behavior, attention deficits, hyperactivity, hyperarousal, and sensory abnormalities (Merenstein et al., 1996, Lozano et al., 2016).

A number of different approaches have been taken to get a better understanding of FXS and the role of FMRP in health and disease. The help of different genetically modified organisms, most importantly Drosophila (Zhang et al., 2001) and knock-out mice (Consortium, 1994) have brought a wealth of findings that are important for human patients. In fact much of what we know today about the function of FMRP in vivo was originally discovered in studies using those two animal models. Fmr1, which is the homologue gene in the mouse of the human *Fmr1* is 97% identical to the human gene at the amino acid level and to 95% identical at the nucleotide level in the coding region (Ashley et al., 1993). Also the expression patterns of *Fmr1* and Fmr1 are similar in human and mouse tissues (Verheij et al., 1995). The first Fmr1

knockout (Fmr1KO) mouse was generated by introducing a neomycin gene into exon 5 of the murine Fmr1 gene through homologous recombination in embryonic stem cells (Consortium, 1994). Many parallels to human FXS patients have been found in the Fmr1KO mouse model regarding biochemical and behavioral characterization (Bakker and Oostra, 2003, Frank Kooy, 2003). For example, Fmr1KO mice also suffer from cognitive impairments, even though they are less severe than those described in FXS patients (Dobkin et al., 2000, Van Dam et al., 2000, Frank Kooy, 2003). The knockout mice also display macroorchidism (Consortium, 1994), which is common in male FXS patients and various other important aspects of the disease, including sensory hypersensitivity and thin, immature dendritic spines. Although Fmr1 KO mice do not express FMRP, the Fmr1 promoter in those mice is intact and residual Fmr1 transcription was found in these mice. To resolve the uncertainty whether the residual transcript functions in some way a second line of Fmr1 KO mouse line, a complete null knockout mouse, has been created by excision of the Fmr1 promoter and first exon (Mientjes et al., 2006). Nowadays, this animal model is, the best-characterized rodent model of FXS is the Fmr1 knockout (KO) mouse. As it occurs in FXS patients, analogous deficits in spine number and morphology have been found in Fmr1 KO mice Over time however the picture has become increasingly complex and the initially thought striking phenotype is not found in all brain areas and actually, for unclear reasons, several studies could not confirm the previous findings. Figure 10 summarizes the complicating findings concerning the spine phenotype in mouse models of FXS. The prevalent opinion today is that Fmr1KO mice have an increased number of spines due to defects in dendritic pruning (Comery et al., 1997, Galvez and Greenough, 2005) but several studies reported the deficits occur just transiently (Nimchinsky et al., 2001, Galvez and Greenough, 2005). A general agreement involve the overabundance of immature dendritic spines in cortical pyramidal neurons (He and Portera-Cailliau, 2013).

Fmr1-KO mice reproduce many phenotypes of FXS patients, including impaired social interactions, repetitive behavior, hyperactivity and cognitive deficits (Pietropaolo et al., 2011, Hebert et al., 2014, Kazdoba et al., 2014). Cognitive rigidity and reduced flexibility in paradigms that involve task reversal have been reported in Fmr1-KO mice (Kramvis et al., 2013, Kazdoba et al., 2014), but behavioral aversion to changes in the environment (a feature well described in FXS patients) has not been much studied in this FXS animal models.

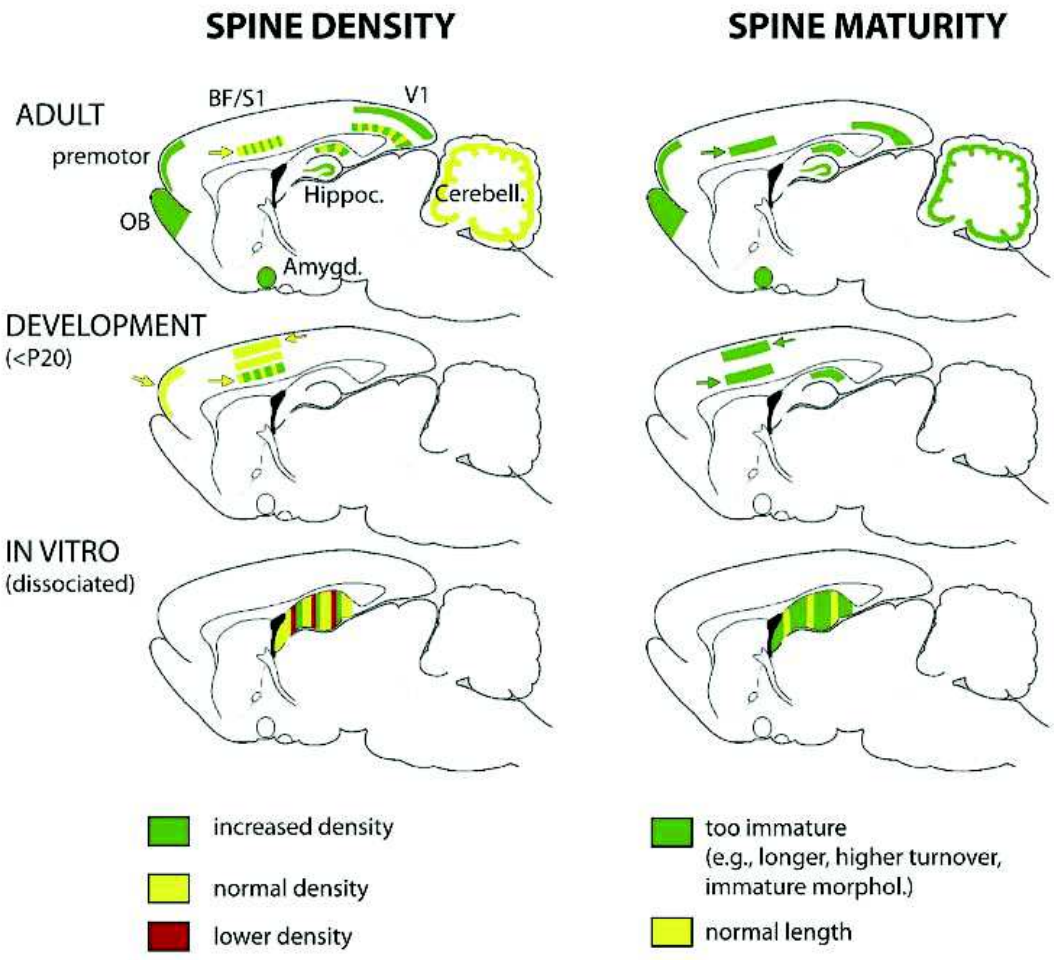

Figure 10. The spine phenotype in the Fragile X knock-out mouse model. Regional distributions of reported spine defects in the brain of Fmr1 KO mice. Data on dendritic spines in Fmr1 KO mice are displayed on a sagittal view of the mouse brain. Data from the adult brain, developing brain (P20), and in vitro results from dissociated neurons in culture (hippocampus only) are shown in the top, middle and bottom rows, respectively. Colored stripes indicate the existence of published studies reporting different results on either spine density or maturity. The relative thickness of the colored stripes reflects approximately the relative number of studies supporting one finding or another. Studies that used imaging in living neurons (in vivo or in acute/organotypic brain slices) are indicated by arrowheads next to the stripes. Note that results of studies are much more consistent for the spine immaturity phenotype than for the spine density phenotype. Abbreviations used in the figures: BF: barrel field; OB: olfactory bulb; S1: somatosensory cortex; V1: visual cortex. Figure adapted from (He and Portera-Cailliau, 2013).

Among the presynaptic mechanisms, the potential role of FMRP in modulating neurotransmitter release and synaptic strength during neuronal activity is of particular interest.

Indeed, rapid activity-dependent modulation of synaptic strength, also known as short-term plasticity (STP), is widely believed to serve several essential neural functions such as information processing, working memory and decision making (Deng and Klyachko, 2011). Moreover, recent information-theoretic analyses have shown that STP plays a critical role in synaptic information transmission by determining the optimal amount of information that synapses transmit in response to specific patterns of neuronal activity (Rotman et al., 2011). On rapid time scales relevant to information processing, the release of neurotransmitter is determined in large part by the shape, frequency and pattern of presynaptic action potentials (APs)(Bean, 2007). In particular, AP duration is an important determinant of release, controlling the amount of presynaptic calcium influx. Modulation of AP duration thus represents a precise and powerful mechanism to control and regulate neurotransmitter release. The AP duration is controlled primarily by the activity of voltage-gated K+ channels (VGKCs) (Bean, 2007). In central neurons, the large conductance Ca2+-activated K+ channels, also called "big" potassium channels (BK) are among the major determinants of AP duration during repetitive activity, owing to their activation being both voltage- and calcium-regulated (Bean, 2007). BK channels are spread over different body tissues, being abundantly expressed in both central and peripheral neurons, with prominent expression reported in both the cell body and pre-synaptic terminals. Functionally, these channels are key regulators of neuronal excitability, as channel opening will reduce action potential (AP) amplitude and duration, increase the magnitude of the fast after-hyperpolarization immediately following repolarization and limit the frequency of AP burst firing(Kyle and Braun, 2014). Diversity of BK channel function is accomplished in part by the presence of two identified auxiliary β subunits: β2 and β4. Deng et al. demonstrated that FMRP can bind directly to the β4 subunit of BK channels (Deng et al., 2013). The absence of FMRP in fmr1 KO neurons presumably affects the co-assembly of β4 subunits with the pore-forming subunits of BK channels and lowers the calcium sensitivity (Brenner et al., 2000). The net effect of this would be reduced IBK and more pronounced action potential broadening during repetitive firing. Indeed it has been shown that FMRP regulates neurotransmitter release and STP in cortical and hippocampal pyramidal neurons by modulating AP duration via BK channels (Deng et al., 2013, Zhang et al., 2014). In WT neurons FMRP acts to limit AP broadening during repetitive activity by modulating the activity of BK channels, specifically their calcium sensitivity. Thus, loss of FMRP causes reduced BK channel activity and excessive AP broadening, leading in turn to elevated presynaptic calcium influx, increased synaptic transmission and thus neuronal hyperexcitability by sensory stimulus.

This neuronal hyperexcitability directly points to a causative role for neocortical circuit

defects in sensory processing described in FXS. Several lines of evidence suggest that altered sensory processing may participate in the generation of major behavioral problems in FXS. Indeed, sensory processing and integration have major roles in human development and this processing has two important components: sensory discrimination and sensory modulation. Sensory discrimination is the process in which sensory stimuli are distinguished, given their meaning and use. Problems with sensory discrimination can cause poor recognition and interpretation of sensory stimuli. Sensory modulation is how the sensory stimuli are used and responded to. Problems with this process can cause hyper-response, over-activity, poor attention and poor coping. The most common sensory modulation difficulty reported in FXS is hyperarousal. Indeed, individuals with FXS have an enhanced sympathetic response to sensory stimuli (Klusek et al., 2013).

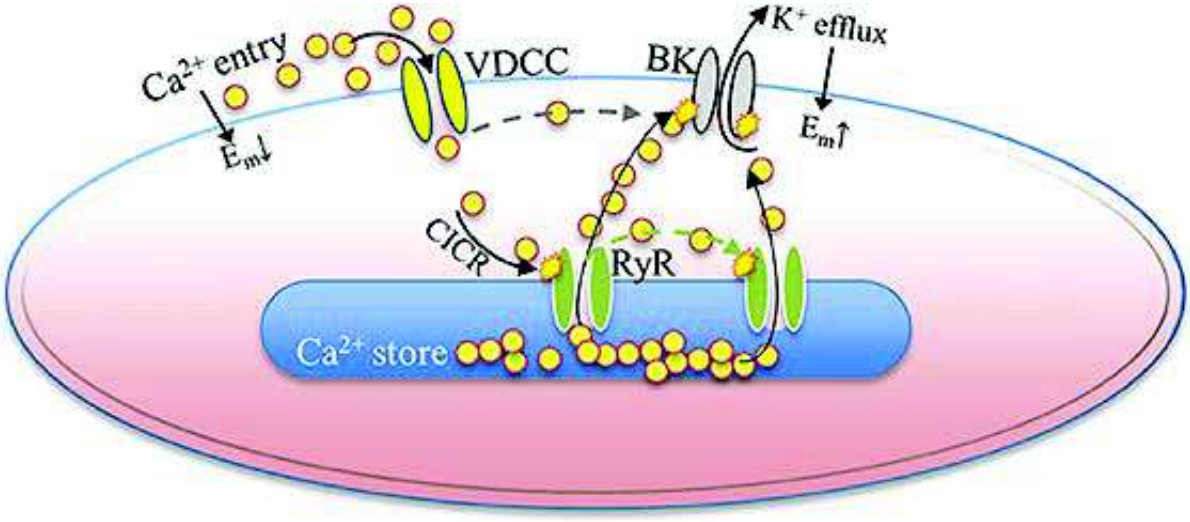

Figure 11. A summary of select physiological mechanisms leading to BK channel activation. Ca2+ –dependent activation of BK channels hyperpolarizes the membrane potential. Depolarization of the membrane potential activates voltage-dependent Ca2+ channels, leading to Ca2+ entry and Ca2+-induced Ca2+ release from nearby ryanodine receptors. Released Ca2+ promotes BK channel activation, which drives the membrane potential in the negative (hyperpolarized) direction. Ca2+ influx via VDCCs may also contribute directly to BK channel activation (dotted line) as a result of the spatial proximity of these two channels within membrane nano/micro-domains (Kyle and Braun, 2014)

Examples of the processing problem are difficulty tolerating bright lights and loud noises, crowded places overstimulation, difficulty making good eye contact, and trouble

tolerating certain clothes. These problems are related to a lack of normal habituation to stimuli of various sensory modalities (Miller et al., 1999, Bruno et al., 2014, Ethridge et al., 2016) . This phenomenon, termed sensory defensiveness, correlates with the expression of repetitive motor patterns and behavioral rigidity in autistic children (Baranek et al., 1997, Miller et al., 1999). Thus, sensory defensiveness has been proposed as the primary cause of hyperactivity, hyperarousal, and various deleterious behaviors such as stereotypies and even self-injury in FXS patients when confronted to change in their habits (Baranek et al., 1997, Miller et al., 1999, Symons et al., 2003, Contractor et al., 2015).

The hypothesis that altered neuronal sensory processing may participate in the generation of deleterious behavior is attractive and may offer physiological targets for therapeutic intervention in FXS.

In relation to this, previous work has shown that independently of its function as a translation regulator, FMRP also interacts with the β4 regulatory subunit of big conductance voltage and Ca2+-activated K+ channels (BKCa) in hippocampal and cortical excitatory neurons, which influence action potential duration and neurotransmitter release (Deng et al., 2013, Myrick et al., 2015, Deng and Klyachko, 2016). Accordingly, recent work from our group has shown that specific alterations in potassium channels are responsible for increased cortical excitability and sensory-hypersensitivity in Fmr1-KO mice(Zhang et al., 2014). In this study, a dysfunction of dendritic HCN1(neocortical h-channel subunit 1)-containing channels (responsible for I_h) as well as of dendritic and somatic BKCa in pyramidal neurons of the primary somatosensory cortex was found to result in increased intrinsic excitability by increasing input resistance, augmenting the spatial and temporal summation of excitatory synaptic potentials and by promoting the efficacy by which action potentials backpropagate into the dendrites and trigger dendritic spikes. Moreover, BKCa channel agonists such as BMS-191011 or BMS-204352 were efficient in reversing cortical hyper-excitability in vitro and increased acoustic startle in behaving Fmr1-KO mice, a widely recognized behavioral readout of sensory sensitivity previously used to assess sensory hypersensitivity in Fmr1-KO mice (Michalon et al, 2012; Nielsen et al, 2002).

In this thesis we have investigated how environmental changes affect *Fmr1*-KO mice behavior, and how these behavioral perturbation might be rescued by BMS-204352, an agonist of potassium BK-Ca channels.

Alzheimer's disease

General symptoms

Alzheimer's disease (AD) is the most common form of progressive cognitive decline. Its clinical symptoms include well-known impairment of memory and learning but also deficiencies in many other intellectual functions such as orientation, abstract thinking, and speech. These clinical signs are in a first stage progressive learning and memory deficits affecting short-term then, in later stages of the disease, long-term memories are disrupted too. Non-cognitive symptoms like disturbances in diurnal activity, aggressiveness, symptoms of affective and paranoid-schizophrenic disease are often associated with AD. Most notably, a fragmented sleep–wake pattern characterized by decreased daytime activity and disrupted nighttime sleep is a common complaint in patients with early AD (Bonanni et al., 2005).

A-Beta

As originally described by Alois Alzheimer in 1907, this form of dementia is associated with amyloid plaque formation as well as neurofibrillary tangles in the brain of affected patients. Amyloid plaques are extracellular deposits of Aβ (or β-amyloid), a 39 to 43 amino acid peptide derived from a larger precursor protein, APP (β-amyloid precursor protein). In contrast to diffuse deposits that do not show any further pathology, compact plaques containing Aβ fibrils are generally associated with hypertrophic astrocytes, activated microglia cells, and various other typical features of inflammatory processes. In addition, dystrophic neurites are present in these amyloid structures. The intracellular neurofibrillary tangles consist of paired helical filaments formed by the cytoskeletal protein tau in an abnormal, hyperphosphorylated state. They are found both in association with fibrillar amyloid plaques as well as apart from them. A reduction in synapse number in the neocortex and neuron loss in distinct regions of AD brain has been observed. Several neurotransmitter systems such as the cholinergic system are impaired in this disease.

There have been numerous clinic-pathological studies attempting to correlate β-amyloid plaques with the cognitive deficits seen in AD. However the strongest correlation between β-amyloid plaques and cognition is in the early stages of the disease and this association weakens as neurofibrillary tangles and gross neocortical neurodegeneration become more widespread (Webster et al., 2014). As the disease progresses into the later stages, there is little evidence to support a continued contribution by β-amyloid plaques to the late-stage AD cognitive decline. In contrast to this, a large number of studies have arrived at a

common finding, namely, there is a strong link between neocortical neurofibrillary tangles and cognitive decline. Although neurofibrillary tangles are not specific for AD (they are rather a secondary response to injury), the density and the neuroanatomic localization of those neurofibrillary tangles are important parameters in AD neuropathology. Neurofibrillary degeneration restricted to subcortical sites is often subclinical, whereas widespread neocortical NFTs are almost always associated with severe cognitive impairment in more than 1 disease state (Nelson et al., 2012).

β-amyloid plaques alone do not seem to be a sufficient substrate for advanced clinical AD dementia. However, in contrast to neurofibrillary (tau) pathology, there seems to be a strong association between AD genetics and amyloid plaque formation. All high-penetrance AD genetic risk alleles (i.e. apolipoprotein E ε4 allele, Down syndrome, APP mutations and duplications, PSEN1 and PSEN2 mutations) have been linked in various experimental systems with increased β-amyloid plaques deposition and increased formation of putative toxic Aβ peptide species (Reitz and Mayeux, 2009).

The concordance of genetics and Aβ deposition is aligned with clinic-pathologic correlation studies that indicate that β-amyloid plaques may be a temporally "upstream" feature of the neocortical disease, with the caveats that brainstem and medial temporal lobe pretangles and neurofibrillary tangles are seen in subjects without Aβ deposition in all age categories. Thus, β-amyloid plaques and neurofibrillary tangles are the hallmark features of AD but do not develop in the human brain according to the same temporal or anatomic pattern (Nelson et al., 2012).

Cholinergic and noradrenergic neurons are highly sensitive to amyloid toxicity, therefore the decline in the number of these neurons starts in the early phase of the disease. The reduced noradrenergic signaling probably contributes significantly to the pathological process in the later phases of AD by exacerbating ongoing neuroinflammation (Bilkei-Gorzo, 2014). The biggest loss in the number of neurons can be observed in the cortex and hippocampus in the advanced phase of AD leading to hypometabolism and atrophy in the affected brain areas. The presence of amyloid plaques and dying neurons activates the immune system leading to neuroinflammatory changes, which significantly contribute to the further progression of AD (Hensley, 2010). When dementia is diagnosed, the patients already show severe histopathological changes in the brain.

All the previously mentioned molecular and cellular alterations observed in AD brains are known to affect excitatory and inhibitory synaptic transmission. Indeed, alterations in network activities in AD are accompanied by an early imbalance of excitation and inhibition

that elites overall changes in theta activity as a hallmark of hippocampal functioning (Scott et al., 2012). These alterations due to Aβ-induced neuronal hyperexcitability (Minkeviciene et al., 2009) are accompanied by decreased GABAergic transmission within the hippocampus and can trigger seizure activity (Palop et al., 2007). Interestingly, AD patients (Goutagny and Krantic, 2013) and various mouse models of AD (Siwek et al., 2015) exhibit alterations in neural rhythmicity at different frequency ranges.

Although clinical AD is etiologically heterogeneous, genetic factors confer approximately 70% of an individual's risk for AD (Bertram et al., 2010). Analyses of both clinical and pathological features have provided important insights into how the pathology correlates with cognitive status. To complement studies in humans it has been the development preclinical model systems of AD pathology. It can be assumed that genetic modifications of these dominant mutations may initiate pathogenic mechanisms in laboratory animals similar to those in human AD patients. These preclinical animal models, especially mouse models, have been extremely useful to test mechanistic hypotheses about AD pathophysiology and to predict outcomes from pharmacological interventions. Figure 12 shows an overview of the progression of cognitive deficits in human AD (A) and in mouse models of AD (B). In humans, the earliest AD-symptoms are episodic memory impairment and semantic memory deficits. In mice models, the progression of the disease shows similar patterns. These impairments are studied in terms of spatial working memory, associative learning and reference memory assessed by water maze, maze alternation and fear conditioning, respectively (Figure 12).

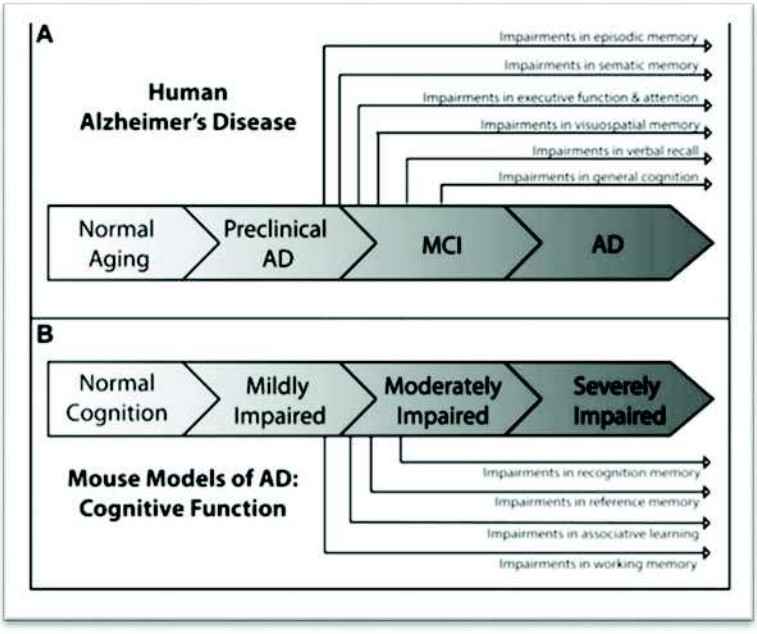

Figure 12. Overview of the progression of cognitive deficits in human AD (A) and in mouse models of AD (B) (Webster et al., 2014).

Animal models of AD:

Several transgenic mouse models are available, that recapitulate major cellular and cognitive features of AD, although no animal model recapitulates the entirety of AD in humans (Webster et al., 2014). A general overview of advantages and limitations of the most widely used or promising transgenic lines is shown in Table 1.

Validity of the most widely used genetic mouse models of Alzheimer's disease.						
		Tg2576	APP23	APP/PS1	3xtg AD	5xFAD
Face validity	Late onset, progressive	Yes	Yes	No late onset	Yes	No late onset
	Learning/memory impairment	Yes	Yes	Yes	Yes	Yes
	Diurnal cycle disturbances	Yes	Yes	Yes	Yes	Not
	Increased anxiety level	No	Yes	Yes	Yes	No
Constructive validity	Amyloid plaques	Yes	Yes	Yes	Yes	Yes
	Tau-hyperphosphorylation	No	Yes	Yes	Yes	No
	Neurofibrillary tangles	No	No	No	Yes	No
	Neuroinflammation	Yes	Yes	Yes	Yes	Yes
	Loss of noradrenergic neurons	Yes	Yes	Yes	Yes	Yes
	Loss of cholinergic neurons	No	Yes/no	Yes	Yes	Yes
	Massive neuronal loss in cortex, hippocampus	No	No	No	No	No
Predictive validity	Free from false negative findings	Yes	Yes	Yes	Yes	Yes
	Free from false positive findings	No	No	No	No	Not known

Table 1: Validity of the most widely used genetic mouse models of Alzheimer's disease. From (Bilkei-Gorzo, 2014).

Among the different genetic mouse lines of AD, APP/PS1 and 3xtg AD are the most commonly used. The 3tg AD is a triple-transgenic model that express three major genes associated with familial AD, namely APP_{Swe}, $PS1_{M146V}$, and tau_{P301L}. The 3×Tg-AD mice develop extracellular Aβ deposits prior to tangle formation, consistent with the amyloid cascade hypothesis (Karran et al., 2011). Indeed, intracellular Aβ immunoreactivity is apparent between 3 and 4 months of age in the neocortex of 3×Tg-AD mice and by 6 months of age in the CA1 hippocampal region. Regarding tau pathology it first appear in the hippocampus of the 3×Tg-AD, particularly within pyramidal neurons of the CA1 subfield, and then later

progresses to involve cortical structures. Although Aβ and tau pathology initiate in different brain regions in the 3×Tg-AD mice (i.e., cortex for Aβ and hippocampus for tau), it is not inconsistent with the notion that Aβ influences tau pathology. These changes are accompanied by significant loss of noradrenergic (Manaye et al., 2013) and cholinergic neurons (Girao da Cruz et al., 2012) and upregulation of microglial activity (Mastrangelo and Bowers, 2008). Furthermore, an imaging study highlighted disturbances in glucose uptake in brain areas similar to those of AD patients even in the early phase of the pathogenic process (Nicholson et al., 2010). These mice exhibit deficits in synaptic plasticity, including long-term potentiation (LTP) that occurs at 6 months old, prior to extracellular Aβ deposition and tangles (Oddo et al., 2003). However no decrease of synapse number nor density in CA1 pyramidal layer has been observed at that ages(Puzzo et al., 2015). These mice have been shown to exhibit a trend towards less daytime activity and more activity during the night at 6 months, however total activity over the light/dark (LD) cycle appears to be roughly the same over time and between genotypes. Decreased amplitude in locomotor activity and arrhythmic behavior has also been noted prior to the development of AD-pathology, although general locomotor ability was not impaired (Sterniczuk et al., 2010). As in humans, locomotor activity has been seen to increase during the typically inactive phase of the 24-h cycle. 3tg AD mice also decrease the amount of activity during the nocturnal (active) phase, although the amplitude of this activity remained comparable to controls. Circadian rhythm in the wheel running has been also shown to be disrupted in 3tg AD mice (Stover et al., 2015). 3xTg-AD mice show enhanced performance on the Rotarod, whereas they have poorer performance on other motor behaviour tasks such as the grip suspension task, indicating that their motor behaviour phenotype is more complex than previously reported (Stover et al., 2015). Increased age-related anxiety and fearfulness have been also reported (Puzzo et al., 2015).

Although numerous transgenic models have been developed to mimic and understand the mechanisms underlying AD, not all express AD pathology in an age-dependent manner along with the associated behavioral changes (Lee et al., 2005, Sterniczuk et al., 2010) as the 3xTg-AD mice do. Only this model expresses three major genes associated with familial AD(Oddo et al., 2003), and exhibits the neuropathological changes and corresponding behavioral manifestations that occur as the disease progresses in human patients The large number of similarities between this model and AD suggests a high level of face validity of the 3xtg AD line (Bilkei-Gorzo, 2014).

Alzheimer's Disease and Dopamine

Classical views consider that Alzheimer's disease is mostly related with cognitive impairment due to deficits in cholinergic systems, and Parkinson's disease with motor impairment due to deficits in dopaminergic systems. Recent results have challenged this view and provided evidence for the involvement of dopaminergic components as well as motor deficits in Alzheimer's disease (Scarmeas et al., 2004, Guzman-Ramos et al., 2012, Martorana and Koch, 2014a).

DA system undergoes several changes during physiological aging process. In general, decreased release of DA from its terminals, reduced DA receptor expression in particular D2 subtypes, reduced DAT expression in caudate putamen, hippocampus and frontal cortex of humans are features commonly observed in the brain during brain aging. The occurrence of apathy, gait disturbances and decline of executive functions are suggested to be the consequence of the impairment of DA transmission both elderly and AD (Martorana and Koch, 2014a).

Some studies claim that the earlier the impairment of DA system occurs, the fastest the cognitive decline goes (Martorana and Koch, 2014a). This consideration is in contrast with early neuropathological studies that found no neuronal loss but only degenerative changes like Lewy bodies or neurofibrillary tangles. These findings suggest that extrapyramidal signs (EPS) appearance could be dependent on extra-nigral mechanisms, given that there is a lack of severe pathology of DA system in AD (Burns et al., 2005). However, several recent experimental evidences renewed interest on DA involvement in AD pathogenesis. Indeed, experimental data from transgenic mice AD showed how the dopaminergic pathology and amyloid deposition are closely related, suggesting a causative role for amyloid on dopamine dysfunction (Perez et al., 2005). Moreover, the restoration of DA transmission was demonstrated to play a role in memory and learning in a mouse model of AD, strengthening the central role of DA in cognitive tasks (Guzman-Ramos et al., 2012). Finally, in AD patients, dopamine agonists treatment has been shown to restore the altered mechanisms of LTP-like cortical plasticity in AD patients (Koch et al., 2014).

Prospective clinical studies have revealed that motor symptoms often precede cognitive symptoms in AD by several years, and analysis of gait parameters has been proposed as a complement to cognitive evaluation to evaluate the risk of developing AD-related dementia at a later stage (Buchman and Bennett, 2011, Laske et al., 2015). In fact, it has been proposed that executive functions and motor ability are related and both get degraded in parallel during aging

and AD (Beauchet et al., 2012, Ijmker and Lamoth, 2012). But techniques to evaluate motor functions maybe more efficient than those to detect cognitive or executive functions, possibly due to more elaborate compensatory mechanisms for cognition than for motor function, so that cognitive deficits can be clearly identified and diagnosed only at a very advanced stage of neuronal impairment. The advantage of early detection of motor symptoms may allow for therapeutic intervention to preserve neuronal networks involved in cognitive functions before they get too much degraded. Therefore, identifying quantitative gait markers of preclinical dementia is a promising approach that may lead to new insights into early disease stages, improve diagnostic assessments and identify new preventive strategies.

Most of the commonly used AD mouse models exhibit altered locomotor activity, stereotypic behaviors, and home cage activity disturbances and the onset of the disturbances is different for each model (Webster et al., 2014). It is important to take into account that no one animal model fully replicates the pathogenesis of AD, no one model recapitulates all of the cognitive deficits observed in human AD. While most AD research has focused on the neurobiological mechanisms underlying the cognitive deficits seen in AD pathogenesis, there is a wide range of non-cognitive neuropsychiatric symptoms also associated with the disease. Most of the studies using mouse models of AD have focused on understanding/correcting the cognitive deficits associated with the disease. However, AD is not just a memory disorder, rather it is a complex disease with many different non-cognitive neuropsychiatric symptoms which are an important source of distress. These non-cognitive symptoms are present across many of the different mouse models of AD and more emphasis should be placed on understanding/correcting these deficits.

Nowadays, it is known that the pathological process that leads to AD begins years if not decades before clinical symptoms occur (Arendt et al., 2015). This long preclinical phase of AD is of pivotal importance to understand the origin of the disease and may provide a promising time window for potential therapeutic intervention. Clinical findings have opened up the possibility of relating motor skills to cognitive skills in patients with Alzheimer's disease (Buchman and Bennett, 2011). It may be possible to obtain predicting variables, such as dexterity or motor activity, in young patients prior to full-blown Alzheimer's symptomatology, thereby providing more targeted treatment options, a more personalized risk stratification for prevention, and early detection of the disease. Exact knowledge on the pathological process occurring during this preclinical phase, however, is difficult to obtain. Even though the identification of early motor symptoms is providing promising results in the clinical practice, few studies have addressed the question of gait analysis and motor function in AD.

Parkinson's Disease

Parkinson's Disease (PD) is the second most common neurodegenerative disorder in the world after Alzheimer disease (Feng and Maguire-Zeiss, 2010). It was initially described by James Parkinson in 1817, who published “an assay on the shaking palsy” where first described the clinical syndrome, as a neurological disorder, consisting of resting tremor and a peculiar form of progressive motor disability (Samii et al., 2004) that was later to bear his name (Parkinson, 2002).

The pathologic hallmark of the disease is the degeneration of dopaminergic neurons in the substantia nigra compacta (SN) of the midbrain and the presence of Lewy bodies, cytoplasmic aggregations in brain neurons formed by more than 25 compounds, but principally alpha-synuclein and ubiquitine with a diameter of 8-30 μm (Samii et al., 2004). The loss of cells from the SN in PD results in profound dopaminergic depletion in the striatum, lateral nigral projections to putamen being most affected (Kish et al., 1988).

Both motor and non-motor symptoms are associated to PD. Clinical signs of PD are evident when about 80% of striatal dopamine and 50-60% of nigral neurons are lost (Fearnley and Lees, 1991). However, nigral damage is always accompanied by extensive extranigral pathology, including that in the dorsal motor nucleus of glossopharyneal and vagal nerves and anterior olfactory nucleus. In fact, some nuclei of the reticular formation and the raphe system, the coeruleus-subcoeruleus complex, the magnocellular nuclei of the basal forebrain and many subnuclei of the thalamus and amygdale are affected as well. Thus, apart from the nigrostriatal dopaminergic system other neurotransmitter systems are involved, such as the glutamatergic, serotonergic, noradrenergic or cholinergic (Hornykiewicz, 1998). Therefore, PD is by no means exclusively a disease of dopaminergic neurons but rather damage is seen within a significant number of other nerve cell types.

The cardinal features of PD are mainly motor symptoms and include tremor at rest, rigidity and bradykinesia. Tremor and rigidity are considered as “positive” phenomena, while bradykinesia together with postural reflex abolition and the freezing are considered as “negative” phenomena. These latter “negative” phenomena are the most disabling problems for PD patients. Tremor is the most common and easy recognized symptom. It is unilateral and occurs at a frequency between 4 and 6 Hz. Rigidity is an increase in passive muscle tone in flexor and extensor muscle groups that extends through the range of movement. Bradykinesia refers to slowness of movements and is the most characteristic clinical feature of PD. Postural instability is sometimes judged as a cardinal feature, but is non-specific and is usually absent early in the disease. This latter feature refers to the gradual development of poor balance,

leading to an increased risk of falls.

Non-motor extra SN symptoms are common and often underappreciated and can be as disabling as motor symptoms (Sullivan et al., 2007). These include, cognitive and psychiatric changes, autonomic dysfunction and sleep disturbances. In fact, the presence of cognitive impairment or dementia in patients with PD is associated with loss of independence, a lower quality of life and a reduction in survival time. In addition, other symptoms such as hypotension, sweating, sphincter and erectile dysfunction have been escribed (Jankovic, 2008).

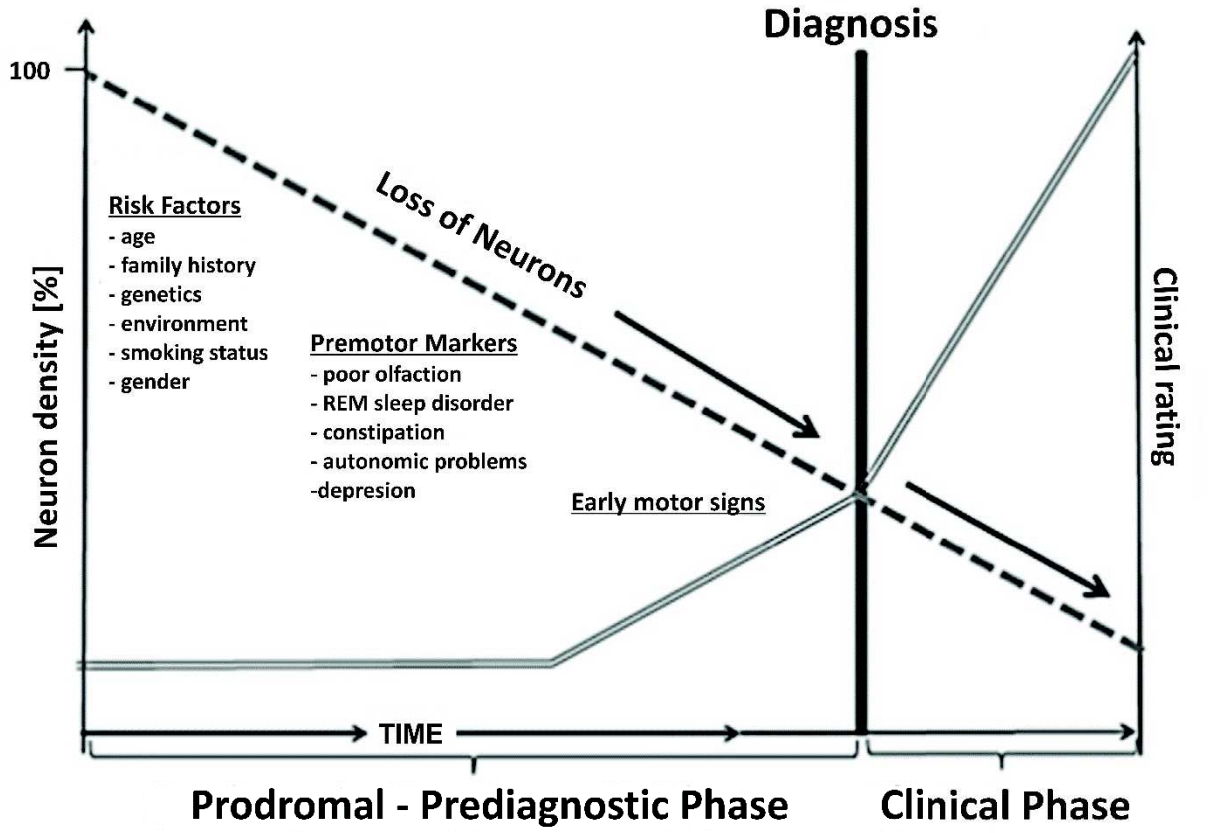

Figure 13: Factors and premotor markers associated with loss of neurons (————) prior to onset of motor signs and clinical diagnosis (====). Adapted from (Miller and O'Callaghan, 2015).

Nowadays, the pharmacological treatment is the first election to treat the PD in the early stages. Generally, the surgery is reserved for patients who do not tolerate the medication, present strong side effects or have small therapeutic benefit/profit. The continuous research on pharmacology has facilitated the development of several drugs since the late 60s when the 3,4-dihydroxyphenylalanine (L-DOPA) was first utilized in PD patients.

L-DOPA is considered the standard/essential drug for the treatment of PD, although dopaminergic agonists can be used in any stages of the disease. L-DOPA is the precursor of dopamine that cross the blood-brain barrier through a large amino acid transporter (Kageyama et al., 2000) and its administration is an attempt to replace exogenously the characteristic deficit of dopamine of PD. Normally, L-DOPA is administered with a dopamine decarboxylase inhibitor, such as carbidopa or benserazide that does not cross the blood- brain barrier, in order to avoid the peripheral transformation of L-DOPA in dopamine. L- DOPA induces the improvement of the striatal dopaminergic transmission, producing a rapid/quick improvement of the motor signs and symptoms of the PD. However, unfortunately, L-DOPA does not stop the development of the disease and its efficacy decreases over the time. Moreover, the prolonged treatment with L-DOPA produces motor complications, such as dystonia or L-DOPA-induced dyskinesia (LID) which appears in the 50% of patient after 5 years of treatment. This side effect could cause an important functional disability in patients and nowadays is one of the most frequent and difficult therapeutic problem of the PD.

Neurotoxic models

Basically, animal models of PD can be classified into three main categories: those based on neurotoxins or neuropharmacological agents targeting catecholaminergic neurons, those based on genetic manipulations relevant to PD (sometimes these two approaches are combined), and others (such as “MitoPark” model is based on the inactivation of a mitochondrial transcription factor selectively in DAergic neurons). None of the current models is able to fully mimic PD and reproduce its pathology and symptoms. This is mostly due to the fact that each model is based on the production of one or few pathological processes of PD, which are either artificially induced in a way that is seldom relevant to the disease (such as toxin models), or that is relevant to PD but produces only a small part of the pathology (such as genetic models)(Gubellini and Kachidian, 2015).

The neurotoxin and pharmacological models of PD are based on the systemic or intracerebral administration of neurotoxins capable of inducing selective degeneration of the nigrostriatal system (Blandini et al., 2008). Among them the hydroxylated analogue of dopamine (6-OHDA) model has resulted to be the most extensively used model in rats for reproducing the loss of dopaminergic neurons in the SN occurred in PD. Other neurotoxins such as paraquat (N,N_-dimethyl-4-4-4_-bypiridinium), MPTP (1-methyl-4-phenyl-1,2,3,6-tetrahydropyridine) and rotenone can be used to induce nigrostriatal lesion.

The 6-OHDA is a toxin-inducing degeneration of dopaminergic neurons in the nigro-

striatal tract (Ungerstedt, 1968). Since 6-OHDA does not efficiently cross the blood–brain barrier it requires direct injection into the brain. This is undoubtedly one of its main drawbacks as specialized stereotaxic surgical instruments and training are required. The injection is commonly carried out unilaterally, with the contralateral hemisphere serving as control. Bilateral injections are generally avoided, due to the high mortality rate associated with this procedure (Blandini et al., 2008).

6-OHDA is injected into the nigro-striatal tract at one of three locations: into the substantia nigra compacta (SN) where the dopaminergic cell bodies are located; into the median forebrain bundle (MFB), through which the dopaminergic nigro-striatal tract ascends; or into the terminal region, the striatum (Duty and Jenner, 2011). Intrastriatal 6-OHDA administration induces a progressive, retrograde degeneration of the nigrostriatal pathway and tends to form a more progressive partial lesion (about 60-80% loss of dopamine in the caudate putamen complex). The administration of 6-OHDA into MFB or SN causes an anterograde degeneration of the nigrostriatal dopaminergic system and trend to form a complete model.

Following its injection, 6-OHDA is taken up into the dopaminergic neurons via the dopamine transporter, DAT. Given that 6-OHDA also shows high affinity for the noradrenaline transporter, NET (Luthman et al., 1989) systemic injection of the NET inhibitor, despiramine, given 30–60 min before 6-OHDA, ensures improved specificity of the toxin for dopaminergic neurons.

Once 6-OHDA enters the neuron, it accumulates in the cytosol and being oxidized leads to increased ROS and quinines production which, in turn, through oxidative stress mechanisms, inactivate biological macromolecules, reduce antioxidant enzyme levels in striatum and increase iron levels in SN (Duty and Jenner, 2011). This elevated iron interacts with the Complex-I and Complex-III of mitochondria and leads to an inhibition of the respiratory chain and further oxidative stress (figure 11).

These mechanisms of 6-OHDA toxicity are considered as the pathological events of human PD; therefore, it makes the model applicable. Although the 6-OHDA model does not allow to study the progressivity of PD neither it generates Lewy body inclusions, this model is the most powerful to degenerate nigrostriatal DA neurons, which assures the proper study of advanced stages of PD (Gubellini and Kachidian, 2015). A schematic representation about the mechanisms adopted by the different agent used to induce animal models of PD is expressed in figure 11.

A major advantage of the 6-OHDA model is a quantifiable motor deficit (rotation) and its usefulness in the pharmacological screening of agents that have effects on DA and its

receptors (Deumens et al., 2002).

Typically, two drugs are used for induction of the rotational behavior in unilaterally lesioned animals: amphetamine and apomorphine. Amphetamine acts as an agonist of dopamine inducing the fast and almost complete release of the neuromediator/neuromodulator dopamine from the presynaptic terminals (Sulzer et al., 2005). Apomorphine, a short-acting dopamine D1 and D2 receptor agonist, functions postsynaptically (Picada et al., 2005).

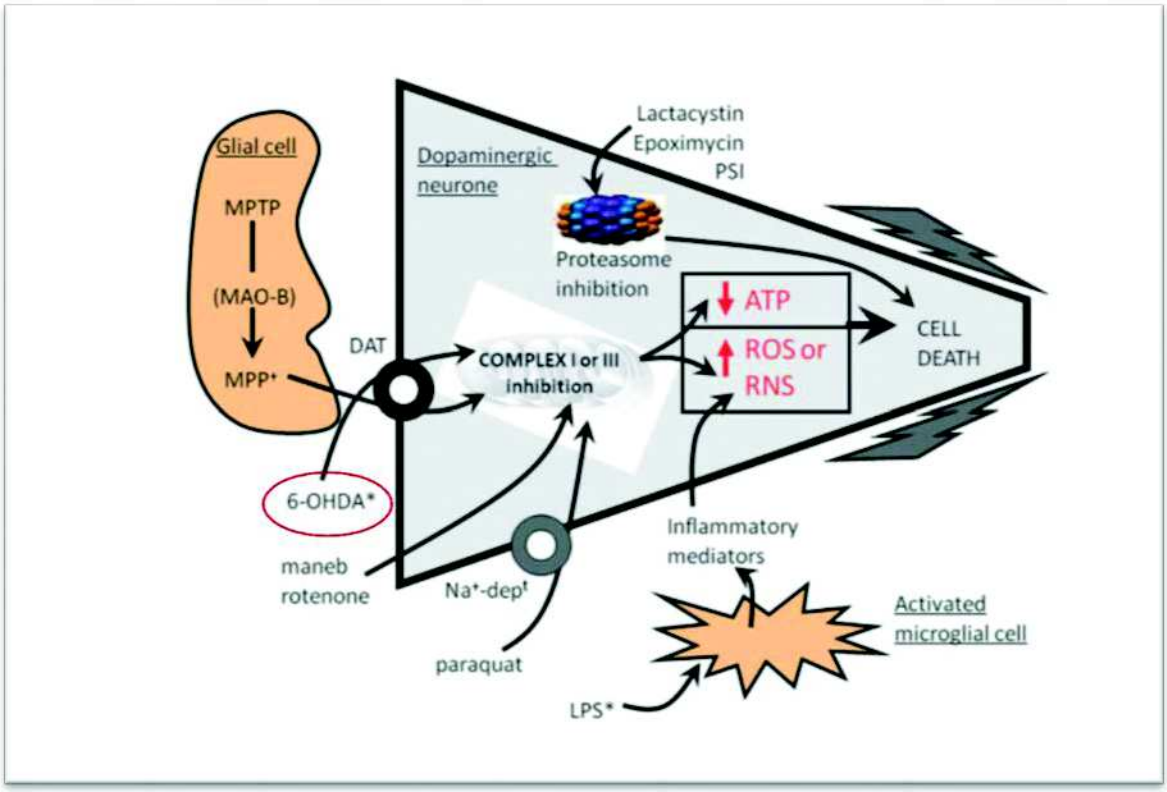

Figure 14. Schematic representation of a dopaminergic SN neuron showing the molecular targets for the various agents used to induce animal models of PD (modified from (Duty and Jenner, 2011).

AIM OF THE THESIS

The main objective of my PhD has been to explore various approaches for behavioural phenotyping, which appears to me as a fundamental and rapidly developing field of neuroscience. My work has relied on several experimental paradigms, including classical behavioural tests such as fear conditioning or nest building, but also had the ambition to further explore less controlled conditions such as spontaneous behaviour in an open field. The technical approaches for data acquisition include classical video recordings, but also a novel device that consists in an open field platform resting on highly sensitive pressure sensors, allowing to detect the slightest animal movement with unprecedented sensitivity and time resolution. I have explored the potential of this novel experimental system on a variety of behavioural conditions such as free exploration, sleep, post-surgery pain and fear, as well as on a variety of animals models of pathologies, such as Fragile-X syndrome / autism spectrum disorders, Alzheimer's and Parkinson's diseases. Applying sophisticated signal-analysis tools such as time frequency decomposition, machine learning algorithms and non linear estimations of signal complexity (ie permutation entropy and Lyapunov equation), I here demonstrate that this device can bring invaluable information for behavioural phenotyping in general, in addition to very original observations in the specific fields of fear and neurodevelopemental and neurodegenerative disorders.

In the next section, I will present my results in the following order:

1. a manuscript entitled "**Potential involvement of impaired BKCa channel function in sensory defensiveness and some behavioral disturbances induced by unfamiliar environment in a mouse model of FXS**", now published in Neuropsychopharmacology (Carreno et al., 2017)
2. a manuscript in preparation, " **Detecting fine and elaborate movement with piezo sensors, from heart beat to the temporal organization of behavior**" (Carreno et al.)
3. a manuscript entitled " **First approach to the analysis of spontaneous activity of mice based on Permutation Entropy**", now published as a proceedings of conference (IWOBI, 2015)
4. a manuscript entitled "**A non-linear dynamic approach to mouse behavioral discrimination using piezoelectric signals.**" , now in revision in Frontiers in Computational Neuroscience

RESULTS

The main objective of my PhD has been to explore various approaches for behavioural phenotyping, which appears to me as a fundamental and rapidly developing field of neuroscience. My work has relied on several experimental paradigms, including classical behavioural tests such as fear conditioning or nest building, but also had the ambition to further explore less controlled conditions such as spontaneous behaviour in an open field.

The first part of my results will present my work on the study on the phenotype of Fmr1-KO mice, a model of Fragile-X syndrome (FXS), which is a neurodevelopmental disorder characterized by a high incidence of autism spectrum disorders (ASD). During my PhD, I have found that as FXS/ASD patients, Fmr1-KO mice are very perturbed by novelty or changes in routine, resulting in hyper-activity, impaired nest building and excessive grooming of the back. These behavioral alerations are considered signs of dyscomfort. I have performed experiments to challenge the interesting clinical hypothesis of sensory defensiveness, which proposes that many behavioral problems in FXS/ASD patients result from the sensory hyper-sensitivity that is a striking characteristic of this syndrome. I have tested the effects of an agonist of potassium channels (BK-Ca cehnnels) previously shown to restore normal neuronal excitability and sensory sensitivity in *Fmr1*-KO mice, and found that it efficiently rescued the observed behavioral abnormalities. This work is now published in now published in Neuropsychopharmacology (Carreno et al., 2017) as a manuscript entitled "**Potential involvement of impaired BKCa channel function in sensory defensiveness and some behavioral disturbances induced by unfamiliar environment in a mouse model of FXS**".

The second section will present a combination of methodological and basic research results that I have performed with a novel device that consists in an open field platform resting on highly sensitive pressure sensors, allowing to detect the slightest animal movement with unprecedented sensitivity and time resolution. I have explored the potential of this novel experimental system on a variety of behavioural conditions such as free exploration, sleep, post-surgery pain and fear, as well as on a variety of animals models of pathologies, such as Fragile-X syndrome / autism spectrum disorders, Alzheimer's and Parkinson's diseases. Applying sophisticated signal-analysis tools such as time frequency decomposition, machine learning algorithms and non linear estimations of signal complexity (ie permutation entropy and Lyapunov equation), I here demonstrate that this device can bring invaluable information

for behavioural phenotyping in general, in addition to very original observations in the specific fields of fear and neurodevelopemental and neurodegenerative disorders. This work is presented as a manuscript in preparation for a methodological journal with the title "**Detecting fine and elaborate movement with piezo sensors, from heart beat to the temporal organization of behavior**" (Carreno et al.), a manuscript entitled " **First approach to the analysis of spontaneous activity of mice based on Permutation Entropy**" (Carreno et al., 2015), now published as a proceedings of conference (IWOBI, 2015), and a manuscript entitled "**A non-linear dynamic approach to mouse behavioral discrimination using piezoelectric signals**" (Moujahid et al.), now in revision in Frontiers in Computational Neuroscience.

My PhD is therefore expected to directly lead to the publication of at least 4 manuscripts, 2 of them published, one in revision, and one in preparation. Nevertheless, depending on editorial consideration of our manuscript in preparation for a methodological journal, we consider reorganizing these results and split them into 2 manuscripts, one centered on the methodological aspects, and the other specifically dedicated to our results demonstrating early motor symptoms presumably involving degeneration of the dopaminergic system in Alzheimer's disease.

Manuscript N. 1
Neuropsychopharmacology. 2017 Jul 19

Manuscript N. 1

Neuropsychopharmacology. 2017 Jul 19

Potential involvement of impaired BKCa channel function in sensory defensiveness and some behavioral disturbances induced by unfamiliar environment in a mouse model of FXS

Maria Isabel Carreno-Munoz[1,2,3], Fabienne Martins[1,2], Maria Carmen Medrano[1,2], Elisabetta Aloisi[1,2], Susanna Pietropaolo[4,5], Corentin Dechaud[1,2], Enejda Subashi[1,2], Guillaume Bony[1,2], Melanie Ginger[1,2], Abdelmalik Moujahid[3], Andreas Frick[1,2] & Xavier Leinekugel[1,2]

Neuropsychopharmacology (2017), 1–11

www.neuropsychopharmacology.org

Potential Involvement of Impaired BK_{Ca} Channel Function in Sensory Defensiveness and Some Behavioral Disturbances Induced by Unfamiliar Environment in a Mouse Model of Fragile X Syndrome

Maria Isabel Carreno-Munoz[1,2,3], Fabienne Martins[1,2], Maria Carmen Medrano[1,2], Elisabetta Aloisi[1,2], Susanna Pietropaolo[4,5], Corentin Dechaud[1,2], Enejda Subashi[1,2], Guillaume Bony[1,2], Melanie Ginger[1,2], Abdelmalik Moujahid[3], Andreas Frick[1,2] and Xavier Leinekugel[*,1,2]

[1]INSERM, Neurocentre Magendie, U1215, Bordeaux, France; [2]University of Bordeaux, Neurocentre Magendie, U1215, Bordeaux, France; [3]University of the Basque Country (UPV/EHU), Donostia, Spain; [4]University of Bordeaux, INCIA, Pessac, France; [5]CNRS, INCIA, UMR 5287, Pessac, France

In fragile X syndrome (FXS), sensory hypersensitivity and impaired habituation is thought to result in attention overload and various behavioral abnormalities in reaction to the excessive and remanent salience of environment features that would normally be ignored. This phenomenon, termed sensory defensiveness, has been proposed as the potential cause of hyperactivity, hyperarousal, and negative reactions to changes in routine that are often deleterious for FXS patients. However, the lack of tools for manipulating sensory hypersensitivity has not allowed the experimental testing required to evaluate the relevance of this hypothesis. Recent work has shown that BMS-204352, a BK_{Ca} channel agonist, was efficient to reverse cortical hyperexcitability and related sensory hypersensitivity in the *Fmr1*-KO mouse model of FXS. In the present study, we report that exposing *Fmr1*-KO mice to novel or unfamiliar environments resulted in multiple behavioral perturbations, such as hyperactivity, impaired nest building and excessive grooming of the back. Reversing sensory hypersensitivity with the BK_{Ca} channel agonist BMS-204352 prevented these behavioral abnormalities in *Fmr1*-KO mice. These results are in support of the sensory defensiveness hypothesis, and confirm BK_{Ca} as a potentially relevant molecular target for the development of drug medication against FXS/ASD.
Neuropsychopharmacology advance online publication, 16 August 2017; doi:10.1038/npp.2017.149

INTRODUCTION

Fragile X syndrome (FXS) is the most common inherited form of mental retardation and a leading known cause of autism spectrum disorder (ASD). A CGG trinucleotide repeat expansion in the promoter region of the *FMR1* gene is responsible for its transcriptional silencing (Verkerk *et al*, 1991). The resulting absence or reduced expression of the Fragile X Mental Retardation Protein (FMRP) induces a complex phenotype that often includes intellectual disability, social and communication impairment, stereotypic behavior, attention deficits, hyperactivity, hyperarousal, and sensory abnormalities (Hagerman, 2006; Merenstein *et al*, 1996).

Several lines of evidence suggest that altered sensory processing may participate in the generation of major behavioral problems in FXS. In normal individuals, sensory habituation is a progressively reduced neuronal response to repeated exposure to the same sensory stimulation, so that irrelevant stimuli can be progressively ignored and attention focused on the most salient and relevant aspects of the environment. In contrast, sensory hypersensitivity and deficit in habituation are prominent features of FXS, causing enhanced and persistent responses to stimuli of various sensory modalities (Andrea *et al*, 2013; Castrén *et al*, 2003; Ethridge *et al*, 2016; Miller *et al*, 1999; Schneider *et al*, 2013), and adverse behavioral responses to otherwise neutral sensory stimuli. This phenomenon, termed sensory defensiveness, correlates with the expression of repetitive motor patterns and behavioral rigidity in autistic children (Baranek *et al*, 1997; Miller *et al*, 1999), and has been proposed as the primary cause of hyperactivity, hyperarousal, and various deleterious behaviors such as stereotypies and even self-injury in FXS patients when confronted to change in their habits (Baranek *et al*, 1997; Contractor *et al*, 2015; Hagerman, 2006; Merenstein *et al*, 1996; Miller *et al*, 1999; Symons *et al*, 2003). The hypothesis that altered neuronal sensory processing may participate in the generation of deleterious behavior is attractive and may offer physiological

*Correspondence: Dr X Leinekugel, Neurocentre Magendie, INSERM U1215, Université de Bordeaux, 146 rue Leo Saignat, 33077 Bordeaux, France, Tel: +33 6 09 55 53 39, Fax: +33 5 57 57 36 69, E-mail: xavier.leinekugel@inserm.fr
Received 24 February 2017; revised 12 June 2017; accepted 8 July 2017; accepted article preview online 19 July 2017

targets for therapeutic intervention in FXS. However, this is yet mostly based on correlative clinical observations and it remains to be demonstrated that restoring normal sensory sensitivity can also rescue behavioral response to novelty or to changes in habits. Recent advances in preclinical research using the *Fmr1*-knockout (KO) mouse model of FXS offer tools to test this hypothesis.

The best-characterized rodent model of FXS is the *Fmr1*-KO mouse that lacks FMRP because of a disruption in the *Fmr1* gene (The Dutch-Belgian Fragile X Consortium, 1994; Mientjes *et al*, 2006). *Fmr1*-KO mice reproduce many phenotypes of FXS patients, including impaired social interactions, repetitive behavior, hyperactivity, and cognitive deficits (Hébert *et al*, 2014; Kazdoba *et al*, 2014; Michalon *et al*, 2012; Oddi *et al*, 2015; Peier *et al*, 2000; Pietropaolo *et al*, 2011). Cognitive rigidity and reduced flexibility in paradigms that involve task reversal have been reported in *Fmr1*-KO mice (Kazdoba *et al*, 2014; Kramvis *et al*, 2013), but behavioral aversion to novelty has not been much studied in this model. Interestingly, sensory hypersensitivity and impaired habituation have been shown at both behavioral and neuronal levels in *Fmr1*-KO mice (Arnett *et al*, 2014; Lovelace *et al*, 2016; Moon *et al*, 2006; Restivo *et al*, 2005; Zhang *et al*, 2014). There is clear evidence that the neocortex of *Fmr1*-KO mice is hyperexcitable (Gibson *et al*, 2008; Goncalves *et al*, 2013; Rotschafer and Razak, 2013; Zhang *et al*, 2014), pointing to a causative role for neocortical circuit defects in sensory hypersensitivity in FXS. In fact, previous work has shown that independently of its function as a translation regulator, FMRP also interacts with the $\beta 4$ regulatory subunit of big conductance voltage and Ca^{2+}-activated K+ channels (BK_{Ca}) in hippocampal and cortical excitatory neurons that influence action potential duration and neurotransmitter release (Deng and Klyachko, 2016; Deng *et al*, 2013; Myrick *et al*, 2015). Accordingly, recent work has shown that specific alterations in potassium channels are responsible for increased cortical excitability and sensory hypersensitivity in *Fmr1*-KO mice (Zhang *et al*, 2014). In this study, a dysfunction of dendritic HCN1-containing channels (responsible for I_h) as well as of dendritic and somatic BK_{Ca} in pyramidal neurons of the primary somatosensory cortex was found to result in increased intrinsic excitability by increasing input resistance, augmenting the spatial and temporal summation of excitatory synaptic potentials and by promoting the efficacy by which action potentials backpropagate into the dendrites and trigger dendritic spikes. Moreover, BK_{Ca} channel agonists such as BMS-191011 or BMS-204352 were efficient in reversing cortical hyperexcitability *in vitro* and increased acoustic startle in behaving *Fmr1*-KO mice, a widely recognized behavioral readout of sensory sensitivity previously used to assess sensory hypersensitivity in *Fmr1*-KO mice (Michalon *et al*, 2012; Nielsen *et al*, 2002).

In the present study, we have investigated the behavioral responses of *Fmr1*-KO mice exposed to novel and familiar environments differing from their home cage, and found that BMS-204352 was effective in preventing the major behavioral disturbances expressed by *Fmr1*-KO mice when removed from their usual environment. These results provide support for the sensory defensiveness hypothesis, and confirm BK_{Ca} as a pertinent molecular target for the development of drug medication against FXS/ASD.

MATERIALS AND METHODS

Animals

Naive 12–14-week-old second-generation *Fmr1*-KO mice ($n=37$) and their wild-type (WT, $n=44$) littermates were used in our study, bred and housed as in prior study from our laboratory (Zhang *et al*, 2014). Compared with the original *Fmr1* − /y mouse line (The Dutch-Belgian Fragile X Consortium *et al*, 1994), second-generation *Fmr1* knockout (Fmr1 − / − ; Fmr1 − /y) mice (Mientjes *et al*, 2006) are deficient for both FMR1 RNA and FMR protein. WT and KO male mice, socially housed in standard cages enriched with Nestlets, were individually isolated in similar standard cages 1 week before the starting point of the experimental protocol. Animals were maintained on a 12 h:12 h light/dark schedule and provided with *ad libitum* access to food and water. Pharmacological testing included intraperitoneal injection of either vehicle (type-1, vehicle for BMS-204352: 0.9% NaCl, 1.25% DMSO, 1.25% Tween-80, 10 ml per kg of body weight; type-2, vehicle for DZ: 0.9% NaCl, 0.2% alcohol, 10 ml per kg of body weight), the BK_{Ca} agonist BMS-204352 (Tocris, 2 mg per kg of body weight, dissolved in type-1 vehicle solution), as in prior studies using BMS-204352 (Hébert *et al*, 2014; Zhang *et al*, 2014), or the anxiolytic diazepam (DZ, Sigma-Aldrich, 1.5 mg/kg, dissolved in type-2 vehicle solution). All experiments were performed during the light period under constant mild luminosity (60–70 Lux). All experimental procedures were performed in accordance with the EU directives regarding the protection of animals used for experimental and scientific purposes, 86/609/EEC and 2010/63/EU. All experiments were performed in accordance with the French law and approved by the Ethical committee CEEA50 (saisine 5012024-A).

Locomotor Activity

At 30 min after injection of either vehicle or BMS-204352, the animal was individually introduced into an empty open-field chamber (45 × 33 cm arena, surrounded by 50 cm high walls and wiped clean with 70% ethanol before introduction of each animal) for behavioral monitoring. Continuous video recording was performed at a rate of 25 frames/s with a video camera (Logitech HD Webcam C270) placed 1 m above the platform, and processed offline with Ethovision XT software (Noldus Technology, Wageningen, The Netherlands) for animal tracking (X–Y coordinates of the body center). Parameters analyzed were: total distance moved, total number of rotations (ie, turn angle $>180°$ within 1 cm during locomotion periods at speed >2 cm/s), total time resting (speed <1 cm/s for at least 2 s) and ratios of total time spent in center (distance from the walls >10 cm) *vs* total time in the session, and time resting in center *vs* total time resting in the session. Self-grooming (back, belly, nose, and ears) was identified offline and tagged manually by a trained experimenter blinded to the genotype, so that we could quantify the durations of individual episodes of each type of grooming. In a series of additional control experiments, video monitoring was performed of animals placed in a new cage with nest building material and pretreated (15 min before recording) with either vehicle or the anxiolytic DZ. Locomotion was then quantified as the total distance run during the initial 1 h recording period.

Nest Building

Nest building behavior was assessed in home cage (dimensions $20 \times 10 \times 15$ cm) 1 week after individual housing, in a new environment (new and wider cage, dimensions $30 \times 15 \times 20$ cm, fresh litter, located in a different room) 4 days after testing in the home cage, and in the open field chamber after familiarization (1 h per day during 10–11 days). Nest building scoring was performed by a trained experimenter blinded to the genotype at different delays (1 to 7 h) after placing the animal in the presence of nesting material (Nestlet, 2.7 g, 2.5×2.5 cm and 5 mm thick compressed cotton), using the following standardized scoring scale (Deacon, 2006): 1: Nestlet not noticeably shredded; 2: Nestlet 10 to 50% shredded, not used as a nest; 3: Nestlet shredded 50 to 90%, but the shredded material remains scattered in the cage and is not used as a nest; 4: Nestlet shredded $>90\%$, and shredded material used as a flat nest; and 5: Nestlet shredded $>90\%$ and used as a rounded nest with sides covering the mouse. In a series of control experiments performed to validate this scaling method with an objective measure, the nest building score was additionally quantified as the normalized weight of the remaining unshredded nesting material using the following standardized scoring scale: 1: above 85% of Nestlet unshredded; 1.5: between 65 and 85% of Nestlet unshredded; 2: between 47.5 and 65% of Nestlet unshredded; 2.5: between 30 and 47.5% of Nestlet unshredded; 3: between 22.5 and 30% of Nestlet unshredded; 3.5: between 15 and 22.5% of Nestlet unshredded; 4: between 7.5 and 15% of Nestlet unshredded; and 5: $<7.5\%$ of Nestlet unshredded. As illustrated in Supplementary Figure S1, both methods for evaluation of nest building provided very similar results (correlation coefficient $= 0.91$, $p < 0.001$, $n = 66$ nests from 8 WT and 14 *Fmr1*-KO mice).

Statistics

Data processing was performed with homemade scripts and functions from the Matlab statistics toolbox (Mathworks). Descriptive statistics for all experiments are presented in Supplementary Tables S1–S3. Data were systematically tested for normal distribution with the Lilliefors test, a modification of the Kolmogorov–Smirnov test recommended for small sample sizes (Razali and Bee Wah, 2011). Data following a normal distribution were analyzed using parametric tests: ANOVA with genotype and drug condition as factors (and *post hoc* Turkey's test) for independent data sets, and Student's *t*-test for paired data. Data following nonnormal distributions were analyzed using nonparametric tests: Kruskal–Wallis (and *post hoc* Mann–Whitney *U*-test) for independent data sets and Wilcoxon signed-ranks test for paired data. Differences were considered statistically significant for values of $p < 0.05$. Data are presented as mean ± SEM.

RESULTS

In order to test the hypothesis that reversing sensory hypersensitivity may help prevent various deleterious behaviors such as stereotypies or self-injury expressed by FXS individuals when confronted to changes in their habits, we have evaluated the potential behavioral improvement of reversing sensory hypersensitivity in *Fmr1*-KO mice exposed to a novel environment. Control (WT) and *Fmr1*-KO mice pretreated with either vehicle or BMS-204352 (2 mg/kg), a drug recently shown to restore normal cortical excitability and sensory sensitivity in *Fmr1*-KO mice, were exposed for 1 h to an open-field arena that they had never visited before (novel environment). Compared with WT, *Fmr1*-KO mice placed in the novel open field showed increased total distance moved (ANOVA, $F_{genotype}(1, 53) = 49.64$, $p < 0.001$), decreased total resting time (Kruskal–Wallis $\chi^2(3, 53) = 22.17$, $p < 0.001$), and increased number of rotations ($F_{genotype}(1, 53) = 38.86$, $p < 0.001$), indicative of hyperactivity. *Fmr1*-KO mice also spent more time in the center of the arena (total time: $F_{genotype}(1, 53) = 11.93$, $p < 0.001$; resting time: $\chi^2(3, 53) = 14.63$, $p = 0.001$), possibly indicating reduced anxiety. As illustrated in Figure 1a and b, all these parameters were significantly rescued by BMS-204352 (distance moved, $F_{drug}(1, 53) = 5.72$, $p = 0.006$; total time resting, $\chi^2(3, 53) = 22.17$, $p = 0.001$; number of rotations, $F_{drug}(2, 53) = 5.89$, $p < 0.001$; total time in center, $F_{drug}(2, 41) = 11.4$, $p = 0.013$; time resting in center, $\chi^2(3, 53) = 14.63$, $p = 0.045$), being fully restored to WT values for time resting in center $\chi^2(3, 53) = 14.63$, $p = 0.75$) and time in center ($F_{genotype \times drug}(1, 53) = 17.17$, $p = 0.59$). BMS-204352 had no significant effect on WT mice.

From the literature it is not clear whether hyperactivity, one of the most consistently reported features in FXS studies (The Dutch-Belgian Fragile X Consortium, 1994; Dansie *et al*, 2013; de Diego-Otero *et al*, 2008; Kramvis *et al*, 2013; Michalon *et al*, 2012; Mineur *et al*, 2002; Oddi *et al*, 2015; Olmos-Serrano *et al*, 2011; Peier *et al*, 2000; Pietropaolo *et al*, 2011; Restivo *et al*, 2005; Spencer *et al*, 2011; The Dutch-Belgian Fragile X Consortium *et al*, 1994) is a permanent behavioral phenotype of *Fmr1*-KO mice or an adverse reaction to novelty or change in habits (due for instance to being taken away from the home cage for testing). As illustrated in Figure 2, when *Fmr1*-KO mice were exposed to the open-field chamber after a familiarization of 5 days, 1 h/day, they did not show any increase in total distance moved ($F(2, 21) = 1.89$), total time resting ($F(2, 21) = 3.84$), number of rotations ($F(2, 21) = 2.88$), total time in center ($F(2, 19) = 1.43$), or total time resting in center ($F(2, 19) = 1.45$). This suggests that hyperactivity is not a permanent phenotypic character of *Fmr1*-KO mice but rather a reaction to change. Altogether, these data suggest that restoring normal sensory sensitivity with the BK_{Ca} agonist BMS-204352 provides a rescue from the hyperactivity observed in *Fmr1*-KO mice in reaction to their exposure to a novel environment.

Beside general locomotor activity, nest building has been proposed as a highly sensitive and well-characterized assay for well-being and ability to perform activities of daily living in mice (Deacon, 2012; Jirkof, 2014). We have therefore used this test to evaluate the global behavioral perturbation induced by confronting *Fmr1*-KO mice to a change in routine (ie, either transferring them to a new cage or to a familiar environment but distinct from their home cage), and the potential benefice of restored sensory sensitivity for restoring normal behavior and well-being. As illustrated in Figure 3, WT and *Fmr1*-KO mice provided with nest building material in their home cage performed elaborated

nests within a couple of hours (no difference between WT and *Fmr1*-KO in nest building score after 2 h, Mann–Whitney, $U = 80.0$, $p = 0.66$). On the other hand, whereas WT mice were minimally perturbed in nest building when tested in a new cage or in the familiar open-field chamber (being exposed 1 h/day for 10 days before testing), *Fmr1*-KO mice appeared strongly affected by changing environment as they performed poorly in nest building in both the new cage (after 1 h, $W = 145$, $p = 0.002$; after 2 h, $W = 183.5$, $p < 0.001$) and familiar open field (cf. Figure 3b). As illustrated in Figure 4a, nest building performance in a new cage was significantly rescued in *Fmr1*-KO mice after pretreatment with BMS-204352, injected 15 min before testing (after 1 h, $\chi^2(3, 26) = 24.09$, $p = 0.008$, after 2 h, $\chi^2(3, 26) = 21.50$, $p = 0.002$), so that *Fmr1*-KO mice then performed as well as WT (after 1 h $\chi^2(3, 26) = 24.09$, $p = 0.84$, after 2 h, $\chi^2(3, 26) = 21.5$, $p = 0.76$). On the other hand, no improvement in nest building was observed in *Fmr1*-KO mice injected with DZ (after 1 h, $W = 1$, $p = 1$; after 2 h, $W = 10$, $p = 0.13$) at a dose and timing promoting anxiolytic rather than sedative effects (Dailly *et al*, 2002), as verified by the absence of statistically significant difference in locomotion between pretreatment with Vehicle or DZ (total distance run, WT+Veh *vs* WT+DZ, $t(6) = 0.80$, $p = 0.45$; KO+Veh *vs* KO +DZ, $t(7) = -1.51$, $p = 0.17$), suggesting that their impaired performance was not due to increased anxiety. In order to evaluate more precisely the potential of BMS-204352 for preventing the behavioral perturbations induced by a change in routine, *Fmr1*-KO mice were tested for nest building on 3 consecutive days in the familiar open field. As illustrated in Figure 4b, *Fmr1*-KO mice pretreated with vehicle performed poorly compared with WT for nest building in the open field

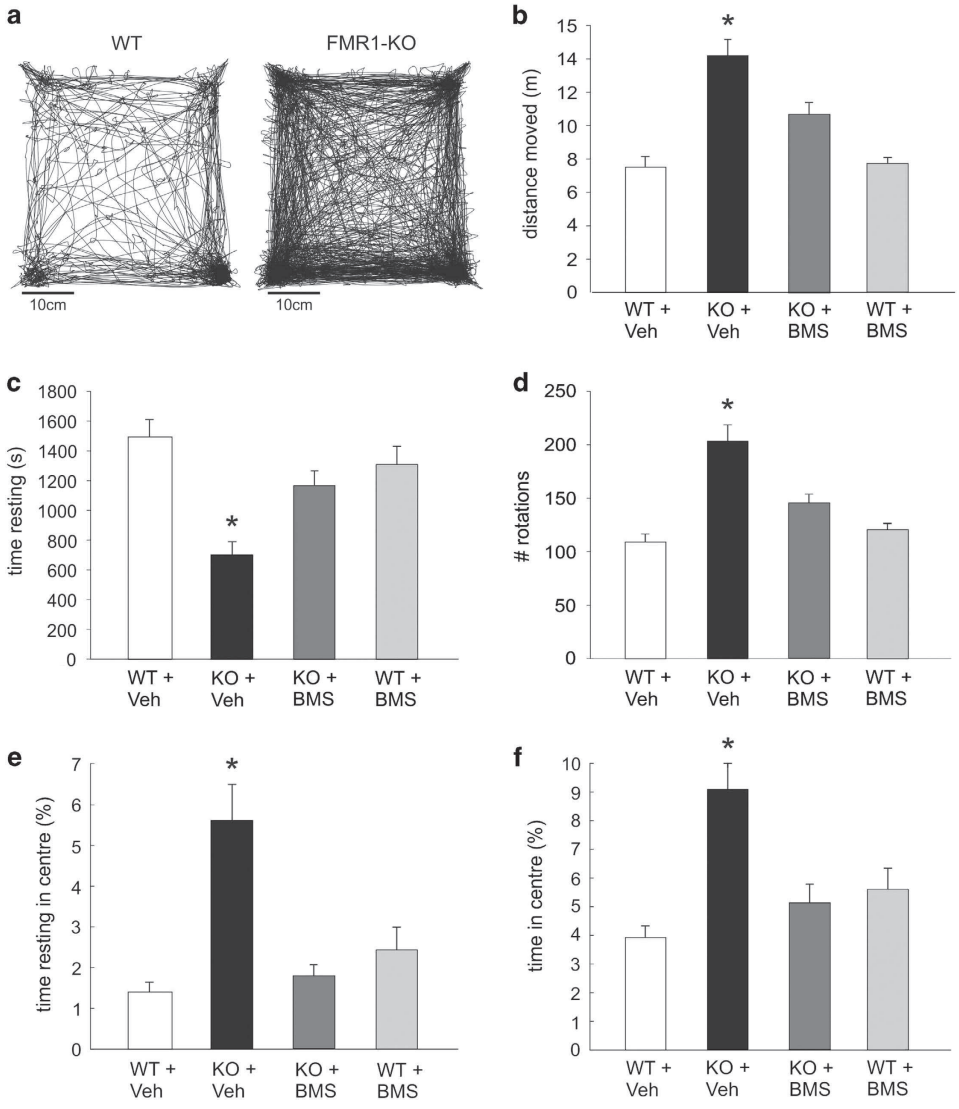

Figure 1 BMS-204352 rescue of the hyperactivity phenotype of *Fmr1*-KO mice in a novel environment. (a) Single animal (left, WT; right, *Fmr1*-KO) total trajectory during a 1 h exposure to an open field never visited before. (b–f) Summary plots of locomotor activity during the initial 1 h spent in a novel open field for WT and *Fmr1*-KO mice pretreated with either vehicle or BMS-204352 (IP injection 30 min before introduction into the open field). WT+Veh, $n = 16$, KO+Veh, $n = 13$, KO+BMS-204352, $n = 13$, WT+BMS-204352, $n = 15$. (b) Total distance moved; (c) total time resting; (d) number of rotations (angle $> 180°$); (e) total time resting in center; and (f) total time in center. *Statistically significant difference compared with all other groups ($p < 0.05$). Note the general hyperactivity of KO mice, rescued by BMS-204352 treatment.

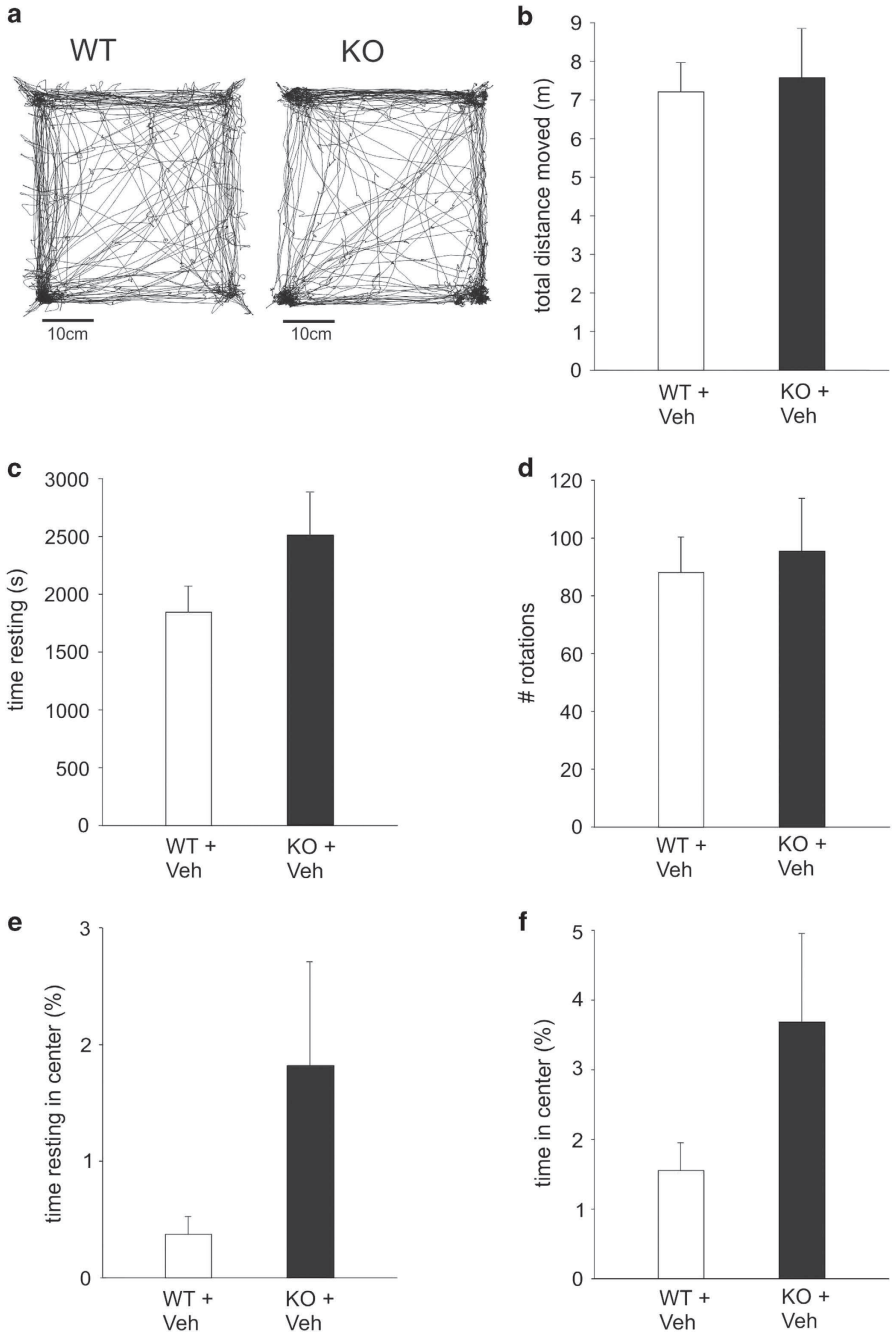

Figure 2 *Fmr1*-KO mice are not hyperactive in a familiar environment. (a) Single animal (left, WT; right, *Fmr1*-KO) total trajectory during a 1 h exploration session of an open field after familiarization (1 h/day during 5 days). (b–f) Summary plots of locomotor activity during the 1 h recording period in the familiar open field for WT and *Fmr1*-KO mice. WT, $n=8$, KO, $n=8$. (b) Total distance moved; (c) total time resting; (d) number of rotations (angle $>180°$); (e) total time resting in center; and (f) total time in center. No statistically significant effect of genotype.

after 10 days of familiarization (1 h/day) (WT+Veh *vs Fmr1*-KO+Veh on day 10: after 2 h, $U=130.0$, $p<0.001$). Their performance increased significantly when tested again the next day, after pretreatment with BMS-204352 (*Fmr1*-KO +Veh day 10 *vs Fmr1*-KO+BMS day 11: after 2 h, paired Wilcoxon signed-ranks test, $W=0$, $p=0.007$) that, on the other hand, had no significant effect on WT mice (WT+Veh day 10 *vs* WT+BMS day 11: after 2 h, Wilcoxon signed-ranks, $W=9$, $p=0.25$). The beneficial effect of BMS-204352 on *Fmr1*-KO mice was reversible as this improvement was no longer observed upon further testing for a third day, after pretreatment of the same animals with vehicle (*Fmr1*-KO +Veh day 10 *vs Fmr1*-KO+Veh day 12, after 2 h, $W=19.5$, $p=0.75$).

Therefore, *Fmr1*-KO mice are deeply perturbed by changes in environment or in daily routine, as FXS patients in whom such situations promote repetitive behavior and even often self-injury. Because repetitive behavior in mice can be expressed as excessive self grooming, we compared the amount of time that WT and *Fmr1*-KO mice exposed to a

novel environment dedicated to grooming activity. As illustrated in Figure 5, we found no effect of genotype (WT *vs Fmr1*-KO) or drug (Veh *vs* BMS) on total grooming time ($\chi^2(3, 28) = 3.04$). On the other hand, when we discriminated between distinct types of self-grooming (ie, back, belly, nose, and ears), we did observe that *Fmr1*-KO mice had excessive grooming of the back, both in terms of number and duration of grooming episodes (total time $F_{genotype}(1, 28) = 2.5$, $p = 0.001$; number of events $\chi^2(3, 28) = 12.92$, $p = 0.047$; mean duration of events $F_{genotype}(1, 28) = 2.79$, $p = 0.001$). As illustrated in Figure 5 and Supplementary Figure S2, this increase was specific to grooming the back, because there was no difference in the number or duration of belly-, nose-, or ears-grooming episodes (belly: total time, $\chi^2(3, 28) = 6.16$; number of events, $F_{genotype}(1, 28) = 0.91$, mean duration of events, $F_{genotype}(1, 28) = 0.69$; nose: total time, $\chi^2(2, 18) = 3.66$, number of events, $F_{genotype}(1, 28) = 0.25$, mean duration of events, $\chi^2(2, 18) = 5.41$; ears: total time, $F_{genotype}(1, 28) = 0.7$, number of events, $F_{genotype}(1, 28) = 0.47$, mean duration of events, $\chi^2(2, 18) = 6.04$). Moreover, increased grooming of the back was rescued to normal levels by pretreatment with BMS-204352 (*Fmr1*-KO *vs Fmr1*-KO +BMS: total time, $F_{drug}(1, 28) = 3.28$, $p = 0.001$; number of events, $\chi^2(3, 28) = 12.93$, $p = 0.037$; mean duration of events $F_{drug}(1, 28) = 4.03$, $p < 0.001$; WT *vs Fmr1*-KO+BMS: total time, $F_{genotype \times drug}(1, 28) = 20.18$, $p = 0.998$; number of events, $\chi^2(3, 28) = 12.93$, $p = 0.999$; mean duration of events, $F_{genotype \times drug}(1, 28) = 18.9$, $p = 0.995$). Even though the effect did not reach statistical significance, there was a tendency for increased grooming of the back following pretreatment with BMS-204352 in WT mice (*WT*+Veh *vs WT*+BMS: total time, $F_{drug}(1, 28) = 3.28$, $p = 0.25$; number of events, $\chi^2(3, 28) = 12.93$, $p = 0.08$; mean duration of events, $F_{drug}(1, 28) = 4.03$, $p = 0.37$). This side effect does not account for the recovery exerted by BMS-204352 pretreatment in *Fmr1*-KO

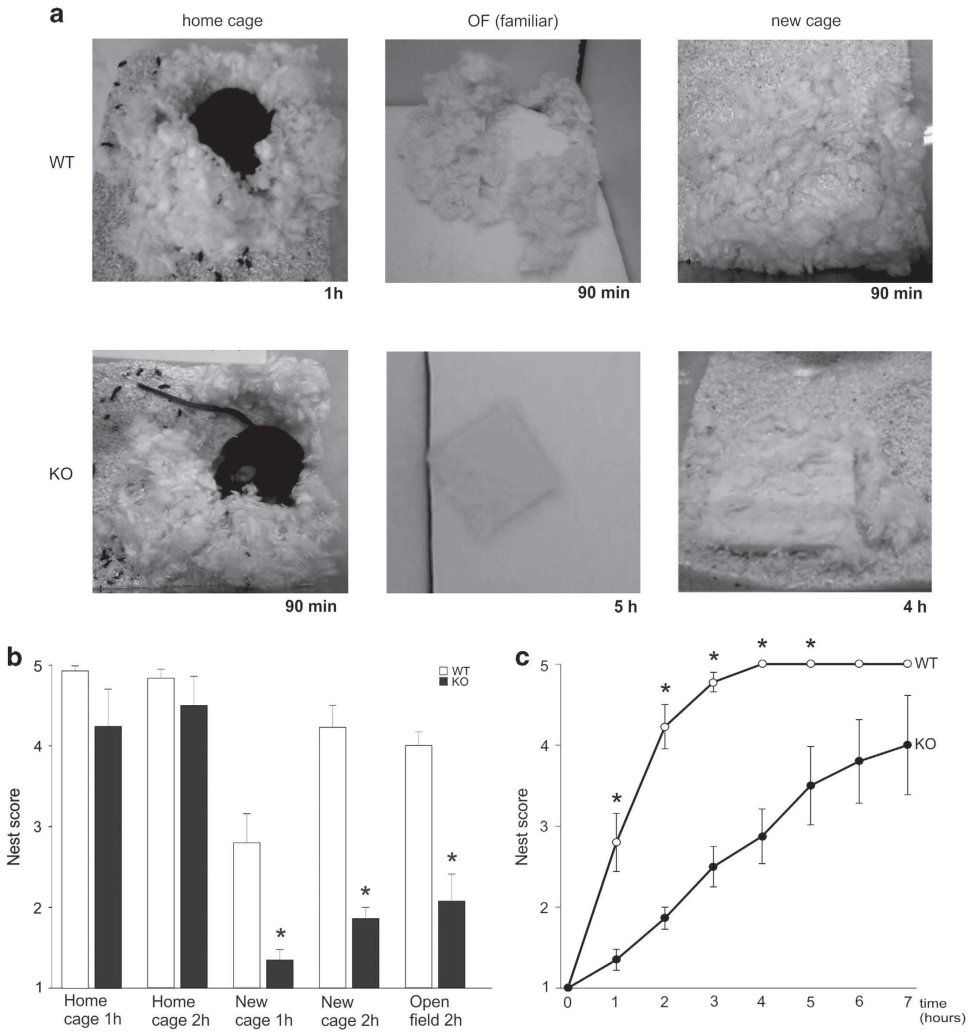

Figure 3 Impaired nest building for *Fmr1*-KO mice outside home cage. (a) Illustration of nest building performance for individual WT and *Fmr1*-KO mice in their home cage (left), familiar open field (OF, familiarization 1 h/day during 9 days), and new cage (right). The pictures were taken at the time indicated (between 1 h and 5 h after introduction of the nest building material). Note that the WT mouse had terminated nest building after 90 min in all tested conditions, whereas the KO mouse performed well in its home cage but not in the familiar open field or in a new cage. (b) Summary plots of nest building scores in home cage, new cage, and familiar open field for WT and *Fmr1*-KO mice. (c) Summary plot of nest building over time for WT and *Fmr1*-KO mice in a new cage. Note that WT mice complete nest building within 2 to 3 h in any tested condition, whereas KO mice have delayed nest building. (b, c) *Statistically significant effect of genotype ($p < 0.05$).

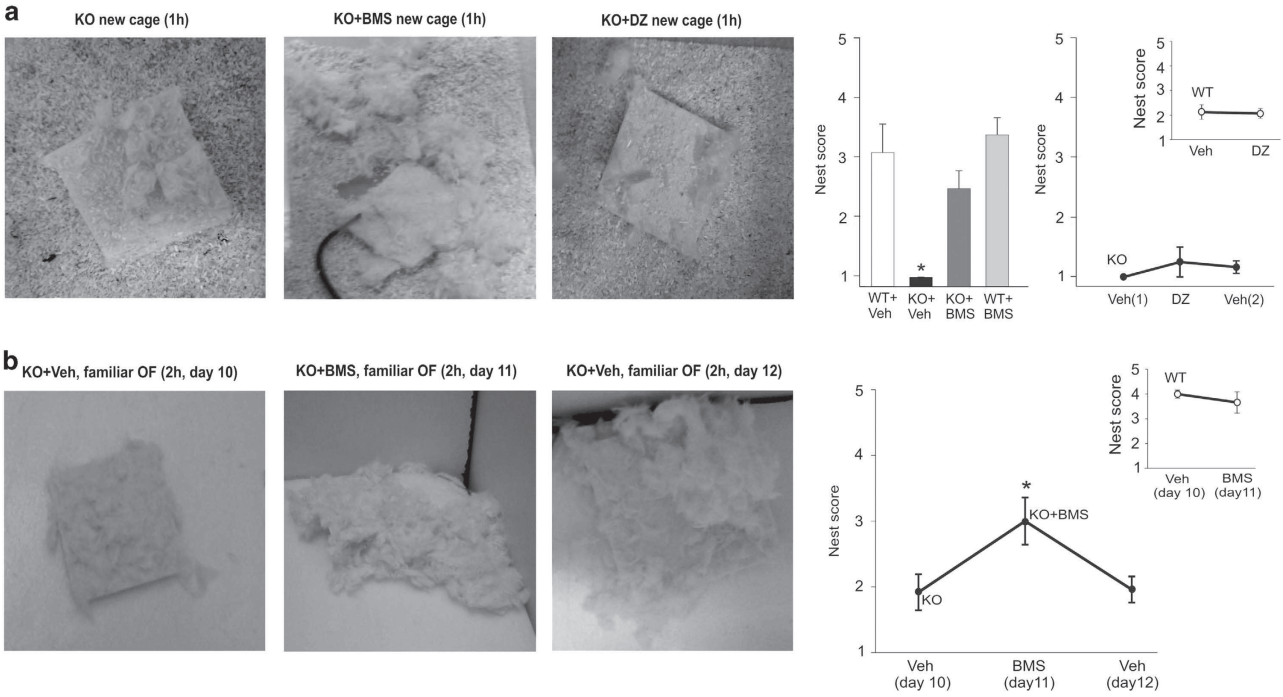

Figure 4 BMS-204352 but not diazepam rescue of nest building in familiar open field and new cage. (a) Illustration of nest building performance of *Fmr1*-KO mice after 1 h in a new cage after vehicle (left), BMS-204352 (middle), or diazepam (DZ, right) injection. Summary plots of nest building performance after 1 h, following treatment with either vehicle or BMS-204352 (left, 5 WT+Veh, 5 WT+BMS, 12 *Fmr1*-KO+Veh, and 9 *Fmr1*-KO+BMS). The effect on nest building of the anxiolytic DZ, tested against that of vehicle (Veh) on the same animals but on consecutive days (8 WT and 6 *Fmr1*-KO mice tested consecutively with vehicle, DZ, and for *Fmr1*-KO mice vehicle again), is illustrated on the right plots. *$P<0.05$ compared with all other groups. (b) Illustration of nest building performance of *Fmr1*-KO mice treated either with vehicle (days 10 and 12) or BMS-204352 (day 11) after 2 h in a familiar (1 h/day during 9 days) open field. Summary plot of nest building performance on days 10 (treatment = vehicle), 11 (BMS-204352), and 12 (vehicle) for *Fmr1*-KO ($n=15$) mice. Inset, nest building performance on days 10 (treatment = vehicle) and 11 (BMS-204352) for WT mice ($n=12$). *$P<0.05$ compared with Veh (day 10) and Veh (day 12). Note the reversible rescue of nest building performance in *Fmr1*-KO mice with the BMS-204352 treatment.

mice, with which grooming of the back was reduced to WT level.

DISCUSSION

The main objective of this study was to experimentally address the hypothesis, derived from clinical observations, that specific physiological deficits in cortical circuits, responsible for sensory hypersensitivity and lack of habituation, are also involved in the sensory defensiveness and major behavioral disturbances expressed by FXS patients exposed to unusual environmental situations or changes in their routine. Even though mouse studies do not always allow to predict the outcome of human studies, we have used *Fmr1*-KO mice as a model of FXS, and the BK_{Ca} agonist BMS-204352 as a tool to restore normal cortical excitability and sensory sensitivity in *Fmr1*-KO mice. Treated and untreated animals were exposed to changes in their daily routine by being transferred to a new environment or removed from their home cage for 1 to 2 h. We found that in such cases, *Fmr1*-KO mice expressed a range of behavioral perturbations. Normalizing neuronal excitability with the BK_{Ca} channel agonist BMS-204352, at a dose previously shown to rescue behaviorally measured sensory hyperresponsiveness (Zhang *et al*, 2014), prevented these behavioral disorders in *Fmr1*-KO mice. These results lend support to the sensory defensiveness hypothesis, by considering a relationship between altered sensory sensitivity and alterations in behaviors only indirectly related to sensory processing. Nevertheless, the case of a patient carrying a point mutation in *FMR1* (R138Q), which was shown in *FMR1*-KO mice to result in impaired FMRP-mediated modulation of BK_{Ca} channels (Myrick *et al*, 2015), emphasizes the complexity of FXS. This patient presented a history of intellectual disability and intractable epilepsy, but not the other maladaptive behaviors commonly associated with FXS or autism, such as stereotypic behaviors, hyperactivity, impulsivity, physical aggressiveness, difficulty with changes or transitions, or problems with sleeping or eating. Although this observation suggests a direct link between BK_{Ca} impairment, severe neurodevelopmental deficits and dysregulation in circuit excitability, it also points at the involvement of other factors, potentially interacting with BK_{Ca} impairment, in the variety of phenotypic traits associated with FXS. Moreover, it is important to note that BK_{Ca} channels are expressed ubiquitously. Consequently, the beneficial effects of BMS-204352 may also be mediated by a variety of physiological targets independent of cortical excitability and sensory sensitivity. Further studies will be necessary to evaluate in which respect other deficits reversed in *Fmr1*-KO mice by the restoration of BK_{Ca} function, such as altered hippocampal physiology, impaired social interactions, and spatial memory (Deng and Klyachko, 2016; Hébert *et al*, 2014), involve or not the reversal of cortical

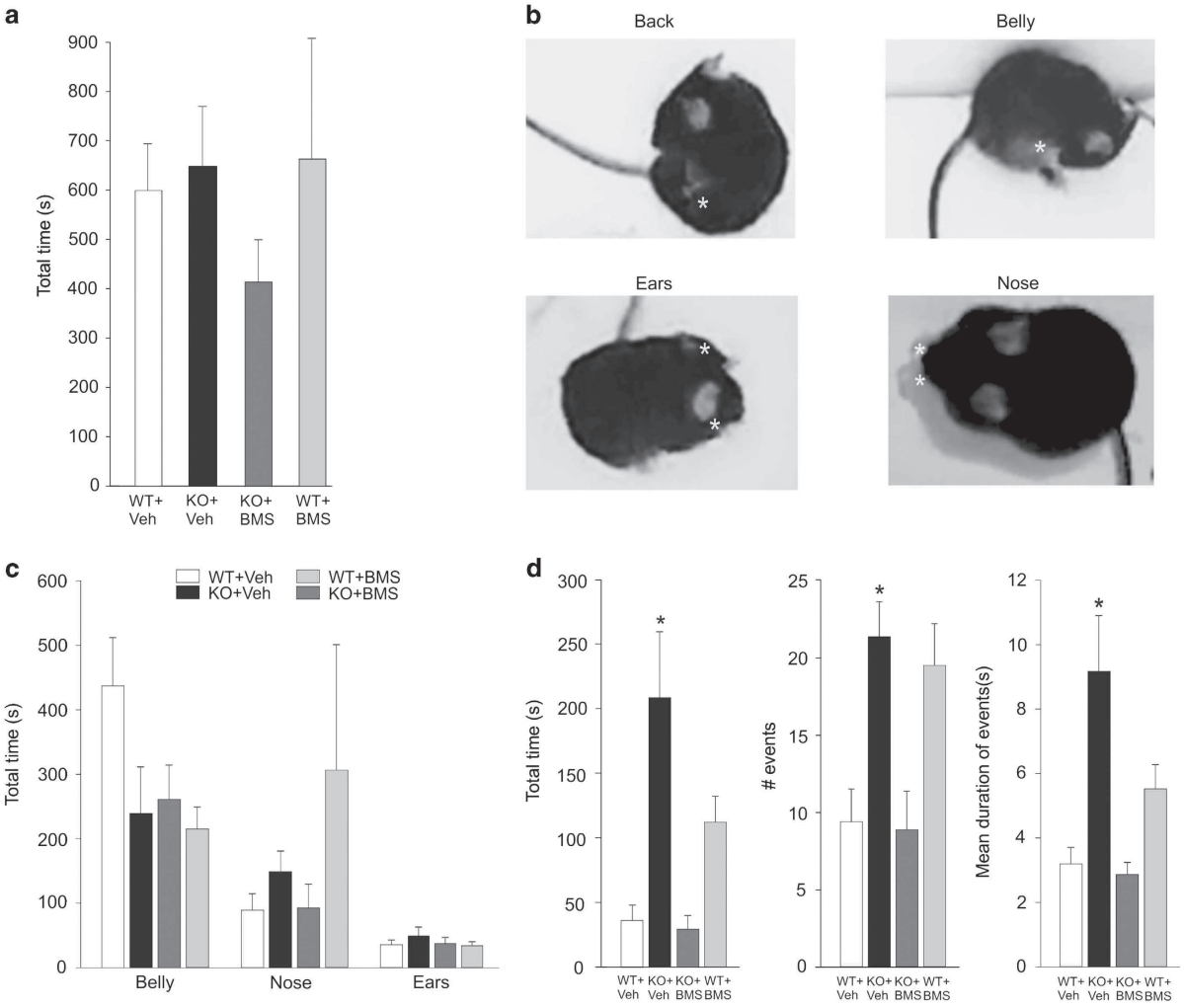

Figure 5 BMS-204352 prevents excessive self-grooming of the back in *Fmr1*-KO mice exposed to a novel environment. Wild-type (WT) and *Fmr1*-KO mice (KO) treated either with vehicle (Veh) or BMS-204352 (BMS) were exposed for 1 h to a novel open field. Total grooming time (a) or specific grooming of the back, belly, nose, or ears (b–d) were quantified (number of animals: 8 WT, 8 *Fmr1*-KO). (a) Total self-grooming time. (b) Pictures showing the four different types of self-grooming activities quantified in (c, d) (*position of paws). (c) Total time spent in grooming the belly, nose, or ears. (d) Total time (left plot), number (middle), and mean duration (right) of events for grooming the back. $^{*}P<0.05$ compared with WT+Veh and KO+BMS. Note the excessive grooming of the back in *Fmr1*-KO mice, an effect fully rescued by BMS-204352.

hyperexcitability and sensory hypersensitivity. Altogether, our results provide further evidence for BK_{Ca} as a potentially important molecular target for the development of drug medication against FXS/ASD. The BK_{Ca} channel agonist BMS-204352 has been approved for human use, having no toxicity or adverse effects (Jensen, 2002). Provided that our observations prove relevant to humans, it is an interesting candidate for clinical trials involving FXS patients, as a complement or alternative to approaches targeting mGluR1-/5 that proved effective in mice but not yet in patients (Krueger and Bear, 2011; Michalon *et al*, 2012).

Some concerns have been expressed in the literature regarding dissimilarities between sensory processing alterations in FXS patients and *Fmr1*-KO mice. Acoustic startle is often considered a behavioral readout of sensory sensitivity and prepulse inhibition (PPI) of acoustic startle to reflect sensory gating. Increased startle and decreased PPI are consistently observed in FXS patients (Frankland *et al*, 2004; Kazdoba *et al*, 2014; Perry *et al*, 2007; Yuhas *et al*, 2011), reflecting increased sensory sensitivity and decreased gating. On the other hand, both increased and decreased startle responses have been reported in *Fmr1*-KO mice, and PPI has often but not always been reported to be increased in *Fmr1*-KO mice, as discussed in a recent review (Kazdoba *et al*, 2014). A potential cause of discrepancy is that startle and PPI in mice seem to depend on stimulus intensity, with increased startle and decreased PPI at low intensities but the opposite with loud auditory stimuli (Nielsen *et al*, 2002). Decreased PPI in *Fmr1*-KO mice has thus been proposed to result from increased perception of the weak prestimulus (Chen and Toth, 2001). Moreover, all studies directly measuring spontaneous cortical activity or the neuronal response to sensory stimulations in *Fmr1*-KO mice reported increased neuronal excitability (Goncalves *et al*, 2013; Zhang *et al*, 2014) and sensory responses (Arnett *et al*, 2014; Rotschafer and Razak, 2013; Zhang *et al*, 2014) that can even lead to audiogenic seizures (Chen and Toth, 2001; Dansie *et al*, 2013; Musumeci *et al*, 2000). In addition, studies in

which habituation has been tested directly, either from behavior (Moon *et al*, 2006; Restivo *et al*, 2005) or neuronal (Lovelace *et al*, 2016) readout, have reported impaired habituation in *Fmr1*-KO mice. Therefore, sensory hypersensitivity and reduced habituation seem clearly established in both *Fmr1*-KO mice and clinical FXS. Furthermore, pharmacological interventions using the *Fmr1*-KO mouse have demonstrated predictive validity for this model (Kazdoba *et al*, 2014), as the results from several drug studies in *Fmr1*-KO mice have paralleled findings from human FXS treatment trials (eg, minocycline (Paribello *et al*, 2010) and lithium (Berry-Kravis *et al*, 2008)). We therefore believe that our results may have translational value for defining pharmacological intervention to treat FXS patients.

The behavioral readouts of our study include locomotor activity, nest building, and self-grooming. The preclinical literature contains some uncertainty regarding whether hyperactivity is a reaction to novelty (Kramvis *et al*, 2013) or a permanent phenotype (de Diego-Otero *et al*, 2008) of FXS. Our results suggest that this is a reaction to novelty, because we did not observe an hyperactive phenotype after familiarization. It is interesting to note that *Fmr1*-KO mice were previously found to be still hyperactive after 24 h in the testing environment (de Diego-Otero *et al*, 2008), suggesting that habituation is less stressful for *Fmr1*-KO mice when performed progressively over several days (1 h/day for 5 to 10 days in our study).

Expression of increased grooming has been reported in *Fmr1*-KO mice as an emotional response to cognitive or social challenge (McNaughton *et al*, 2008; Moon *et al*, 2008). In keeping with a previous study on *Fmr1*-KO mice exposed to a novel open field (Mineur *et al*, 2002), our results do not show any difference in total self-grooming time. However, analysis of distinct grooming types revealed specific excessive grooming of the back in *Fmr1*-KO mice exposed to the novel open field, a phenotype reversed by pretreatment with BMS-204352. Previous work has shown that the behavioral microstructure of self-grooming in rodents may serve as a sensitive marker of stress levels, even without significant change in overall grooming time (Song *et al*, 2016). Increased caudal self-grooming has been reported as a response to relatively moderate aversive conditions such as bright light and novelty exposure (Meshalkina and Kalueff, 2016; van Erp *et al*, 1994). We therefore suggest that in our mouse line, grooming of the back may be a relevant index of FXS-related repetitive behavior, and that this sign of discomfort can be alleviated by BMS-204352, a treatment rescuing cortical hyperexcitability, sensory hypersensitivity, and behavioral hyperarousal.

Nest building has been proposed as an index of well-being and the ability to perform activities of daily living (Jirkof, 2014) that is finally one of the most important objectives of clinical intervention. The fact that *Fmr1*-KO mice showed a clear impairment in nest building suggests that they are highly perturbed when exposed to novelty or even to situations out of their daily routine, as also are FXS or ASD patients. The behavioral rescue provided by BMS-204352 is compatible with the clinical hypothesis that restoring normal sensory sensitivity may indeed be a decisive way of restoring well-being in FXS or ASD, and points to BK_{Ca} as a potentially relevant physiological target for therapeutic drug development. Our protocol of alternation of vehicle and BMS-204352 treatment on 3 consecutive days nevertheless shows that the effects of BMS-204352 on nest building performance are transitory. Further studies are awaited to evaluate the potential beneficial effects of chronic BMS-204352 delivery, as well as the development of more stable molecules allowing long-term corrective action on BK_{Ca} channels.

FUNDING AND DISCLOSURE

The authors declare no conflict of interest.

ACKNOWLEDGMENTS

We thank Nora Abrous and Guillaume Lucas for feedback on the manuscript. This work was supported by funding from INSERM, CNRS, and Agence Nationale pour la Recherche (ANR). We thank the Animal Housing and Genotyping facilities, supported by funding from INSERM and LabEX BRAIN (ANR-10-LABX-43). MICM was supported by an international PhD fellowship (ANR-10-IDEX--03-02). The funders had no role in study design, data collection and analysis, decision to publish, or preparation of the manuscript.

AUTHOR CONTRIBUTIONS

XL conceived the project. MICM, MG, AF, and XL planned the research. MICM, FM, MCM, EA, CD, ES, GB, MG, and XL performed data acquisition. MICM, FM, EA, CD, SP, GB, AM, and XL analyzed the data. MICM and XL wrote the paper and all other authors provided feedback.

REFERENCES

Andrea S, Jacena LM, Patrick A, Rawi N, Tasleem C, John O *et al* (2013). Electrocortical changes associated with minocycline treatment in fragile X syndrome. *J Psychopharmacol (Oxford, England)* **27**: 956–963.

Arnett MT, Herman DH, McGee AW (2014). Deficits in tactile learning in a mouse model of fragile X syndrome. *PLoS ONE* **9**: e109116.

Baranek GT, Foster LG, Berkson G (1997). Tactile defensiveness and stereotyped behaviors. *Am J Occup Ther* **51**: 91–95.

Berry-Kravis E, Sumis A, Hervey C, Nelson M, Porges SW, Weng N *et al* (2008). Open-label treatment trial of lithium to target the underlying defect in fragile X syndrome. *J Dev Behav Pediatr* **29**: 293–302.

Castrén M, Pääkkönen A, Tarkka IM, Ryynänen M, Partanen J (2003). Augmentation of auditory N1 in children with fragile X syndrome. *Brain Topogr* **15**: 165–171.

Chen L, Toth M (2001). Fragile X mice develop sensory hyperreactivity to auditory stimuli. *Neuroscience* **103**: 1043–1050.

Contractor A, Klyachko VA, Portera-Cailliau C (2015). Altered neuronal and circuit excitability in fragile X syndrome. *Neuron* **87**: 699–715.

Dailly E, Hascoët M, Colombel MC, Jolliet P, Bourin M (2002). Relationship between cerebral pharmacokinetics and anxiolytic activity of diazepam and its active metabolites after a single intraperitoneal administration of diazepam in mice. *Hum Psychopharmacol* **17**: 239–245.

Dansie LE, Phommahaxay K, Okusanya AG, Uwadia J, Huang M, Rotschafer SE *et al* (2013). Long-lasting effects of minocycline on

behavior in young but not adult Fragile X mice. *Neuroscience* **246**: 186–198.

de Diego-Otero Y, Romero-Zerbo Y, Bekay RE, Decara J, Sanchez L, Fonseca FR-D *et al* (2008). [alpha]-Tocopherol protects against oxidative stress in the fragile X knockout mouse: an experimental therapeutic approach for the Fmr1 deficiency. *Neuropsychopharmacology* **34**: 1011–1026.

Deacon R (2012). Assessing burrowing, nest construction, and hoarding in mice. *J Vis Exp*: e2607.

Deacon RMJ (2006). Assessing nest building in mice. *Nat Protoc* **1**: 1117–1119.

Deng PY, Klyachko VA (2016). Genetic upregulation of BK channel activity normalizes multiple synaptic and circuit defects in a mouse model of fragile X syndrome. *J Physiol* **594**: 83–97.

Deng PY, Rotman Z, Blundon JA, Cho Y, Cui J, Cavalli V *et al* (2013). FMRP regulates neurotransmitter release and synaptic information transmission by modulating action potential duration via BK channels. *Neuron* **77**: 696–711.

The Dutch-Belgian Fragile X Consortium, Bakker CE, Verheij C, Willemsen R, van der Helm R, Oerlemans F *et al* (1994). Fmr1 knockout mice: a model to study fragile X mental retardation. *Cell* **78**: 23–33.

Ethridge LE, White SP, Mosconi MW, Wang J, Byerly MJ, Sweeney JA (2016). Reduced habituation of auditory evoked potentials indicate cortical hyper-excitability in fragile X syndrome. *Transl Psychiatry* **6**: e787.

Frankland PW, Wang Y, Rosner B, Shimizu T, Balleine BW, Dykens EM *et al* (2004). Sensorimotor gating abnormalities in young males with fragile X syndrome and Fmr1-knockout mice. *Mol Psychiatry* **9**: 417–425.

Gibson JR, Bartley AF, Hays SA, Huber KM (2008). Imbalance of neocortical excitation and inhibition and altered UP states reflect network hyperexcitability in the mouse model of fragile X syndrome. *J Neurophysiol* **100**: 2615–2626.

Goncalves JT, Anstey JE, Golshani P, Portera-Cailliau C (2013). Circuit level defects in the developing neocortex of Fragile X mice. *Nat Neurosci* **16**: 903–909.

Hagerman RJ (2006). Lessons from fragile X regarding neurobiology, autism, and neurodegeneration. *J Dev Behav Pediatr* **27**: 63–74.

Hébert B, Pietropaolo S, Même S, Laudier B, Laugeray A, Doisne N *et al* (2014). Rescue of fragile X syndrome phenotypes in Fmr1 KO mice by a BKCa channel opener molecule. *Orphanet J Rare Dis* **9**: 1–10.

Jensen BS (2002). BMS-204352: a potassium channel opener developed for the treatment of stroke. *CNS Drug Rev* **8**: 353–360.

Jirkof P (2014). Burrowing and nest building behavior as indicators of well-being in mice. *J Neurosci Methods* **234**: 139–146.

Kazdoba TM, Leach PT, Silverman JL, Crawley JN (2014). Modeling fragile X syndrome in the Fmr1 knockout mouse. *Intractable Rare Dis Res* **3**: 118–133.

Kramvis I, Mansvelder H, Loos M, Meredith R (2013). Hyperactivity, perseveration and increased responding during attentional rule acquisition in the fragile X mouse model. *Front Behav Neurosci* **7**: 172.

Krueger DD, Bear MF (2011). Toward fulfilling the promise of molecular medicine in fragile X syndrome. *Annu Rev Med* **62**: 411–429.

Lovelace JW, Wen TH, Reinhard S, Hsu MS, Sidhu H, Ethell IM *et al* (2016). Matrix metalloproteinase-9 deletion rescues auditory evoked potential habituation deficit in a mouse model of Fragile X Syndrome. *Neurobiol Dis* **89**: 126–135.

McNaughton CH, Moon J, Strawderman MS, Maclean KN, Evans J, Strupp BJ (2008). Evidence for social anxiety and impaired social cognition in a mouse model of fragile X syndrome. *Behav Neurosci* **122**: 293–300.

Merenstein SA, Sobesky WE, Taylor AK, Riddle JE, Tran HX, Hagerman RJ (1996). Molecular-clinical correlations in males with an expanded FMR1 mutation. *Am J Med Genet* **64**: 388–394.

Meshalkina DA, Kalueff AV (2016). Commentary: Ethological evaluation of the effects of social defeat stress in mice: beyond the social interaction ratio. *Front Behav Neurosci* **10**: 155.

Michalon A, Sidorov M, Ballard Theresa M, Ozmen L, Spooren W, Wettstein Joseph G *et al* (2012). Chronic pharmacological mGlu5 inhibition corrects fragile X in adult mice. *Neuron* **74**: 49–56.

Mientjes EJ, Nieuwenhuizen I, Kirkpatrick L, Zu T, Hoogeveen-Westerveld M, Severijnen L *et al* (2006). The generation of a conditional Fmr1 knock out mouse model to study Fmrp function in vivo. *Neurobiol Dis* **21**: 549–555.

Miller LJ, McIntosh DN, McGrath J, Shyu V, Lampe M, Taylor AK *et al* (1999). Electrodermal responses to sensory stimuli in individuals with fragile X syndrome: a preliminary report. *Am J Med Genet* **83**: 268–279.

Mineur YS, Sluyter F, Wit S, Oostra BA, Crusio WE (2002). Behavioral and neuroanatomical characterization of the Fmr1 knockout mouse. *Hippocampus* **12**: 39–46.

Moon J, Beaudin AE, Verosky S, Driscoll LL, Weiskopf M, Levitsky DA *et al* (2006). Attentional dysfunction, impulsivity, and resistance to change in a mouse model of fragile X syndrome. *Behav Neurosci* **120**: 1367–1379.

Moon J, Ota KT, Driscoll LL, Levitsky DA, Strupp BJ (2008). A mouse model of fragile X syndrome exhibits heightened arousal and/or emotion following errors or reversal of contingencies. *Dev Psychobiol* **50**: 473–485.

Musumeci SA, Bosco P, Calabrese G, Bakker C, De Sarro GB, Elia M *et al* (2000). Audiogenic seizures susceptibility in transgenic mice with fragile X syndrome. *Epilepsia* **41**: 19–23.

Myrick LK, Deng P-Y, Hashimoto H, Oh YM, Cho Y, Poidevin MJ *et al* (2015). Independent role for presynaptic FMRP revealed by an FMR1 missense mutation associated with intellectual disability and seizures. *Proc Natl Acad Sci USA* **112**: 949–956.

Nielsen DM, Derber WJ, McClellan DA, Crnic LS (2002). Alterations in the auditory startle response in Fmr1 targeted mutant mouse models of fragile X syndrome. *Brain Res* **927**: 8–17.

Oddi D, Subashi E, Middei S, Bellocchio L, Lemaire-Mayo V, Guzman M *et al* (2015). Early social enrichment rescues adult behavioral and brain abnormalities in a mouse model of fragile X syndrome. *Neuropsychopharmacology* **40**: 1113–1122.

Olmos-Serrano JL, Corbin JG, Burns MP (2011). The GABA-A receptor agonist THIP ameliorates specific behavioral deficits in the mouse model of fragile X syndrome. *Dev Neurosci* **33**: 395–403.

Paribello C, Tao L, Folino A, Berry-Kravis E, Tranfaglia M, Ethell IM *et al* (2010). Open-label add-on treatment trial of minocycline in fragile X syndrome. *BMC Neurol* **10**: 91.

Peier AM, McIlwain KL, Kenneson A, Warren ST, Paylor R, Nelson DL (2000). (Over)correction of FMR1 deficiency with YAC transgenics: behavioral and physical features. *Hum Mol Genet* **9**: 1145–1159.

Perry W, Minassian A, Lopez B, Maron L, Lincoln A (2007). Sensorimotor gating deficits in adults with autism. *Biol Psychiatry* **61**: 482–486.

Pietropaolo S, Guilleminot A, Martin B, D'Amato FR, Crusio WE (2011). Genetic-background modulation of core and variable autistic-like symptoms in Fmr1 knock-out mice. *PLoS ONE* **6**: e17073.

Razali NM, Bee Wah Y (2011). Power comparisons of Shapiro-Wilk, Kolmogorov-Smirnov, Lilliefors and Anderson-Darling tests. *J Stat Model Analyt* **2**: 21–33.

Restivo L, Ferrari F, Passino E, Sgobio C, Bock J, Oostra BA *et al* (2005). Enriched environment promotes behavioral and

morphological recovery in a mouse model for the fragile X syndrome. *Proc Natl Acad Sci USA* **102**: 11557–11562.

Rotschafer S, Razak K (2013). Altered auditory processing in a mouse model of fragile X syndrome. *Brain Res* **1506**: 12–24.

Schneider A, Leigh MJ, Adams P, Nanakul R, Chechi T, Olichney J *et al* (2013). Electrocortical changes associated with minocycline treatment in fragile X syndrome. *J Psychopharmacol* **27**: 956–963.

Song C, Berridge KC, Kalueff AV (2016). 'Stressing' rodent self-grooming for neuroscience research. *Nat Rev Neurosci* **17**: 591–591.

Spencer CM, Alekseyenko O, Hamilton SM, Thomas AM, Serysheva E, Yuva-Paylor LA *et al* (2011). Modifying behavioral phenotypes in Fmr1KO mice: genetic background differences reveal autistic-like responses. *Autism Res* **4**: 40–56.

Symons FJ, Clark RD, Hatton DD, Skinner M, Bailey DB (2003). Self-injurious behavior in young boys with fragile X syndrome. *Am J Med Genet A* **118A**: 115–121.

van Erp AMM, Kruk MR, Meelis W, Willekens-Bramer DC (1994). Effect of environmental stressors on time course, variability and form of self-grooming in the rat: handling, social contact, defeat, novelty, restraint and fur moistening. *Behav Brain Res* **65**: 47–55.

Verkerk AJMH, Pieretti M, Sutcliffe JS, Fu Y-H, Kuhl DPA, Pizzuti A *et al* (1991). Identification of a gene (FMR-1) containing a CGG repeat coincident with a breakpoint cluster region exhibiting length variation in fragile X syndrome. *Cell* **65**: 905–914.

Yuhas J, Cordeiro L, Tassone F, Ballinger E, Schneider A, Long JM *et al* (2011). Brief report: sensorimotor gating in idiopathic autism and autism associated with fragile X syndrome. *J Autism Dev Disord* **41**: 248–253.

Zhang Y, Bonnan A, Bony G, Ferezou I, Pietropaolo S, Ginger M *et al* (2014). Dendritic channelopathies contribute to neocortical and sensory hyperexcitability in Fmr1(− /y) mice. *Nat Neurosci* **17**: 1701–1709.

Supplementary Information accompanies the paper on the Neuropsychopharmacology website (http://www.nature.com/npp)

SUPPLEMENTARY INFORMATION

Figure S1: Nest building quantification and scoring method
Nest building scores quantified as described in the Methods section, comparing the normalized subjective scale (Nest score, Y axis) and the nestlet shredding quantification (based on the normalized weight of shredded/unshredded material, X axis). Linear regression analysis indicates a correlation coefficient of 0.91 ($p<0.0001$, n=66 nests from 8 WT and 14 *Fmr1*-KO mice).

Figure S2: Grooming of the nose, ears or belly in *Fmr1*-KO mice exposed to a novel environment
Summary plots of the number (A) and mean duration (B) of events for grooming the belly, nose or ears in WT and *Fmr1*-KO treated either with vehicle (Veh) or BMS-204352 (BMS) and exposed for 1h to a novel open field (number of animals: 8 WT+Veh, 8 *Fmr1*-KO+Veh, 8 WT+BMS, 8 *Fmr1*-KO+BMS). No statistically significant effect of genotype or drug.

Table S1: Locomotor activity, descriptive statistics

Table S2: Nest building, descriptive statistics

Table S3: Grooming, descriptive statistics

Mean duration of events (s)

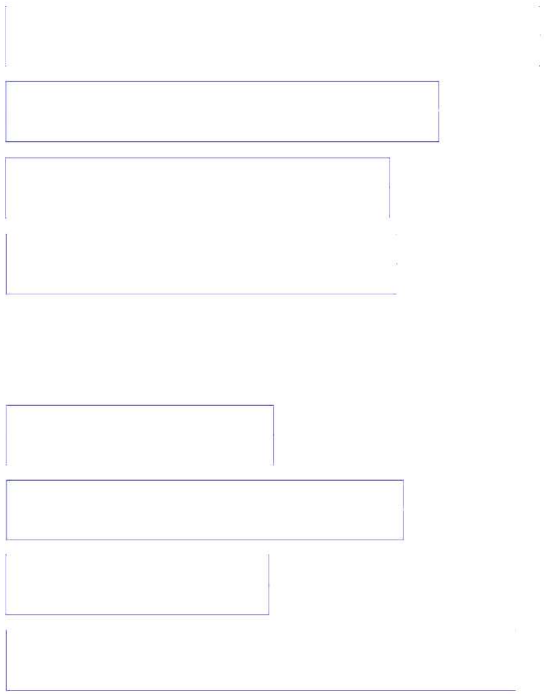

events

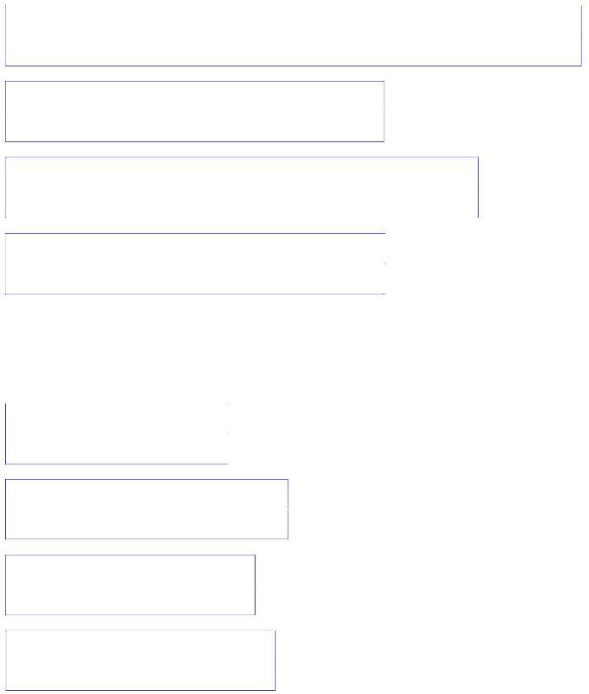

Manuscript N.2
Manuscript in preparation

Detecting fine and elaborate movement with piezo sensors, from heart beat to the temporal organization of behavior

Maria Isabel Carreno-Muñoz*, Maria Carmen Medrano*, Maelys Bompart, Fabienne Martins, Cristina Miguelez, Marc Landry, Andreas Frick, Manuel Grana & Xavier Leinekugel

Detecting fine and elaborate movement with piezo sensors, from heart beat to the temporal organization of behavior

Maria Isabel Carreño-Muñoz*, Maria Carmen Medrano*, Maelys Bompart, Fabienne Martins, Cristina Miguelez, Marc Landry, Franck Aby, Manuel Grana & Xavier Leinekugel

* equally contributing authors
correspondance: xavier.leinekugel@inserm.fr

Author contributions

XL conceived the project and collected pilot data. MIC, MCM and XL planned the research. MIC, MCM, MB, FM, CM, ML, FA and XL participated in animal preparation. MIC, MCM, MB, FM and XL performed data acquisition. MIC, MCM, MB, FM, MG and XL analyzed the data. MIC, MCM, MG and XL wrote the paper

Abstract

Behavioral phenotyping devices have been successfully used to build ethograms, but studying the temporal dynamics of individual movements during spontaneous, ongoing behavior, remains a challenge. We now report on a novel device, the Phenotypix, which consists in an open-field platform resting on highly sensitive piezoelectric (electro-mechanical) pressure-sensors, with which we could detect the slightest movements from freely moving rats and mice. The combination with video recordings and signal analysis based on time-frequency decomposition, clustering and machine learning algorithms allowed to quantify various behavioral components with unprecedented accuracy, such as individual heart beats and breathing cycles during rest, tremor and shaking in response to pain, fear or as motor symptoms of neurodegenerative diseases, and the dynamics of balance within individual footsteps during spontaneous locomotion. We believe that this novel device represents a significant progress and offers new opportunities for the awaited advance of behavioral phenotyping.

Introduction

With the advent of molecular genetics and techniques allowing to manipulate neuronal physiology with unprecedented versatility and precision, the number of animal models is growing considerably, supporting a renewed interest for integrative physiology and behavioral phenotyping. The possibility to generate animal models in which psychological, cognitive and physiological functions can be manipulated experimentally is a considerable source of progress in neuroscience and medical research, allowing to establish causal relationships between brain structure and function, as well as to reproduce and rescue the pathological changes responsible for pathologies that are major societal concerns. However, the presumably limited introspection and language capabilities of laboratory animals promote the need for designing sophisticated behavioral readout of internal cognitive states.

Our knowledge of the extent of the behavioral repertoire largely depends on the technologies available for the acquisition of relevant biological information. For now, most studies in behavioral phenotyping rely on our visual sense. The development of video devices and tools for image processing is increasingly sophisticated and sustains fast progress in behavioral phenotyping. Recent examples include 3D video acquisition[1,2], which combined with machine learning algorithms allowed to identify a number of postures and dynamics of spontaneous behavior, organized at the sub-second timescale [2]. The combination of video recordings and specific experimental devices could successfully identify the positions of the paws and other body parts, providing detailed information about the dynamic coordination of paws and body movement during locomotion[3-5]. However, most (if not all) internal movements underlying behavior, such as heart beat, breathing, shivering, or the dynamics of balance

during locomotion, remain out of reach from pure visual inspection. A number of these, such as breathing or heart beat are too small to be captured by visual inspection. Others such as the strength involved in muscle activity and balance are just not visual signals. A number of invasive techniques such as electromyogram or electrocardiogram are available to reach this information, but as all invasive approaches, they are likely to seriously interfere with spontaneous behavior. An interesting approach is that of pressure sensors positioned below the floor plate. Piezoelectric technology offers sensors of exquisite sensitivity, and can be used to collect the dynamics of movement with very high temporal precision in a totally non-invasive manner. Plates resting of piezo sensors or accelerometers have successully been used to distinguish various behaviors such as sleep, rest, grooming, etc...[3,6-12]. However, these systems were either used to detect strong movements (eg startle), or global properties of movement in order to identify specific behaviors. But none of them provides detailed information about movement and forces involved in single movements during spontaneous, ongoing behavior. We now report on a novel device, the Phenotypix, which consists in an open-field platform resting on highly sensitive piezoelectric (electro-mechanical) pressure-sensors, with which we could detect the slightest movements from freely moving rats and mice. The combination with video recordings and signal analysis based on time-frequency decomposition, clustering and machine learning algorithms allowed to quantify various behavioral components with unprecedented accuracy, such as individual heart beats and breathing cycles during rest, tremor and shaking in response to pain, fear or as motor symptoms of neurodegenerative diseases, and the dynamics of balance within individual footsteps during spontaneous locomotion. We believe that this novel device represents a significant progress and offers new opportunities for the awaited advance of behavioral phenotyping.

Results

The behavioral phenotyping device (Phenotypix) was designed to transmit any applied pressure to the underlying piezoelectric sensors, for a faithful transmission of any movement of the animal. The output signal of the piezoelectric sensors was recorded in synchrony with the video (cf Figure 1A), but at much higher sampling rate (20KHz instead of 25 frames/s). The dynamics of animal movement can therefore be resolved with high temporal precision. As illustrated in Figure 1B, frequency decomposition (power spectral density) of the electromechanical (EM) signal retracing the spontaneous behavior of a WT mouse during a 1h open field session suggests that animal movements are mostly expressed at frequencies between 0 and 15Hz. A closer examination of specific behaviors such as walking, self grooming or sniffing revealed that although the signal amplitude and shape was different for each behavior, frequency decomposition of the signal indeed showed a common expression of main temporal dynamics around 10Hz. Another interesting observation is that the high frequency response of the device and sampling rate of the signal allowed to resolve individual movements within complex behaviors. As illustrated in Figure 1 C-F, frame/frame analysis of movement related to specific behaviors revealed that individual footsteps during locomotion, paw movements during self grooming of the nose, body twitches during grooming of the back, or coordinated head and nose movements during sniffing, could be identified and quantified, providing the time course and amplitude of individual movements within complex behaviors. This may be of interest in specific applications such as the experimental study of scratching behavior. As illustrated in Figure S1A, the number of paw movements during scratching episodes induced by chloroquine in the mouse could be readily quantified from the EM signal, while this procedure is tedious when performed from the frame/frame analysis of video recordings. The rapid switch between one type of movement and the other during grooming episodes can also be difficult to perform with accuracy from inspection of video recordings. As illustrated in Figure S1B, this can be facilitated by the simultaneous monitoring of the EM signal, which shows distinct dynamics for instance between grooming of the back and grooming of the belly, one being characterized by the presence of a plateau while the other contains a fast peak and is devoid of plateau. But beyond such incidental observation, one information readily obtained from the EM signal and most likely out of reach with visual inspection, is the strength or

precise amplitude involved in individual movements such as back or belly grooming. Recent work suggests that *Fmr1*-KO mice, a model of Fragile X syndrome, express subtle changes in grooming behavior as a sign of stress when exposed to a novel environment. We have here quantified the amplitude of the EM signal associated with grooming of the back and belly in *Fmr1*-KO mice, and found an increase in amplitude of the movements underlying grooming of the back (WT vs Fmr1-KO $t(4)=-2.887$, $p=0.044$) but not of the belly (WT vs Fmr1-KO $t(6)=0.1278$; $p=0.097$, Figure S1 C-H).

Other very subtle movements hardly at reach from video recordings, that can also serve as an index of emotional reaction, are breathing and heart beat. Within the EM signal obtained from a rat during sleep and immobility, we actually noticed events that seemed to correspond to breathing and heart beat (Figure S2). The signal / noise ratio was highest during sleep and lower during rest, probably because the movements issued from the heart and chest were transferred less directly to the sensors when the animal was resting on his legs than when his chest was in direct contact with the floor-plate. We did observe more regular breathing during slow wave sleep (SWS) than during REM sleep, the two main brain states here identified by the theta/delta ratio simultaneously recorded from the hippocampus, as described in the literature. But more direct evidence was provided by concomittant recording of heart activity using invasive electrocardiogram (ECG) monitoring under urethane anesthesia. As illustrated in Figure 2A-B, in addition to the large and slow signal related to breathing movement, fast events occuring at about 10Hz were exactly concomittant with individual heart beats readily visible in the ECG of both rats and mice. Taking advantage of the possibility to monitor heart beat and breathing in a totally non invasive manner, we compared the EM signal obtained from WT freely moving mice before and after contextual fear conditioning, and observed statistically significant increases in breathing rate ($t(5)=-9.63$; $p<0.001$), heart rate ($t(5)=-8.045$; $p<0,001$) and heart/breathing rates ratio ($t(5)=-4.56$; $p=0,006$), as expected from the literature. Because heart rate is an index of vagal/parasympathetic tonus, considered to be misregulated in Fragile-X syndrome (FXS), we investigated the EM signal obtained from *Fmr1*-KO mice (a transgenic mouse model of FXS) at rest in a familiar environment. As illustrated in Figure S3A, we found that *Fmr1*-KO mice had increased basal heart rate compared to WT mice ($t(17)=-7.26$; $p<0.001$), rescued to normal levels by the BK_{Ca} channel agonist BMS-204352 (paired ttest KO vs KO+BMS: $t(4)=6.62$; $p=0.003$, and independent samples ttest WT vs KO+BMS: $t(17)=-1.39$; $p=0.18$). This is compatible with the clinical hypothesis that abnormal parasympathetic activation may participate in the anxiety, behavioral distress, and gaze avoidance typically observed in FXS children [13-15], and confirms BK_{Ca} as a potentially relevant molecular target for the development of drug medication against FXS / ASD[16].

Although the temporal dynamics of normal movements seem to be mostly confined to frequencies within the 0-15Hz range, we did notice faster components in specific experimental conditions. For example, following surgical intervention (craniotomy), high amplitude intermittent events in the 10-30Hz frequency range could be detected (Figure 2A, left). Because we could feel during direct handling contact, that the animal was shaking/shivering, we thought this might be a reaction to post-surgery pain. Indeed, the events were efficiently suppressed a few minutes after injection of the pain killer buprenorphine ($T(5)=3.746$, $p= 0.0134$; Figure 2A, right). They were not observed either in response to local inflammation produced by CFA injection in a rear paw (data not shown), suggesting that shaking is rather a signature of generalized pain. We did not detect either shaking in mice after surgery, suggesting that rats and mice do not fully share behavioral responses to pain. .

Another condition in which shaking is expected is in response to depletion of dopamine (DA), because tremor is a hallmark of Parkinson's disease (PD). We have therefore recorded the EM signal from mice after dopaminergic lesions induced by 6-OHDA injections in either the MFB or Striatum, two classical models of PD, and observed the clear expression of shaking events in the 20-30Hz frequency range in both MFB ($F(2,4)=17.02$, $p=0.0126$) and striatum ($F(2,4)=17.0204$, $p=0.018$) lesioned animals, that were not present in control mice (Figure 3B). Interestingly, these events were resistent to L-DOPA, and shaking events in the same frequency range could also be induced in mice after a depletion of acetylcholine induced by the injection of reserpine (Figure S4), in line with the ambiguity concerning the cholinergic vs dopaminergic origin of tremor in PD.

On the other hand, as illustrated in Figure 4A, we also noticed the expression of much higher frequency (80-100Hz) shaking events in the DA-depleted mice, in which the direct involvement of DA was confirmed by L-DOPA, which totally eliminated the high-frequency shaking events. Interestingly, high frequency shaking was also observed in a mouse model of Alzheimer's disease (AD). As illustrated in Figure 4B, adult 3Tg-AD mice expressed events (WT vs 3xTg-AD, t(4)=-4.72; p=0,009) in the same frequency range (80-100Hz) and with a similar rate of occurence (5Hz) as MFB or Striatum 6-OHDA DA depleted mice. Shaking events in 3Tg-AD mice were expressed already at 3 weeks of age (Figure S5B), and were eliminated by L-DOPA (50mg/kg) in both adult (t(8)=5.1639, p=0.001; Figure S5A) and young (t(8)=3.69, p=0.03; S5B) mice, but not by the anxiolytic Diazepam (2mg/kg) neither in young (Wilcoxon test, W=2, p=0.1), nor in adult mice (W=12, p=0.84; Figure S5D). The pain killer meloxicam did not have an effect on the shaking behavior in 3xtgAD mice (3mg/kg, t(1)=0.4805, p=0.7 Figure S5E). They were also observed in APP-PS1 mice (t(8)=-3.86 p=0.04; Figure S5F), another mouse model of AD. Shaking behavior in this mice model was also sensitive to L-dopa (t(5)=-3.56; p=0,02). Altogether these results suggest very early motor symptoms and degeneration of the DA system in Alzheimer's disease.

Another behavioral condition of interest is that of fear conditioning, characterized by the active suppression of movement (freezing). Because freezing behavior is classically quantified manually, we looked for its potential specific signature in the time-frequency composition of the EM signal of mice after contextual fear conditioning. While episodes of total immobility could indeed be detected with high efficiency and reliability using a script collecting periods of EM signal below a manually set threshold of power in the 0-100Hz frequency range (Figure 5A), we also noticed the high incidence of high frequency (70-100Hz) shaking events when the animal was inserted in the recording arena after fear conditioning (Figure 5 B-C). When we compared the times of occurrence of shaking and freezing in different behavioral conditions (Figure 5C-F), we found that shaking was predominantly expressed as a behavioral response to context but not to the conditionned stimulus (F(2,7)=21,4545; p=0,002), while it was the opposite for freezing (F(2,7)= 29,562; p<0,001), raising the possibility that shaking may be a behavioral response to diffuse threat and freezing to imminent threat. A confounding factor with freezing is that it was difficult from visual inspection to distinguish between immobility periods due to the real expression of fear from behavioral immobility associated with active scanning of the environment. In the litterature, a classical approximation is to consider immobility periods longer than 2s as freezing and ignore those of shorter durations. Accordingly, mice inserted in a novel environment expressed shaking only during the first few minutes while virtually no freezing behavior (>2s) could be identified. Short immobility periods (<2s) were detected by our algorithm during the first minutes of exploration. Further investigation may evaluate whether these brief immobility periods are related with mild anxiety and increased attention to potential alerts in the ambient environment. Distinct signatures of fear were further suggested by the behavioral reaction of mice exposed to the presence of a rat, one of their natural predators, which induced the immediate and remarkable expression of shaking, while inducing little freezing (Figure S6). In addition, *Fmr1*-KO mice exposed for 1h to a novel environment expressed persistent shaking compared to WT mice in which this initial reaction fades away within a few minutes of habituation, in line with our observation of altered vagal tonus (Figure S3) and with the clinical literature pointing a deficit of habituation in FXS patients. Therefore, the Phenotypix proved remarkably efficient to detect and quantify movements almost invisible to the eye of an experienced observer.

Another interesting aspect of pressure sensors is the possibility to evaluate the dynamics of the coordination and strengths of limb movements involved in locomotion. Locomotion has been extensively studied using various experimental paradigms associated with image processing tools allowing to gather increasingly sophisticated spatio-temporal information about stride or stance. Nevertheless, it has remained quite out of reach to get non invasive information about the dynamics of strengths, which can not be evaluated by visual inspection, however sophisticated. We observed that the EM signal provides some information about the dynamics of locomotion. Frame by frame analysis of the synchronously recorded video signal allows to depict the EM signature of individual footsteps. In the short sample of spontaneous locomotion illustrated in Figure 6A, one can distinguish a few initial footsteps of small amplitude, that correspond to orienting behavior (the mouse was

changing direction but not moving forward). The EM signature of locomotion, with the animal really starting to move ahead, then becomes much more visible, as series of 5 to 10 footsteps of increasing and then decreasing amplitude, displaying a spindle pattern that turned out to be very typical of the mouse locomotion. Because the EM signal is the result of the dynamic distribution of weight and of all the forces generated by a multitude of muscles within the animal's body, it is a complex mixture that depends on the coordination of the various limbs and strengths involved in movement. Nevertheless, we think that the very stereotypical signature of spontaneous locomotion in WT mice may serve as a reference template for the detection of motor impairment in various models of pathology. As a first example, we recorded the EM signal of mice injected with CFA in one of the rear paws, producing local inflammation so that the animal tended to avoid pressing on the sore paw. Using a linear Support Vector Machine (SVM) classifier approach combining autoregression, k-means clustering and machine learning algorithms (Figure S7), we identified clusters of footsteps that differenciated control from CFA mice. Visual inspection of the discriminating clusters guided our interest towards the time course of footsteps EM signature. As illustrated in Figure 6B, some footsteps of CFA mice appeared smaller (amplitude, $t(16)=2,756$; $p=0,0141$) and displayed a slower time course than those of control mice (half-width, $t(16)=-7.2562$; $p<0.001$), which reflects in the distributions of amplitude and half-width of the EM signal underlying individual footsteps during steady locomotion (15-20 cm/s, stats). This is compatible with the likely consequence that CFA mice tend to avoid pressing on their sore paw, although our system does not offer the resolution of individual paws. Alzheimer's and Parkinson's diseases are also associated with motor impairment. Upon visual inspection of locomotion in 3xTg-AD and 6-OHDA lesioned mice (respective models of AD and PD), we noticed a disruption of the typical spindle pattern characteristic of WT mice. As illustrated in Figure 6C, this was confirmed by the quantification of the correlation coeficient between the lower and upper enveloppes of the EM signal associated with steady locomotion, suggesting altered balance and movement coordination in AD ($F(2,10)=25,26$; $p=0.012$) and PD ($F(2,10)=25,26$; $p=0.009$).

Discussion

A novel device (the Phenotypix), made of an open-field plateform resting on highly sensitive piezoelectric pressure sensors, povided access in a totally non invasive manner to very fine components of rat or mouse spontaneous behaviors. Existing systems[6-8] based on similar principles, combined with spectral decomposition and automatic classification, are used for behavioral phenotyping by the generation of an ethogram, attributing each time bin of the recording to the most likely ongoing behavior such as walking, eating, drinking, walking, seizures etc... But in contrast to existing devices, the fine sensitivity and high sampling rate of the Phenotypix allow to resolve individual movements such as individual breathing cycles, heart beats or single footsteps during locomotion. Through the study of various behavioral conditions and transgenic models, we could identify and quantify novel behavioral components that can be useful for the study of several fields of behavioral neuroscience such as sleep, stress, pain, motor symptoms of neurodegenerative diseases and locomotion.

Although existing devices were shown to have good performance for the detection of various kinds of self-grooming behavior[6,8], they are not used, to our knowledge, for the quantification of the strength or amplitude of individual self-grooming body movements. The possibility to count the number of body movements during scratching, as demonstrated here in the chloroquine model, is of interest to itch research in which this quantification is usually made manually[17,18], which is a tedious and repetitive task for the experimenter. The observation of increased amplitude of body movement in self-grooming of the back in *Fmr1*-KO mice is also an interesting complement to recent studies pointing at fine alterations in self-grooming behavior in the mouse under stressful conditions[19-21], because it may help better understand repetitive and self-injury behavior in FXS/ASD patients[16,22-24].

The direct and non-invasive evaluation of breathing and heart rate may prove useful for the study of sleep apneas, a pathological condition we still poorly understand. These vital parameters are also strongly related to emotions, an aspect of behavior difficult to identify in animal studies. Anxiety

is classically evaluated as the avoidance of situation of innate aversion such as exposed or bright areas (eg center of an open field, open arms of a maze)[25]. We have observed increased basal rates and reduced habituation of breathing and heart beat in *Fmr1*-KO mice exposed to an open field environment, which might represent an alternative expression of anxiety less affected by confounding factors such as hyperactivity, a major pathological component of some FXS/ASD patients and *Fmr1*-KO mice[16,26]. Fear on the other hand, a more acute and stronger behavioral reaction to perceived threat, is classically quantified as freezing immobility in rat and mouse studies. From our results, we propose high-frequency (80-100Hz) shaking as a complementary and more sensitive index of fear in the mouse, expressed during exposition to a fearful situation such as a novel environment, the presence of a predator or a context previously associated with fear conditioning.

We found high frequency shaking to be expressed also as a spontaneous behavioral signature of chronic pain in the rat. Most studies about pain in rats and mice rely on the quantification of reactive pain, such as the latency between the presentation of a painful stimulus and the retraction of the affected limb (eg of the paw in response to von Frey filaments, of the tail in response to local heating of the skin). But these are poor models of chronic and spontaneous pain, conditions of major clinical relevance[27,28]. A remarkable recent study proposed a "mouse grimace scale" as a standardized classification of facial expression to quantify subjective pain in response to noxious stimuli of moderate duration[29]. This approach has not been tested for persistant pain, and requires a good visual access to the face of the animal. With the Phenotypix, spontaneous pain is likely easier and more reliable to detect because the measure by itself should not depend on the precise moment of estimation, nor on any specific position of the animal relative to the camera.

A novel finding here is the expression of early motor symptoms in 3xTg-AD and APP-PS1 mice, two different mouse models of Alzheimer's disease. High frequency shaking was detected already at 21 days of age in 3xTg-AD mice. This is earlier than any reported cognitive or motor symptoms in this strain[30], and interesting in the perspective that motor function abnormalities precede the diagnosis of AD dementia by many years[31,32]. In both 3xTg-AD and APP-PS1 mice, shaking was rescued by the dopaminergic agonist L-DOPA. Moreover, shaking could be induced experimentally in WT mice by dopaminergic excitotoxic lesions by injection of 6-OHDA in the MFB or in the Striatum. These results suggest the involvement of early degeneration of dopaminergic systems in AD, in line with the recent description of cognitive rescue with L-DOPA in mouse models of AD[31,33]. Altogether, these results point towards potentially common mechanisms between Alzheimer's and Parkinson's disease that could help better understand the complex etiology of these devastating neurodegenerative diseases.

In addition to shaking and tremor that constitute isolated motor symptoms in AD and PD, our device allowed the detection of abnormalities in the execution of locomotion, a fundamental motor function. While a number of systems are available to measure the spatio-temporal organisation of gait, analyzing the sequence of positions of the various limbs during locomotion[3-5,34], the Phenotypix allowed to reveal subtle alterations in the pressure signature of individual footsteps. This compound output is the result of complex interactions, that we can not yet dissociate, between the muscular strengths and the coordination of the individual limbs involved in each footstep. Nevertheless, we could access the time course of the impulse that corresponds to each footstep, and identify its reduced amplitude and slower time course in limping mice. Moreover, global analysis of the dynamics of successive footsteps revealed that locomotion is typically organized as series of 5 to 10 footsteps of increasing and then decreasing amplitude. Sophisticated analysis based on classifiers and machine learning algorithms pointed to alterations of this pattern in both AD and PD mouse models, suggesting access to novel criteria for gait analysis that may shed new light in the understanding of various forms of ataxia.

Figures

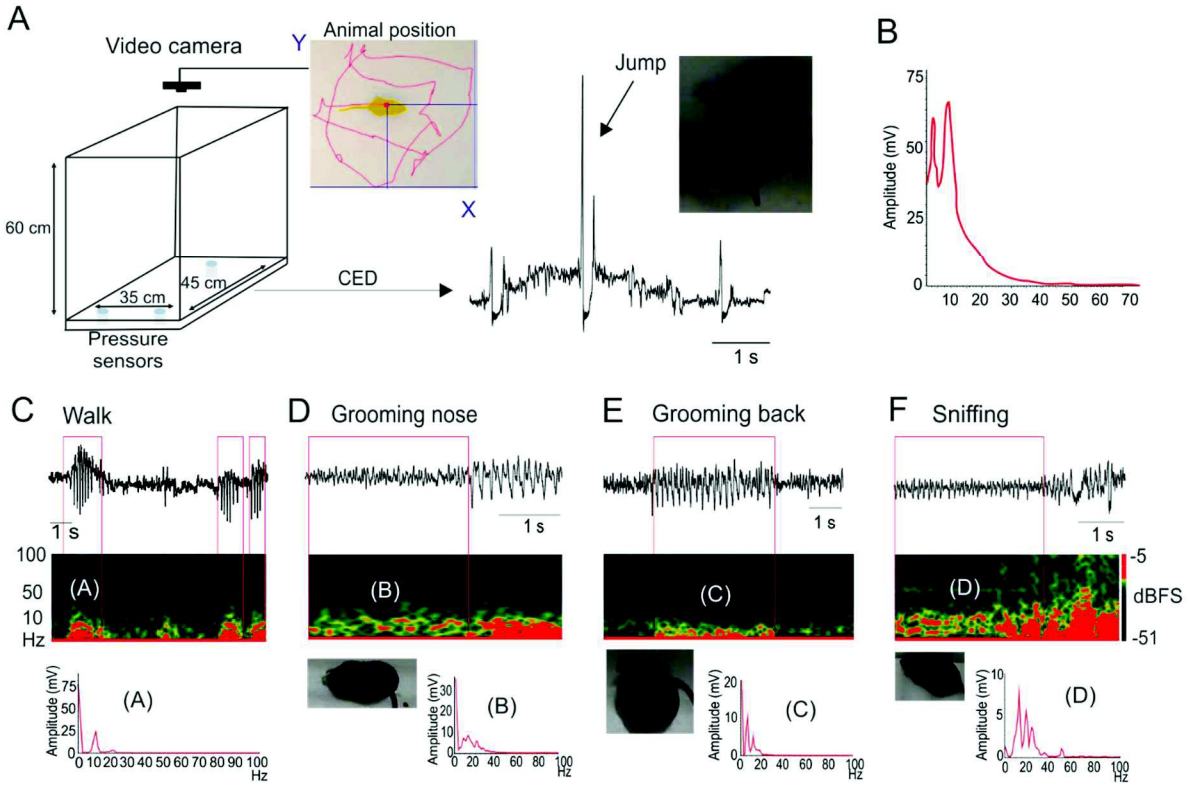

Figure 1: Pressure-sensor-derived detection of various body movements with the Phenotypix system

The Phenotypix system is an open field platform connected to pressure sensors allowing to detect various body movements of a freely moving rat or mouse with high sensitivity and fine time resolution. Spike2 software is used to synchronize the video (25fps) and analog signal (20kHz) from the pressure sensors with the CED recording system. The software also allows synchronized replay offline for analysis. Offline analysis of the video file with the Noldus Ethovision software provides continuous tracking of the position (x, y) of the animal.

A. Schema of the Phenotypix acquisition system and the sensor-derived signal elicited by jumping of the mouse.

B. Spectral composition (power spectral density) of the EM signal recorded during 1h of free open field exploration.

C-F, typical EM signal generated by different behaviors. Below each trace, time-frequency spectrogram and power spectral density (PSD) of the portion of data included in the red box. C, locomotion (>13 x cm/s); **D,** nose grooming (each cycle of front paw movement appears as a separate deflection in the mechanical signal); **E**, grooming of the back; **F,** sniffing (each deflection corresponds to an individual nose-movement).

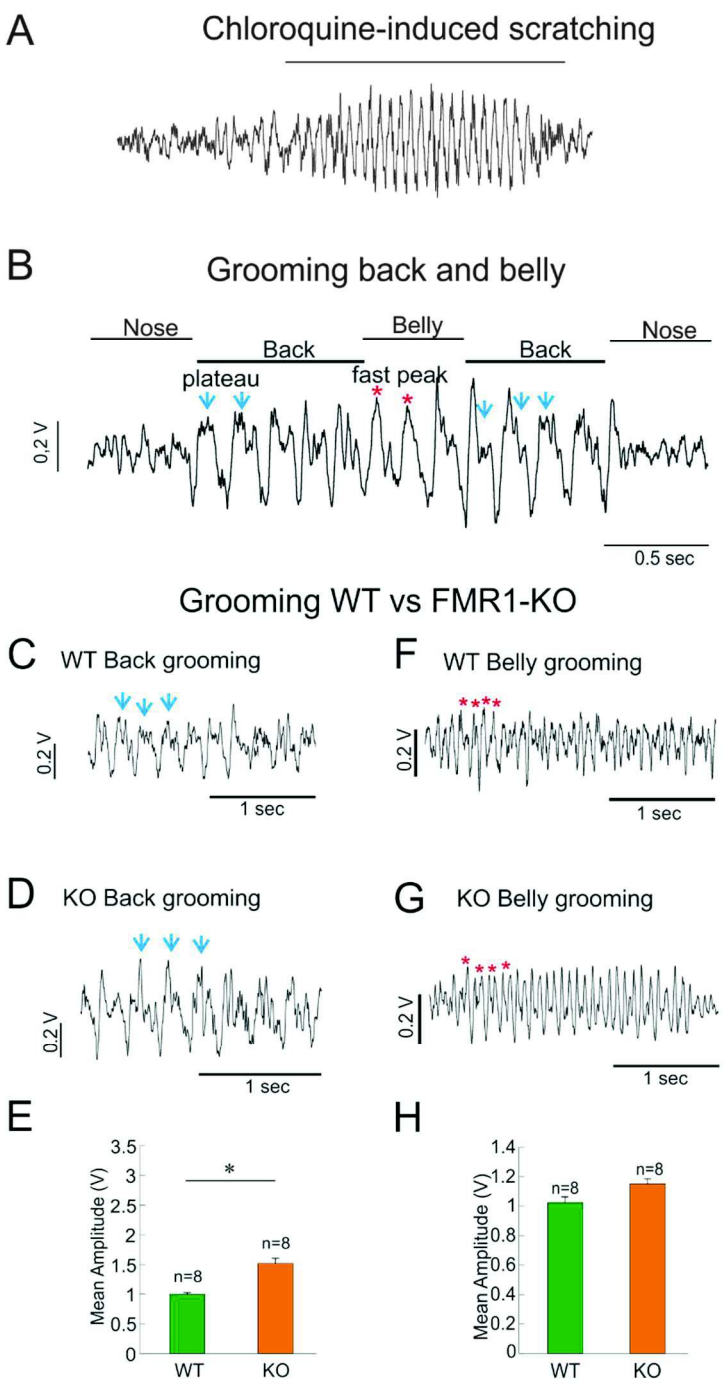

Figure S1: Pressure-sensor-derived signature of various types of grooming in the mouse

A. Sensor-derived signature of a mouse scratching in reaction to application. Each deflection in the mechanical signal is an individual front paw scratching movement.

B. Sensor-derived signature of grooming the back and the belly in the mouse. Note the difference in signal shape when grooming the back (blue arrow, plateau) or the belly(red stars, fast peak).

C-H. Sensor-derived signature of grooming the back and the belly in WT and FMR1-KO mice. The signal indicates larger movements in FMR1-KO mice during grooming of the back (**C**, signal for WT; **D**, signal for FMR1-KO; **E**, quantified amplitude) or the belly (**F**, signal for WT; **G**, signal for FMR1-KO; **H**, quantified amplitude).

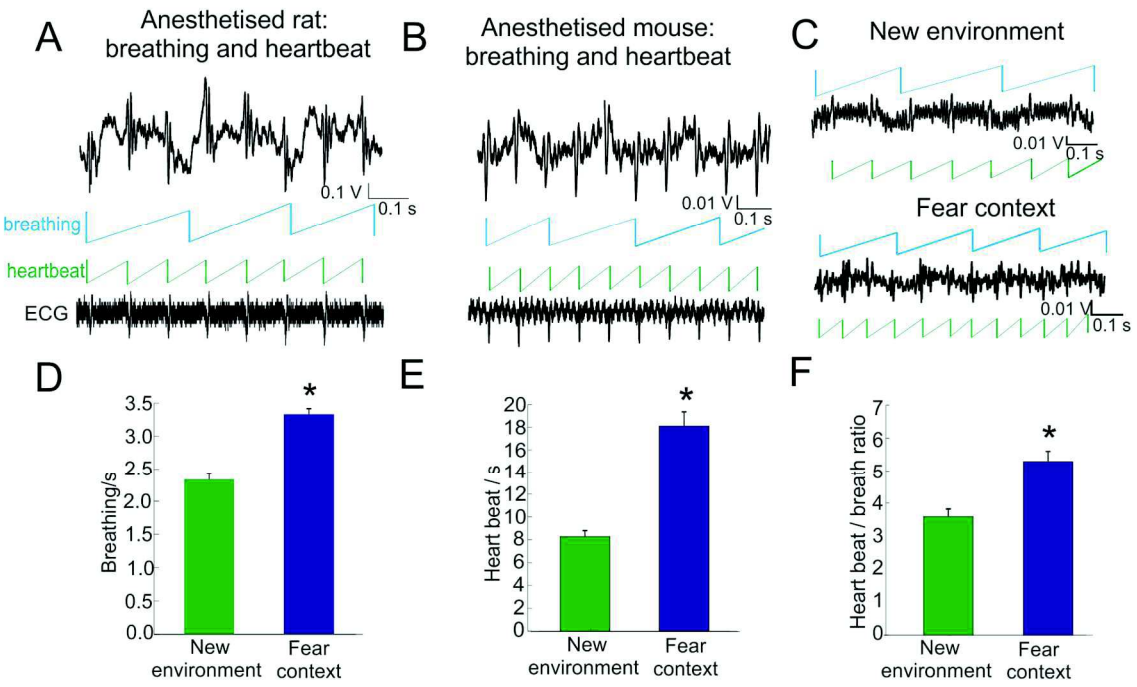

Figure 2: Pressure-sensor-derived detection of breathing and heart-beat

A-B. Simultaneously recorded sensor-derived signal and electro-cardiogram (ECG) from anesthetized rat (**A**) and mouse (**B**). Upper traces: raw sensor-derived signal (body movements). Lower traces: ECG (electrical heart beat signal). Note the slow and higher frequency components of the sensor-derived signal, respectively represented in middle traces as blue line (linearized phase of breathing rhythm) and green line (linearized phase of heart-beat).

C. Sensor-derived signal and linearized breathing (blue line) and heart-beat (green line) rhythms from a mouse during natural immobility in a neutral context of after fear conditioning.

D-F. Note faster breathing (**D**), heart rate (**E**) and number of heart-beats per breathing cycle (**F**) after fear conditioning.

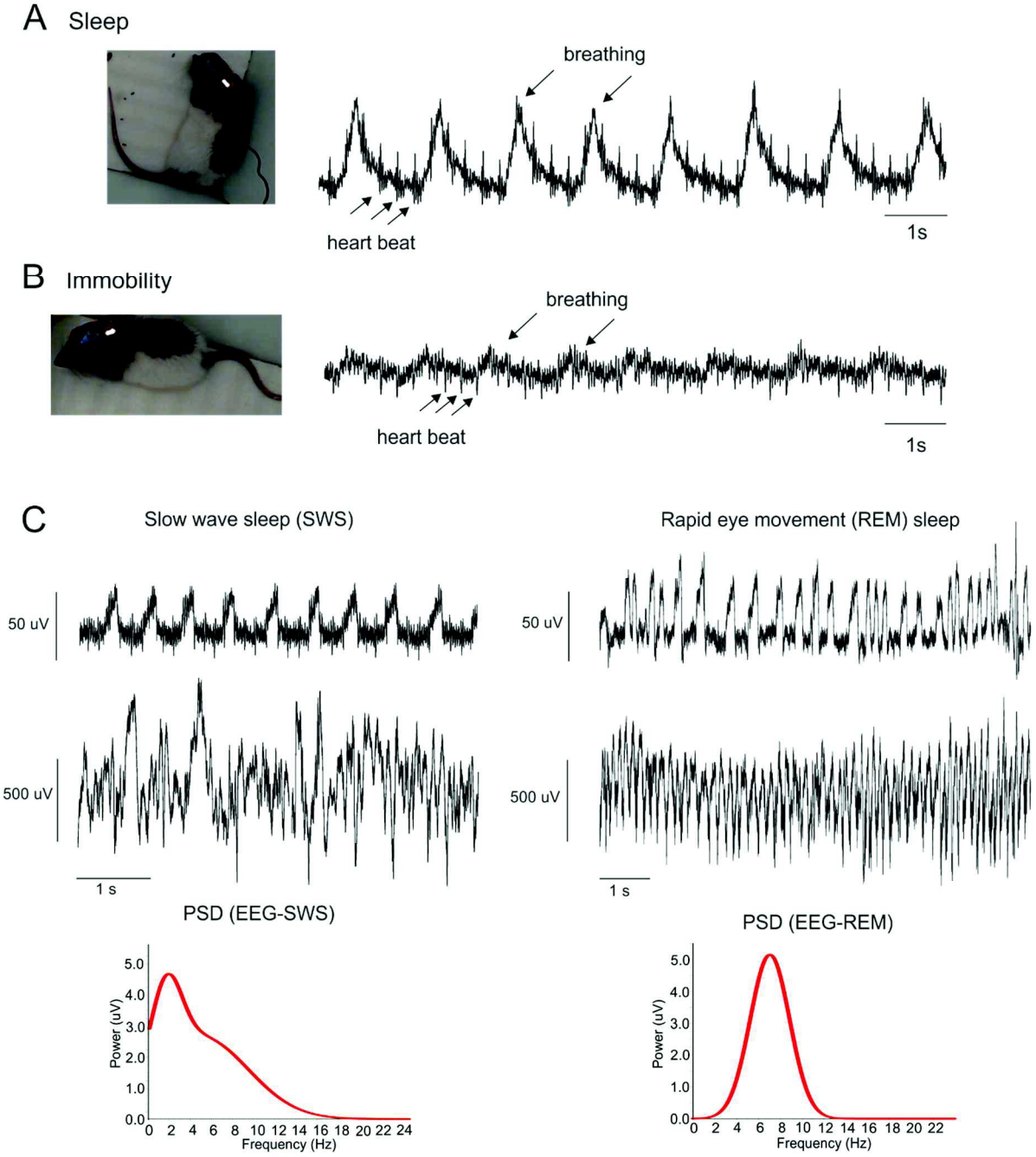

Figure S2: Pressure-sensor-derived detection of breathing and heart-beat during immobility and sleep
A-B. Sensor-derived signal from a rat during sleep and immobility. Note the higher amplitude of breathing signal when the animal is lying on the floor (A, Sleep) compared to resting on his paws (B, immobility).
C. Simultaneously recorded sensor-derived (upper trace) and EEG (lower trace) signal from a mouse during sleep. Power spectral decomposition of EEG traces (below) identify slow wave sleep (SWS, left traces) as high delta (0-4Hz) and low theta (6-10Hz) power, and REM sleep (right traces) as low delta and high theta power. Note that SWS is characterized by very regular breathing and heart beat in absence of any other movement, while REM sleep shows irregular breathing and heart beat as well as occasional movements (twitches).

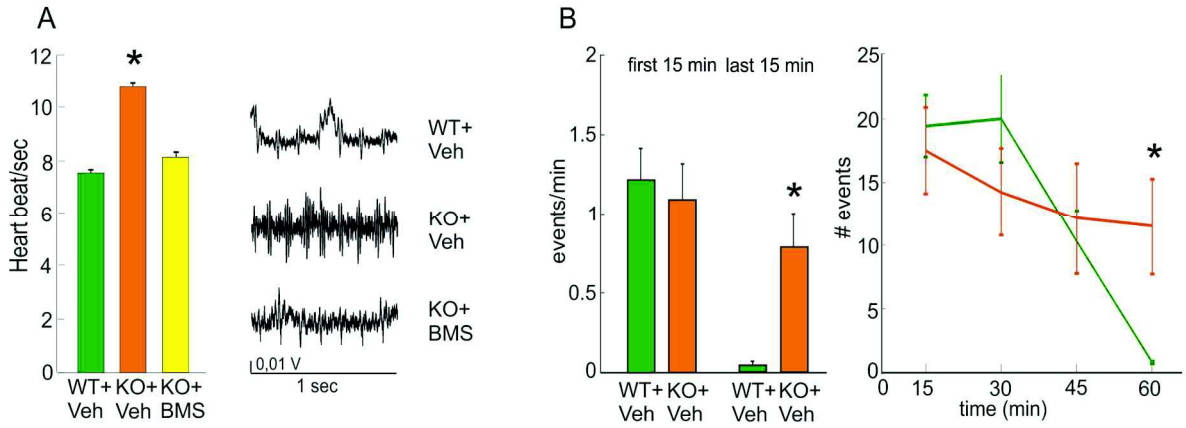

Figure S3: Increased heart beat and persistent shaking in *Fmr1*-KO mice

A. Bar plot (left), showing an increased heart rate in *Fmr1*-KO mice, corrected by BMS-204352. Examples of EM signal traces (right) corresponding to sleep are shown for the three animal groups: WT (upper trace), KO (middle trace) and KO+BMS-204352 (lower trace).

B. Bar plots showing no difference in the shaking frequency of occurrence between WT and KO mice during the first 15 minutes of exposition to a novel environment (left). However statistical difference (*) is revealed after 45 minutes of exposition (right). The time course (right) show the evolution of mean shaking appearance during the whole 1-hour recording.

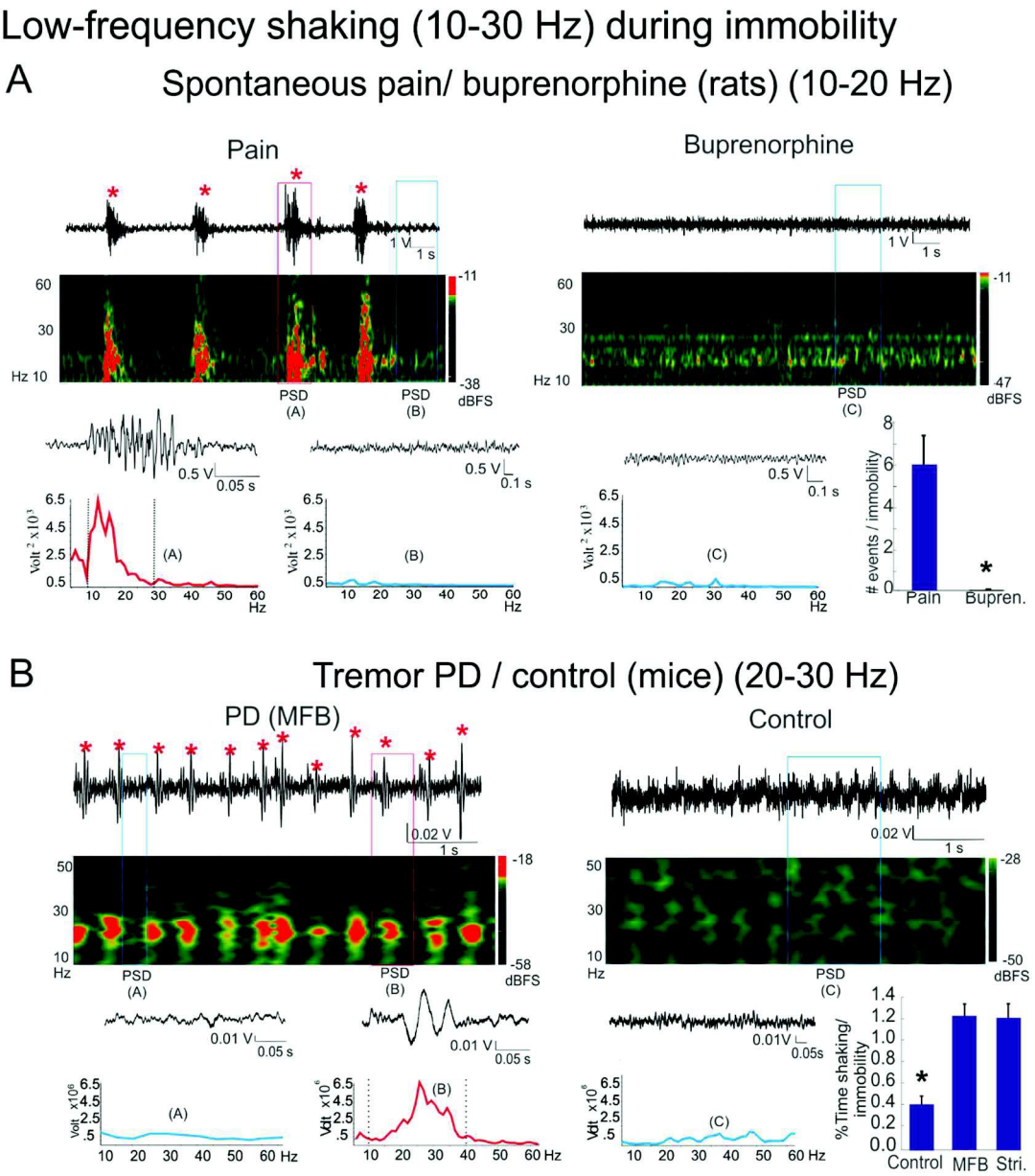

Figure 3: Pressure-sensor-derived detection of low frequency shaking (10-30Hz)

A. Sensor-derived signal (**top traces**, raw data) and associated time-frequency spectrogram (**underneath color plots**, left scale is frequency range, color scale indicates power) show the presence of transient 10-30Hz oscillations in the signal (**left**, *****) during behavioural rest from a rat on the next day after surgery, that are not expressed after a pharmacological treatment against pain (**right, Buprenorphine**). Below are shown a single shaking event (**red box**) and a section of equivalent duration out of shaking events (**blue box**), displayed at wider time scale above the corresponding Power Density Spectra (**PSD**). Note the high power in the 10-30Hz frequency range during pain-related shaking.

The **right bar plot** shows the comparison in frequency of occurrence of 10-30Hz shaking events (detected as supra-threshold power in the 10-30Hz frequency range) between Pain and Buprenorphine conditions.

B. Sensor-derived signal (**top traces**, raw data) and associated time-frequency spectrogram (**underneath color plots**, left scale is frequency range, color scale indicates power) show the presence of transient 10-30Hz oscillations in the signal (**left, ***) during behavioural rest from a mouse after MFB lesion, that are not expressed in control mice (**right, Control**). Below are shown a single shaking/tremor event (**red box**) and a section of equivalent duration out of shaking events (**blue box**), displayed at wider time scale above the corresponding Power Density Spectra (**PSD**). Note the high power in the 10-40Hz frequency range during shaking/tremor.

The **right bar plot** shows the frequency of occurrence of 10-30Hz shaking events (detected as supra-threshold power in the 10-30Hz frequency range) in control conditions and after 6-OHDA lesions of the MFB or of the Striatum.

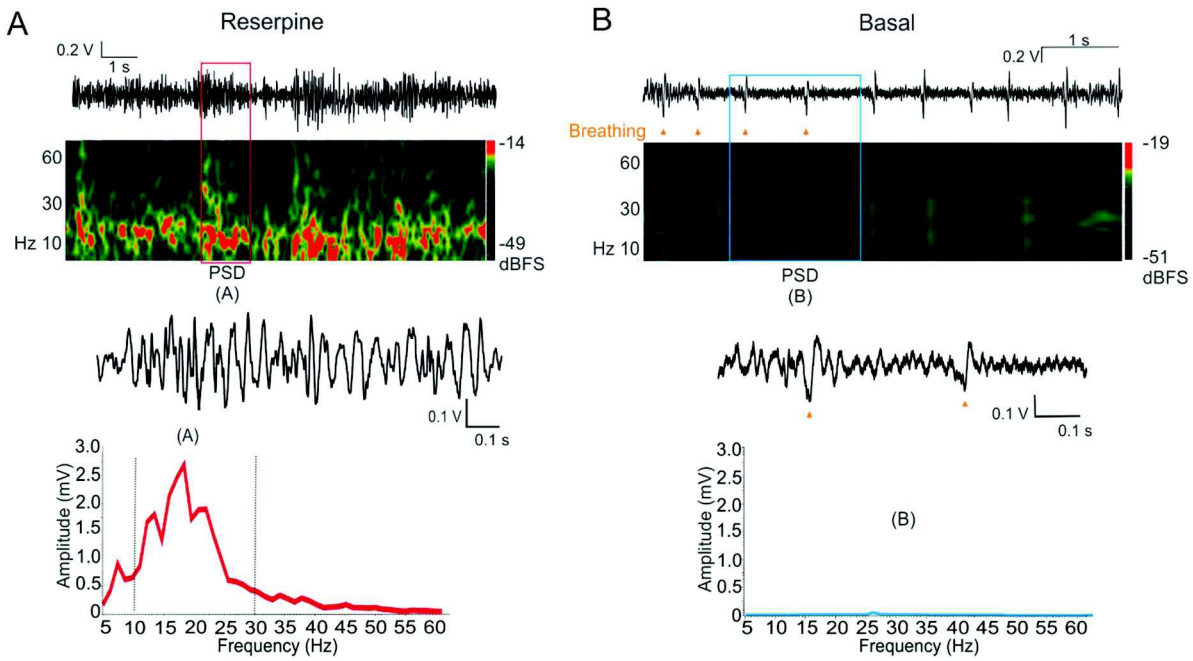

Figure S4: Pressure-sensor-derived detection of low frequency tremor in reserpine-treated mice
Sensor-derived signal (**top traces**, raw data) and associated time-frequency spectrogram (**underneath color plots**, left scale is frequency range, color scale indicates power) show the presence of 10-30Hz oscillations in the signal (**A, reserpine**) during behavioural rest from a mouse after reserpine injection, that were not expressed in the same mouse before the injection (**B, Basal**). Below are shown traces of a tremor period (**red box**) vs basal condition (**blue box**), displayed at wider time scale above the corresponding Power Density Spectra (**PSD**). The yellow arrows in Basal condition point to breathing-related movements. Note the high power in the 10-30Hz frequency range during tremor.

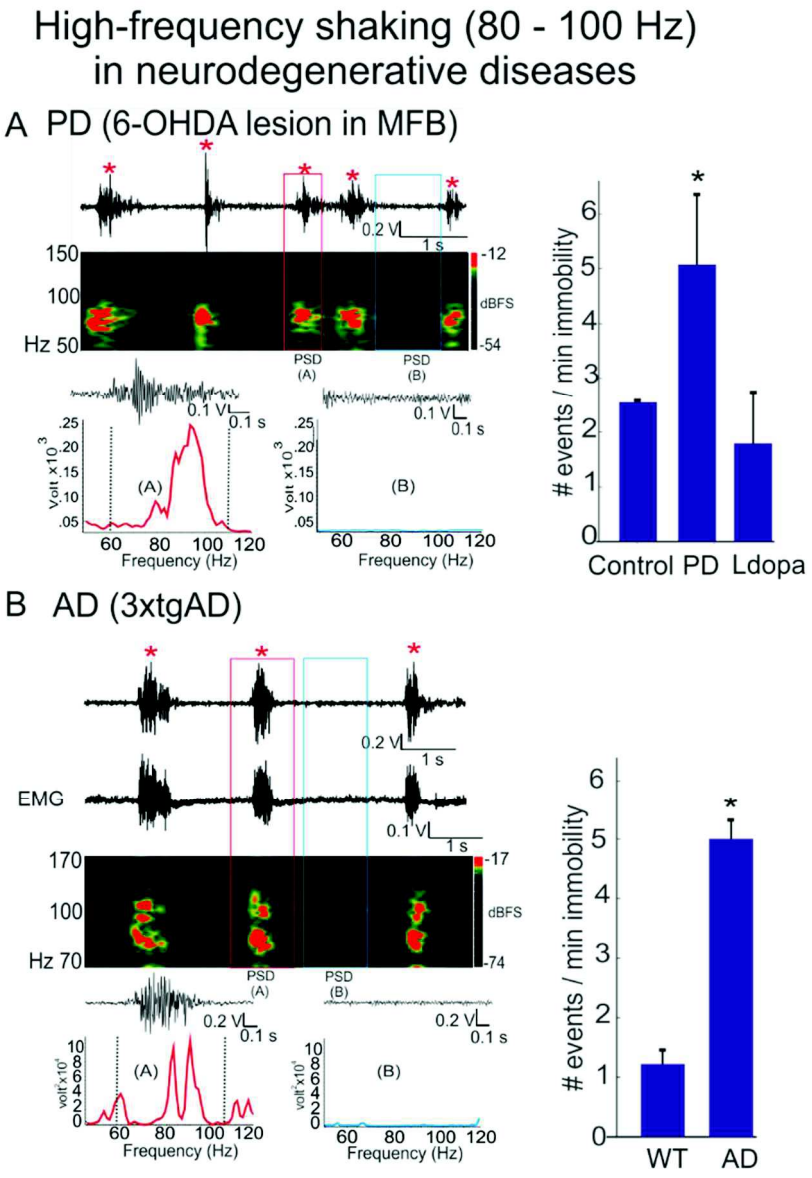

Figure 4: Pressure-sensor-derived detection of high frequency shaking (80-110Hz)

A. Sensor-derived signal (**top trace**, raw data) and associated time-frequency spectrogram (**underneath color plot**, left scale is frequency range, color scale indicates power) show the presence of transient 80-110Hz oscillations in the signal (red *****) during behavioural rest from a mouse after 6-OHDA-lesion (MFB/Striatum). Below are shown a single shaking event (**red box**) vs basal condition (**blue box**), displayed at wider time scale above the corresponding Power Density Spectra (**PSD**). Note the high power in the 80-110Hz frequency range during shaking.

The **bar plot** on the **right** shows the frequency of occurrence of 80-110Hz shaking events (detected as supra-threshold power in the 80-110Hz frequency range) in before (control) and after (PD the lesion) as well as after treatment with L-DOPA. Note that L-DOPA abolished the lesion-induced 80-110Hz shaking to normal levels (*).

B. Sensor-derived signal (**top trace**, raw data) and associated time-frequency spectrogram (**underneath color plot**, left scale is frequency range, color scale indicates power) show the presence of transient 80-110Hz oscillations in the signal (red *****) during behavioural rest from a 3xTg-AD mouse (a model of Alzheimer's disease). Below are shown a single shaking event (**red box**) vs basal condition (**blue box**), displayed at wider time scale above the corresponding Power Density Spectra (**PSD**). Note the high power in the 80-110Hz frequency range during shaking.

The **bar plot** on the **right** shows the frequency of occurrence of 80-110Hz shaking events (detected as supra-threshold power in the 80-110Hz frequency range) in WT and age-matched (3-4months) 3xTg-AD mice.

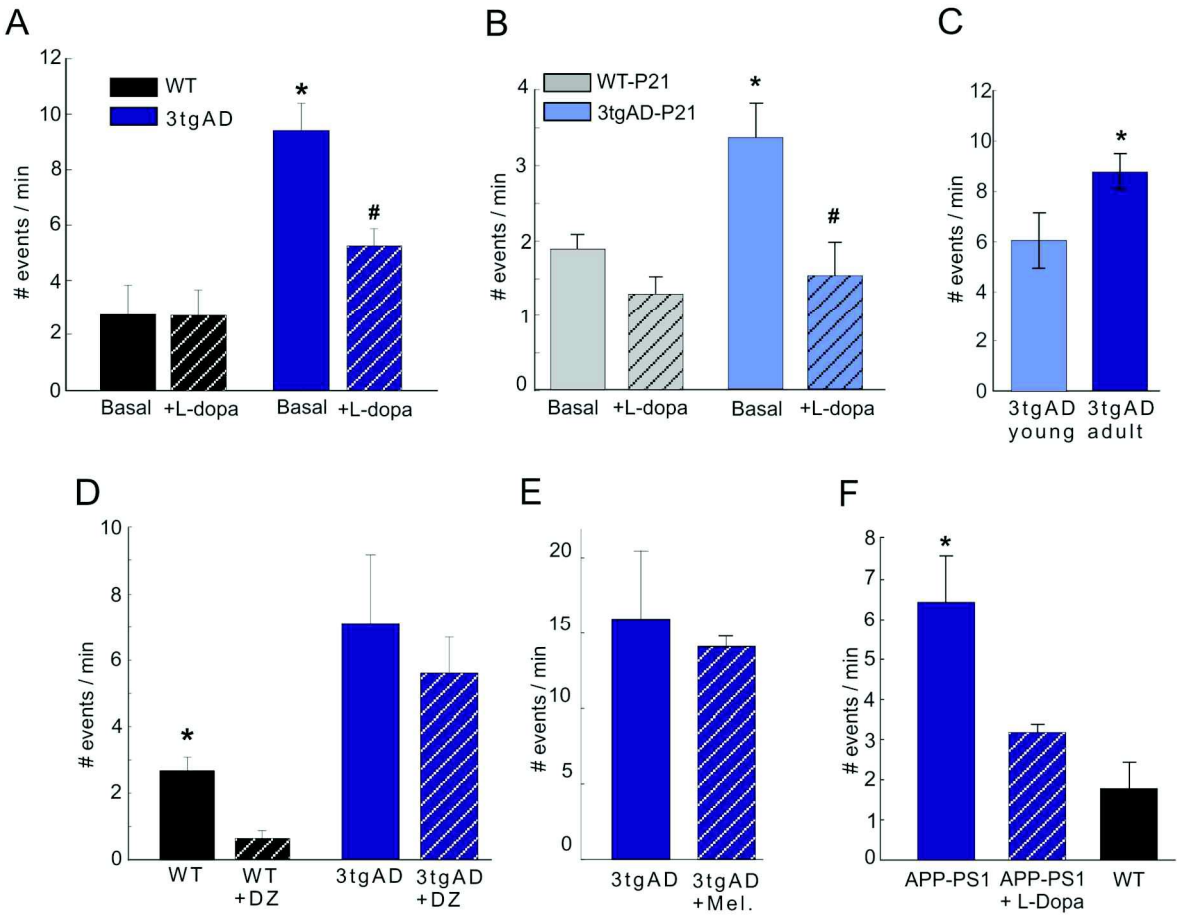

Fig S5: Pharmacology of shaking symptoms in 3xtgAD and APP-PS1 mice.

A-B. Bar plots showing an increased rate of shaking events in 3tgAD mice compared to WT (*) in adult (A) and p21 (B) mice. Plots also show the positive effect of Ldopa (striped pattern) revealed by paired statistics (#) in both adult (A) and p21 (B) mice, having no significant effect on adult and young WT mice.

C. Plot shows the progressive evolution of shaking events with age in 3tgAD mice.

D. Plots showing the positive effect of DZ on adult WT mice (*) and no effect on 3tgAD mice.

E. Plot showing no effect of the analgesic meloxicam on shaking in adult 3Tg-AD mice.

F. Shaking and L-dopa rescue in APP-PS1 mice

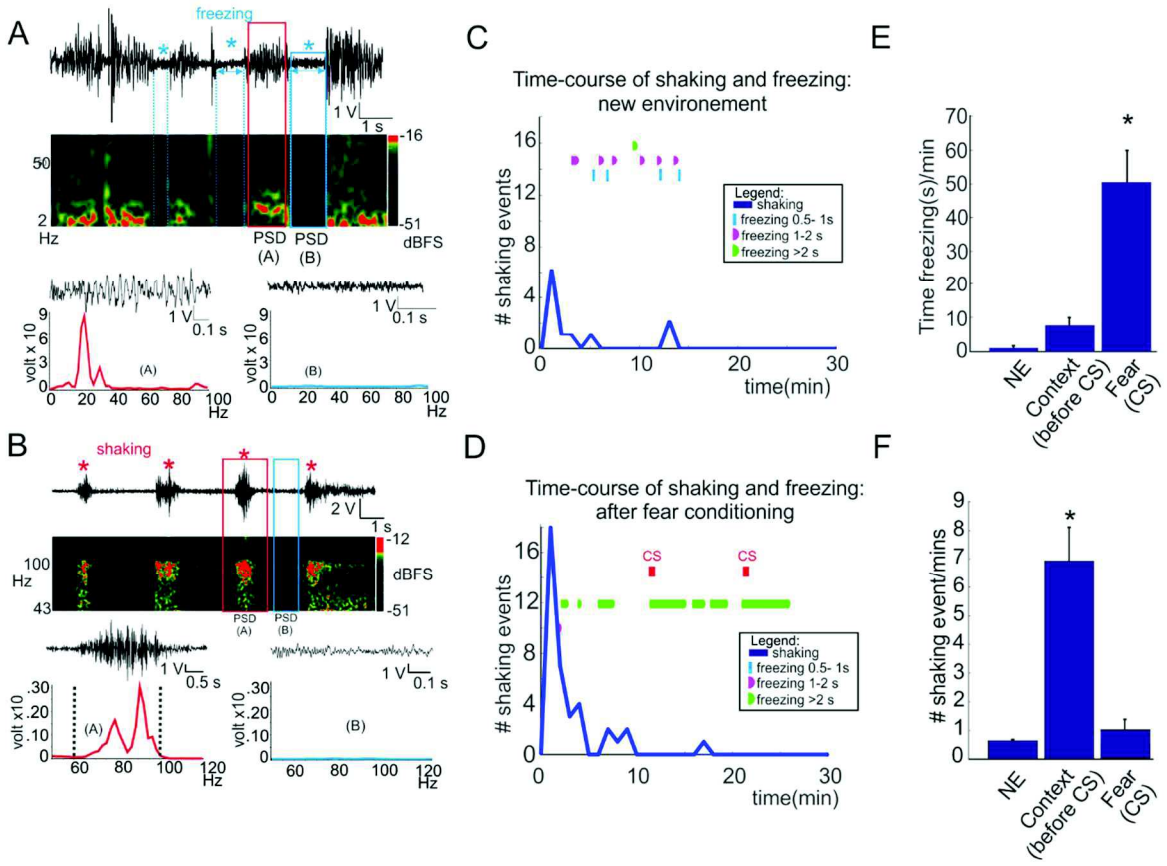

Figure 5: Pressure-sensor-derived detection of fear-related freezing and shaking

A. Sensor-derived signal (**top trace**, raw data) and associated time-frequency spectrogram (**underneath color plot**, left scale is frequency range, color scale indicates power) show the presence of transient immobility periods (freezing, blue *) during spontaneous exploration of a novel environment in a naive mouse. Below are shown a single freezing event (**blue box**) vs basal resting condition (**red box**), displayed at wider time scale above the corresponding Power Density Spectra (**PSD**). Note the strong drop in power at all frequencies during freezing.

B. Sensor-derived signal (**top trace**, raw data) and associated time-frequency spectrogram (**underneath color plot**, left scale is frequency range, color scale indicates power) show the presence of spontaneous transient 60-100Hz oscillations in the signal (red *) during behavioural rest from a mouse after contextual fear conditioning. Below are shown a single shaking event (**red box**) vs basal resting condition (**blue box**), displayed at wider time scale above the corresponding Power Density Spectra (**PSD**). Note the high power in the 60-100Hz frequency range during shaking.

C-D. Time course of occurrence of freezing (color coded **vertical bars**, detected as infra-threshold power in the 0-100Hz frequency range) and shaking (**blue line**, detected as supra-threshold power in the 80-110Hz frequency range) events over 30min of recording before (**C**) and after (**D**) contextual fear conditioning. Freezing episodes are indicated according to their duration: brief (<1s, **cyan ticks**), intermediate (1-2s, in **magenta ticks**), long (>2s, in **green ticks**). **CS** indicates delivery of conditioned sound.

E-F. Bar plots of global expression of spontaneous freezing (**E**) and 80-110Hz shaking events (**F**) before (**New environment**) and after (**Context before CS**) contextual fear conditioning as well as in response to the CS (**Fear CS**). Note that while freezing is the dominant behavioural expression of fear in response to CS, shaking is the dominant expression of context-related fear.

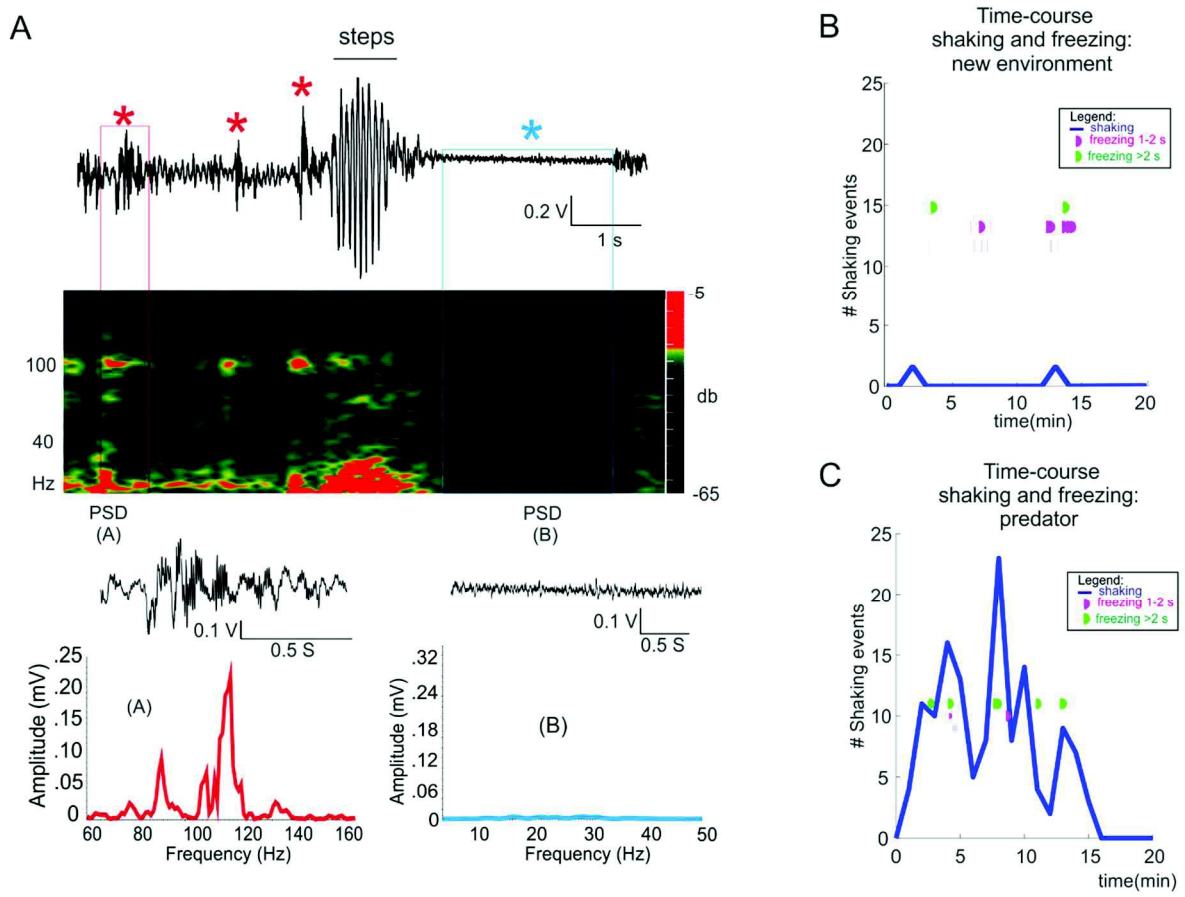

Figure S6: Pressure-sensor-derived detection of fear of predator

A. Sensor-derived signal (**top trace**, raw data) and associated time-frequency spectrogram (**underneath color plot**, left scale is frequency range, color scale indicates power) show the presence of both freezing (**blue ***) and 80-120Hz shaking (**red ***) during exposure of a naive mouse to a predator (a rat behind bars on the side of the open field, so that the mouse can see and smell but not get in direct physical contact with it). Below are shown a single freezing event (**blue box**) vs 80-120Hz shaking event (**red box**), displayed at wider time scale above the corresponding Power Density Spectra (**PSD**). Note the high power in the 80-120Hz frequency range during shaking vs the strong drop in power at all frequencies during freezing.

B-C. Time course of occurrence of freezing (color coded **vertical bars**) and shaking (**blue line**) events over 20min before (**B**) and during (**C**) exposition to the predator. Freezing episodes are indicated according to their duration: short (1-2s, in **magenta ticks**), long (>2s, in **green ticks**). Note that shaking is the dominant expression of fear in response to exposure to the predator.

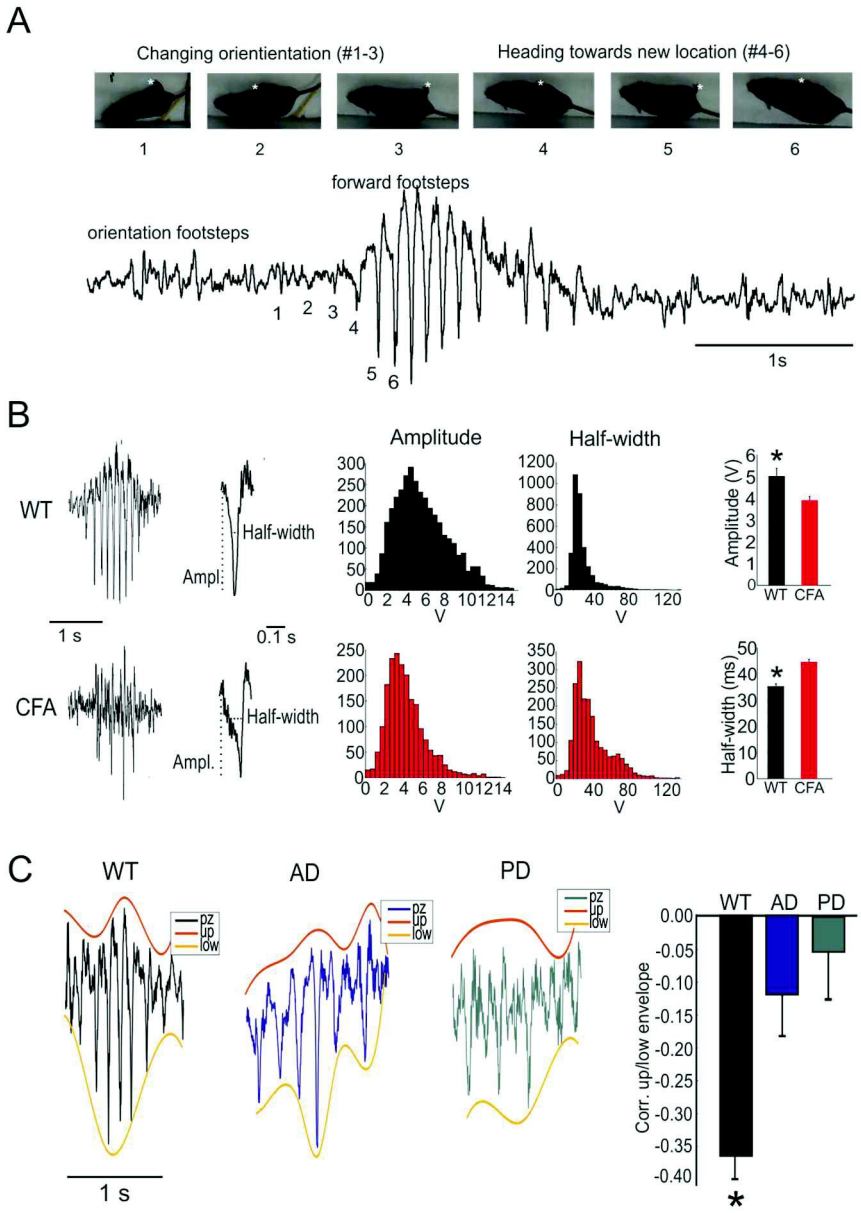

Figure 6: Pressure-sensor-derived signature of individual footsteps during spontaneous locomotion

A. Typical sensor-derived signature of a walking mouse. Images 1-6, successive video frames (***** right rear paw). Each footstep appears as a fast downward deflection in the sensor-derived signal. Note the very light mechanical signal generated by orientation footsteps (**#1-3**, when the mouse is changing orientation) compared to the strong signature of forward footsteps (**#5-6**, when the mouse is giving a strong impulsion to move forward)

B. The signature of individual footsteps during locomotion is affected in mice with a sore paw. Sensor-derived signal of walking mice (locomotor event 15-20 cm/s, with a zoom on an individual footstep), either in normal conditions (**WT, upper traces**) or after CFA-induced inflammatory pain in the left rear paw (**CFA, lower traces**). Amplitude and half-width quantification indicates significant differences (*) in locomotion between WT and CFA animals (bar plots on the right). Amplitude and half-width histograms show a different distribution of foot step characteristics in both groups.

C. The upper and lower sensor-derived signal envelopes (**orange and yellow lines**) were computed as an indication of global time-organization of footsteps in control (**WT**), 3xTg-AD (**AD**) and 6-OHDA lesioned (**PD**) walking mice (**traces on the left**). As indicated in the **bar plot quantification on the right**, the correlation coefficient between upper and lower envelopes is different in WT vs AD and PD mice.

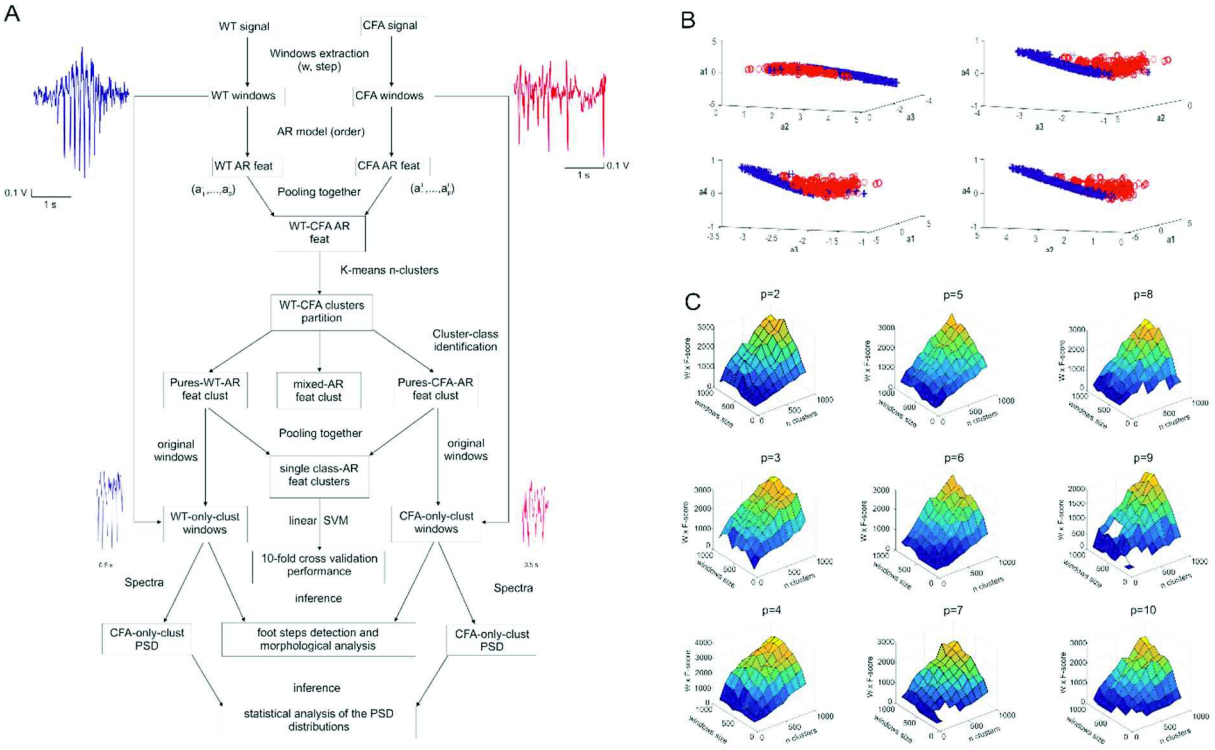

Figure S7. Clustering of foot step: methodological description of classification process

A. Schematic diagram of the computational pipeline. First, overlapping sliding windows of the signal are extracted from signal regions above the selected velocity threshold (15-20 cm/s) (on the left, a blue signal window example of a WT mouse locomotion; and on the right a red signal window shows a typical locomotion period in CFA mice). Every signal window is used to fit an autoregressive model (AR) of order=p (one model per window). The coefficients of these AR models become the AR features which encode the dynamic and spectral characteristics of each window. After pooling together WT and CFA AR features we perform a k-means clustering. Resulting clusters are sorted into 3 different groups according to the original mice class: pure clusters containing only feature samples from WT locomotion periods, idem only from CFA locomotion periods, and mixed clusters including features from both classes. In order to identify discriminant patterns of both experimental groups we built a reduced feature dataset containing only the samples from pure clusters. Then we perform a classification cross-validation process using a linear support vector machine (SVM) classifier to confirm the discrimination power between both groups. On a second phase of the computational pipeline, for each sample in the pure feature dataset we retrieve the corresponding original signal windows. Finally, we could extract each foot step and perform morphological analysis (amplitude, half width, time to peak, decay time and inter-footsteps interval) on the signal chunks composed of selected pure clusters of signal windows. Power Density Spectra (PSD) analysis were also performed on these signal chunks as shown in Fig. 6.

B. 3D Scatter plots of WT (blue) and CFA (red) pure AR feature clusters depending on the AR coefficients (upper left: a1 vs a2 vs a3; bottom left: a1 vs a3 vs a4; upper right: a2 vsa3 vs a4; and bottom right: a1 vs a2 vs a4). Note that there are two well separated point clouds representing each experimental mice group.

C. Results of grid search given by 3D plots of weighted F-score (F-score * number of samples obtained for each group) vs the windows size (w) vs the number of clusters (k) for each AR order (p) from 2 to 10. Maximal weighted F-score (4000) corresponds to p=4, window size of 1000 points, and the number of clusters (k) was fixed to 1000.

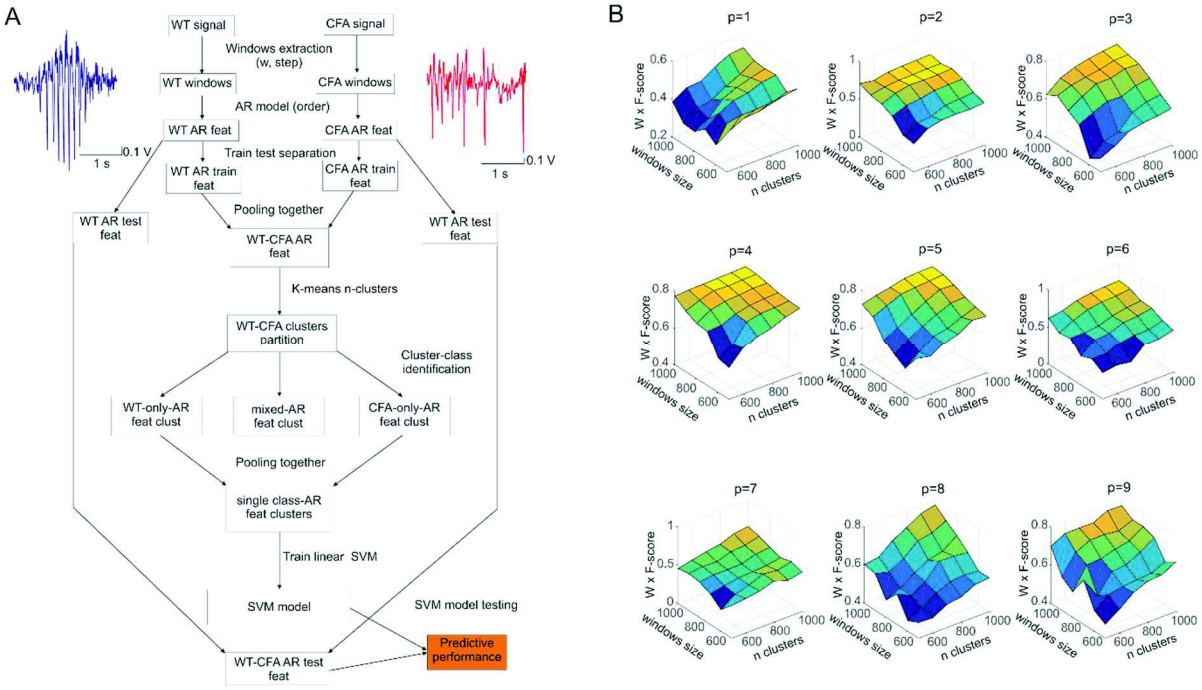

Figure S8. Clustering of foot step: methodological description of predictive analysis

A. Schematic diagram of the computational pipeline: Overlapping sliding windows of the signal are extracted from signal regions above the selected velocity threshold (15-20 cm/s) (on the left, a blue signal window example of a WT mouse locomotion; and on the right a red signal window shows a typical locomotion period in CFA mice). Every signal window is used to fit an autoregressive model (AR) of order=p (one model per window). The coefficients of these AR models become the AR features which encode the dynamic and spectral characteristics of each window. We split the feature dataset into independent training and test datasets at each cross-validation fold. Training dataset is used for model building according to the following steps: first, we carry out a k-means clustering, second, we identify pure clusters of AR features containing samples from only one class of mice, third, we built the reduced training dataset with samples from the pure clusters, finally, we train a linear SVM model on the reduced training dataset. We apply this model on the independent test dataset (note that it has not been "purified" of confusing data samples) to obtain predictive performance measures (F-score). Samples for which the model provides uncertain classification probabilities (i.e. too close to 0.5) are considered confusing samples and removed from the performance computation.

B. Results of the grid search given by 3D plots of weighed F-score (Fscore * number of samples obtained for each group) vs the windows size (w) vs the number of clusters (k) for each AR order (p) from 2 to 10.

Methods

Animals

Two mouse models of Alzheimer's disease were used, for a total of 30 3xTg-AD mice, 15 APP-PS1 mice, and their WT controls (respectively 67 and 15 animals). The 3xTg-AD mouse line contains three mutations associated with familial Alzheimer's disease that are the APP Swedish, MAPT P301L, and PSEN1 M146V (Oddo et al., 2003), while the APP-PS1 line contains the human transgenes for both APP and PSEN1. Another 8 Fmr1-KO mice (mouse model of Fragle X Syndrome) and their 8 WT controls were used for arousal (heartbeat) and anxiety (shaking) analysis. A total of 6 *Sprague*-Dawley adult rats were used in pain and breathing/heart-beat and sleep studies (4 and 2 animals respectively). 3 WT mice were used for itching analysis. Animals were bred in collective enriched cages in the laboratory animal facility, and then transfered to individual cages for the duration of the experiments. Animals were kept on a 12h/12h light/dark cycle (artificial light), provided with nesting material and food and water ad libitum. All experiments were performed during day time, between 10am and 7pm. All efforts were made to minimize suffering and keep the number of animals to a minimum.

Behavioral conditions

Open field exploration: Animals were placed in the recording chamber (45l × 35 w × 60 h cm) in which they were continuously recorded for durations ranging from 5min to 3h.
EEG under anesthesia: Rats and mice were deeply anesthetized with urethane (15mg/kg), placed on the floor of the recording plateform, and the electrocardiogram recorded as the different voltage fluctuations between 2 electrical wires positioned sub-cutaneously in the forepaw and hindpaw.
Itch / scratching: The fur on the nape of the neck was shaved and mice were habituated to the recording chamber 30 minutes prior to testing. The animal received an intradermal 50 µl injection of Chloroquine (40mg/10ml saline (0.9%) and was placed on the recording arena 10 minutes after.
***Fmr1*-KO mice heart beat:** 8 Fmr1-KO mice and their 8 WT controls were familiarized to the recording chamber for 3 days (1 hour/day). Every day during familiarization, mice were i.p. injected with vehicle (0.9% NaCl, 1.25% DMSO, 1.25% Tween 80, 10 ml per kg of body weight). On the fourth day, a single i.p. injection of BMS-204352 (2 mg per kg of body weight, dissolved in vehicle solution), was given to the animals 30 minutes before the recording session.
Pain: WT mice received a subcutaneous injection of complete Freund's adjuvant (CFA) in a hind paw as a model of inflammatory pain. The mice were recorded in the open field 24 hours after the injection, for a duration of 1h. Four adult Sprague-Dawley rats and three 3xTg-WT mice were anesthetized with isoflurane and implanted with intracranial electrodes for electrophysiological recordings. After 10min of recovery from anesthesia, animals were individually placed on the piezoelectric platform for a 5 min. recording session. Inmediatelly after, animals were injected with a single dose of the pain killer buprenorphine (0,05mg/Kg; 0.1ml/ 10g animal), and 10 minutes after injection, they were recorded again for 5 min.
Fear conditioning: On day 1, four 3xtg-WT mice were given a 5 minutes acclimation period to the conditioning chamber, followed by 5 trials consisting of 10 intermittent white tones (10 x 500ms tones separated by 1.5s) paired to 5x 1-sec footschocks (1 sec interval between each foot-shock). Intertrial interval was randomly chosen lasting 5-10 minutes.. On day 2, all mice were tested for context fear in the recording chamber (same experimental room with the same contextual configuration) during the first 10 minutes of exposition. Immediately after, 3 trials of tones were presented. Shaking and freezing behaviors were analyzed during the whole 30 minutes session.
Exposition to a predator: WT mice were individually pre-exposed to the recording chamber for 1 hour and the next day in the same platform they were exposed to an adult Sprague-Dawley rat. To do so, one of the arena walls was removed and a grid separated the rat (separated compartment) from the mouse (placed on the piezo platform). Shaking and freezing behaviors were analyzed during the 15-min recording session.

Tremor associated to neurodegenerative diseases:

- Parkinson mouse models: after 2 weeks of post-surgery recovery 6 dopamine-depleted (3 MFB and 3 striatum) and 2 sham mice were familiarized to the recording chamber for 3 days (1 hour/day) and at the fourth day, basal activity was measured for 1 hour. The following day, L-Dopa (sigma, 6 mg/kg) was injected i.p. together with benserazide (Sigma, 12 mg/kg, to inhibit peripheral DopaDecarboxylase) one hour before the 1-hour recording session.
- Alzheimer mouse model: 24 adult and 6 young 3xtg-AD mice and their WT controls (18 adults and 6 young) were used following the same behavioral protocol than for Dopamine depleted animals. In this case, Ldopa concentration was higher (50 mg/ kg) and additional sessions were applied to test Diazepam anxiolytic effect and Meloxicam analgesic effect. Two consecutive days after L-dopa injection, mice received an i.p injection of Diazepam (Sigma; 2mg/kg) 30 mins before the 30-min recording session. The following day, a single dose of Meloxicam (3mg/kg) was i.p. injected 60 min prior the 30-min recording session. Same experiments were also performed on 5 adults and 5 young APP-PS1 mice and their respective WT controls (5 adult and 6 young WT mice).

All drugs were injected with a dose of 0.1ml/ 10g animal.

Reserpine-induced tremor: Basal activity of two 3xtg-WT mice was measured during a 30-min recording session. Immediately after, and 30 min prior to the testing session animals were injected a single i.p. dose of reserpine (1mg/Kg). Mice spontaneous activity was then recorded for 30 minutes.

Dopaminergic lesions

Mice were injected with 6 hydroxylated analogue of dopamine (6-OHDA). 6-OHDA is generally used to generate toxin-inducing degeneration of dopaminergic neurons. Two groups of animas are defined here depending on the injection site: MFB (N=3) and striatum (N=3). In MFB animals, 6-OHDA was injected into the median forebrain bundle (MFB) through which the dopaminergic nigro-striatal tract ascends into the terminal region, the striatum. This lesion is more invasive since all the dopaminergic nigro-striatal tract are affected, together with the striatum. In the striatum group, 6-OHDA injection was applied directly in the striatum, so only the striatum is affected. 2 more animals were used as control, in which the same surgery was performed, but using vehicle instead of 6-OHDA.

Animals were first placed on the piezo platform after 2 weeks of post-surgery recovery. In order to test if the 6-OHDA injection had properly lesioned the dopaminergic population of neurons, single ip L-dopa injections (50 mg) were administered. The appearance of rotations and dyskinesia confirmed dopaminergic damage.

Data acquisition

The mice were introduced individually onto the recording plateform (Phenotypix, Imetronic, Bordeaux, France), a dimly illuminated open field environment (45x35cm), surrounded by 50cm-high walls and equipped with video monitoring. In this system, the floor plate is resting on piezoelectric pressure sensors, providing continuous analog signal generated by the subtle changes in floor-plate pressure due to animal movement. Video signal was acquired at a sample rate of 25 frames/s with a webcam placed 1.5 m above the platform, and piezo signal was recorded continuously at a 20 kHz sampling frequency. Both signals were acquired synchronously using Spike2 software (CED) and stored on a PC for offline analysis with EthoVision XT software (Noldus) and custom-made matlab scripts (Mathworks). Ethovision software provided automated animal detection and tracking (X-Y coordinates).

Data analysis

The derived-signal pattern identification of spontaneous behaviours was performed by first exploring visually video recording and the corresponding piezo-electric derived-signal. After visualization of the raw data, tagging of the different observed behaviour was manually performed using Spike2 software. Sonic Visualizer software, which allowed real-time frequency decomposition, was used to explore the main frequency that piezo derived-signal revealed about the whole battery of detected behaviours. Normal voluntary movements such as grooming, sniffing, running or scratching turned out to share a common frequency band at 5-20 Hz (figure C, D, E, and F). Running periods were selected automatically

based on the animal velocity calculated from the XY coordinates. A velocity threshold (15-20 cm/s) has been established in order to select this goal directed behaviour during locomotion, and not the dubitative orientating displacement. Shaking detection was done only during preselected periods of immobility (speed <1 cm/s).

Heart beat detection was corroborated by simultaneous electrocardiogram (ECG) recordings performed in urethane anesthetized animals placed over the piezo platform.

Clustering of footsteps

We show an automated procedure which allows to identify signal windows that show significant differences between WT and CFA (control and treated) mice. We assume that there are many confusing signal windows, so the task is to remove them to retain the discriminant ones. We propose machine learning approaches illustrated in supplementary figures S7 and S8. We have used linear approaches because they are the minimal complexity data models, parameter tuning is easy, risk of over fitting is lower than for non-linear approaches, and they are well understood by the scientific community. The first step is a feature extraction process in order to obtain an informative lower dimension representation of the data. We achieve dimensionality reduction by fitting an autorregressive model [35] of order *p* and using the regression coefficients as features. Thus we have a linear generative model of each signal window, which captures its dynamic and spectral characteristics. Secondly, we carry out a k-means clustering [36] of all the features, which induces a partition of the feature dataset. Next we identify which clusters are pure, i.e. containing only samples from one class of mice. We built a reduced feature dataset containing only the samples belonging to these clusters. We assume that this reduced feature dataset show significant differences between classes, so we confirm their discrimination power by means of a classification cross validation process using a linear support vector machine (SVM) [37] classifier approach. In order to find the largest feature dataset with the highest classification performance, we conduct a grid search on the following parameters: AR order (p), window size (w) and number of clusters (k) maximizing an objective function defined by the product of the feature dataset size and the classification performance measured by F-score [38]. From the feature dataset maximizing the objective function we retrieve the corresponding signal windows, merging them to obtain the signal chunks where discrimination has been detected. Finally, on these signal chunks we carry out the extraction of manually defined descriptive features, which show significant differences (as shown in fig. 6). Moreover, it is possible to build predictive models of the mice class following this approach as shown by crossvalidation experiments (described in figure S8) where there is a separation of train and test data before the selection process and the construction of the SVM model, ensuring that there is not double dipping effect [39]in the estimation of the classification performance. F-score results reach 0.80 which is well above random choice classification.

References

1. Ou-Yang, T.H., Tsai, M.L., Yen, C.T. & Lin, T.T. An infrared range camera-based approach for three-dimensional locomotion tracking and pose reconstruction in a rodent. *J Neurosci.Methods* **201**, 116-123 (2011).
2. Wiltschko, A.B.*, et al.* Mapping Sub-Second Structure in Mouse Behavior. *Neuron* **88**, 1121-1135 (2015).
3. Clarke, K.A. & Still, J. Gait analysis in the mouse. *Physiology & behavior* **66**, 723-729 (1999).
4. Machado, A.S., Darmohray, D.M., Fayad, J., Marques, H.G. & Carey, M.R. A quantitative framework for whole-body coordination reveals specific deficits in freely walking ataxic mice. *eLife* **4**, e07892 (2015).
5. Zorner, B.*, et al.* Profiling locomotor recovery: comprehensive quantification of impairments after CNS damage in rodents. *Nat Meth* **7**, 701-708 (2010).
6. Brodkin, J.*, et al.* Validation and implementation of a novel high-throughput behavioral phenotyping instrument for mice. *J.Neurosci.Methods* **224**, 48-57 (2014).
7. Wood, N.I.*, et al.* Increased thirst and drinking in Huntington's disease and the R6/2 mouse. *Brain Research Bulletin* **76**, 70-79 (2008).
8. Chen, S.-K.*, et al.* Hematopoietic Origin of Pathological Grooming in Hoxb8 Mutant Mice. *Cell* **141**, 775-785 (2010).
9. Mang, G.M.*, et al.* Evaluation of a piezoelectric system as an alternative to electroencephalogram/ electromyogram recordings in mouse sleep studies. *Sleep* **37**, 1383-1392 (2014).
10. Donohue, K.D., Medonza, D.C., Crane, E.R. & O'Hara, B.F. Assessment of a non-invasive high-throughput classifier for behaviours associated with sleep and wake in mice. *Biomed.Eng Online.* **7**, 14 (2008).
11. Daldrup, T.*, et al.* Expression of freezing and fear-potentiated startle during sustained fear in mice. *Genes, Brain and Behavior* **14**, 281-291 (2015).
12. Sato, S. Quantitative evaluation of ontogenetic change in heart rate and its autonomic regulation in newborn mice with the use of a noninvasive piezoelectric sensor. *American Journal of Physiology - Heart and Circulatory Physiology* **294**, H1708-H1715 (2008).
13. Boccia, M.L. & Roberts, J.E. Behavior and autonomic nervous system function assessed via heart period measures: the case of hyperarousal in boys with fragile X syndrome. *Behavior research methods, instruments, & computers : a journal of the Psychonomic Society, Inc* **32**, 5-10 (2000).
14. Roberts, J.E., Tonnsen, B., Robinson, A. & Shinkareva, S.V. Heart Activity and Autistic Behavior in Infants and Toddlers with Fragile X Syndrome. *American journal on intellectual and developmental disabilities* **117**, 90-102 (2012).
15. Hessl, D.*, et al.* Cortisol and behavior in fragile X syndrome. *Psychoneuroendocrinology* **27**, 855-872 (2002).
16. Carreno-Munoz, M.I.*, et al.* Potential Involvement of Impaired BKCa Channel Function in Sensory Defensiveness and Some Behavioral Disturbances Induced by Unfamiliar Environment in a Mouse Model of Fragile X Syndrome. *Neuropsychopharmacology* (2017).
17. Liu, Q.*, et al.* Sensory Neuron-Specific GPCR Mrgprs Are Itch Receptors Mediating Chloroquine-Induced Pruritus. *Cell* **139**, 1353-1365 (2009).
18. Inoue, A., Uchida, H., Nakazawa, T., Yamamoto, T. & Ito, S. Phosphorylation of NMDA receptor GluN2B subunit at Tyr1472 is important for trigeminal processing of itch. *European Journal of Neuroscience* **44**, 2474-2482 (2016).
19. Song, C., Berridge, K.C. & Kalueff, A.V. 'Stressing' rodent self-grooming for neuroscience research. *Nat Rev Neurosci* **17**, 591-591 (2016).
20. van Erp, A.M.M., Kruk, M.R., Meelis, W. & Willekens-Bramer, D.C. Effect of environmental stressors on time course, variability and form of self-grooming in the rat: Handling, social

contact, defeat, novelty, restraint and fur moistening. *Behavioural Brain Research* **65**, 47-55 (1994).
21. Meshalkina, D.A. & Kalueff, A.V. Commentary: Ethological Evaluation of the Effects of Social Defeat Stress in Mice: Beyond the Social Interaction Ratio. *Frontiers in Behavioral Neuroscience* **10**(2016).
22. Baranek, G.T., Foster, L.G. & Berkson, G. Tactile Defensiveness and Stereotyped Behaviors. *American Journal of Occupational Therapy* **51**, 91-95 (1997).
23. Merenstein, S.A*., et al.* Molecular-clinical correlations in males with an expanded FMR1 mutation. *American Journal of Medical Genetics* **64**, 388-394 (1996).
24. Symons, F.J., Clark, R.D., Hatton, D.D., Skinner, M. & Bailey, D.B. Self-injurious behavior in young boys with fragile X syndrome. *American Journal of Medical Genetics Part A* **118A**, 115-121 (2003).
25. Prut, L. & Belzung, C. The open field as a paradigm to measure the effects of drugs on anxiety-like behaviors: a review. *Eur J Pharmacol* **463**, 3-33 (2003).
26. de Diego-Otero, Y*., et al.* [alpha]-Tocopherol Protects Against Oxidative Stress in the Fragile X Knockout Mouse: an Experimental Therapeutic Approach for the Fmr1 Deficiency. *Neuropsychopharmacology* **34**, 1011-1026 (2008).
27. Mogil, J.S., Davis, K.D. & Derbyshire, S.W. The necessity of animal models in pain research. *Pain* **151**, 12-17 (2010).
28. Mogil, J.S. & Crager, S.E. What should we be measuring in behavioral studies of chronic pain in animals? *Pain* **112**, 12-15 (2004).
29. Langford, D.J*., et al.* Coding of facial expressions of pain in the laboratory mouse. *Nat.Methods* **7**, 447-449 (2010).
30. Webster, S.J., Bachstetter, A.D., Nelson, P.T., Schmitt, F.A. & Van Eldik, L.J. Using mice to model Alzheimer's dementia: an overview of the clinical disease and the preclinical behavioral changes in 10 mouse models. *Front Genet.* **5**, 88 (2014).
31. Guzmán-Ramos, K*., et al.* Restoration of dopamine release deficits during object recognition memory acquisition attenuates cognitive impairment in a triple transgenic mice model of Alzheimer's disease. *Learning & Memory* **19**, 453-460 (2012).
32. Ijmker, T. & Lamoth, C.J.C. Gait and cognition: The relationship between gait stability and variability with executive function in persons with and without dementia. *Gait & Posture* **35**, 126-130 (2012).
33. Ambrée, O*., et al.* Levodopa ameliorates learning and memory deficits in a murine model of Alzheimer's disease. *Neurobiology of Aging* **30**, 1192-1204 (2009).
34. Brooks, S.P. & Dunnett, S.B. Tests to assess motor phenotype in mice: a user's guide. *Nat.Rev.Neurosci* **10**, 519-529 (2009).
35. Mills, T.C. *Time Series Techniques for Economists*, (Cambridge University Press, 1991).
36. Hartigan, J.A. & Wong, M.A. Algorithm AS 136: A k-means clustering algorithm. *Applied Statistics* **28**, 100-108 (1979).
37. Cortes, C. & Vapnik, V. Support-Vector Networks. *Machine Learning* **20**, 273-297 (1995).
38. Rijsbergen, C.J.V. *Information Retrieval*, (Butterworth-Heinemann, 1979).
39. Kriegeskorte, N., Simmons, W.K., Bellgowan, P.S.F. & Baker, C.I. Circular analysis in systems neuroscience – the dangers of double dipping. *Nature neuroscience* **12**, 535-540 (2009).

Manuscript N. 3

Manuscript in revision in Frontiers in Computational Neuroscience

A non-linear dynamic approach to mouse behavioral discrimination using piezoelectric signals.

A. Moujahid, M.I. Carreño-Muñoz, K. Lopez-de-Ipiña, A. D'Anjou, X. Leinekugel

A Non-linear Dynamic Approach to Mouse Behavior Discrimination Using Piezoelectric Signals.

A. Moujahid[d], M.I. Carreño[f], K. López-de-Ipiña[1], A. D'Anjou[1], X. Leinekugel[f]

[a]*Signal Theory and Communications Department (DTSC), Carlos III University of Madrid (UC3M), Spain*
[b]*INSERM, Neurocentre Magendie, Physiopathologie de la plasticité neuronale, U862, Bordeaux, France*
[c]*University of the Basque Country UPV/EHU*

Abstract

The general idea that the complexity of physiological and behavioral systems decreases with aging and disease is debated. It has been reported that changes in complexity are dependent on the convergence of the different constraints governing the system dynamics. Here we provide evidence, using a novel technical approach for the study of FMR1-KO mice, that hyperactivity in Fragile X Syndrome (FXS) is associated with a decrease in behavior complexity. Based on nonlinear dynamical measures such as the correlation dimension (CD) and largest Lyapunov exponent (LLE), we have analyzed the underlying dynamics of the time series obtained from global spontaneous behavior content in piezoeletric signals. The results reveal that the dynamics of FXS mice seems to be confined in a low dimensional space characterized by decreased values of CD and LLE.

Keywords:

A Non-linear Dynamic Approach to Mouse Behavior Discrimination Using Piezoelectric Signals.

A. Moujahid[d], M.I. Carreño[f], K. López-de-Ipiña[1], A. D'Anjou[1], X. Leinekugel[f]

[d]*Signal Theory and Communications Department (DTSC), Carlos III University of Madrid (UC3M), Spain*
[e]*INSERM, Neurocentre Magendie, Physiopathologie de la plasticité neuronale, U862, Bordeaux, France*
[f]*University of the Basque Country UPV/EHU*

1. Introduction

Understanding the underlying mechanisms of complex behavior and the behavioral abnormalities product of neuropsychiatric disorders represent a critical issue in biomedical research. Behavioral phenotyping is indeed a keystone step to exploit a multitude of animal models and potentially useful pharmacological agents made available by academic and industrial medical research. Thus the behavioral examination of animals conditioned to controlled environmental situations can be used to evaluate specific aspects of mood or cognition such as anxiety or memory. On the other hand, analyzing spontaneous behavior of unconditioned animals can be also very informative about a whole variety of psychological, motor and cognitive components.

In the present study, we have investigated the spontaneous behavioral activity of pathological and normal mice exposed to novel and familiar environments different from their home cage. In order to perform a complete behavioral description over time, we adopted the piezoelectric technology which bring more precise information about the strength and architecture of each single animal movement. In fact, the Piezo system is provided with very sensitive pressure sensors that allow to detect slight animal movements leading to a very rich but also very complex signal that has been shown to provide a useful complement to video signals [1, 2, 3].

These signals often exhibit a range of nonlinear temporal behaviors and structural patterns that make traditional linear analysis methods unsuitable

to detect all irregular behaviors and quantify the fractal scaling and related correlation properties underlying physiological processes.

Over the past decades, various methods based on nonlinear dynamics theory have been proposed as alternative approaches to the traditional analysis of physiological time series which often tends to focus on averages, histograms and simple power spectra of physiological variables. Nonlinear analysis methods revealed that physiological processes generally operate far from equilibrium, their fluctuations exhibit long-range correlations that extend across many time scales, and underlying dynamics can be nonlinear driven by deterministic chaos [4]. In the same line, but based on complex network theory, many recent works have reported successful results about the study of experimental time series of time dependent complex systems. These include data from climate system [5], rhythmic dynamics in human gait [6] and spontaneous magnetoencephalographic (MEG) signals of epileptic patients and healthy subjects [7].

In particular, chaos inspired methods such as largest Lyapunov exponent (LLE) [8, 9, 10] and correlation dimensions [11, 12], have been increasingly used to characterize dynamical properties of a wide range of biological nonlinear systems, and are useful to study the structure of the underlying dynamics of the system. The main reasons of their relevance is the invariance under smooth transformations of the state space. Specifically, Lyapunov exponents refer to the average exponential rates of divergence or convergence of neighboring trajectories in the system phase space. And, correlation dimensions account for a quantitative characterization of the attractor geometry in the phase space.

During the last years, these methods have been used to characterize the complexity for a variety of physiological signals ranging from EEG recordings, perception and control to voice signals [13, 14]. In fact, fractal dimension has been proposed as a valid tools to characterize and classify electroencephalographic (EEG) time series [15]. Also, it has been used to diagnose some important vascular diseases such as the stenos and the arterio-venous malformations from the X-ray angiography [16]. Largest Lyapunov exponent, however, has been used to analyze alterations in Heart rate variability signals [17], to distinguish healthy controls from Parkinson's disease patients [18], or recently to investigate whether changes in state anxiety can modulate nonlinear dynamics of heart rate [19].

While these measures are well-known tools for describing and analyzing physiological signals, to the best of our knowledge, no work has addressed

their relevance in characterizing piezoelectric pressure like signals.

According to the experiment set-up adopted in this study to collect the data, we believe that the piezoelectric signals are not compatible with the assumption that they are created by a Gaussian random process with only linear correlations. In addition, it seems that their frequency spectra show an inverse power-law scaling pattern which is consistent with long range fractal correlation. And therefore, nonlinear measures such as correlation dimension and Lyapunov exponents can be useful to characterize the apparent nonlinear dynamics governing these physiological signals.

Therefore, the purpose of this study is twofold: first, discriminating between pathological (Fmr1 *knockout* (KO)) and normal (Wild type (WT)) mice behaviors and, secondly, characterizing the underlying dynamics governing the physiological process behind the exploring pattern of these mice and drawing some conclusions about their complex nature. The genetic condition known as Fragile X syndrome is the most common inherited form of mental retardation and one of the leading genetic causes for autism spectrum disorder. And, is caused by loss of expression of the fragile X mental retardation protein (FMRP), an RNA-binding protein that negatively regulates protein synthesis [20, 21, 22, 23, 24, 25, 26]. Absence of FMRP in mice leads to macroorchidism, learning deficits, hyperactivity and hypersensitivity as reported for FXS patients [27, 28].

2. Material and Methods

In the following we briefly review some basic concepts from the theory of dynamical systems to introduce how one can estimate nonlinear measures such as correlation dimension and largest Lyapunov exponents from time series. For detailed mathematical backgrounds the reader is referred to specialist texts [29, 30, 31].

The existence of the strange or chaotic attractor in the phase space is perhaps the main intrinsic property of a large class of nonlinear dissipative systems. The dynamical behavior of such systems is generally studied experimentally by recording a sequence of scalar measurements of some quantity. Let x_n $(1 \leq n \leq N)$ be a time series, where N is the sample size. The first step is therefore the reconstruction of the phase space which is the basis of almost all nonlinear time series analysis methods.

The most important phase space reconstruction technique is the method of delays. Vectors in a new space, the embedding space, are formed from

time delayed values of the scalar measurements.

A delay reconstruction in a m-dimensional space is formed by the vectors $\mathbf{X}_n$, given as:

$$\mathbf{X}_n = (x_n, x_{n+\tau}, ..., x_{n+(m-1)\tau})^T, \tag{1}$$

where τ is the time delay, and T stands for vector transpose. If τ is small compared to the internal time scales of the system, successive elements in the delay vectors are strongly correlated. However, if τ is very large, successive values are already almost independent, and the points fill a large cloud in the state space. A good and most natural estimate for finding a compromise between these extrema is the autocorrelation function of the time series which is intimately related to the shape of the attractor in the reconstructed space, and gives hints about stationarity and typical time scales.

2.1. Correlation dimension

The correlation dimension introduced by Grassberger and Procaccia [11, 12] is the most frequently used measure of complexity. This measure is based upon the correlation integral $C(\epsilon)$ which refers to the likelihood that any two randomly chosen points on the attractor will be closer than a given distance ϵ; usually $C(\epsilon)$ is determined for a range of values ϵ, and plotted as a function of ϵ in a double logarithmic plot. The crucial point of the Grassberger and Procaccia algorithm is that, for a sufficiently high embedding dimension m, the slope of a linear scaling region of $log(C(\epsilon))/log(\epsilon)$ gives an estimate of the correlation dimension.

The correlation integral is given as follows:

$$C(\epsilon) = \frac{1}{N(N-1)} \sum_{i=1}^{N} \sum_{j=i+1}^{N} \Theta(\epsilon - \|x_i - x_j\|), \tag{2}$$

where Θ is the Heaviside step function, $\Theta = 0$ if $x \leq 0$ and $\Theta = 1$ for $x > 0$. The sum just count the pairs (x_i, x_j) whose distance is smaller then ϵ. In the limit of an infinite amount of data and for smaller ϵ, it is expected that C scales like a power law, that is, $C(\epsilon) \propto \epsilon^D$, where D is defined as the correlation dimension as follows:

$$d(N, \epsilon) = \frac{\partial \ln C(\epsilon, N)}{\partial \ln \epsilon} \tag{3}$$

$$D = \lim_{\epsilon \to 0} \lim_{N \to \infty} d(N, \epsilon). \tag{4}$$

The correlation dimension D corresponds to the slope of the $\ln C$ versus $\ln \epsilon$ plot, and generally estimated by a least-square fit of a straight line over a certain range of ϵ, called the region (or *plateau*). The correlation dimension D is expected to have a non-integer value if the attractor is a fractal set. The above definitions of the correlation sum and dimension involve phase space vectors as the locations of points on an attractor. Thus, to compute these measures we have reconstructed the phase space by the embedding method considering two time delays given by the times where the autocorrelation function decays to $1/e$ and 0. The embedding dimension has been varied from 2 to 12.

Unfortunately, correlation dimension like other quantitative measures of time series analysis can be biased by temporal correlations. The most important temporal correlations comes from the fact that data close in time are also close in space. Indeed, successive elements of a time series are not usually independent. In particular for highly sampled flow data subsequent delay vectors are highly correlated. In order to obtain a consistent estimator of the correlation dimension, the correlation sum (Eq. 2) should cover a random sample of points drawn independently according to the invariant measure on the attractor. Theiler [32, 33] suggested to remove this spurious effect by simply ignoring all pairs of points in Eq.2 whose time indices differ by less than w, where w should be chosen generously. For a more detailed discussion about the optimal values of the Theiler window w, we refer the reader to the references [34, 35].

2.2. The largest Lyapunov exponent (LLE)

The exponential divergence or convergence of nearby trajectories is conceptually the strongest indication of the existence of chaos. The main idea behind most methods to compute Lyapunov exponents is to consider a small number of nearby points on the attractor, and to quantify the exponential increase or decrease of the inter vector distances over time intervals.

One can define as many different Lyapunov exponents as there are phase space dimensions, that is, for a m-dimensional embedding space there are λ_i, $i = 1, ..., m$ exponents. By convention, the Lyapunov exponents are always ordered so that $\lambda_1 > \lambda_2, ..., \lambda_m,$.

Among these exponents, the most important one is the largest Lyapunov exponent, λ_1, which is a strong signature of chaos.

To measure the LLE from our data, we used the algorithm introduced by Rosenstein et al. (1993) [8] and by Kantz [10] independently. It proceeds as

follows: Choose a reference point x_{t_0} of the time series in embedding space and select all neighbors with distance smaller than ϵ. Compute the average over the distance of all neighbors to the reference part of the trajectory as a function of the relative time. The logarithm of the average distance at time δ_t is some effective expansion rate over the time span δ_t containing all the deterministic fluctuations due to projection and dynamics. Repeating this for very many values t_0, the fluctuations of the effective expansion rate will average out. Based on this understanding, one has to compute:

$$x(\delta_t) = \frac{1}{N}\sum_{t_0=1}^{N} \ln\{\frac{1}{|\nu(x_{t_0})|}\sum_{x_t \in \nu(x_{t_0})} |x_{t_0+\delta_t} - x_{t+\delta_t}|\}. \quad (5)$$

where $\nu(x_{t_0})$ is the neighborhood of the reference point x_{t_0} with diameter given by ϵ. The size of the neighborhood should be as small as possible, but large enough such that on average each reference point has at a least a few neighbors. If $x(\delta_t)$ shows a linear increase with identical slope for all embedding dimensions m larger than some m_0 and for a reasonable range of ϵ, then this slope can be taken as an estimate of the LLE λ_1.

2.3. Ethical considerations

All experimental procedures were performed in accordance with the French and EU legislation regarding the protection of animals used for experimental and scientific purposes, 86/609/EEC and 2010/63/EU. The experiments have been approved by "Comit dEthique pour l'Exprimentation Animale de Bordeaux CEEA50 (agr par le ministre de la recherche)".

2.4. Animals

Mice were housed in an animal facility and kept on a 12 h:12 h light:dark cycle with ad libitum access to food and water. All experiments have been performed during the light period. Second generation Fmr1 knockout mice were used in our study [36].

Compared to the original Fmr1/y mouse line [24], these animals are deficient for both Fmr1 RNA and FMRP protein. Mice were backcrossed six generations into a C57BL/6J (Charles River) background and maintained in this mixed background for all experiments. Male wild-type and Fmr1/y littermates were generated by crossing Fmr1+/ females with a wild-type mouse from the same background. Given that Fmr1 is carried on the X chromosome, the resulting male progeny were either Fmr1+/y (wild-type) and Fmr1+/

(Fmr1-KO) mice. A total of 16 animals were used in this study of which 8 WT and 8 Fmr1-KO.

2.5. Experimental setup

Mice were introduced individually for a single 1 hour recording session onto the recording platform (Phenotypix, Imetronic, Bordeaux, France), a dimly illuminated open field environment (45x35cm), surrounded by 50cm-high walls and equipped with video monitoring. In this system, the floor plate is resting on piezoelectric pressure sensors, providing continuous analog signal generated by the subtle changes in floor-plate pressure due to animal movement. This environment was novel to the animal. Piezo signal was recorded continuously at 20 kHz sampling frequency, and acquired using Spike2 software (CED) and stored on a PC for offline analysis with EthoVision XT software (Noldus) [37] and custom-made Matlab scripts (Mathworks). Piezo signals (downsampled at 1250 Hz) were further analyzed. Finally, TISEAN 3.0.1 a software package for the analysis of time series with methods based on dynamical system theory were used to compute both correlation dimensions and Lyapunov exponents [38, 39].

2.6. Statistics

Data were analyzed using scripts and functions from the Matlab statistics toolbox (Matworks). Data were systematically tested for normal distribution with the Lilliefors test, a modification of the Kolmogorov-Smirnov test recommended for small sample sizes [45]. Data following non-normal distributions were analyzed using non-parametric tests: Kruskal-Wallis for independent data sets, Wilcoxon signed-ranks test for paired data. Data following a normal distribution were analyzed using parametric tests: ANOVA for independent data sets, and Student t-test for paired data. Results were considered significant for values of $p < 0.05$.

3. Results and discussion

The content of this section is divided into two main subsections which report the results obtained from linear and nonlinear methods respectively. The linear analysis consists mainly in computing measures such as the instantaneous variance, the auto-correlation and the power spectrum. The

nonlinear approach, however, focuses on computing the correlation dimension and the largest Lyapunov exponent from piezoelectric time series which allows to characterize both the underlying system attractor and dynamics.

Figure 1 contains box plots showing a visual summary of the distribution of the piezo signals of the different subjects from each experimental group. Three successive time periods corresponding to 20 minutes of recording have been considered for a better appreciation of the data distribution over time. In each of these plots the presence of outliers is evident for all time series. This is due mainly to the very sensitive pressure sensors characterizing the piezoelectric platform which allow to detect very slight animal movements ranging from heartbeat or breathing to large movements like walking, jumping or scratching. In these box plots, points are drawn as outliers if they are larger than $Q_3 + W(Q_3 - Q_1)$ or smaller than $Q_1 - W(Q_3 - Q_1)$, where $W = 1.5$, and Q_1 and Q_3 are the 25th and 75th percentiles, respectively.

In fact, the visual inspection of the exploring activity of these mice is characterized by repetitive jumps of the animals on the platform which may explain the presence of large peaks in the signals. This hyperactive behavior seems to be relaxed in time for WT than for KO mice (See the decreasing scale of the box plots for WT subjects).

3.1. **Linear analysis**

The first step to analyze these signals is to check for the non-stationarity property characterizing most of real data. In fact, temporal changes of the spontaneous dynamics are unavoidable and very natural when working with experimental data.

On the other hand, it is widely known that stochastic and nonlinear deterministic mechanisms generally give rise to fluctuations over multiple time scales, and typically show a frequency spectra with an inverse power-law scaling pattern which is a characteristic of fractal processes. This suggest that irregularity observed in long time recording looks similar (statistically) to that observed in a time series over a few minutes.

Non-stationarity has been analyzed using a very simple test which consists in computing the running variance for non-overlapping time windows of length 60 seconds, each containing 75000 data points. Within each time window, the standard error of the estimated mean ($\bar{x}$) is given by $\sqrt{\frac{\sum_1^N (x-\bar{x})^2}{N(N-1)}}$.

Figure 2 shows the area graphs of standard deviation of the piezoelectric time series from WT and Fmr1-KO averaged over all subjects.

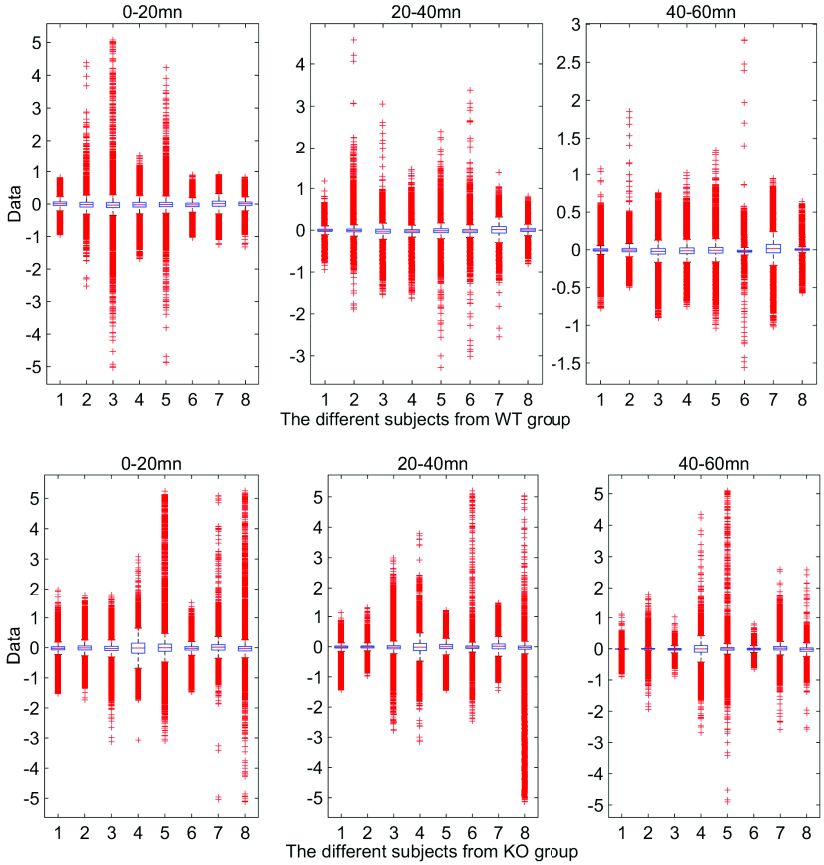

Figure 1: Boxplots for piezoelectric signals of the different subjects from each experimental group. Each experimental group is represented by 8 mice.

Non-stationarity is clearly visible in both signals as evidenced by small variations beyond the statistical fluctuations. Nevertheless, we can see a significant difference in variability between WT and KO time series (ANOVA, $F(1, 116) = 26.3$, $p < 0.001$). In fact, KO mice show higher variability with mean value of about 37% greater than WT ones ($\overline{var}_{KO} = 0.125$ and $\overline{var}_{WT} = 0.091$). On the other hand, the decreasing pattern of the running variance in KO mice seems to suffer a break towards the end of the recording.

The scaling behavior, however, were addressed considering the frequency spectra of the piezoelectric signals which has been computed using the Welch's method [41]. This method uses average values of power spectral density es-

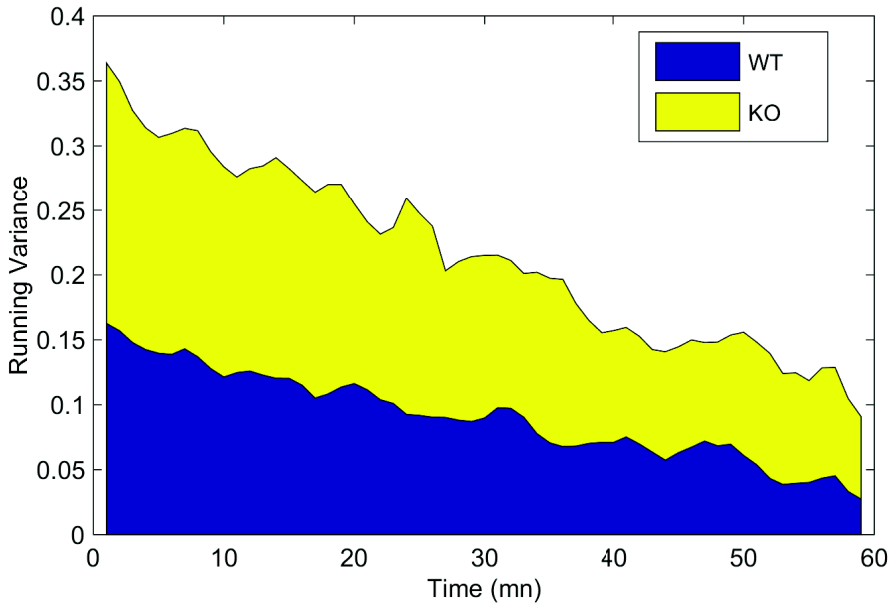

Figure 2: Area graphs of the running variance of piezoelectric signals from WT (blue) and Fmr1-KO (yellow). Values have been averaged over all subjects from each experimental group.

timates of different segments of the time series allowing a reduction of variability, and gives approximately uncorrelated estimates of the true power spectral density.

The frequency spectrum corresponding to two piezoelectric signals (from WT and KO groups) is shown in Fig. 3. The inverse power-law scaling pattern is clearly visible, and it seems to occurs in two different scaling regions. The first region corresponds to frequencies in the interval $[0.1-1Hz]$, and is characterized by the coefficients $\alpha_{WT} = -2.71$ and $\alpha_{KO} = -2.54$ for WT and KO subjects respectively. The second region, however, is identified at frequencies approximately higher than 10Hz with coefficients $\alpha_{WT} = -2.87$ and $\alpha_{KO} = -2.61$.

3.2. Non-linear analysis

After inspecting data both visually and based on running variance and frequency analysis for obvious non-stationarity and scale invariance, we have addressed the non-linear approach which consists in computing both the

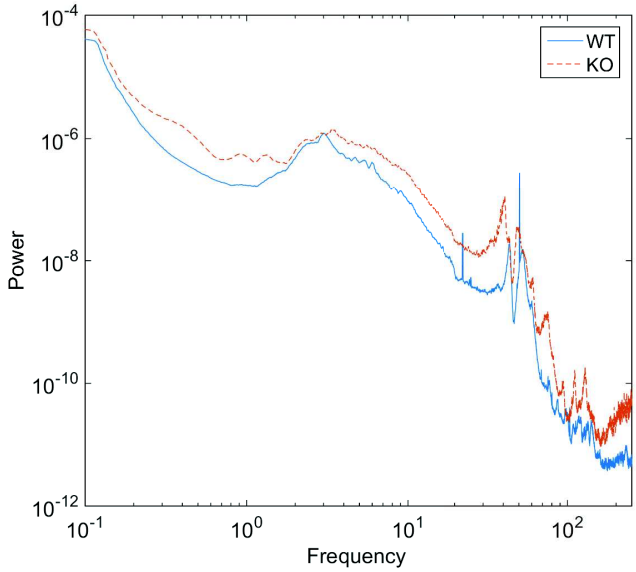

Figure 3: Frequency spectrum of piezoelectric signal from a WT subject (blue solid line) and Fmr1-KO (red dashed line). The frequency spectrum shows an inverse power-law scaling pattern consistent with long-range fractal correlations.

correlation dimension (D) and the largest Lyapunov exponents (LLE) for the piezoelectric signals.

3.2.1. Practical considerations

To compute these non-linear measures, we have divided each time series into non-overlapping time windows of length given by 180 seconds assuming stationarity at each time window. For each time window, the correlation sum (Eq. 2) and the average separation of neighbors (Eq. 5) have been computed for different embedding dimensions and time delays. The estimated values of D and LLE have been then averaged over all time windows giving a characteristic measure of each time series.

The embedding dimension has been varied from $m = 2$ to $m = 12$ and the time delay τ has been chosen according to the times where the auto-correlation function decays both to the values $1/e$ and 0 (e been the base of the natural logarithms). For the time series considered in this work, these times correspond, in average, to delays between $\tau = 5$ and $\tau = 8$ seconds.

To numerically compute the correlation sum given by Eq. 2, we have

considered the following parameters:

(i) the number of pairs covered by the sums is limited to 5000 pairs of points selected randomly (typically 1000 pairs will suffice). This number is sufficient to avoid statistical fluctuations;

(ii) the maximal length scale corresponds to the max data interval while the minimum length scale is a thousandth part of this interval;

(iii) the number of ϵ points is 100.

Similarly, to compute the average separation of neighbors given by Eq. 5, we have fixed:

(i) the minimal length scale to search neighbors to $range(data)/1000$;

(ii) the maximal length scale to search neighbors to $range(data)/100$;

(iii) the number of reference points to 10000 excluding those reference points which have no more that 20 neighbors closer than ϵ;

(iv) the number of relative time span (number of iterations) δ_t to 30.

Both correlation dimension and Lyapunov estimates may be affected by serial correlations between reference points and neighbors. Therefore, to exclude those correlated reference points we have chosen a Theiler w according to the first zero of the autocorrelation function.

3.2.2. Estimated values of the correlation dimension

Figure 4 reports, in top panels, the evolution of the average correlation dimension versus the embedding dimension (D) for a time delay $\tau = 8$ sec. The different curves refer to the different time series from each experimental group. As it can be appreciated, for values of embedding m greater than 5, the correlation dimension D tends to saturate. To study either this saturated regime is affected by the time delay, we have represented the average correlation dimension versus embedding for different time delays (See bottom panel).

As discussed in Method section, the values of the correlation dimension D correspond to the slopes of the $\ln C(\epsilon)$ versus $\ln \epsilon$ plots, and have been estimated by a linear fit of a straight line over a certain range of ϵ. For the time series considered in this work, this range is identified for ϵ values

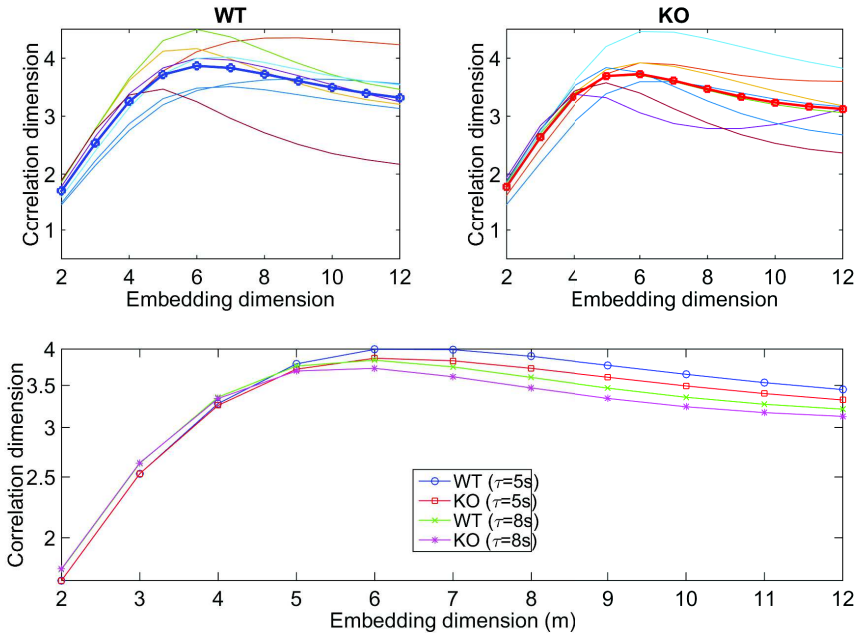

Figure 4: (Top) Correlation dimension (D) versus embedding dimension (m) for each subject from each experimental group ($\tau = 8s$). Lines with markers represent the average correlation dimensions over the different subjects. (Bottom) Average correlation dimension over the different subjects from each group. Two time delays were considered corresponding to the times where the auto-correlation function decays to $1/e$ and 0 respectively.

between $[10^{-2}, 10^{-1}]$ (See Figure 5). The power law behavior of $C(\epsilon)$ as a signature of self-similarity can be clearly appreciated from the local slopes. In fact, the desired power law for the correlation sum is the one where $d(\epsilon)$ is approximately independent of m and $C(\epsilon)$. That is, when the different curves of $d(\epsilon)$ corresponding to different embedding dimensions, show approximately the same value for a given range of $C(\epsilon)$.

To further understand the complexity behavior of the these mice, we have considered the temporal evolution of the average correlation dimension (D) over all subject characterizing each experimental group. The embedding dimension was fixed to $m = 10$ and time delay to $\tau = 8$ sec. In fact, for embedding dimension $m >= 8$, the correlation dimension saturates with m. Box plots disclosed in Fig. 6(a) show that WT mice, in average, seem

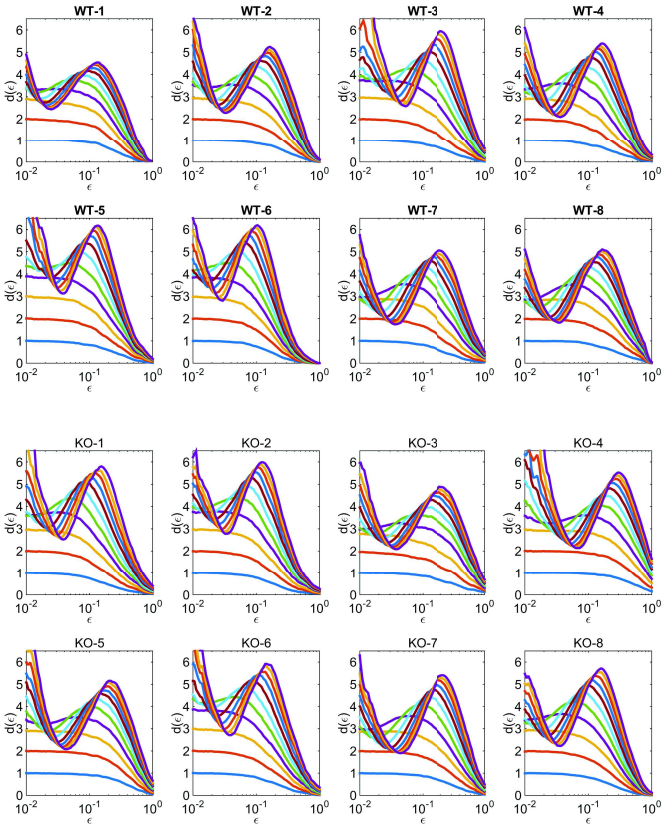

Figure 5: (Top) Local slopes $d(\epsilon)$ of the correlation integral for 3-minute intervals of the piezoelectric signals from WT (first 8 plots) and KO (last 8 plots) subjects. $d(\epsilon)$ is depicted versus ϵ in double logarithmic plot. The different curves were obtained for embedding dimensions $m = 2$ (lowest curve) to $m = 12$ (uppermost curve), and $\tau = 8$ sec.

to evolve in a high dimensional space compared to KO ones resulting in a significantly difference (Kruskal Wallis $H(1, 38) = 8.53$, $p = 0.0035$).

These results suggest that the low dimensional state space characterizing Ko mice could suggest a less complex patterns of variability in the exploring behavior of these mice. This observation is in agreement with the theory that there is a loss in the complexity of physiological and behavioral systems with aging and disease [42, 43].

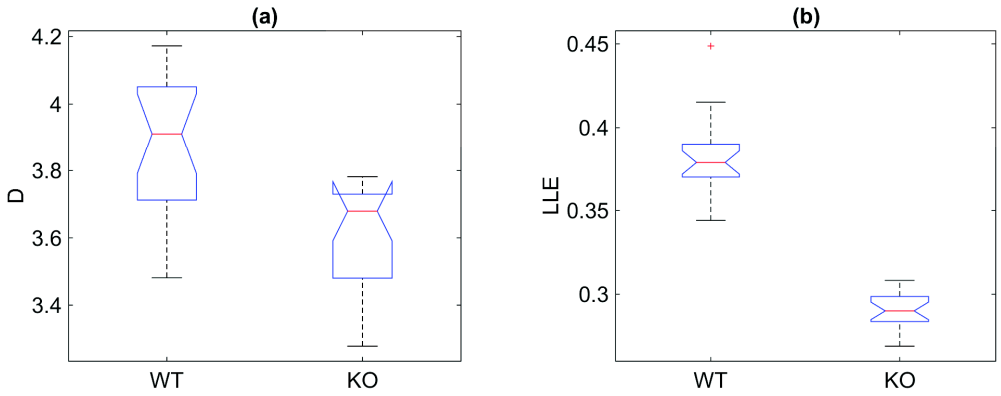

Figure 6: The average correlation dimension (D) (panel (a)) and the largest Lyapunov exponents (panel (b)) computed over all subjects from each experimental group. The embedding dimension was set to $m = 10$ and time delay $\tau = 8$ sec. For Lyapunov exponents the delay time was 8750 units (equivalent to 7 seconds).

3.2.3. Estimated values of the largest Lyapunov exponent

On the other hand, Lyapunov exponents reflect the tendency of small disturbances to grow exponentially, and therefore give a typical time scale for the divergence of nearby trajectories. According to our results (See Fig. 6(panel (b))), WT mice are characterized by largest Lyapunov exponents with values significantly higher than those of KO mice (ANOVA $F(1, 38) = 237$, $p << 0.0001$). And consequently, their prediction horizon (2.6 time unit) is one unit time shorter than the one of KO mice (3.6 time unit) [44].

4. Discussion

This paper discusses the use of nonlinear dynamical measures to discriminate between normal and pathological mouse behavior based on the global spontaneous activity of freely moving mice recorded for one hour in a novel open field environment. In fact, this work is only a part of an extensive study, still in progress, in which wild type (WT) and Fmr1-KO mice are injected with either vehicle solution or a candidate drug to restore normal behavior in Fragile X syndrome mice model.

To conduct this study, continuous analog signals generated by the changes in floor-plate pressure due to animal movement were recorded for 8 animals from each experimental group (WT and Fmr1-KO). These signals was

recorded continuously at 20 kHz sampling frequency and then down-sampled to 1250 Hz.

First, we performed a quantitative analysis which consist in computing measures such as the running variance, auto-correlation function and power spectrum. Two main conclusions could be drawn from this analysis: (i) the piezoelectric signals are non-stationary; (ii) the frequency spectrum of these signals shows an inverse power-law scaling pattern which is an immediate consequence of the exponentially decaying auto-correlation function.

Then, we carried out a non-linear analysis in order to characterize, for one hand, the underlying dynamics governing the physiological process behind the exploring pattern of these mice, and for the other hand, to draw some conclusions about their behavioral complexity. In fact, the main goal was to validate the hypothesis that the complexity of physiological and behavioral systems decreases with aging and disease. Results obtained show that the dynamics of Fmr1-KO mice is confined in a low dimensional space characterized by decreased values of CD and LLE. This suggests that in spite of hyperactivity [40, 27], the behavior is decreased in complexity in FMR1-KO mice, while this is not the case for all behavioral parameters in other diseases [42].

Acknowledgments

This work was performed thanks to the following funding sources: INSERM (XL), Region Aquitaine (XL) and ANR-13-BSV4-0011-02 (XL), UPV/EHU58/14 project (KLI). This project has also received public funding, provided by the National Research Agency (ANR) within the framework program *Investments for the Future, Excellence Initiative IdEx Bordeaux* under the reference ANR-10-IDEX-03-02 (MC).

[1] A.A.H.P. Megens, J. Voeten, J. Rombouts, T.F. Meert, and C.J.E. Niemegeers. Behavioural activity of rats measured by a new method based on the piezo-electric principle. *Psychopharmacology*, 93(3):382–388, 1987.

[2] Géraldine M Mang, Jérôme Nicod, Yann Emmenegger, Kevin D Donohue, Bruce F O'Hara, and Paul Franken. Evaluation of a piezoelectric system as an alternative to electroencephalogram/electromyogram recordings in mouse sleep studies. *Sleep*, 37(8):1383, 2014.

[3] Aaron E Flores, Judith E Flores, Hrishikesh Deshpande, Jorge A Picazo, Xinmin Xie, Paul Franken, H Craig Heller, Dennis A Grahn, and Bruce F O'Hara. Pattern recognition of sleep in rodents using piezoelectric signals generated by gross body movements. *Biomedical Engineering, IEEE Transactions on*, 54(2):225–233, 2007.

[4] AL. Goldberger. Complex systems. *Proceedings of the American Thoracic Society*, 3(6):467–471, 2006.

[5] J.F. Donges, Y. Zou, N. Marwan, J. Kurths, The backbone of the climate network, *Europhys. Lett.* 87 (2009) 48007.

[6] J. Zhang, K. Zhang, J.F. Feng, M. Small, Understanding rhythmic dynamics and synchronisation in human gait through dimensionality reduction, *PLoS Comput. Biol.* 6 (2010) e1001033.

[7] M. Chavez, M. Valencia, V. Navarro, V. Latora, and J. Martinerie Functional Modularity of Background Activities in Normal and Epileptic Brain Networks *Phys. Rev. Lett.* 104, 118701 Published 18 March 2010

[8] Michael T. Rosenstein, James J. Collins, and Carlo J. De Luca. A practical method for calculating largest lyapunov exponents from small data sets. *Physica D: Nonlinear Phenomena*, 65(1):117–134, 1993.

[9] Alan Wolf, Jack B. Swift, Harry L. Swinney, and John A. Vastano. Determining lyapunov exponents from a time series. *Physica D: Nonlinear Phenomena*, 16(3):285 – 317, 1985.

[10] Holger Kantz. A robust method to estimate the maximal lyapunov exponent of a time series. *Physics Letters A*, 185(1):77–87, 1994.

[11] Peter Grassberger and Itamar Procaccia. Measuring the strangeness of strange attractors. *Physica D: Nonlinear Phenomena*, 9(12):189 – 208, 1983.

[12] Peter Grassberger and Itamar Procaccia. Characterization of strange attractors. *Phys. Rev. Lett.*, 50:346–349, Jan 1983.

[13] Oliver Faust and Muralidhar G. Bairy. Nonlinear analysis of physiological signals: A review. *Journal of Mechanics in Medicine and Biology*, 12(04):1240015, 2012.

[14] C.J. Stam. Nonlinear dynamical analysis of {EEG} and meg: Review of an emerging field. *Clinical Neurophysiology*, 116(10):2266 – 2301, 2005.

[15] M. Phothisonothai and M. Nakagawa. Eeg signal classification method based on fractal features and neural network. In *2008 30th Annual International Conference of the IEEE Engineering in Medicine and Biology Society*, pages 3880–3883, Aug 2008.

[16] I. Tache, D. Popescu, and C. Vasseur. Fractal dimension for the analysis of vascular diseases on x-ray angiography. In *2015 20th International Conference on Control Systems and Computer Science*, pages 650–655, May 2015.

[17] L. Li, C. Liu, C. Liu, Q. Zhang, and B. Li. Physiological signal variability analysis based on the largest lyapunov exponent. In *2009 2nd International Conference on Biomedical Engineering and Informatics*, pages 1–5, Oct 2009.

[18] Paolo Pascolo, Fausto Barazza, and Roberto Carniel. Considerations on the application of the chaos paradigm to describe the postural sway. *Chaos, Solitons & Fractals*, 27(5):1339 – 1346, 2006.

[19] DA. Dimitriev, EV. Saperova, and AD. Dimitriev. State anxiety and nonlinear dynamics of heart rate variability in students. *PLoS ONE*, 11(1):564 – 570, 2016.

[20] Michael R. Santoro, Steven M. Bray, and Stephen T. Warren. Molecular mechanisms of fragile x syndrome: A twenty-year perspective. *Annual Review of Pathology: Mechanisms of Disease*, 7(1):219–245, 2012. PMID: 22017584.

[21] Dilja D Krueger and Mark F Bear. Toward fulfilling the promise of molecular medicine in fragile x syndrome. *Annual review of medicine*, 62:411, 2011.

[22] Anne Gallagher and Brian Hallahan. Fragile x-associated disorders: a clinical overview. *Journal of neurology*, 259(3):401–413, 2012.

[23] K. De-Boulle, A.J.M.H. Verkerk, E. Reyniers, L. Vits, J. Hendrickx, B. Van Roy, F. Van Den Bos, E. de Graaff, Ben A. Oostra, and P. J. Willems. A point mutation in the fmr-1 gene associated with fragile x mental retardation. *Nature Genetics*, 3(6):31–35, 1993.

[24] Cathy E Bakker, Coleta Verheij, Rob Willemsen, Robert van der Helm, Frank Oerlemans, Marcel Vermey, Anne Bygrave, AndréT Hoogeveen, Ben A Oostra, Edwin Reyniers, et al. Fmr1 knockout mice: a model to study fragile x mental retardation. *Cell*, 78(1):23–33, 1994.

[25] Peng Jin and Stephen T. Warren. Understanding the molecular basis of fragile x syndrome. *Human Molecular Genetics*, 9(6):901–908, 2000.

[26] Tatiana M Kazdoba, Prescott T Leach, Jill L Silverman, and Jacqueline N Crawley. Modeling fragile x syndrome in the fmr1 knockout mouse. *Intractable & rare diseases research*, 3(4):118, 2014.

[27] Yann S Mineur, Frans Sluyter, Sanne de Wit, Ben A Oostra, and Wim E Crusio. Behavioral and neuroanatomical characterization of the fmr1 knockout mouse. *Hippocampus*, 12(1):39–46, 2002.

[28] Simon Baron-Cohen, Emma Ashwin, Chris Ashwin, Teresa Tavassoli, and Bhismadev Chakrabarti. Talent in autism: hyper-systemizing, hyper-attention to detail and sensory hypersensitivity. *Philosophical Transactions of the Royal Society B: Biological Sciences*, 364(1522):1377–1383, 2009.

[29] J. P. Eckmann and D. Ruelle. Ergodic theory of chaos and strange attractors. *Rev. Mod. Phys.*, 57:617–656, Jul 1985.

[30] HG. Schuster. *Deterministic chaos. An introduction.* Weinheim: VCH Verlagsgesellschaft mbH, 1995.

[31] DT. Kaplan and L. Glass. *Understanding nonlinear dynamics.* New York: Springer Verlag, 1995.

[32] J. Theiler, Spurious dimensions from correlation algorithms applied to limited time-series data. *Phys. Rev. A* 34, 2427-2432, 1986.

[33] J. Theiler, Some comments on the correlation dimensionof $1/f^{\alpha}$ noise. *Phys. Lett. A*2155, 480, 1991.

[34] J. Theiler, Estimating fractal dimension *J. Opt. Soc. Amer. A* 7, 1055 (1990).

[35] H. Kantz and T. Schreiber, Dimension Estimates and Physiological Data *CHAOS* 5, 143 (1995);

[36] EJ Mientjes, I Nieuwenhuizen, L Kirkpatrick, T Zu, M Hoogeveen-Westerveld, L Severijnen, M Rife, R Willemsen, DL Nelson, and BA Oostra. The generation of a conditional fmr1 knock out mouse model to study fmrp function in vivo. *Neurobiology of disease*, 21(3):549–555, 2006.

[37] A.J Spink, R.A.J Tegelenbosch, M.O.S Buma, and L.P.J.J Noldus. The ethovision video tracking systema tool for behavioral phenotyping of transgenic mice. *Physiology & Behavior*, 73(5):731 – 744, 2001. Molecular Behavior Genetics of the Mouse.

[38] Rainer Hegger, Holger Kantz, and Thomas Schreiber. Practical implementation of nonlinear time series methods: The tisean package. *Chaos: An Interdisciplinary Journal of Nonlinear Science*, 9(2):413–435, 1999.

[39] Thomas Schreiber and Andreas Schmitz. Surrogate time series. *Physica D: Nonlinear Phenomena*, 142(3-4):346 – 382, 2000.

[40] Betty Hébert, Susanna Pietropaolo, Sandra Même, Béatrice Laudier, Anthony Laugeray, Nicolas Doisne, Angélique Quartier, Sandrine Lefeuvre, Laurence Got, Dominique Cahard, et al. Rescue of fragile x syndrome phenotypes in fmr1 ko mice by a bkca channel opener molecule. *Orphanet J. Rare Dis*, 9(124):10–1186, 2014.

[41] P. Welch. The use of fast fourier transform for the estimation of power spectra: A method based on time averaging over short, modified periodograms. *IEEE Transactions on Audio and Electroacoustics*, 15(2):70–73, Jun 1967.

[42] David E Vaillancourt and Karl M Newell. Changing complexity in human behavior and physiology through aging and disease. *Neurobiology of Aging*, 23(1):1 – 11, 2002.

[43] R.K.A. Rao and V.K. Yeragani. Decreased chaos and increased nonlinearity of heart rate time series in patients with panic disorder. *Autonomic Neuroscience: Basic and Clinical*, 88(1-2):99–108, 2001.

[44] M. Sano and Y. Sawada. Measurement of the lyapunov spectrum from a chaotic time series. *Phys. Rev. Lett.*, 55:1082–1085, Sep 1985.

[45] NM. Razali , Y. Bee Wah. Power comparisons of Shapiro-Wilk, Kolmogorov-Smirnov, Lilliefors and Anderson-Darling tests. *Journal of Statistical Modeling and Analytics*, 2(1): 21-33, 2011.

Manuscript N. 4

Conference proceedings – 4th International Work Conference on Bioinspired Intelligence (IWOBI)
197-204 (2015)

First approach to the analysis of spontaneous activity of mice based on Permutation Entropy

M.I. Carreño-Muñoz, K. Lopez-de-Ipiña, B. Beitia, A. Moujahid, A. Frick, X. Leinekugel

First approach to the analysis of spontaneous activity of mice based on Permutation Entropy

M.I Carreno, K. López de Ipiña, B. Beitia, A. Moujahid

Engineering School and Computer Sciences Faculty
20018, Donostia-San Sebastian Spain
Universidad del País Vasco/Euskal Herriko Unibertsitatea
{karmele.ipina, mariablanca.beitia,
abdelmalic.moujahid}@ehu.eus

M.I Carreno, A. Frick, X. Leinekugel

1. INSERM, Neurocentre Magendie, Physiopathologie de la plasticité neuronale, U862, Bordeaux, France.
2. University of Bordeaux, Neurocentre Magendie, Physiopathologie de la plasticité neuronale, U862, Bordeaux, France.
maria-isabel.carreno@u-bordeaux.fr,
xavier.leinekugel@inserm.fr; andreas.frick@inserm.fr

***Abstract*: Animal behavior is usually assessed by categorical classification. Here we used an alternative approach, based on the global quantification of video and pressure sensor derived signals, in order to characterize normal and pathological mouse behavior. Freely moving mice were recorded for 1h in a novel open field environment. In this preliminary study we have tested the use of permutation entropy applied to spatial information (Cartesian and polar coordinates of instantaneous position, provided by automatic video-tracking analysis) and movement-derived signal (ie total animal movement detected using piezoelectric pressure-sensors). We report that this approach could discriminate between wild type and transgenic Fmr1-KO mice, a model of neurodevelopmental disorder affecting cognitive functions and behavior in open field conditions.**

Keywords— Behavioral Phenotyping, Permutation Entropy, Piezo-electric pressure sensors.

I. INTRODUCTION

Behavioral phenotyping is a required step to exploit a multitude of transgenic mouse models and potentially useful pharmacological agents made available by academic and industrial medical research. While the examination of animals in controlled behavioral conditions can be used to evaluate specific aspects of mood or cognition such as anxiety or memory, analyzing spontaneous behavior in unsupervised conditions can also be very informative about a whole variety of psychological, motor and cognitive components. For example, previous studies based on the analysis of spontaneous rat or mouse activity in an open-field environment have identified specific behavioral correlates of different mouse strains or pharmacological drugs [1-6].

Identification of various behaviors is most often performed from video recordings [7-9]. Based on pixel by pixel analysis and sometimes sophisticated computational procedures such as pattern recognition or template matching, a number of behaviors such as rest, locomotion or grooming can be automatically identified by commercially available algorithms, although with less performance than trained human operators. A limitation of video signal is that it is sometimes difficult to discriminate between behaviors involving «stationary" movement such as grooming, sniffing, eating or drinking. In this respect, very sensitive pressure sensors are available, that can help detect slight animal movements [10;11]. One interesting thing about such movement-related signal is that it reflects the summed activity of all the muscles of the animal. Depending on the coordination of these myriads of muscles, their mechanical signature can sum up or cancel each other. This is therefore a very rich but also very complex signal that has been shown to provide a useful complement to video signal for the identification of a number of behaviors [10-12].

Nevertheless, behavioral characterization is a very complex matter and the more precise and sensitive the tool, the more potential categories to classify behavior, so that it may finally become a very tedious and difficult task. Accordingly, it has been reported recently that trained human operators requested to classify each second of a recording session had major problems attributing up to 44% of individual seconds to any specific behavior [13]. This evidence has lead our interest towards synthetic parameters such as Permutation Entropy (PE), a physical measure commonly used to characterize the non-linear dynamics of biosignals, an approach well suited to studying biological system's complexity [14]. Indeed, PE directly accounts for the temporal information contained in the time series derived from chaotic signals, so that the more regular, predictable and less complex the series, the lower its entropy. This is furthermore a fast, robust and cost-effective method that can be performed automatically without human supervision. It has already been used with some success to characterize rat locomotor behavior [15] or to detect behavioral alterations of schools of fish exposed to pollution [16].

We have tested the use of permutation entropy applied to spatial tracking and movement-derived signal (ie total animal movement detected using piezoelectric pressure-sensors), and report that it could discriminate between wild type and transgenic FMR1-KO mice, a model of neurodevelopmental disorder affecting cognitive functions and behavior in open field conditions.

Fragile X syndrome (FXS) is the most common heritable form of intellectual disability and is the leading known monogenic cause for autism spectrum disorders (ASD), with a third of FXS patients fulfilling the criteria for ASD [17-19]. FXS is caused by transcriptional silencing of Fmr1, which encodes the fragile X mental retardation protein (FMRP) [20]. Absence of FMRP in mice leads to macroorchidism, learning deficits, hyperactivity and hypersensitivity as reported for FXS patients [20-23]. Increased locomotor activity of Fmr1-KO has been observed in freely moving animals [22]. Our study provides evidence that permutation entropy applied to spatial tracking (instantaneous X-Y coordinates) and piezoelectric pressure-sensor signal also discriminates between wild type and Fmr1-KO mice.

The materials are described in section II. Section III presents the used methods. The results and discussion are described in section IV finally concluding remarks are included in section V.

II. Materials

A. Ethical considerations

All experimental procedures were performed in accordance with the French and EU legislation regarding the protection of animals used for experimental and scientific purposes, 86/609/EEC and 2010/63/EU. The experiments have been approved by the Ethical committee CEEA50 (saisine 50120167).

B. Animals

Mice were housed in an animal facility and kept on a 12 h:12 h light:dark cycle with ad libitum access to food and water. All experiments have been performed during the light period. Second generation Fmr1 knockout (Fmr1−/−; Fmr1−/y) mice were used in our study [24]. Compared to the original Fmr1−/y mouse line [20], these animals are deficient for both Fmr1 RNA and FMRP protein. Mice were backcrossed six generations into a C57BL/6J (Charles River) background and maintained in this mixed background for all experiments. Male wild-type and Fmr1−/y littermates were generated by crossing Fmr1+/− females with a wild-type mouse from the same background. Given that Fmr1 is carried on the X chromosome, the resulting male progeny were either Fmr1+/y (wild-type) or (0- still in progress, in which wild type (WT) and Fmr1-KO mice are injected with either vehicle solution or a candidate drug to restore normal behavior in this model [21;24;25]. Because the number of animals studied is still too low to draw any conclusion regarding the physiological effect of the drug, we are presenting here only the results obtained from 2 Fmr1-KO and 2 WT mice in control conditions (i.e. injected with a single intraperitoneal dose of 10 ml/kg vehicle solution containing 0.9 M NaCl supplemented with 1.25% DMSO and 1.25% Tween 80). Thirty minutes after the injection, the mice were introduced individually for a single 1 hour recording session onto the recording plateform (Phenact 2, Addenfi, Paris, France), a dimly illuminated open field environment (45x35cm), surrounded by 50cm-high walls and equipped with video monitoring. In this system, the floor plate is resting on piezoelectric pressure sensors, providing continuous analog signal generated by the subtle changes in floor-plate pressure due to animal movement. This environment was novel to the animal. Video signal was acquired at a sample rate of 25 frames/s with a webcam placed 1.5 m above the platform, and piezo signal was recorded continuously at a 20 kHz sampling frequency. Both signals were acquired synchronously using Spike2 software (CED) and stored on a PC for offline analysis with EthoVision XT software (Noldus) and custom-made matlab scripts (Mathworks). Ethovision software provided automated animal detection and tracking (X-Y coordinates).

III. Methods

A. Behavioral assessment system

This method paper reports the initial part of a larger study, still in progress, in which wild type (WT) and Fmr1-KO mice are injected with either vehicle solution or a candidate drug to restore normal behavior in this model [21;24;25]. Because the number of animals studied is still too low to draw any conclusion regarding the physiological effect of the drug, we are presenting here only the results obtained from 2 Fmr1-KO and 2 WT mice in control conditions (i.e. injected with a single intraperitoneal dose of 10 ml/kg vehicle solution containing 0.9 M NaCl supplemented with 1.25% DMSO and 1.25% Tween 80). Thirty minutes after the injection, the mice were introduced individually for a single 1 hour recording session onto the recording plateform (Phenact 2, Addenfi, Paris, France), a dimly illuminated open field environment (45x35cm), surrounded by 50cm-high walls and equipped with video monitoring. In this system, the floor plate is resting on piezoelectric pressure sensors, providing continuous analog signal generated by the subtle changes in floor-plate pressure due to animal movement. This environment was novel to the animal. Video signal was acquired at a sample rate of 25 frames/s with a webcam placed 1.5 m above the platform, and piezo signal was recorded continuously at a 20 kHz sampling frequency. Both signals were acquired synchronously using Spike2 software (CED) and stored on a PC for offline analysis with EthoVision XT software (Noldus) and custom-made matlab scripts (Mathworks). Ethovision software provided automated animal detection and tracking (X-Y coordinates).

B. Permutation Entropy

As Shannon entropy, permutation entropy (PE) quantifies the disorder of a system [27-30]. Bandt and Pompe [14] introduce this method that takes into account time causality by comparing neighboring values in a time series. PE has shown a good ability to measure complexity for large time series and basically converts a time series into an ordinal patterns series where the order of relations between the present and a fixed number of equidistant past values at a given time are described. Moreover it has the quality of simplicity, robustness and very low computational cost [16,28,29].

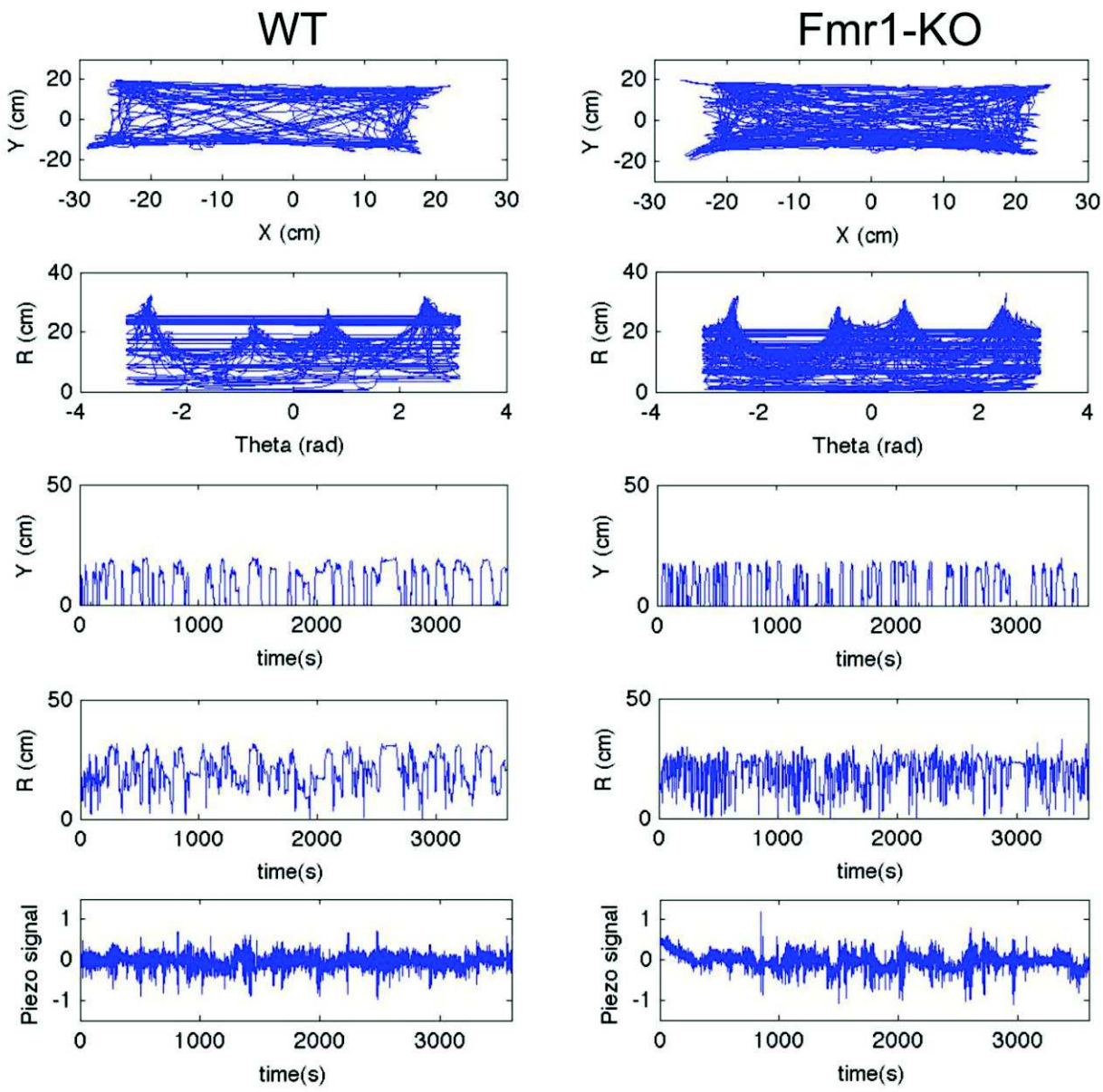

Figure 1. Instantaneous position (spatial coordinates) and whole body movement (piezoelectric sensor signal) from WT and Fmr1-KO mice in an open field A-B. Instantaneous position (Cartesian (XY) and polar (ZR) coordinates) in WT and Fmr1-KO mice recorded during the first 20min of exposition to a novel open-field environment. C-E. Instantaneous Y, Z and P, over time. Spatial coordinates were measured on every video frame (abscise, time, 25 frames/s). Piezo signal was sampled at 1.25 KHz (abscise, time, sample #).

The appropriate symbol sequence arises naturally from the time series, with no prior knowledge assumed [28]. The Permutation entropy (PE) is calculated for a given time series of length N $\{x_1, x_2, \ldots, x_N\}$ as a function of the scale factor s. Simple PE is calculated for s=1 and depends on two-parameters: the embedding dimension, m, and a time-lag, τ, where m is the number of samples belonging to the segment, and τ represents the distance between the sample points spanned by each section of the motif [14,29]. Then in order to compute the PE over the time series, the series of vectors of length m are generated. Thus for m different samples, there will be $m!$ (also known as permutation of m) possible ordinal patterns, π, which are also called "motifs".[29]. If $f(\pi)$ denotes its frequency in the time series, its relative frequency is $p(\pi) = f(\pi)/(N - m + 1)$. The permutation entropy is then defined as:

$$PE = -\sum_{i=1}^{m!} p(\pi_i) \ln p(\pi_i) \qquad (1)$$

Being the maximum value of PE is log2(d!), which implies that all patterns have equal probability. The smallest value is zero when the series is very regular with a repetition of the same basic pattern [29]. m should be > 2.

Summarizing, permutation entropy refers to the local order structure of the time series, which can give a quantitative measure of complexity for dynamical time series. This calculation depends on the selection of the m parameter, which is strictly related with the length N of the analyzed signal. In the experimentation m=4 and t=1.

C. Signal Analysis

Each animal recording is divided in 90 chunks and the following signal analysis is carried out:

- (*Analysis of spacial mice's trajectories* based on cartesian (X,Y) and polar (θ,R) coordinates. Evolution of these signals across the time. θ will be named Z in figures.
- Analysis of piezoelectric signal (P) across the time.
- *Permutation Entropy (PE)* of the signal of previously defined coordinates (X,Y, θ and R) and P. One point for each chunk.

IV. Results

Wild type (WT) and Fmr1-KO (KO) mice were introduced individually in the open field device and recorded for 1 hour, during which they became progressively familiar with this novel environment. As illustrated in Fig.1, video tracking analysis provided the instantaneous Cartesian (XY) and polar (θ R) coordinates, which were analyzed together with the signal, derived from piezoelectric pressure-sensors (P), reflecting up to subtle animal's movement. Instantaneous permutation entropy (PE) was computed on the variables X, Y, θ and P.

As appears in the boxplot representation shown in Fig.2, confirmed with statistical analysis with the non-parametric Kruskal Wallis test, applied to the whole recording period (1h), there was a significant ($p<0.05$) group effect on PE for X, Y, θ and P with an increased entropy in WT compared to KO mice.

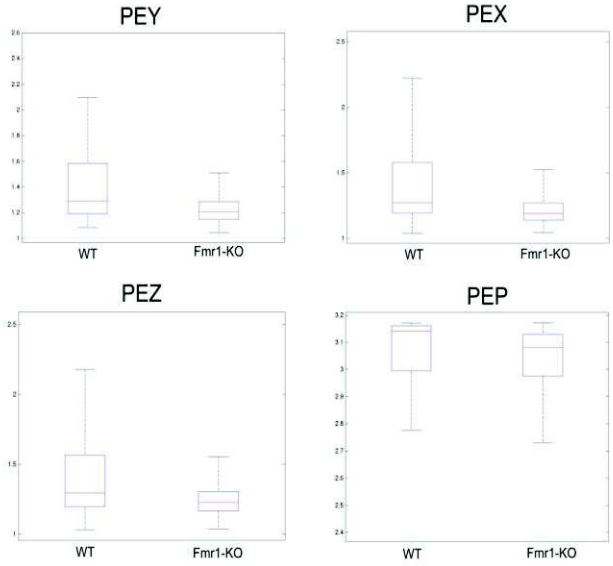

Figure 2: Permutation Entropy of X, Y, θ and Piezoelectric signal in WT and FMR1-KO mice for the whole 1 hour session. X (PEX), Y (PEY), θ (PEZ) and P (PEP) are significantly higher in WT than in Fmr1-KO.

Therefore, PE applied to animal tracking data obtained from video analysis as well as to movement-related signal obtained from piezoelectric pressure-sensors could discriminate between WT and Fmr1-KO phenotypes, indicating behavioral differences over a 1h exposure to a novel open field environment.

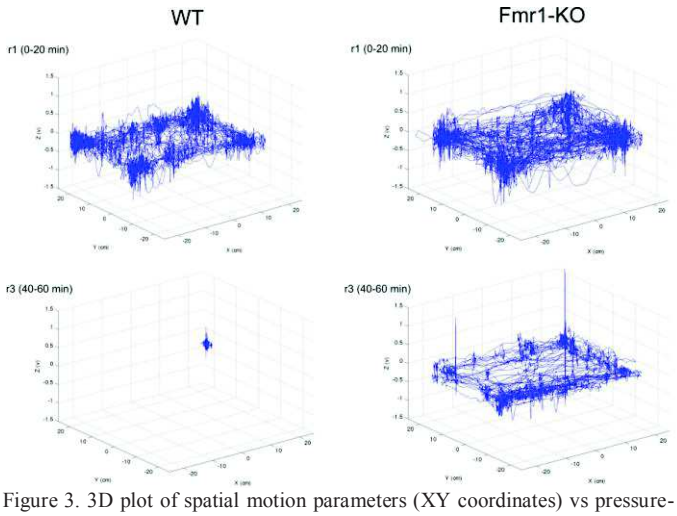

Figure 3. 3D plot of spatial motion parameters (XY coordinates) vs pressure-sensors signal reflecting global body-movement (P) during the first (r1) and last (r3) 20 minutes of exposition for WT and Fmr1-KO mice.

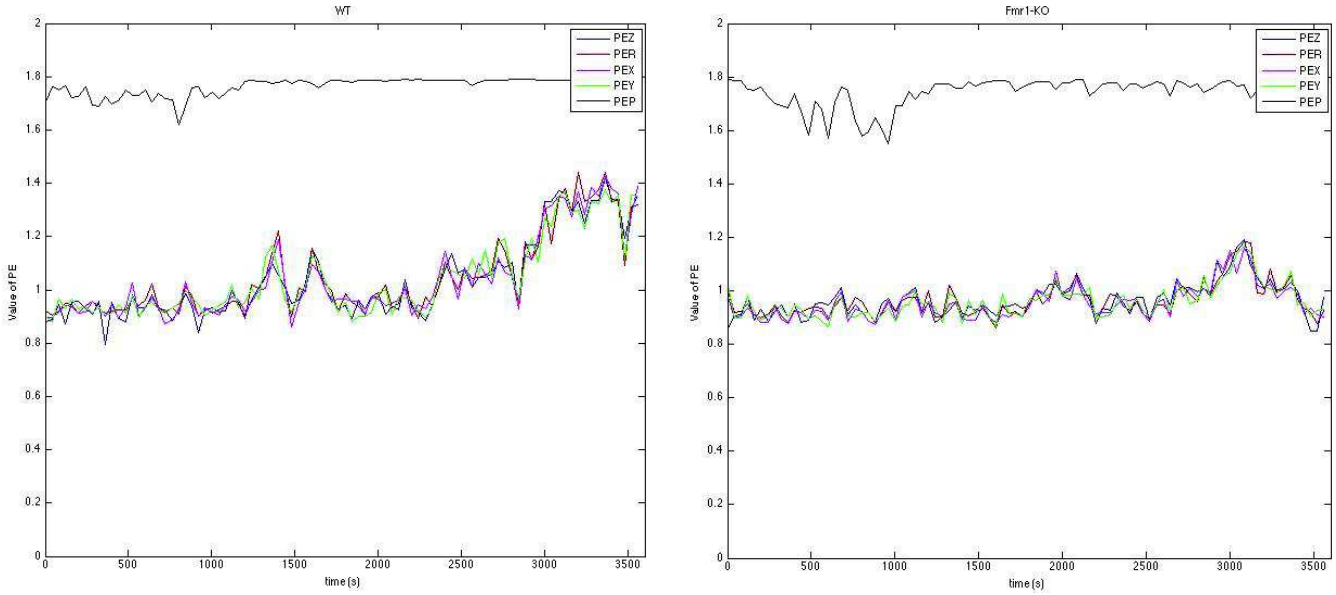

Figure 4. Permutation Entropy of spatial coordinates (X,Y, θ (Z) and R; colour lines) and Piezoelectric signal (black line) over time (s) in WT (left) and Fmr1-KO (right) mice during one hour exposition to a novel environment. Note general increase of PE over time. Note higher PE mean in WT compared to Fmr1-KO mice for positional information (Y).

We next investigated how mice behavior changed over the course of exposure to the open field. As illustrated in Fig.3, WT mice that were all actively exploring the environment during the initial 20 min then showed a trend to decrease in explorative behavior, spending some time in grooming and finally getting asleep before the end of the 1h session. In contrast, Fmr1-KO mice kept a high level of explorative behavior throughout the 1h period. Interestingly, PE analysis also allowed to recognize that changes in behavior occur as a function of time exposure to a novel environment. The evolution of PE values over the 1h recording is illustrated in Fig.4. Beside a transient decrease for PEP during the initial part of the recording, it appears that PE values are increasing with time in both WT and KO for the parameters reflecting the position of the animal (XY, θ R), although a difference between WT and KO mice progressively appears with time, with higher PE in WT than in KO mice during the last 20min of exposure. As illustrated in Fig.5, and confirmed by Kruskal Wallis test on the animals ($p<0.05$), it appears that PE was increased for all parameters measured (XY, θ, P) between the initial and last 20min of the 1h recording session, potentially pointing to less predictable behavior when the environment is getting more familiar, both in terms of exploration and gross body movement.

Even though the low number of animals at this stage does not allow us to make any conclusion regarding differences between genotypes, it appears from the data shown in Fig.5 that this increase in PE could be much less strong in Fmr1-KO mice than in WT. Together with tracking data (Fig.3), *t*hese preliminary results therefore point to a major potential difference between WT and Fmr1-KO mice, suggesting that the behavior of Fmr1-KO mice might be much less sensitive to familiarization than that of WT mice at the 1h time scale.

V. Discussion and Conclusions

In conclusion, our preliminary study suggests that PE applied to animal movement can be used to detect differences in behavior in respect to genotype and time spent in a new environment. The potential contribution of spatial memory deficit and associative learning impairment [25] to persistent explorative behavior in Fmr1-KO mice remains to be investigated in more detail.

Interestingly, PE calculations provided here different genotyping signatures when applied to spatial motion parameters (XY/ θ coordinates) vs pressure-sensors detected body-movement (P). Understanding the physiological basis of these differences will require more specific behavioral investigation. We expect the piezoelectric platform to be useful as a complement to video recording to identify and quantify specific behaviors, so that we can pin down which specific aspects of animal behavior are affected in various diseases such as Fragile-X related neurodevelopmental disorders.

But the combination of global quantification measures such as PE and technological tools recording specific and global aspects of behavior such as video and piezo signals appears as a promising approach for behavioral phenotyping. In ongoing works this study will be extended with regard to animal number and to the methodology by introducing Multiscale Permutation Entropy.

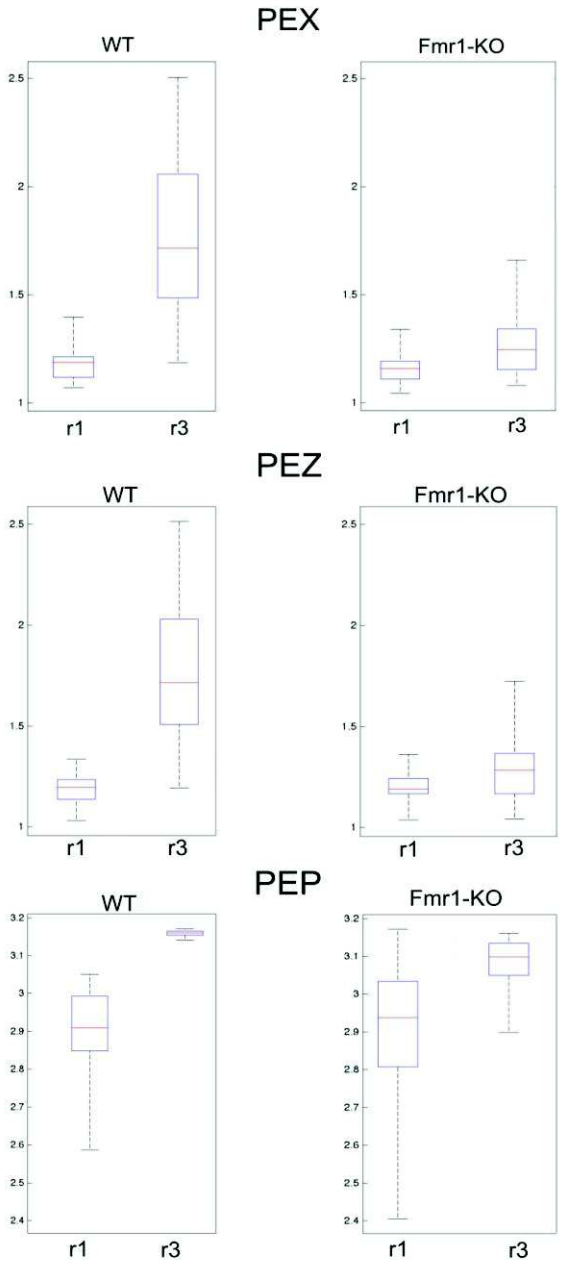

Figure 5. PEX, PEZ (PE, θ) and PEP values for WT and Fmr1 mice over time. r1, first 20min of exposition to the environment; r3, last 20min of the 1h recording session. Note the significant increase in PE with time in WT but not in Fmr1-KO mice.

ACKNOWLEDGMENTS

This work was performed thanks to the following funding sources: INSERM (XL), Region Aquitaine (XL) and ANR-13-BSV4-0011-02 (XL), UPV/EHU—58/14 project (KLI) This project has also received public funding, provided by the National Research Agency (ANR) within the framework program "Investments for the Future, Excellence Initiative IdEx Bordeaux" under the reference ANR-10-IDEX-03-02 (MC) . We thank Enejda Subashi for technical assistance with mice recording.

REFERENCES

[1] N. Maubourguet, A. Lesne, J. P. Changeux, U. Maskos, and P. Faure, "Behavioral sequence analysis reveals a novel role for beta2* nicotinic receptors in exploration," PLoS. Comput. Biol., vol. 4, no. 11, p. e1000229, Nov.2008.

[2] L. Prut and C. Belzung, "The open field as a paradigm to measure the effects of drugs on anxiety-like behaviors: a review," Eur. J. Pharmacol., vol. 463, no. 1-3, pp. 3-33, Feb.2003.

[3] D. Lipkind, A. Sakov, N. Kafkafi, G. I. Elmer, Y. Benjamini, and I. Golani, "New replicable anxiety-related measures of wall vs center behavior of mice in the open field," J Appl. Physiol, vol. 97, no. 1, pp. 347-359, July2004.

[4] A. Dvorkin, Y. Benjamini, and I. Golani, "Mouse cognition-related behavior in the open-field: emergence of places of attraction," PLoS. Comput. Biol., vol. 4, no. 2, p. e1000027, Feb.2008.

[5] C. M. Thiel, C. P. Muller, J. P. Huston, and R. K. Schwarting, "High versus low reactivity to a novel environment: behavioural, pharmacological and neurochemical assessments," Neuroscience, vol. 93, no. 1, pp. 243-251, 1999.

[6] U. Maskos, B. E. Molles, S. Pons, M. Besson, B. P. Guiard, J. P. Guilloux, A. Evrard, P. Cazala, A. Cormier, M. Mameli-Engvall, N. Dufour, I. Cloez-Tayarani, A. P. Bemelmans, J. Mallet, A. M. Gardier, V. David, P. Faure, S. Granon, and J. P. Changeux, "Nicotine reinforcement and cognition restored by targeted expression of nicotinic receptors," Nature, vol. 436, no. 7047, pp. 103-107, July2005.

[7] R. K. Schwarting, R. Goldenberg, H. Steiner, J. Fornaguera, and J. P. Huston, "A video image analyzing system for open-field behavior in the rat focusing on behavioral asymmetries," J. Neurosci. Methods, vol. 49, no. 3, pp. 199-210, Sept.1993.

[8] D. Drai and I. Golani, "SEE: a tool for the visualization and analysis of rodent exploratory behavior," Neurosci Biobehav. Rev., vol. 25, no. 5, pp. 409-426, July2001.

[9] A. J. Spink, R. A. Tegelenbosch, M. O. Buma, and L. P. Noldus, "The EthoVision video tracking system--a tool for behavioral phenotyping of transgenic mice," Physiol Behav., vol. 73, no. 5, pp. 731-744, Aug.2001.

[10] A. A. Megens, J. Voeten, J. Rombouts, T. F. Meert, and C. J. Niemegeers, "Behavioral activity of rats measured by a new method based on the piezo-electric principle," Psychopharmacology (Berl), vol. 93, no. 3, pp. 382-388, 1987.

[11] G. M. Mang, J. Nicod, Y. Emmenegger, K. D. Donohue, B. F. O'Hara, and P. Franken, "Evaluation of a piezoelectric system as an alternative to electroencephalogram/ electromyogram recordings in mouse sleep studies," Sleep, vol. 37, no. 8, pp. 1383-1392, 2014.

[12] A. E. Flores, J. E. Flores, H. Deshpande, J. A. Picazo, X. S. Xie, P. Franken, H. C. Heller, D. A. Grahn, and B. F. O'Hara, "Pattern recognition of sleep in rodents using piezoelectric signals generated by gross body movements," IEEE Trans. Biomed. Eng, vol. 54, no. 2, pp. 225-233, Feb.2007.

[13] J. Brodkin, D. Frank, R. Grippo, M. Hausfater, M. Gulinello, N. Achterholt, and C. Gutzen, "Validation and implementation of a novel high-throughput behavioral phenotyping instrument for mice," J. Neurosci. Methods, vol. 224, pp. 48-57, Mar.2014.

[14] C. Bandt and B. Pompe, "Permutation Entropy: A Natural Complexity Measure for Time Series," Phys. Rev. Lett., vol. 88, no. 17, p. 174102, Apr.2002.

[15] M. P. Paulus, M. A. Geyer, L. H. Gold, and A. J. Mandell, "Application of entropy measures derived from the ergodic theory of dynamical systems to rat locomotor behavior," Proc. Natl. Acad. Sci. U. S. A, vol. 87, no. 2, pp. 723-727, Jan.1990.

[16] H. Eguiraun, K. LÃ³pez-de-IpiÃ±a, and I. Martinez, "Application of Entropy and Fractal Dimension Analyses to the Pattern Recognition of Contaminated Fish Responses in Aquaculture," Entropy, vol. 16, no. 11, pp. 6133-6151, 2014.

[17] M. R. Santoro, S. M. Bray, and S. T. Warren, "Molecular mechanisms of fragile X syndrome: a twenty-year perspective," Annu. Rev. Pathol., vol. 7, pp. 219-245, 2012.

[18] D. D. Krueger and M. F. Bear, "Toward fulfilling the promise of molecular medicine in fragile X syndrome," Annu. Rev. Med., vol. 62, pp. 411-429, 2011.

[19] A. Gallagher and B. Hallahan, "Fragile X-associated disorders: a clinical overview," J. Neurol., vol. 259, no. 3, pp. 401-413, Mar.2012.

[20] "Fmr1 knockout mice: a model to study fragile X mental retardation. The Dutch-Belgian Fragile X Consortium," Cell, vol. 78, no. 1, pp. 23-33, July1994.

[21] Y. Zhang, A. Bonnan, G. Bony, I. Ferezou, S. Pietropaolo, M. Ginger, N. Sans, J. Rossier, B. Oostra, G. LeMasson, and A. Frick, "Dendritic channelopathies contribute to neocortical and sensory hyperexcitability in Fmr1(-/y) mice," Nat. Neurosci., vol. 17, no. 12, pp. 1701-1709, Dec.2014.

[22] Y. S. Mineur, F. Sluyter, W. S. de, B. A. Oostra, and W. E. Crusio, "Behavioral and neuroanatomical characterization of the Fmr1 knockout mouse," Hippocampus, vol. 12, no. 1, pp. 39-46, 2002.

[23] S. Baron-Cohen, E. Ashwin, C. Ashwin, T. Tavassoli, and B. Chakrabarti, "Talent in autism: hyper-systemizing, hyper-attention to detail and sensory hypersensitivity," Philos. Trans. R. Soc. Lond B Biol. Sci., vol. 364, no. 1522, pp. 1377-1383, May2009.

[24] E. J. Mientjes, I. Nieuwenhuizen, L. Kirkpatrick, T. Zu, M. Hoogeveen-Westerveld, L. Severijnen, M. Rife, R. Willemsen, D. L. Nelson, and B. A. Oostra, "The generation of a conditional Fmr1 knock out mouse model to study Fmrp function in vivo," Neurobiol. Dis., vol. 21, no. 3, pp. 549-555, Mar.2006.

[25] B. Hebert, S. Pietropaolo, S. Meme, B. Laudier, A. Laugeray, N. Doisne, A. Quartier, S. Lefeuvre, L. Got, D. Cahard, F. Laumonnier, W. E. Crusio, J. Pichon, A. Menuet, O. Perche, and S. Briault, "Rescue of fragile X syndrome phenotypes in Fmr1 KO mice by a BKCa channel opener molecule," Orphanet. J. Rare. Dis., vol. 9, p. 124, 2014.

[26] S. Pietropaolo, A. Guilleminot, B. Martin, F. R. D'Amato, and W. E. Crusio, "Genetic-background modulation of core and variable autistic-like symptoms in Fmr1 knock-out mice," PLoS. One., vol. 6, no. 2, p. e17073, 2011.

[27] Shannon, C.; Weaver, W. The Mathematical Theory of Communication; University of Illinois Press: Champaign, IL, USA, 1949.

[28] Zanin M., L Zunino, OA Rosso, D Papo. Permutation entropy and its main biomedical and econophysics applications: a review. Entropy 14 (8), 1553-1577.

[29] Morabito F.C., D. Labate, F. La Foresta, A. Bramanti, G. Morabit, and I. Palamara. Multivariate Multi-Scale Permutation Entropy for Complexity Analysis of Alzheimer's Disease EEG. Entropy 14(7):1186-1202 (2012).

[30] Costa, M.; Goldberger, A.; Peng, C.-K. Multiscale entropy analysis of biological signals. Phys. Rev. E 2005, 71, 021906:1–021906:18. - See more at: http://www.mdpi.com/1099-4300/16/11/6133/htm#sthash.ufFUh4mq.dpuf, 2005.

DISCUSSION AND PERSPECTIVES

The main objective of my PhD has been to explore various approaches for behavioural phenotyping, which appears to me as a fundamental and rapidly developing field of neuroscience. My work has relied on several experimental paradigms, including classical behavioural tests such as fear conditioning or nest building, but also had the ambition to further explore less controlled conditions such as spontaneous behaviour in an open field. The technical approaches for data acquisition include classical video recordings, but also a novel device (the Phenotypix) that consists in an open field platform resting on highly sensitive pressure sensors, allowing to detect the slightest animal movement with unprecedented sensitivity and time resolution. I have explored the potential of this novel experimental system on a variety of behavioural conditions such as free exploration, sleep, post-surgery pain and fear, as well as on a variety of animals models of pathologies, such as Fragile-X syndrome / autism spectrum disorders, Alzheimer's and Parkinson's diseases. Applying sophisticated signal-analysis tools such as time frequency decomposition, machine learning algorithms and non linear estimations of signal complexity (ie permutation entropy and Lyapunov equation), I here demonstrate that this device can bring invaluable information for behavioural phenotyping in general, in addition to very original observations in the specific fields of fear and neurodevelopemental and neurodegenerative disorders.

The results I have obtained with *Fmr1*-KO mice suggest that sensory-hypersensitivity and impaired habituation due to sensory hyperexcitability from deficient potassium channels in neocortical circuits might participate in the sensory defensiveness expressed by patients with Fragile X syndrome / autism spectrum disorders. This clinical hypothesis could not be tested before, due to the lack of tools to manipulate sensory excitability in patients. I have found that exposing *Fmr1*-KO mice to novel or unfamiliar environments resulted in multiple behavioural perturbations, ranging from hyperactivity to impaired nest building and excessive grooming of the back, confirming that in addition to sensory hyperesensitivity, *Fmr1*-KO mice express symptoms relevant to the FXS/ASD condition. Reversing sensory hypersensitivity with BMS-204352 prevented these behavioral abnormalities in *Fmr1*-KO mice. Using the Phenotypix, I could provide further elements along the same line. I could observe excessive amplitude/strength of individual movements involved in grooming of the back specifically (and not of the belly for example). I also observed increased heart rate in basal condition, as well as persistent fear-related shaking in response to exploration of a novel environment, in support of

the hypothesis of persistently altered regulation of autonomic functions in FXS/ASD (Roberts et al., 2012). In normal individuals, autonomic regulation represents a behavioral flexibility, so that energy can be mobilized in response to potentially dangerous or stressful conditions. It has been proposed that FXS/ASD patients would suffer from chronic autonomic activation, so that not only the system would be stressed already in basal conditions, but would also loose its ability to respond apropriately to potentially dangerous or stressful conditions such as confrontation to novelty. In fact, such situations would push the system out of its physiological limits, resulting in pathological behavioral manifestations such as stereotypies, withdrawal from others and social activities. It would be interesting to investigate in which respect these original results apply to other models of ASD, such as BTBR, Ts65Dn and VPA mouse models. There is also some discrepancy between the clinical indications that FXS/ASD patients are very anxious, while the classical behavioral tests (eg time in center of the open field, time in the open arm of the elevated plus maze) suggest decreased anxiety in Fmr1-KO mice (Kazdoba et al., 2014). One possible explanation resides in the hyperactivity phenotype, that may perturb the evaluation of anxiety in tests based on locomotor activity. Even though normalized by the total distance run, attentional disorders may modify the ratio of time spent in the various locations during locomotion in a confounding way for the evaluation of anxiety. Attentional disorders might therefore modify the relationships between anxiety as a background mood and the effects of anxiety on locomotor behavior. In this respect, the high-frequency shaking we describe in response to fear may be an interesting alternative index of anxiety to consider, because it does not seem to be affected by hyperactivity. Further investigation is required with different models or conditions affecting specifically attention and/or anxiety in order to clarify the relationships between this internal psychological state and its behavioral readout.

With the Phenotypix, I could identify shaking as a signature of pain, which was certainly known before (shaking is easily felt during handling), but to our knowledge not available for objective and automatic quantification in scientific studies. Even though this behavioral phenotype does not seem to be expressed in mice, rats are commonly used as a preclinical model in pain research. From personal experience, I can say that the measured shaking is indeed a sign of pain also experienced by other animals, but further work is required to clarify what it represents exactly. I might be for example the signature of certain kinds of pain but not others, which would be compatible with our observation that local inflammation with CFA, considered a model of pain, was not associated with shaking. Alternatively, it might be associated with the magnitude of pain, being expressed for example only above a certain

threshold. If so, then we might investigate whether this is an all or none reaction, or conversely proportional to the subjective pain. In order to answer these questions, it would be useful to investigate in a systematic manner different models of pain, as well as the dose-response effects of analgesic drugs. This research might prove very important in pain research, in which the development of methods to measure spontaneous pain is definitely required to investigate a number of clinical conditions not yet addressed with available animal models (Mogil and Crager, 2004).

The high-frequency shaking detected in animal models of neurodegenerative diseases also proved to be a potentially interesting parallel between Alzheimer's (AD) and Parkinson's (PD) disease. Classical views consider AD pathology related with deficits in cholinergic systems and PD with deficits in dopaminergic systems. Recent results have challenged this view and provided evidence for the involvement of cholinergic components in PD and dopaminergic components in AD (Ambrée et al., 2009, Guzmán-Ramos et al., 2012, Müller and Bohnen, 2013, Martorana and Koch, 2014b). We have reported here the presence of a dopaminergic system-dependent motor signature of AD, expressed as early as weaning time (P21) in 3xTg-AD mice. The pharmacology of these episodes suggests that shaking episodes expressed by 3xTg mice are not due to fear or pain but rather the sign of a dopaminergic deficit because they are eliminated by L-DOPA but not affected by the analgesic meloxicam or the anxiolytic diazepam. They could be reproduced (and rescued by L-DOPA) in WT mice by neurotoxic lesions of the dopaminergic system, as classically performed to mimick Parkinson's disease. We also observed shaking in APP-PS1 mice, another mouse model of AD. These results suggest very early deficit in dopaminergic systems in AD. I have performed preliminary EEG recordings from freely moving mice, revealing the presence of oscillations in the beta band frequency during locomotion, another striking characteristic of DA deficits as expressed in Parkinson's disease. Further investigation with histological, immuno-chemical and electrophysiolical approaches are required to understand the exact origin and mechanisms of this deficit in AD. One puzzling observation is that the rescue of shaking in 3xTg-AD and APP-PS1 mice by L-DOPA required doses 10 times higher than to rescue shaking in 6-OHDA lesioned mice. Further investigation is required to understand whether this is due to unspecific effects of L-DOPA or to the distinct degenerative state of DA systems in AD compared to PD. Through a local collaboration, we have started to investigate the dosage of DA and other monoamines (NA, 5-HT) in various source and target regions that may explain the shaking and the rescuing effect of L-DOPA.

Investigating the dynamics of the electromechanic signal underlying locomotion, I have also found evidence for altered gait in a mouse with sore paw and in both AD and PD mouse models. This illustrates the potential complementarity between the Phenotypix and existing systems to study gait. Sophisticated devices exist that can provide very accurate spatio-temporal information regarding body movements and the successive positions of the paws during locomotion (Clarke and Still, 1999, Zorner et al., 2010, Machado et al., 2015). However, the Phenotypix adds information regarding the dynamics of the muscular efforts underlying individual footsteps, an information out of reach before. In addition to potentially help understanding gait alterations in ataxia and in a variety of models of motor impairment, it is also an opportunity to study the relationships between neuronal activity and the time organization of behavior. For example, a wealth of literature has established tight links between hippocampal theta oscillations and locomotion. Both the amplitude and frequency of theta have been proposed to be proportional to the locomotion speed (Whishaw and Vanderwolf, 1973, Bland, 2004, Geisler et al., 2007). Theta has been proposed to be both part of the preparation of action and a process of sensori-motor integration (Vanderwolf, 1969, Bland and Oddie, 2001, Geisler et al., 2007, Fuhrmann et al., 2015). There is however a paucity of data to compare theta and behavior at a time scale relevant to individual theta oscillations (10s to 100s of ms) or individual behavioral actions. Previous work from our group (Molter et al., 2012) has suggested that although the correlation between theta amplitude and running speed does not hold at short times scales (<1s), endogenous and regular fluctuations of theta power might underlie the time organization of behavior. I have performed pilot electrophysiological recordings of mice during locomotion in the Phenotypix platform, and observed correlations between individual theta cycles of individual footsteps, that are broken in 3xTg-AD mice. Further work is required to better understand the precise relationships between theta oscillations and the time organization of behavior at the sub second time scale.

Finally, this device has the potential to allow significant progress in the field of behavioral phenotyping. During my PhD I have started to move towards computational ethology, which is a most promising and rapidly developing field of neuroscience. I believe that computational approaches can be very useful for supervised as well as unsupervised investigation of behavior. The analysis performed to quantify the complexity of the signal could for now be considered as unsupervised, in the sense that the use of computational tools provides information that still needs to be interpreted afterwards by biologists and ethologists.

The use of machine learning algorithms and unsupervised clustering methods will certainly help to discover basic behavioral elements and their organization into ethograms of higher resolution and complexity than considered today. Here also, the need of interpretation and identification by the human eye means going back and forth between supervised and unsupervised approaches, because as a complement to learning from the algorithm, it is also safe to build our own definition and test our ability to train the algorithm to detect what we think we have understood from this complex field.

References

Abasolo D, Hornero R, Espino P, Alvarez D, Poza J (2006) Entropy analysis of the EEG background activity in Alzheimer's disease patients. Physiological measurement 27:241-253.

Ambrée O, Richter H, Sachser N, Lewejohann L, Dere E, de Souza Silva MA, Herring A, Keyvani K, Paulus W, Schäbitz W-R (2009) Levodopa ameliorates learning and memory deficits in a murine model of Alzheimer's disease. Neurobiology of Aging 30:1192-1204.

Anagnostaras SG, Wood SC, Shuman T, Cai DJ, Leduc AD, Zurn KR, Zurn JB, Sage JR, Herrera GM (2010) Automated assessment of pavlovian conditioned freezing and shock reactivity in mice using the video freeze system. Front BehavNeurosci 4.

Anderson David J, Perona P (2014) Toward a Science of Computational Ethology. Neuron 84:18-31.

Ängeby Möller K, Kinert S, Størkson R, Berge O-G (2012) Gait Analysis in Rats with Single Joint Inflammation: Influence of Experimental Factors. PLoS ONE 7:e46129.

Angoa-Perez M, Kane MJ, Briggs DI, Francescutti DM, Kuhn DM (2013) Marble Burying and Nestlet Shredding as Tests of Repetitive, Compulsive-like Behaviors in Mice. J Vis Exp 50978.

Arendt T, Brückner MK, Morawski M, Jäger C, Gertz H-J (2015) Early neurone loss in Alzheimer's disease: cortical or subcortical? Acta Neuropathologica Communications 3:10.

Arentsen T, Raith H, Qian Y, Forssberg H, Heijtz RD (2015) Host microbiota modulates development of social preference in mice. Microb Ecol Health Dis 26:10.

Ashley C, Wilkinson K, Reines D, Warren S (1993) FMR1 protein: conserved RNP family domains and selective RNA binding. Science 262:563-566.

Bakker CE, Oostra BA (2003) Understanding fragile X syndrome: insights from animal models. Cytogenetic and Genome Research 100:111-123.

Balbir A, Lande B, Fitzgerald RS, Polotsky V, Mitzner W, Shirahata M (2008) Behavioral and respiratory characteristics during sleep in neonatal DBA/2J and A/J mice. Brain research 1241:84-91.

Baranek GT, Foster LG, Berkson G (1997) Tactile Defensiveness and Stereotyped Behaviors. American Journal of Occupational Therapy 51:91-95.

Barlow C, Hirotsune S, Paylor R, Liyanage M, Eckhaus M, Collins F, Shiloh Y, Crawley JN, Ried T, Tagle D, Wynshaw-Boris A (1996) Atm-deficient mice: a paradigm of ataxia telangiectasia. Cell 86:159-171.

Basbaum AI, Bautista DM, Scherrer G, Julius D (2009) Cellular and Molecular Mechanisms of Pain. Cell 139:267-284.

Bassell GJ, Warren ST (2008) Fragile X Syndrome: Loss of Local mRNA Regulation Alters Synaptic Development and Function. Neuron 60:201-214.

Bastianini S, Alvente S, Berteotti C, Lo Martire V, Silvani A, Swoap SJ, Valli A, Zoccoli G, Cohen G (2017) Accurate discrimination of the wake-sleep states of mice using non-invasive whole-body plethysmography. Scientific Reports 7:41698.

Bean BP (2007) The action potential in mammalian central neurons. Nat Rev Neurosci 8:451-465.

Beauchet O, Annweiler C, Montero-Odasso M, Fantino B, Herrmann FR, Allali G (2012) Gait control: a specific subdomain of executive function? Journal of NeuroEngineering and Rehabilitation 9:12-12.

Bertram L, Lill CM, Tanzi RE (2010) The Genetics of Alzheimer Disease: Back to the Future. Neuron 68:270-281.

Bilkei-Gorzo A (2014) Genetic mouse models of brain ageing and Alzheimer's disease. Pharmacology & Therapeutics 142:244-257.

Blanchard CG, Guy; Nutt, David (2008) Handbook of Anxiety and Fear. 2008: Elsevier Science

Blanchard DC, Griebel G, Nutt DJ (2011) Handbook of Anxiety and Fear: Elsevier Science.

Bland BH (2004) The power of theta: providing insights into the role of the hippocampal formation in sensorimotor integration. Hippocampus 14:537-538.

Bland BH, Oddie SD (2001) Theta band oscillation and synchrony in the hippocampal formation and associated structures: the case for its role in sensorimotor integration. Behavioural Brain Research 127:119-136.

Blandini F, Armentero M-T, Martignoni E (2008) The 6-hydroxydopamine model: News from the past. Parkinsonism & Related Disorders 14, Supplement 2:S124-S129.

Blessing W, Mohammed M, Ootsuka Y (2012) Heating and eating: Brown adipose tissue thermogenesis precedes food ingestion as part of the ultradian basic rest–activity cycle in rats. Physiology & Behavior 105:966-974.

Bonanni E, Maestri M, Tognoni G, Fabbrini M, Nucciarone B, Manca ML, Gori S, Iudice A, Murri L (2005) Daytime sleepiness in mild and moderate Alzheimer's disease and its relationship with cognitive impairment. Journal of Sleep Research 14:311-317.

Boyer P, Lienard P (2006) Why ritualized behavior? Precaution Systems and action parsing in developmental, pathological and cultural rituals. The Behavioral and brain sciences 29:595-613; discussion 613-550.

Brenner R, Jegla TJ, Wickenden A, Liu Y, Aldrich RW (2000) Cloning and Functional Characterization of Novel Large Conductance Calcium-activated Potassium Channel β Subunits, hKCNMB3 and hKCNMB4. Journal of Biological Chemistry 275:6453-6461.

Brodkin J, Frank D, Grippo R, Hausfater M, Gulinello M, Achterholt N, Gutzen C (2014) Validation and implementation of a novel high-throughput behavioral phenotyping instrument for mice. JNeurosciMethods 224:48-57.

Brown V, Jin P, Ceman S, Darnell JC, O'Donnell WT, Tenenbaum SA, Jin X, Feng Y, Wilkinson KD, Keene JD, Darnell RB, Warren ST (2001) Microarray Identification of FMRP-Associated Brain mRNAs and Altered mRNA Translational Profiles in Fragile X Syndrome. Cell 107:477-487.

Bruno JL, Garrett AS, Quintin E-M, Mazaika PK, Reiss AL (2014) Aberrant face and gaze habituation in fragile X syndrome. The American journal of psychiatry 171:1099-1106.

Bruzzo AA, Gesierich B, Santi M, Tassinari CA, Birbaumer N, Rubboli G (2008) Permutation entropy to detect vigilance changes and preictal states from scalp EEG in epileptic patients. A preliminary study. Neurological Sciences 29:3-9.

Buchman AS, Bennett DA (2011) Loss of motor function in preclinical Alzheimer's disease. Expert Review of Neurotherapeutics 11:665-676.

Burns JM, Galvin JE, Roe CM, Morris JC, McKeel DW (2005) The pathology of the substantia nigra in Alzheimer disease with extrapyramidal signs. Neurology 64:1397-1403.

Buzsaki G, Leung LW, Vanderwolf CH (1983) Cellular bases of hippocampal EEG in the behaving rat. Brain research 287:139-171.

Calvino B, Grilo RM (2006) Central pain control. Joint Bone Spine 73:10-16.

Canavello PR, Cachat JM, Hart PC, Murphy DL, Kalueff AV (2013) Behavioral phenotyping of mouse grooming and barbering. In: Behavioral Genetics of the mouse, vol. 1 (Crusio, W. E. et al., eds), pp 195-104 New York USA: Cambridge university press.

Cao Y, Cai L, Wang J, Wang R, Yu H, Cao Y, Liu J (2015) Characterization of complexity in the electroencephalograph activity of Alzheimer's disease based on fuzzy entropy. Chaos: An Interdisciplinary Journal of Nonlinear Science 25:083116.

Carter RJ, Lione LA, Humby T, Mangiarini L, Mahal A, Bates GP, Dunnett SB, Morton AJ (1999) Characterization of progressive motor deficits in mice transgenic for the human Huntington's disease mutation. JNeurosci 19:3248-3257.

Choleris E, Thomas AW, Kavaliers M, Prato FS (2001) A detailed ethological analysis of the mouse open field test: effects of diazepam, chlordiazepoxide and an extremely low frequency pulsed magnetic field. Neuroscience & Biobehavioral Reviews 25:235-260.

Clarke KA, Still J (1999) Gait analysis in the mouse. Physiology & behavior 66:723-729.

Clarke KA, Still J (2001) Development and consistency of gait in the mouse. Physiol Behav 73:159-164.

Comery TA, Harris JB, Willems PJ, Oostra BA, Irwin SA, Weiler IJ, Greenough WT (1997) Abnormal dendritic spines in fragile X knockout mice: Maturation and pruning deficits. Proceedings of the National Academy of Sciences of the United States of America 94:5401-5404.

Consortium TD-BFX (1994) Fmr1 knockout mice: a model to study fragile X mental retardation. The Dutch-Belgian Fragile X Consortium. Cell 78:23-33.

Contractor A, Klyachko VA, Portera-Cailliau C (2015) Altered neuronal and circuit excitability in Fragile X Syndrome. Neuron 87:699-715.

Crabbe JC, Metten P, Yu C-H, Schlumbohm JP, Cameron AJ, Wahlsten D (2003) Genotypic differences in ethanol sensitivity in two tests of motor incoordination. Journal of Applied Physiology 95:1338-1351.

Crawley J, Goodwin FK (1980) Preliminary report of a simple animal behavior model for the anxiolytic effects of benzodiazepines. PharmacolBiochemBehav 13:167-170.

Crawley JN (2007a) Emotional Behaviors: Animal Models of Psychiatric Diseases. In: What's Wrong With My Mouse? , pp 226-265: John Wiley & Sons, Inc.

Crawley JN (2007b) Motor Functions. In: What's Wrong With My Mouse? , pp 62-84: John Wiley & Sons, Inc.

Crusio WE, Sluyter F, Gerlai T (2013) Ethogram of the mouse. In: Behavioral genetics of the mouse, vol. 1, pp 17-22 New York, USA: Cambridge University press.

Daldrup T, Remmes J, Lesting J, Gaburro S, Fendt M, Meuth P, Kloke V, Pape HC, Seidenbecher T (2015) Expression of freezing and fear-potentiated startle during sustained fear in mice. Genes, Brain and Behavior 14:281-291.

Darnell JC, Van Driesche SJ, Zhang C, Hung KYS, Mele A, Fraser CE, Stone EF, Chen C, Fak JJ, Chi SW, Licatalosi DD, Richter JD, Darnell RB (2011) FMRP stalls ribosomal translocation on mRNAs linked to synaptic function and autism. Cell 146:247-261.

de Oliveira Crisanto K, de Andrade WMG, de Azevedo Silva KD, Lima RnH, de Oliveira Costa MSM, de Souza Cavalcante J, de Lima RRM, do Nascimento Jr ES, Cavalcante JC (2015) The differential mice response to cat and snake odor. Physiology & Behavior 152, Part A:272-279.

Deacon RM (2006) Assessing nest building in mice. NatProtocols 1:1117-1119.

Deacon RM, Raley JM, Perry VH, Rawlins JN (2001) Burrowing into prion disease. Neuroreport 12:2053-2057.

Deng P-Y, Klyachko VA (2011) The diverse functions of short-term plasticity components in synaptic computations. Communicative & Integrative Biology 4:543-548.

Deng P-Y, Rotman Z, Blundon JA, Cho Y, Cui J, Cavalli V, Zakharenko SS, Klyachko VA (2013) FMRP Regulates Neurotransmitter Release and Synaptic Information Transmission by Modulating Action Potential Duration via BK channels. Neuron 77:696-711.

Deng PY, Klyachko VA (2016) Genetic upregulation of BK channel activity normalizes multiple synaptic and circuit defects in a mouse model of fragile X syndrome. J Physiol 594:83-97.

Deumens R, Blokland A, Prickaerts J (2002) Modeling Parkinson's Disease in Rats: An Evaluation of 6-OHDA Lesions of the Nigrostriatal Pathway. Experimental Neurology 175:303-317.

Dickinson SL, Jackson A, Curzon G (1983) Effect of apomorphine on behaviour induced by 5-methoxy-N, N-dimethyl tryptamine: three different scoring methods give three different conclusions. Psychopharmacology 80:196-197.

Dictenberg JB, Swanger SA, Antar LN, Singer RH, Bassell GJ (2008) A Direct Role for FMRP in Activity-Dependent Dendritic mRNA Transport Links Filopodial-Spine Morphogenesis to Fragile X Syndrome. Developmental cell 14:926-939.

Dobkin C, Rabe A, Dumas R, El Idrissi A, Haubenstock H, Ted Brown W (2000) Fmr1 knockout mouse has a distinctive strain-specific learning impairment. Neuroscience 100:423-429.

Drai D, Golani I (2001) SEE: a tool for the visualization and analysis of rodent exploratory behavior. Neurosci BiobehavRev 25:409-426.

Duty S, Jenner P (2011) Animal models of Parkinson's disease: a source of novel treatments and clues to the cause of the disease. British Journal of Pharmacology 164:1357-1391.

Elias WJ, Shah BB (2014) Tremor. JAMA 311:948-954.
Ethridge LE, White SP, Mosconi MW, Wang J, Byerly MJ, Sweeney JA (2016) Reduced habituation of auditory evoked potentials indicate cortical hyper-excitability in Fragile X Syndrome. Translational Psychiatry 6:e787.
Evans DW, Leckman JF, Carter A, Reznick JS, Henshaw D, King RA, Pauls D (1997) Ritual, Habit, and Perfectionism: The Prevalence and Development of Compulsive-Like Behavior in Normal Young Children. Child Development 68:58-68.
Fearnley JM, Lees AJ (1991) AGEING AND PARKINSON'S DISEASE: SUBSTANTIA NIGRA REGIONAL SELECTIVITY. Brain 114:2283-2301.
Feng LR, Maguire-Zeiss KA (2010) Gene Therapy in Parkinson's Disease: Rationale and Current Status. CNS drugs 24:177-192.
Finnerup NB, Haroutounian S, Kamerman P, Baron R, Bennett DLH, Bouhassira D, Cruccu G, Freeman R, Hansson P, Nurmikko T, Raja SN, Rice ASC, Serra J, Smith BH, Treede R-D, Jensen TS (2016) Neuropathic pain: an updated grading system for research and clinical practice. Pain 157:1599-1606.
Fisher SP, Godinho SI, Pothecary CA, Hankins MW, Foster RG, Peirson SN (2012) Rapid assessment of sleep/wake behaviour in mice. J Biol Rhythms 27:48-58.
Flores AE, Flores JE, Deshpande H, Picazo JA, Xie XS, Franken P, Heller HC, Grahn DA, O'Hara BF (2007) Pattern recognition of sleep in rodents using piezoelectric signals generated by gross body movements. IEEE TransBiomedEng 54:225-233.
Fowler SC, Birkestrand BR, Chen R, Moss SJ, Vorontsova E, Wang G, Zarcone TJ (2001) A force-plate actometer for quantitating rodent behaviors: illustrative data on locomotion, rotation, spatial patterning, stereotypies, and tremor. J Neurosci methods 107:107-124.
Frank Kooy R (2003) Of mice and the fragile X syndrome. Trends in Genetics 19:148-154.
Friedman L, Haines A, Klann K, Gallaugher L, Salibra L, Han F, Strohl KP (2004) Ventilatory behavior during sleep among A/J and C57BL/6J mouse strains. J Appl Physiol (1985) 97:1787-1795.
Fuhrmann F, Justus D, Sosulina L, Kaneko H, Beutel T, Friedrichs D, Schoch S, Schwarz MK, Fuhrmann M, Remy S (2015) Locomotion, Theta Oscillations, and the Speed-Correlated Firing of Hippocampal Neurons Are Controlled by a Medial Septal Glutamatergic Circuit. Neuron.
Galvez R, Greenough WT (2005) Sequence of abnormal dendritic spine development in primary somatosensory cortex of a mouse model of the fragile X mental retardation syndrome. American Journal of Medical Genetics Part A 135A:155-160.
Garrity PA, Goodman MB, Samuel AD, Sengupta P (2010) Running hot and cold: behavioral strategies, neural circuits, and the molecular machinery for thermotaxis in C. elegans and Drosophila. Genes & Development 24:2365-2382.
Gaskill BN, Karas AZ, Garner JP, Pritchett-Corning KR (2013) Nest Building as an Indicator of Health and Welfare in Laboratory Mice. J Vis Exp 51012.
Geisler C, Robbe D, Zugaro M, Sirota A, Buzsaki G (2007) Hippocampal place cell assemblies are speed-controlled oscillators. Proceedings of the National Academy of Sciences of the United States of America 104:8149-8154.
Girao da Cruz MT, Jordao J, Dasilva KA, Ayala-Grosso CA, Ypsilanti A, Weng YQ, Laferla FM, McLaurin J, Aubert I (2012) Early increases in soluble amyloid-beta levels coincide with cholinergic degeneration in 3xTg-AD mice. J Alzheimers Dis 32:267-272.
Goldberger AL (1996) Non-linear dynamics for clinicians: chaos theory, fractals, and complexity at the bedside. The Lancet 347:1312-1314.
Goldberger AL (1997) Fractal variability versus pathologic periodicity: complexity loss and stereotypy in disease. Perspectives in biology and medicine 40:543-561.
Goldberger AL, Peng CK, Lipsitz LA (2002) What is physiologic complexity and how does it change with aging and disease? Neurobiology of Aging 23:23-26.

Gomez-Marin A, Partoune N, Stephens GJ, Louis M, Brembs B (2012) Automated tracking of animal posture and movement during exploration and sensory orientation behaviors. PLoSOne 7:e41642.

Goutagny R, Krantic S (2013) Hippocampal Oscillatory Activity in Alzheimer's Disease: Toward the Identification of Early Biomarkers? Aging and Disease 4:134-140.

Gubellini P, Kachidian P (2015) Animal models of Parkinson's disease: An updated overview. Revue Neurologique 171:750-761.

Guzman-Ramos K, Moreno-Castilla P, Castro-Cruz M, McGaugh JL, Martinez-Coria H, LaFerla FM, Bermudez-Rattoni F (2012) Restoration of dopamine release deficits during object recognition memory acquisition attenuates cognitive impairment in a triple transgenic mice model of Alzheimer's disease. Learn Mem 19:453-460.

Guzmán-Ramos K, Moreno-Castilla P, Castro-Cruz M, McGaugh JL, Martínez-Coria H, LaFerla FM, Bermúdez-Rattoni F (2012) Restoration of dopamine release deficits during object recognition memory acquisition attenuates cognitive impairment in a triple transgenic mice model of Alzheimer's disease. Learning & Memory 19:453-460.

Handforth A (2012) Harmaline Tremor: Underlying Mechanisms in a Potential Animal Model of Essential Tremor. Tremor and Other Hyperkinetic Movements 2:02-92-769-761.

Hanson JE, Madison DV (2007) Presynaptic Fmr1 Genotype Influences the Degree of Synaptic Connectivity in a Mosaic Mouse Model of Fragile X Syndrome. The Journal of Neuroscience 27:4014-4018.

Harlow EG, Till SM, Russell TA, Wijetunge LS, Kind P, Contractor A (2010) Critical Period Plasticity Is Disrupted in the Barrel Cortex of Fmr1 Knockout Mice. Neuron 65:385-398.

Hazlett HC, Poe MD, Lightbody AA, Styner M, MacFall JR, Reiss AL, Piven J (2012) Trajectories of Early Brain Volume Development in Fragile X and Autism RH: Trajectory of Brain Volume in Fragile X. Journal of the American Academy of Child and Adolescent Psychiatry 51:921-933.

He CX, Portera-Cailliau C (2013) The trouble with spines in fragile X syndrome: density, maturity and plasticity. Neuroscience 251:120-128.

Hebert B, Pietropaolo S, Meme S, Laudier B, Laugeray A, Doisne N, Quartier A, Lefeuvre S, Got L, Cahard D, Laumonnier F, Crusio WE, Pichon J, Menuet A, Perche O, Briault S (2014) Rescue of fragile X syndrome phenotypes in Fmr1 KO mice by a BKCa channel opener molecule. OrphanetJRareDis 9:124.

Heikamp K, Bajorath J (2014) Support vector machines for drug discovery. Expert Opinion on Drug Discovery 9:93-104.

Heller HC, Salehi A, Chuluun B, Das D, Lin B, Moghadam S, Garner CC, Colas D (2014) Nest building is impaired in the Ts65Dn mouse model of Down syndrome and rescued by blocking 5HT2a receptors. Neurobiology of Learning and Memory 116:162-171.

Hensley K (2010) Neuroinflammation in Alzheimer's Disease: Mechanisms, Pathologic Consequences, and Potential for Therapeutic Manipulation. Journal of Alzheimer's disease : JAD 21:1-14.

Hernandez AB, Kirkness JP, Smith PL, Schneider H, Polotsky M, Richardson RA, Hernandez WC, Schwartz AR (2012) Novel whole body plethysmography system for the continuous characterization of sleep and breathing in a mouse. J Appl Physiol (1985) 112:671-680.

Herold S, Kumar P, Jung K, Graf I, Menkhoff H, Schulz X, B+ñhr M, Hein K (2016) CatWalk gait analysis in a rat model of multiple sclerosis. BMC Neurosci 17:78.

Herrera-Meza G, Manzo J, Hernandez ME, Miquel M, Garcia LI (2014) Induction of mandibular tremor using electrolytic lesion of the ventrolateral striatum or using subchronic haloperidol therapy in male rats: An electromyographic comparison. Neurolog+¡a (English Edition) 29:416-422.

Hess SE, Rohr S, Dufour BD, Gaskill BN, Pajor EA, Garner JP (2008) Home Improvement: C57BL/6J Mice Given More Naturalistic Nesting Materials Build Better Nests. J Am Assoc Lab Anim Sci 47:25-31.

Holter SM, Einicke J, Sperling B, Zimprich A, Garrett L, Fuchs H, Gailus-Durner V, Hrabe de AM, Wurst W (2015) Tests for Anxiety-Related Behavior in Mice. CurrProtocMouseBiol 5:291-309.

Hornykiewicz O (1998) Biochemical aspects of Parkinson's disease. Neurology 51:S2-9.
Huang H-Y, Lin C-J Linear and kernel classification: When to use which? , pp 216-224: SIAM.
Ijmker T, Lamoth CJC (2012) Gait and cognition: The relationship between gait stability and variability with executive function in persons with and without dementia. Gait & Posture 35:126-130.
Imbe H, Iwai-Liao Y, Senba E (2006) Stress-induced hyperalgesia: animal models and putative mechanisms. Frontiers in bioscience : a journal and virtual library 11:2179-2192.
Inouye T, Shinosaki K (1991) Quantification of EEG irregularity by use of the entropy of the power spectrum. Electroencephalogr Clin Neurophysiol 79.
Ivanov PC, Amaral LAN, Goldberger AL, Havlin S, Rosenblum MG, Struzik ZR, Stanley HE (1999) Multifractality in human heartbeat dynamics. Nature 399:461-465.
Jankovic J (2008) Parkinson's disease: clinical features and diagnosis. Journal of Neurology, Neurosurgery & Psychiatry 79:368-376.
Jhuang H, Garrote E, Yu X, Khilnani V, Poggio T, Steele AD, Serre T (2010) Automated home-cage behavioural phenotyping of mice. 1:68.
Jirkof P (2014) Burrowing and nest building behavior as indicators of well-being in mice. In: Journal of Neuroscience methods
Measuring Behavior, vol. 234, pp 139-146.
Jirkof P, Cesarovic N, Rettich A, Nicholls F, Seifert B, Arras M (2010) Burrowing Behavior as an Indicator of Post-Laparotomy Pain in Mice. Front Behav Neurosci 4:165.
Kafkafi N, Lipkind D, Benjamini Y, Mayo CL, Elmer GI, Golani I (2003) SEE locomotor behavior test discriminates C57BL/6J and DBA/2J mouse inbred strains across laboratories and protocol conditions. BehavNeurosci 117:464-477.
Kageyama T, Nakamura M, Matsuo A, Yamasaki Y, Takakura Y, Hashida M, Kanai Y, Naito M, Tsuruo T, Minato N, Shimohama S (2000) The 4F2hc/LAT1 complex transports l-DOPA across the blood–brain barrier. Brain research 879:115-121.
Kalueff AV, Ishikawa K, Griffith AJ (2008) Anxiety and otovestibular disorders: Linking behavioral phenotypes in men and mice. Behavioural Brain Research 186:1-11.
Kamens HM, Phillips TJ, Holstein SE, Crabbe JC (2005) Characterization of the parallel rod floor apparatus to test motor incoordination in mice. Genes, Brain and Behavior 4:253-266.
Karbowski J, Schindelman G, Cronin CJ, Seah A, Sternberg PW (2008) Systems level circuit model of C. elegans undulatory locomotion: mathematical modeling and molecular genetics. Journal of Computational Neuroscience 24:253-276.
Karki J (2000) Signal Conditioning Piezoelectrc Sensors. In: Texas Instruments, pp 1-6.
Karran E, Mercken M, Strooper BD (2011) The amyloid cascade hypothesis for Alzheimer's disease: an appraisal for the development of therapeutics. Nat Rev Drug Discov 10:698-712.
Kazdoba TM, Leach PT, Silverman JL, Crawley JN (2014) Modeling fragile X syndrome in the Fmr1 knockout mouse. Intractable & Rare Diseases Research 3:118-133.
Keisala T, Minasyan A, Järvelin U, Wang J, Hämäläinen T, Kalueff AV, Tuohimaa P (2007) Aberrant nest building and prolactin secretion in vitamin D receptor mutant mice. The Journal of Steroid Biochemistry and Molecular Biology 104:269-273.
Kim KJ, Chang YM, Yoon SUN, Kim HJ (2009) A Novel Piezoelectric PVDF Film-based physiological sensing belt for a complementary respiration and heartbeat monitoring system. In: Integrated Ferroelectrics, vol. 107, pp 53-68: Taylor & Francis.
Kish SJ, Shannak K, Hornykiewicz O (1988) Uneven Pattern of Dopamine Loss in the Striatum of Patients with Idiopathic Parkinson's Disease. New England Journal of Medicine 318:876-880.
Klusek J, Martin GE, Losh M (2013) Physiological Arousal in Autism and Fragile X Syndrome: Group Comparisons and Links With Pragmatic Language. American journal on intellectual and developmental disabilities 118:475-495.
Koch G, Di Lorenzo F, Bonnì S, Giacobbe V, Bozzali M, Caltagirone C, Martorana A (2014) Dopaminergic Modulation of Cortical Plasticity in Alzheimer's Disease Patients. Neuropsychopharmacology 39:2654-2661.

Kovalenko ILGAGS, Dmitry A.; Kudryavtseva, Natalia N. (2015) Hyperactivity and Abnormal Exploratory Activity Developing in CD-1 Male Mice under Chronic Experience of Aggression and Social Defeats. Journal of Behavioral and Brain Science 5:478-490

Kramvis I, Mansvelder HD, Loos M, Meredith R (2013) Hyperactivity, perseveration and increased responding during attentional rule acquisition in the Fragile X mouse model. Frontiers in Behavioral Neuroscience 7:172.

Kulesskaya N, Voikar V (2014) Assessment of mouse anxiety-like behavior in the lightΓÇôdark box and open-field arena: Role of equipment and procedure. Physiology & Behavior 133:30-38.

Kyle BD, Braun AP (2014) The regulation of BK channel activity by pre- and post-translational modifications. Frontiers in Physiology 5.

Lalone R, Strazielle C (2013) Motor Coordination in inbred mouse strains and the crucial role of the cerebellum. In: Behavioral Genetics of the mouse, vol. 1 (Crusio, W. E. S., F.; Gerlai, R. ; Pietropaolo, S., ed), pp 81-87 New York, USA: Cambridge University Press.

Langen M, Durston S, Kas MJH, van Engeland H, Staal WG (2011a) The neurobiology of repetitive behavior: …and men. Neuroscience & Biobehavioral Reviews 35:356-365.

Langen M, Kas MJH, Staal WG, van Engeland H, Durston S (2011b) The neurobiology of repetitive behavior: Of miceΓÇª. Neuroscience & Biobehavioral Reviews 35:345-355.

Langford DJ, Bailey AL, Chanda ML, Clarke SE, Drummond TE, Echols S, Glick S, Ingrao J, Klassen-Ross T, LaCroix-Fralish ML, Matsumiya L, Sorge RE, Sotocinal SG, Tabaka JM, Wong D, van den Maagdenberg AMJM, Ferrari MD, Craig KD, Mogil JS (2010) Coding of facial expressions of pain in the laboratory mouse. Nat Meth 7:447-449.

Laske C, Sohrabi HR, Frost SM, López-de-Ipiña K, Garrard P, Buscema M, Dauwels J, Soekadar SR, Mueller S, Linnemann C, Bridenbaugh SA, Kanagasingam Y, Martins RN, O'Bryant SE (2015) Innovative diagnostic tools for early detection of Alzheimer's disease. Alzheimer's & Dementia 11:561-578.

Lee VMY, Kenyon TK, Trojanowski JQ (2005) Transgenic animal models of tauopathies. Biochimica et Biophysica Acta (BBA) - Molecular Basis of Disease 1739:251-259.

Lewis MH, Tanimura Y, Lee LW, Bodfish JW (2007) Animal models of restricted repetitive behavior in autism. In: Behavioural Brain Research

Animal Models for Autism, vol. 176, pp 66-74.

Line SJ, Barkus C, Coyle C, Jennings KA, Deacon RM, Lesch KP, Sharp T, Bannerman DM (2011) Opposing alterations in anxiety and species-typical behaviours in serotonin transporter overexpressor and knockout mice. European Neuropsychopharmacology 21:108-116.

Lozano R, Azarang A, Wilaisakditipakorn T, Hagerman RJ (2016) Fragile X syndrome: A review of clinical management. Intractable & Rare Diseases Research 5:145-157.

Luo L, Gershow M, Rosenzweig M, Kang K, Fang-Yen C, Garrity PA, Samuel A (2010) Navigational decision-making in Drosophila thermotaxis. The Journal of neuroscience : the official journal of the Society for Neuroscience 30:4261-4272.

Luthman J, Fredriksson A, Lewander T, Jonsson G, Archer T (1989) Effects ofd-amphetamine and methylphenidate on hyperactivity produced by neonatal 6-hydroxydopamine treatment. Psychopharmacology 99:550-557.

Machado AS, Darmohray DM, Fayad J, Marques HG, Carey MR (2015) A quantitative framework for whole-body coordination reveals specific deficits in freely walking ataxic mice. eLife 4:e07892.

Manaye KF, Mouton PR, Xu G, Drew A, Lei D-L, Sharma Y, Rebeck GW, Turner S (2013) Age-related loss of noradrenergic neurons in the brains of triple transgenic mice. Age 35:139-147.

Mang GM, Nicod J, Emmenegger Y, Donohue KD, O'Hara BF, Franken P (2014) Evaluation of a piezoelectric system as an alternative to electroencephalogram/ electromyogram recordings in mouse sleep studies. Sleep 37:1383-1392.

Martin TJ, Buechler NL, Kahn W, Crews JC, Eisenach JC (2004) Effects of laparotomy on spontaneous exploratory activity and conditioned operant responding in the rat: A model for postoperative pain. In: Anesthesiology, vol. 101, pp 191-203.

Martorana A, Koch G (2014a) “Is dopamine involved in Alzheimer's disease?”. Frontiers in Aging Neuroscience 6:252.
Martorana A, Koch G (2014b) “Is dopamine involved in Alzheimer's disease?”. Frontiers in Aging Neuroscience 6.
Masocha W, Pavarthy SS (2009) Assessment of weight bearing changes and pharmacological antinociception in mice with LPS-induced monoarthritis using the Catwalk gait analysis system. Life Sciences 85:462-469.
Mastrangelo MA, Bowers WJ (2008) Detailed immunohistochemical characterization of temporal and spatial progression of Alzheimer's disease-related pathologies in male triple-transgenic mice. BMC Neuroscience 9:81-81.
McLennan Y, Polussa J, Tassone F, Hagerman R (2011) Fragile X Syndrome. Current Genomics 12:216-224.
McShane BB, Galante RJ, Biber M, Jensen ST, Wyner AJ, Pack AI (2012) Assessing REM Sleep in Mice Using Video Data. Sleep 35:433-442.
Mechiel Korte S, De Boer SF (2003) A robust animal model of state anxiety: fear-potentiated behaviour in the elevated plus-maze. In: European Journal of Pharmacology
Animal Models of Anxiety Disorders, vol. 463, pp 163-175.
Meert TF, Rombouts J, Voeten J, Naranji F, Clincke G (1997) A simple, non-invasive method for the measurement of reserpine-induced tremor in rats. Acta NeurobiolExp (Wars) 57:75-81.
Merenstein SA, Sobesky WE, Taylor AK, Riddle JE, Tran HX, Hagerman RJ (1996) Molecular-clinical correlations in males with an expanded FMR1 mutation. American Journal of Medical Genetics 64:388-394.
Mientjes EJ, Nieuwenhuizen I, Kirkpatrick L, Zu T, Hoogeveen-Westerveld M, Severijnen L, Rife M, Willemsen R, Nelson DL, Oostra BA (2006) The generation of a conditional Fmr1 knock out mouse model to study Fmrp function in vivo. NeurobiolDis 21:549-555.
Millan MJ, Brocco M (2003) The Vogel conflict test: procedural aspects, +¦-aminobutyric acid, glutamate and monoamines. In: European Journal of Pharmacology
Animal Models of Anxiety Disorders, vol. 463, pp 67-96.
Miller DB, O'Callaghan JP (2015) Biomarkers of Parkinson's disease: Present and future. Metabolism: clinical and experimental 64:S40-S46.
Miller LJ, McIntosh DN, McGrath J, Shyu V, Lampe M, Taylor AK, Tassone F, Neitzel K, Stackhouse T, Hagerman RJ (1999) Electrodermal responses to sensory stimuli in individuals with fragile X syndrome: A preliminary report. American Journal of Medical Genetics 83:268-279.
Minkeviciene R, Rheims S, Dobszay MB, Zilberter M, Hartikainen J, Fülöp L, Penke B, Zilberter Y, Harkany T, Pitkänen A, Tanila H (2009) Amyloid β-Induced Neuronal Hyperexcitability Triggers Progressive Epilepsy. The Journal of Neuroscience 29:3453-3462.
Miyata K, Kuwaki T, Ootsuka Y (2016) The integrated ultradian organization of behavior and physiology in mice and the contribution of orexin to the ultradian patterning. Neuroscience 334:119-133.
Mogil JS, Crager SE (2004) What should we be measuring in behavioral studies of chronic pain in animals? Pain 112:12-15.
Mogil JS, Graham AC, Ritchie J, Hughes SF, Austin J-S, Schorscher-Petcu A, Langford DJ, Bennett GJ (2010) Hypolocomotion, asymmetrically directed behaviors (licking, lifting, flinching, and shaking) and dynamic weight bearing (gait) changes are not measures of neuropathic pain in mice. Molecular Pain 6:34-34.
Molter C, O'Neill J, Yamaguchi Y, Hirase H, Leinekugel X (2012) Rhythmic modulation of theta oscillations supports encoding of spatial and behavioral information in the rat hippocampus. Neuron 75:889-903.
Morabito FC, Labate D, La Foresta F, Bramanti A, Morabito G, Palamara I (2012) Multivariate multi-scale permutation entropy for complexity analysis of Alzheimer’s disease EEG. Entropy 14:1186-1202.

Moy SS, Riddick NV, Nikolova VD, Teng BL, Agster KL, Nonneman RJ, Young NB, Baker LK, Nadler JJ, Bodfish JW (2014) Repetitive behavior profile and supersensitivity to amphetamine in the C58/J mouse model of autism. Behavioural Brain Research 259:200-214.

Müller MLTM, Bohnen NI (2013) Cholinergic Dysfunction in Parkinson's Disease. Current Neurology and Neuroscience Reports 13:377.

Myrick LK, Deng P-Y, Hashimoto H, Oh YM, Cho Y, Poidevin MJ, Suhl JA, Visootsak J, Cavalli V, Jin P, Cheng X, Warren ST, Klyachko VA (2015) Independent role for presynaptic FMRP revealed by an FMR1 missense mutation associated with intellectual disability and seizures. Proceedings of the National Academy of Sciences 112:949-956.

Nakamura A, Zhang W, Yanagisawa M, Fukuda Y, Kuwaki T (2007) Vigilance state-dependent attenuation of hypercapnic chemoreflex and exaggerated sleep apnea in orexin knockout mice. J Appl Physiol (1985) 102:241-248.

Nelson PT, Alafuzoff I, Bigio EH, Bouras C, Braak H, Cairns NJ, Castellani RJ, Crain BJ, Davies P, Del Tredici K, Duyckaerts C, Frosch MP, Haroutunian V, Hof PR, Hulette CM, Hyman BT, Iwatsubo T, Jellinger KA, Jicha GA, Kövari E, Kukull WA, Leverenz JB, Love S, Mackenzie IR, Mann DM, Masliah E, McKee AC, Montine TJ, Morris JC, Schneider JA, Sonnen JA, Thal DR, Trojanowski JQ, Troncoso JC, Wisniewski T, Woltjer RL, Beach TG (2012) Correlation of Alzheimer Disease Neuropathologic Changes With Cognitive Status: A Review of the Literature. Journal of neuropathology and experimental neurology 71:362-381.

Nicholson RM, Kusne Y, Nowak LA, LaFerla FM, Reiman EM, Valla J (2010) Regional cerebral glucose uptake in the 3xTG model of Alzheimer's disease highlights common regional vulnerability across AD mouse models. Brain research 1347:10.1016/j.brainres.2010.1005.1084.

Nicolaou N, Georgiou J (2012) Detection of epileptic electroencephalogram based on Permutation Entropy and Support Vector Machines. Expert Systems with Applications 39:202-209.

Nimchinsky EA, Oberlander AM, Svoboda K (2001) Abnormal Development of Dendritic Spines inFMR1 Knock-Out Mice. The Journal of Neuroscience 21:5139-5146.

Nimchinsky EA, Sabatini BL, Svoboda K (2002) Structure and function of dendritic spines. Annual review of physiology 64:313-353.

Oddo S, Caccamo A, Shepherd JD, Murphy MP, Golde TE, Kayed R, Metherate R, Mattson MP, Akbari Y, LaFerla FM (2003) Triple-Transgenic Model of Alzheimer's Disease with Plaques and Tangles: Intracellular Aβ and Synaptic Dysfunction. Neuron 39:409-421.

Ootsuka Y, de Menezes RC, Zaretsky DV, Alimoradian A, Hunt J, Stefanidis A, Oldfield BJ, Blessing WW (2009) Brown adipose tissue thermogenesis heats brain and body as part of the brain-coordinated ultradian basic rest-activity cycle. Neuroscience 164:849-861.

Ossowska K, Glowacka U, Kosmowska B, Wardas J (2015) Apomorphine enhances harmaline-induced tremor in rats. Pharmacological Reports 67:435-441.

Ou-Yang TH, Tsai ML, Yen CT, Lin TT (2011) An infrared range camera-based approach for three-dimensional locomotion tracking and pose reconstruction in a rodent. J NeurosciMethods 201:116-123.

Pack AI, Galante RJ, Maislin G, Cater J, Metaxas D, Lu S, Zhang L, Von SR, Kay T, Lian J, Svenson K, Peters LL (2007) Novel method for high-throughput phenotyping of sleep in mice. Physiol Genomics 28:232-238.

Palop JJ, Chin J, Roberson ED, Wang J, Thwin MT, Bien-Ly N, Yoo J, Ho KO, Yu G-Q, Kreitzer A, Finkbeiner S, Noebels JL, Mucke L (2007) Aberrant Excitatory Neuronal Activity and Compensatory Remodeling of Inhibitory Hippocampal Circuits in Mouse Models of Alzheimer's Disease. Neuron 55:697-711.

Parkinson J (2002) An essay on the shaking palsy. 1817. The Journal of neuropsychiatry and clinical neurosciences 14:223-236; discussion 222.

Pedersen CS, Sorensen DB, Parachikova AI, Plath N (2014) PCP-induced deficits in murine nest building activity: Employment of an ethological rodent behavior to mimic negative-like symptoms of schizophrenia. Behavioural Brain Research 273:63-72.

Pellow S, Chopin P, File SE, Briley M (1985) Validation of open:closed arm entries in an elevated plus-maze as a measure of anxiety in the rat. JNeurosci Methods 14:149-167.
Perez SE, Lazarov O, Koprich JB, Chen E-Y, Rodriguez-Menendez V, Lipton JW, Sisodia SS, Mufson EJ (2005) Nigrostriatal Dysfunction in Familial Alzheimer's Disease-Linked APPswe/PS1ΔE9 Transgenic Mice. The Journal of Neuroscience 25:10220-10229.
Picada JN, Roesler R, Henriques JAP (2005) Genotoxic, neurotoxic and neuroprotective activities of apomorphine and its oxidized derivative 8-oxo-apomorphine. Brazilian Journal of Medical and Biological Research 38:477-486.
Pietropaolo S, Guilleminot A, Martin B, D'Amato FR, Crusio WE (2011) Genetic-background modulation of core and variable autistic-like symptoms in Fmr1 knock-out mice. PLoSOne 6:e17073.
Pitzer C, Kuner R, Tappe-Theodor A (2016) Voluntary and evoked behavioral correlates in neuropathic pain states under different social housing conditions. Mol Pain 12:1744806916656635.
Puzzo D, Gulisano W, Palmeri A, Arancio O (2015) Rodent models for Alzheimer's disease drug discovery. Expert opinion on drug discovery 10:703-711.
Reitz C, Mayeux R (2009) Use of Genetic Variation as Biomarkers for Alzheimer's Disease. Annals of the New York Academy of Sciences 1180:75.
Roberts JE, Tonnsen B, Robinson A, Shinkareva SV (2012) Heart Activity and Autistic Behavior in Infants and Toddlers with Fragile X Syndrome. American journal on intellectual and developmental disabilities 117:90-102.
Rotman Z, Deng P-Y, Klyachko VA (2011) Short-Term Plasticity Optimizes Synaptic Information Transmission. The Journal of Neuroscience 31:14800-14809.
Rudelli RD, Brown WT, Wisniewski K, Jenkins EC, Laure-Kamionowska M, Connell F, Wisniewski HM (1985) Adult fragile X syndrome. Acta Neuropathologica 67:289-295.
Rymut R, Slotty E, Kini N (2003) Method and apparatus for monitoring respiration using signals from a piezoelectric sensor mounted on a substrate. Google Patents.
Sachdev NS (2001) Temporal organization of multi-whisker contact in rats. In: Somatosensory & Motor Research, vol. 18, pp 91-100: Taylor & Francis.
Sadovsky E, Polishuk WZ, Yaffe H, Adler D, Pachys F, Mahler Y (1977) Fetal movements recorder, use and indications. IntJGynaecolObstet 15:20-24.
Salamone JD, Mayorga AJ, Trevitt JT, Cousins MS, Conlan A, Nawab A (1998) Tremulous jaw movements in rats:a model of parkinsonian tremor. Progress in Neurobiology 56:591-611.
Samii A, Nutt JG, Ransom BR (2004) Parkinson's disease. The Lancet 363:1783-1793.
Scarmeas N, Hadjigeorgiou GM, Papadimitriou A, Dubois B, Sarazin M, Brandt J, Albert M, Marder K, Bell K, Honig LS, Wegesin D, Stern Y (2004) Motor signs during the course of Alzheimer disease. Neurology 63:975-982.
Schwarting RK, Goldenberg R, Steiner H, Fornaguera J, Huston JP (1993) A video image analyzing system for open-field behavior in the rat focusing on behavioral asymmetries. JNeurosciMethods 49:199-210.
Scott L, Feng J, Kiss T, Needle E, Atchison K, Kawabe TT, Milici AJ, Hajós-Korcsok É, Riddell D, Hajós M (2012) Age-dependent disruption in hippocampal theta oscillation in amyloid-β overproducing transgenic mice. Neurobiology of Aging 33:1481.e1413-1481.e1423.
Seibenhener ML, Wooten MC (2015) Use of the Open Field Maze to measure locomotor and anxiety-like behavior in mice. JVisExp e52434.
Silvani A, Berteotti C, Bastianini S, Cohen G, Lo Martire V, Mazza R, Pagotto U, Quarta C, Zoccoli G (2014) Cardiorespiratory Anomalies in Mice Lacking CB(1) Cannabinoid Receptors. PLoS One 9:e100536.
Silverman JL, Yang M, Lord C, Crawley JN (2010) Behavioural phenotyping assays for mouse models of autism. Nat Rev Neurosci 11:490-502.
Siwek ME, Müller R, Henseler C, Trog A, Lundt A, Wormuth C, Broich K, Ehninger D, Weiergräber M, Papazoglou A (2015) Altered Theta Oscillations and Aberrant Cortical Excitatory Activity in the 5XFAD Model of Alzheimer's Disease. Neural Plasticity 2015:781731.

Spink AJ, Tegelenbosch RA, Buma MO, Noldus LP (2001) The EthoVision video tracking system--a tool for behavioral phenotyping of transgenic mice. Physiol Behav 73:731-744.
Staal WG (2015) Autism, DRD3 and repetitive and stereotyped behavior, an overview of the current knowledge. European Neuropsychopharmacology 25:1421-1426.
Steimer T (2002a) The biology of fear- and anxiety-related behaviors. Dialogues in Clinical Neuroscience 4:231-249.
Steimer T (2002b) The biology of fear- and anxiety-related behaviors. DialoguesClinNeurosci 4:231-249.
Stephenson R, Gucciardi EJ (2002) Theoretical and practical considerations in the application of whole body plethysmography to sleep research. EurJ Appl Physiol 87:207-219.
Sterniczuk R, Dyck RH, LaFerla FM, Antle MC (2010) Characterization of the 3xTg-AD mouse model of Alzheimer's disease: Part 1. Circadian changes. Brain research 1348:139-148.
Stevenson GW, Bilsky EJ, Negus SS (2006) Targeting Pain-Suppressed Behaviors in Preclinical Assays of Pain and Analgesia: Effects of Morphine on Acetic Acid-Suppressed Feeding in C57BL/6J Mice. The Journal of Pain 7:408-416.
Stevenson GW, Mercer H, Cormier J, Dunbar C, Benoit L, Adams C, Jezierski J, Luginbuhl A, Bilsky EJ (2011) Monosodium iodoacetate-induced osteoarthritis produces pain-depressed wheel running in rats: Implications for preclinical behavioral assessment of chronic pain. Pharmacology Biochemistry and Behavior 98:35-42.
Stover KR, Campbell MA, Van Winssen CM, Brown RE (2015) Analysis of motor function in 6-month-old male and female 3xTg-AD mice. Behavioural Brain Research 281:16-23.
Sugiyama M (2016) Introduction to Statistical Machine Learning. Elsevier.
Sullivan KL, Ward CL, Hauser RA, Zesiewicz TA (2007) Prevalence and treatment of non-motor symptoms in Parkinson's disease. Parkinsonism & Related Disorders 13:545.
Sulzer D, Sonders MS, Poulsen NW, Galli A (2005) Mechanisms of neurotransmitter release by amphetamines: A review. Progress in Neurobiology 75:406-433.
Sun M, Gewirtz JC, Bofenkamp L, Wickham RJ, Ge H, Connor MB (2010) Canonical TGF-+¦ Signaling Is Required for the Balance of Excitatory/Inhibitory Transmission within the Hippocampus and Prepulse Inhibition of Acoustic Startle. The Journal of Neuroscience 30:6025.
Svensson M, Rosvall P, Boza-Serrano A, Andersson E, Lexell J, Deierborg T (2016) Forced treadmill exercise can induce stress and increase neuronal damage in a mouse model of global cerebral ischemia. NeurobiolStress 5:8-18.
Symons FJ, Clark RD, Hatton DD, Skinner M, Bailey DB (2003) Self-injurious behavior in young boys with fragile X syndrome. American Journal of Medical Genetics Part A 118A:115-121.
Tagaito Y, Polotsky VY, Campen MJ, Wilson JA, Balbir A, Smith PL, Schwartz AR, Donnell CP (2001) A model of sleep-disordered breathing in the C57BL/6J mouse. Journal of Applied Physiology 91:2758.
Takahashi LK, Chan MM, Pilar ML (2008) Predator odor fear conditioning: Current perspectives and new directions. In: Neuroscience & Biobehavioral Reviews
Predator Odors, 5HT and Emotion, vol. 32, pp 1218-1227.
Tappe-Theodor A, Kuner R (2014) Studying ongoing and spontaneous pain in rodents--challenges and opportunities. The European journal of neuroscience 39:1881-1890.
Terman G, Shavit Y, Lewis J, Cannon J, Liebeskind J (1984) Intrinsic mechanisms of pain inhibition: activation by stress. Science 226:1270-1277.
Thifault S, Girouard N, Lalonde R (1996) Climbing Sensorimotor Skills in Lurcher Mutant Mice. Brain research bulletin 41:385-390.
Tuncel O, Altun K, Barshan B (2009) Classifying Human Leg Motions with Uniaxial Piezoelectric Gyroscopes. In: Sensors, vol. 9.
Ungerstedt U (1968) 6-hydroxy-dopamine induced degeneration of central monoamine neurons. European Journal of Pharmacology 5:107-110.

Van Dam D, D'Hooge R, Hauben E, Reyniers E, Gantois I, Bakker CE, Oostra BA, Kooy RF, De Deyn PP (2000) Spatial learning, contextual fear conditioning and conditioned emotional response in Fmr1 knockout mice. Behavioural Brain Research 117:127-136.

Vanderwolf CH (1969) Hippocampal electrical activity and voluntary movement in the rat. Electroencephalogr Clin Neurophysiol 26:407-418.

Varela M, Ruiz-Esteban R, Mestre de Juan MJ (2010) Chaos, fractals, and our concept of disease. Perspectives in biology and medicine 53:584-595.

Verheij C, de Graaff E, Bakker CE, Willemsen R, Willems PJ, Meijer N, Galjaard H, Reuser AJ, Oostra BA, Hoogeveen AT (1995) Characterization of FMR1 proteins isolated from different tissues. Human molecular genetics 4:895-901.

Vogel JR, Beer B, Clody DE (1971) A simple and reliable conflict procedure for testing anti-anxiety agents. Psychopharmacologia 21:1-7.

Walsh J, Desbonnet L, Clarke N, Waddington JL, O'Tuathaigh CMP (2012) Disruption of exploratory and habituation behavior in mice with mutation of DISC1: an ethologically based analysis. Journal of Neuroscience Research 90:1445-1453.

Webster SJ, Bachstetter AD, Nelson PT, Schmitt FA, Van Eldik LJ (2014) Using mice to model Alzheimer's dementia: an overview of the clinical disease and the preclinical behavioral changes in 10 mouse models. Frontiers in Genetics 5:88.

Whishaw IQ, Vanderwolf CH (1973) Hippocampal EEG and behavior: changes in amplitude and frequency of RSA (theta rhythm) associated with spontaneous and learned movement patterns in rats and cats. BehavBiol 8:461-484.

Willemsen R, Levenga J, Oostra BA (2011) CGG repeat in the FMR1 gene: size matters. Clinical genetics 80:214-225.

Wilson SG, Mogil JS (2001) Measuring pain in the (knockout) mouse: big challenges in a small mammal. Behavioural Brain Research 125:65-73.

Wiltschko AB, Johnson MJ, Iurilli G, Peterson RE, Katon JM, Pashkovski SL (2015a) Mapping sub-second structure in mouse behavior. Neuron 88.

Wiltschko AB, Johnson MJ, Iurilli G, Peterson RE, Katon JM, Pashkovski SL, Abraira VE, Adams RP, Datta SR (2015b) Mapping Sub-Second Structure in Mouse Behavior. Neuron 88:1121-1135.

Wolff JJ, Hazlett HC, Lightbody AA, Reiss AL, Piven J (2013) Repetitive and self-injurious behaviors: associations with caudate volume in autism and fragile X syndrome. Journal of Neurodevelopmental Disorders 5:12-12.

Woolf CJ, Mannion RJ (1999) Neuropathic pain: aetiology, symptoms, mechanisms, and management. The Lancet 353:1959-1964.

Xi M, Zhu G (2015) [Multi-scale Permutation Entropy and Its Applications in the Identification of Seizures]. Sheng Wu Yi Xue Gong Cheng Xue Za Zhi 32:751-756.

Yaghouby F, Donohue KD, OHara BF, Sunderam S (2016) Noninvasive Dissection of Mouse Sleep Using a Piezoelectric Motion Sensor. J Neurosci methods 259:90-100.

Yang M, Augustsson H, Markham CM, Hubbard DT, Webster D, Wall PM, Blanchard RJ, Blanchard DC (2004) The rat exposure test: a model of mouse defensive behaviors. Physiology & Behavior 81:465-473.

Yao Q, Pho H, Kirkness J, Ladenheim EE, Bi S, Moran TH, Fuller DD, Schwartz AR, Polotsky VY (2016) Localizing Effects of Leptin on Upper Airway and Respiratory Control during Sleep. Sleep 39:1097-1106.

Young MS, Li YC, Lin MT (1993) A modularized infrared light matrix system with high resolution for measuring animal behaviors. Physiology & Behavior 53:545-551.

Zhang Y, Bonnan A, Bony G, Ferezou I, Pietropaolo S, Ginger M, Sans N, Rossier J, Oostra B, LeMasson G, Frick A (2014) Dendritic channelopathies contribute to neocortical and sensory hyperexcitability in Fmr1(-/y) mice. NatNeurosci 17:1701-1709.

Zhang YQ, Bailey AM, Matthies HJG, Renden RB, Smith MA, Speese SD, Rubin GM, Broadie K (2001) Drosophila Fragile X-Related Gene Regulates the MAP1B Homolog Futsch to Control Synaptic Structure and Function. Cell 107:591-603.

Zhuo M (2007) Neuronal mechanism for neuropathic pain. Molecular Pain 3:14-14.

Zorner B, Filli L, Starkey ML, Gonzenbach R, Kasper H, Rothlisberger M, Bolliger M, Schwab ME (2010) Profiling locomotor recovery: comprehensive quantification of impairments after CNS damage in rodents. Nat Meth 7:701-708.